

PROCESSING AND FORMULATION STRATEGIES FOR THE STABILIZATION OF THERAPEUTIC PROTEINS

zur Erlangung des akademischen Grades eines
DOKTORS DER INGENIEURWISSENSCHAFTEN (Dr.-Ing.)

der Fakultät für Chemieingenieurwesen und Verfahrenstechnik des
Karlsruher Instituts für Technologie (KIT)

genehmigte
DISSERTATION

von
Dipl.-Ing. Josefine Morgenstern
geboren in Berlin

Referent: Prof. Dr. Jürgen Hubbuch
Korreferent: Prof. Dr. Matthias Franzreb
Tag der mündlichen Prüfung: 20.10.2017



This document is licensed under a Creative Commons Attribution-ShareAlike 4.0 International License (CC BY-SA 4.0):
<https://creativecommons.org/licenses/by-sa/4.0/deed.en>

Danksagung

Bei der Realisierung dieses Projekts habe ich die Unterstützung vieler Menschen erfahren, denen ich meine tiefe und aufrichtige Dankbarkeit ausdrücken möchte.

An erster Stelle gilt mein Dank Prof. Dr. Jürgen Hubbuch für die fachliche Leitung dieser Arbeit und das entgegen gebrachte Vertrauen. Jürgen, darüber hinaus bedanke ich mich für deinen Optimismus sowie deine Leidenschaft und Neugier gegenüber neuen Dingen. Du hast mir beigebracht, nicht genügsam zu sein, Fragen zu stellen, die Sache mal von der anderen Seite zu sehen und Kritik positiv zu begegnen und so meine Forschungsfrage eigenständig zu entwickeln.

Prof. Dr. Matthias Franzreb danke ich für das Interesse an meiner Arbeit sowie die Übernahme des Zweitgutachtens.

Dem Bundesministerium für Bildung und Forschung danke ich für die Finanzierung meiner Forschung im Rahmen des Projektes "Molecular Interaction Engineering".

Mein tiefer Dank gilt der Arbeitsgruppe des MABs. Es hat extrem viel Freude gemacht, mit euch zusammen zu arbeiten. Danke für die gemeinsamen Stunden im Labor, für die zahlreichen und gewinnbringenden fachlichen Diskussionen, für die ehrliche und offene Kritik und natürlich für die gemeinsamen Stunden außerhalb der Arbeitszeiten. Ich bin dankbar für eure Unterstützung und für die wertvollen Freundschaften, die sich aus unserer gemeinsamen Arbeit entwickelt haben. Ein besonderer Dank gilt:

- Meinen fleißigen studentischen Helfern Markus Busch, Carina Brunner, Nicolai Bluthardt, Svenja Strauß, Rebecca Hoffman und Dominik Hiltmann.
- Marion Krenz, Iris Perner-Nochta, Margret Meixner und Michael Wörner für die zuverlässige administrative Unterstützung, ohne welche meine Arbeit nicht so reibungslos abgelaufen wäre.

-
- Unserem Ingenieurteam Marc Hoffmann, Marie-Luise Schwab, Susanna Suhm, Kristina Schleining, Birgit Roser, Cathrin Dürr, Stefanie Limbrunner und Nicolai Bluthardt für die traumhafte Labororganisation.
 - Lara Galm und Pascal Baumann - Ihr wart für mich nicht nur Mentoren, sondern Vorbilder. Von euch lernen zu dürfen war für mich eine große Ehre.
 - Lara Galm, Pascal Baumann, Carsten Radtke und Gang Wang für die gemeinsamen Projektarbeiten.
 - Meinen Bürokollegen für die angenehme Arbeitsatmosphäre, so manchen Insider und dass ihr mein Geknusper am Nachmittag und den Fencheltee ohne Beschwerden ertragen habt.
 - Frank Hämmerling, Pascal Baumann, Kai Baumgartner, Marc Hoffmann, Susanna Suhm, Sarah Gretzinger, Sven Amrhein, Therese Schermeyer und Gang Wang für die vielen unterhaltsamen Kaffeepausen der anderen Art, die 15-Uhr Spezi und das ein oder andere Feierabendbier.

Von Herzen danke ich meinen Freunden Heike, der Karlsruher Gang, den X-Ment-Mädels und meinen Yogis - Ihr habt mich immer öfter daran erinnert, dass es im Leben wichtigere Dinge als eine Doktorarbeit gibt.

Ich möchte meinen Eltern Petra und Andreas und meiner Schwester Paula danken - für eure andauernde Unterstützung und euren Rückhalt, für eure Liebe und euer unerschütterliches Vertrauen in mich und für euer Vorbild. Ohne euch wäre ich nicht der Mensch der ich bin und das bedeutet mir unbeschreiblich viel.

Tobi, du hast stärker an mich geglaubt als ich selbst, hast mein Jammern und Klagen ertragen, Selbstzweifel ausgeräumt und mich aufgebaut, mir Essen gebracht – du warst da, in jedem Augenblick den ich dich brauchte. Wenn es ein bedeutungsvolleres Wort gäbe als "Danke", hätte ich es benutzt, um deine Unterstützung in den letzten Jahren anzuerkennen. Ich möchte dich in meinem Leben nicht mehr missen.

Es gibt ein großes und doch ganz alltägliches Geheimnis. Alle Menschen haben daran teil, jeder kennt es, aber die wenigsten denken je darüber nach. Die meisten Leute nehmen es einfach so hin und wundern sich kein bisschen darüber. Dieses Geheimnis ist die Zeit. Es gibt Kalender und Uhren, um sie zu messen, aber das will wenig besagen, denn jeder weiß, dass einem eine einzige Stunde wie eine Ewigkeit vorkommen kann, mitunter kann sie aber auch wie ein Augenblick vergehen – je nachdem, was man in dieser Stunde erlebt. Denn Zeit ist Leben. Und das Leben wohnt im Herzen.

- aus MOMO von Michael Ende -

Contents

Abstract	I
German Abstract: Zusammenfassung	VII
1 Introduction	1
1.1 Protein Structure and Properties	3
1.2 Intermolecular Protein Interactions	5
1.3 Protein Instabilities	7
1.4 Stabilization Strategies for Biopharmaceutical Proteins	17
1.5 Mechanistic Chromatography Modeling	22
1.6 Hydrogels as Drug Delivery Systems	26
1.7 3D Printing to Synthesize Photopolymerized Hydrogels	27
2 Research Proposal	29
3 Comprehensive Overview of Publications & Manuscripts	33
4 Manipulation of Lysozyme Phase Behavior by Additives	39
4.1 Introduction	41
4.2 Materials and Methods	43
4.3 Results	47
4.4 Discussion	56
4.5 Conclusion	60
4.6 Acknowledgments	61
4.7 References	61
5 Quantification of PEGylated Proteins	67
5.1 Introduction	69
5.2 Materials and Methods	71
5.3 Results and Discussion	79
5.4 Conclusion	90

5.5	Acknowledgments	90
5.6	References	91
6	Physical Stability of PEGylated Lysozyme	97
6.1	Introduction	99
6.2	Materials and Methods	101
6.3	Results and Discussion	107
6.4	Conclusion	118
6.5	Acknowledgments	118
6.6	References	119
7	Alternative Polymers for Protein Conjugation	123
7.1	Introduction	125
7.2	Materials and Methods	127
7.3	Results and Discussion	132
7.4	Conclusion	140
7.5	Acknowledgments	141
7.6	References	141
8	Mechanistic Chromatography Modeling for PEGylated Lysozyme	147
8.1	Introduction	149
8.2	Materials and Methods	151
8.3	Results	158
8.4	Discussion	164
8.5	Acknowledgments	168
8.6	References	169
9	High-Throughput Evaluation of Hydrogels	175
9.1	Introduction	177
9.2	Materials and Methods	179
9.3	Results and Discussion	184
9.4	Conclusion	193
9.5	Acknowledgments	194
9.6	References	194
10	Conclusion and Outlook	199
11	Comprehensive Reference List	203

12 Abbreviations and parameters	235
A Supplementary Figures	

Abstract

The present work contributes to the field of process development and optimization for the manufacturing of recombinant proteins. Recombinant proteins are biological macromolecules, which are produced using genetically modified organisms (GMOs). In addition to the food industry and for the synthesis of organic compounds, industrially produced proteins are mainly used in the field of medicine. There, they make a decisive contribution to the diagnosis, prevention and treatment of various human diseases. The production of protein-based drugs (biopharmaceuticals) and their provision in a stable and bioavailable dosage form (formulation) are a challenge due to the size and complexity of these molecules. On the way to the final drug product, the target protein undergoes a long and complex processing chain consisting of GMO cultivation (upstream processing), purification operations (downstream processing) and formulation steps. The reaction medium for the entire manufacturing process is mainly based on aqueous solutions. Some of the process steps used require extreme conditions such as unphysiological salt concentrations (e.g. in chromatographic purification) or acidic pH values (e.g. virus inactivation); all of which are potential stress factors for the protein integrity. Resulting irreversible changes in protein structure and physical instabilities, e.g. aggregation can affect both drug safety and efficacy. In order to ensure the product quality during the entire manufacturing process, the development of strategies for the stabilization of proteins in aqueous solutions is of paramount importance. From an economic perspective, short development times are desirable in order to reduce the ‘time to market’ of a drug product. Standardized procedures are of great interest for shortening the development times of stabilized protein products and are therefore the subject of this dissertation.

The aim of this work was the development and optimization of methods for the evaluation and implementation of stabilization strategies for proteins in aqueous solutions. The work is composed of an introduction and motivation, followed by six publications/manuscripts, in which different stabilization strategies for proteins as well as their processing are investigated. Due to the desire for fast, reproducible and cost-efficient methods, high-throughput screenings (HTS) as well as computer-based (*in silico*) methods have been used. In case of HTS, robot-based pipetting platforms were used for the automated and parallelized experimentation in microlitre scale. This approach generates large

volumes of data and consequently highly sophisticated analytical methods that simultaneously provide a sufficiently high sample throughput and data quality are required. For the *in silico* process development, mechanistic chromatography models were used and solved using numerical methods. All methods presented in this work have been developed using model proteins.

In the first publication¹, the effect of solution additives on the conformation and the aggregation behavior of proteins is examined. For this purpose, an automated high-throughput method was established for the generation of ternary phase diagrams consisting of protein, precipitant and the respective additive. For the analysis of the protein conformation, Fourier-transformed-infrared (FT-IR) spectroscopy was applied. FT-IR can provide insight into the secondary structure of the measured protein sample. Glycerol, glycine and PEG 1000 (polyethylene glycol having a molecular weight of 1 kDa) were used as sample additives. The results of this study indicate that the additives had a decisive influence on the process-relevant parameters conformation, solubility and aggregation behavior of the investigated protein lysozyme. The additive effect was found to depend on the pH value and the associated conformational stability of lysozyme. At pH values with low conformational protein stability in the unmodified system, glycine enhanced the unfolding and aggregation of the protein, while PEG 1000 and glycerol increased the conformational stability of the protein and altered the protein aggregation behavior. However, no change in the protein solubility was observed. For pH values where the protein conformation was stable in the unmodified system, the investigated additives had no effect on the protein structure, but they affected the solubility, phase transition, crystal size, and morphology. In summary, the presented method provides an efficient tool for selecting suitable solution additives to prevent unwanted phase transitions and instabilities.

The observed stabilization of lysozyme by solution additive initiated the investigation on how the covalent attachment of non-polypeptides to the protein (protein conjugation) influences its aggregation behavior and solubility. The covalent linkage of proteins and synthetic materials produces novel hybrid molecules with combined properties of both reactants. In the pharmaceutical industry, polyethylene glycol (PEG) is state of the art for protein conjugation. The currently used reaction mechanisms utilize naturally occurring binding sites (amino acids) on the protein surface. Since the individual amino acids occur repeatedly in a protein, these approaches result in heterogeneous product mixtures of proteins with different number (conjugation degree) and position (isoforms) of bound polymers. For a fast and material-efficient identification of the different conjugate species

¹Galm et al., *Int. J. Pharm.*, 494/1 (2015): 370-380.

and reaction monitoring a fast and robust analytical method is required.

In the second publication², the development of an analytical method for quantifying the composition of heterogeneous PEG-conjugate mixtures is presented. The basis of this method is a microfluidic-based capillary gel electrophoresis (CGE), which was combined with a precipitation step to conserve the sample composition for structurally unstable proteins. The method was validated using the example of proteases, which are susceptible to autocatalysis. This method was found to be highly effective for large data sets as it provides a low sample consumption of only 2 μL , an analysis time of 40 s per sample, a high resolution allowing for peak baseline separation between conjugates with varying conjugation degree and a high sensitivity down to 0.1 mg/mL of PEGylated protein.

In the third publication³, the influence of covalently bound PEG on the phase behavior, the solubility and the protein conformation of lysozyme was investigated. For this purpose, the automated high-throughput method for the preparation of protein phase diagrams in microbatch experiments from publication 1 was adapted for the application to protein conjugates. The PEG molecular weight (2 kDa, 5 kDa and 10 kDa) and the number of bound PEG molecules (PEGylation degree) were varied as influencing parameters. Higher PEG molecular weights and PEGylation degrees resulted in increased shielding of the protein properties. This resulted in an increase in the conformational protein stability as well as the solubility and a simultaneous decrease in the residual activities of the conjugates. The methodology used is extremely useful for fine-tuning PEG molecular weights and PEGylation degree with respect to the conjugate properties required for specific applications.

While PEG remains useful for the stabilization of therapeutic proteins, some limitations in its clinical use including antibody formation against PEG (anti-PEG), hypersensitivity and vacuolation in various tissues upon repeated exposure have begun to emerge driving the development of alternatives. In addition, the synthesis of activated PEGs with narrow dispersity is complex and therefore expensive. The development of protein conjugates with lower-cost polymers having similar advantages as PEG would increase the availability of stable biopharmaceuticals to a broader mass of the population. For this reason, the synthesis of two alternative, biocompatible polymers (poly-(4-acryloylmorpholine) = PNAM and poly-(oligoethylene glycol methacrylate) = POEGMA) and their effect on lysozyme stability are described in manuscript 4⁴. An increase in protein solubility was achieved for all investigated polymers. Compared to PEG, however, higher molecular

²Morgenstern et al., *J. Chrom. A*, 1462 (2016): 153-164.

³Morgenstern et al., *Int. J. Pharm.*, 519/1-2 (2017): 408-417.

⁴in preparation: Stability Assessment of Protein-Polymer Conjugates: Alternative Polymers to Polyethylene Glycol.

weight polymers or conjugation degrees were required to achieve a comparable effect on solubility, which unfortunately entailed a significant reduction of residual activity. Nonetheless, a positive result of this study was the uncomplicated transferability of the methods for analysis, purification and stability assessment developed using PEG enabling the search for more effective and economically viable alternatives.

Due to the strong differences in the physico-chemical properties of protein conjugates with a varying degree of conjugation, a separation strategie for the individual species is expedient. Ion-exchange chromatography (IEX) is among the most important purification methods for protein conjugates. The separation principle in IEX is based on different transport and adsorption properties of the conjugates within the chromatographic column. Up to now, IEX process design and optimization are mainly performed by empirical approaches, which are time and material consuming. In publication 5⁵ an alternative approach for IEX process development is presented which is based on the *in silico* determination of mass transfer and adsorption parameters needing solely a few experiments. In addition to the use as solution additive and for protein conjugation, PEG can also be functionalized in such a way that a crosslinking to three-dimensional networks is possible. Due to the hydrophilic character of PEG, these networks swell to a multiple of their volume in an aqueous environment without dissolving and are therefore referred to as hydrogels. Due to their high water content and their porous structure, hydrogels offer a physico-chemical similarity to the natural extracellular matrix and provide an mechanical support for incorporated proteins. Both protein stability and release from hydrogels are influenced by various parameters including the mode of crosslinking, the chemistry and molecular weight of the polymer, pH and ionic strength of the surrounding solution, and specific protein properties such as size, three-dimensional structure and surface characteristics. Since the large number and interaction of these parameters complicate a mechanistic prediction of protein-hydrogel interactions, a high-throughput method for their experimental investigation has been established in the last manuscript⁶. The hydrogels were cross-linked to high-throughput compatible structures by means of 3D printing and then screened for their protein uptake and release on an automated pipetting platform. Polyethylene glycol diacrylate (PEG-DA) was used as a polymer and copolymerized with acrylic acid for further functionalization of the hydrogel. In a case study with lysozyme, the data generated by the presented approach was comparable to literature data for the used materials. Compared to conventional methods, however, the

⁵Morgenstern et al., *Biotechnology Journal*, accepted (2017), doi: 10.1002/biot.201700255.

⁶in preparation: Assessment of Hydrogels for Biopharmaceutical Purposes Using a Combination of 3D Printing and High-Throughput Screening.

screening process has been significantly accelerated.

In summary, process development for the stabilization of pharmaceutical proteins as well as their encapsulation into polymeric hydrogels can be significantly accelerated and simplified by the application of the presented methods. For the development and validation of these methods different model proteins were used in this thesis. However, these strategies can readily be transferred to other molecules due to their automation and the reduction of the necessary sample material.

German Abstract: Zusammenfassung

Die vorliegende Arbeit ist in das Themengebiet der Verfahrensentwicklung und -optimierung für die Prozessierung von rekombinanten Proteinen einzuordnen. Rekombinante Proteine sind biologische Makromoleküle, welche mit Hilfe von gentechnisch veränderten Organismen (genetically modified organism - GMO) hergestellt werden. Neben der Anwendung in der Lebensmittelindustrie und für die Synthese von organischen Verbindungen werden industriell hergestellte Proteine vor allem im Bereich der Medizin eingesetzt. Dort leisten sie einen wichtigen Beitrag zur Diagnose, Prävention und Therapie einer Vielzahl menschlicher Krankheiten. Die Produktion von Proteinwirkstoffen (Biopharmazeutika) und deren Bereitstellung in einer stabilen und für den Körper verfügbaren Darreichungsform (Formulierung) stellen aufgrund der Größe und Komplexität der Moleküle eine Herausforderung dar. Auf dem Weg zum fertigen Arzneimittel durchläuft das Zielprotein von der Kultivierung der GMOs (Upstream) über diverse Reinigungsschritte (Downstream) bis hin zur Formulierung eine lange und komplexe Prozesskette. Das Reaktionsmedium für den gesamten Herstellungsprozess basiert dabei hauptsächlich auf wässrigen Lösungen. Manche der eingesetzten Prozessschritte erfordern extreme Bedingungen, wie unphysiologische Salzkonzentrationen (z.B. bei der chromatographischen Aufreinigung) oder saure pH-Werte (z.B. bei der Virus-Inaktivierung), welche potenzielle Stressfaktoren für die Proteinintegrität darstellen. Daraus resultierende irreversible Veränderungen der Proteinstruktur und physikalische Instabilitäten, wie z.B. Aggregation, können sowohl die Arzneimittelsicherheit als auch die -wirksamkeit beeinträchtigen. Um die notwendige Produktqualität während des gesamten Herstellungsprozesses zu gewährleisten, ist die Entwicklung von Strategien zur Stabilisierung von Proteinen in wässrigen Lösungen von höchster Wichtigkeit. Aus ökonomischer Perspektive sind geringe Entwicklungszeiten wünschenswert, um die Markteinführung eines Arzneimittels zu beschleunigen. Die Etablierung standardisierter Vorgehensweisen in der Prozessentwicklung steht in engem Zusammenhang mit der Verkürzung der Entwicklungszeiten und ist daher Gegenstand dieser Dissertation.

Das Ziel dieser Arbeit war die Entwicklung und Optimierung von Methoden zur Bewertung und prozesstechnischen Umsetzung von Stabilisierungsstrategien für Proteine in wässrigen Lösungen. Die Arbeit besteht aus einer Einleitung und Motivation, gefolgt

von sechs Publikationen/Manuskripten, in welchen unterschiedliche Stabilisierungsstrategien für Proteine adressiert werden. Resultierend aus dem Streben nach schnellen, reproduzierbaren und kosteneffizienten Methoden wurden in dieser Arbeit sowohl Hochdurchsatzverfahren (high-throughput screenings - HTS) als auch computerbasierte (*in silico*) Verfahren eingesetzt. Im Falle von HTS wurden robotergestützte Pipettierplattformen für die automatisierte und parallelisierte Durchführung von Experimenten im Mikrolitermaßstab eingesetzt. Durch die Erzeugung großer Datenmengen erfordert diese Herangehensweise Analytikmethoden, die gleichzeitig einen ausreichend hohen Probendurchsatz und eine ausreichend hohe Datenqualität liefern. Bei der *in silico*-Prozessentwicklung wurden mechanistische Modelle für physikalische Prozesse verwendet und mit Hilfe von numerischen Methoden gelöst.

In der ersten Publikation¹ wurde die Wirkung von Lösungsmitteladditiven auf die Konformation und das Aggregationsverhalten von Lysozym aus Hühnereiweiß untersucht. Dazu wurde ein automatisiertes Hochdurchsatzverfahren zur Erstellung ternärer Phasendiagramme, bestehend aus Protein, Fällungsmittel (Präzipitant) und dem jeweiligen Additiv etabliert. Für die Analyse der Proteinkonformation wurde Fourier-Transformations-Infrarotspektroskopie (FT-IR) angewandt, welche basierend auf den Schwingungen des Proteinerückgrats Einblick in die Sekundärstruktur der gemessenen Proteinprobe liefert. Als Additiv wurden exemplarisch Glycerin, Glycin und PEG 1000 (Polyethylenglykol) mit einem Molekulargewicht von 1 kDa) verwendet. Die Ergebnisse dieser Studie zeigten einen deutlichen Einfluss der Lösungsmitteladditive auf prozessrelevante Parameter wie Konformation, Löslichkeit und Aggregationsverhalten von Lysozym. Es wurde ein Zusammenhang zwischen der Wirkung der Additive sowie dem pH-Wert und der damit verbundenen konformellen Stabilität von Lysozym hergestellt. Bei pH-Werten mit niedriger Stabilität der Proteinkonformation im unmodifizierten System verstärkte Glycin die Entfaltung und Aggregation des Proteins, wohingegen PEG 1000 und Glycerin die Stabilität der Proteinkonformation erhöhten und das Aggregationsverhalten veränderten. Es wurde jedoch keine Veränderung der Proteinlöslichkeit beobachtet. Für pH-Werte, bei denen das Protein im unmodifizierten System konformell stabil war, hatten die untersuchten Additive keinen Einfluss auf die Proteinstruktur, beeinflussten jedoch die Löslichkeit, die auftretenden Phasenübergänge und Kristallgröße sowie -morphologie. Zusammenfassend ist festzustellen, dass die vorgestellte Methode ein effizientes Werkzeug zur Auswahl geeigneter Lösungsmitteladditive bietet, um unerwünschte Phasenübergänge und Instabilitäten zu vermeiden.

Die beobachtete Stabilisierung von Lysozym durch Lösungsmitteladditive initiierte die

¹Galm et al., Int. J. Pharm., 494/1 (2015): 370-380.

Untersuchung, wie die kovalente Bindung von Nichtprotein-Molekül an das Protein (Proteinkonjugation) das Aggregationsverhalten und die Löslichkeit beeinflusst. Als Nichtprotein-Moleküle wurden in dieser Arbeit synthetische Polymere untersucht. Die kovalente Verknüpfung von Proteinen und synthetischen Materialien erzeugt neuartige Hybridmoleküle mit einer Kombination der Eigenschaften beider Reaktanten. In der pharmazeutischen Industrie ist Polyethylenglycol (PEG) Stand der Technik für die Proteinkonjugation. Die derzeit verwendeten Reaktionsmechanismen nutzen die Seitenketten natürlich vorkommender Aminosäuren auf der Proteinoberfläche als Bindungsstellen. Da die einzelnen Aminosäuren wiederholt in einem Protein auftreten, entstehen durch diesen Ansatz heterogene Reaktionsgemische aus verschiedenen Produkten, die sich in der Anzahl der gebundenen Polymer-Moleküle (Konjugationsgrad) und Position (Isoformen) unterscheiden. Für eine schnelle und effiziente Identifizierung der unterschiedlichen Konjugatspezies und für eine Überwachung der Konjugationsreaktion ist eine schnelle und robuste Analytikmethode unabdingbar.

In der zweiten Publikation² wird die Entwicklung eines analytischen Verfahrens zur Quantifizierung der Zusammensetzung von heterogenen PEG-Konjugat-Gemischen vorgestellt. Grundlage dieser Methode ist eine Mikrofluidik-basierte Kapillargelelektrophorese, welche für die Analyse von strukturell instabilen Proteinen zusätzlich mit einem Präzipitationsschritt zum Erhalt der Probenzusammensetzung kombiniert wurde. Die Methode wurde am Fallbeispiel von Proteasen validiert, welche anfällig für Autokatalyse sind. Die Methodik zeichnet sich durch einen geringen Probenverbrauch von nur 2 μL , eine Analysezeit von 40 s pro Probe, eine hohe Auflösung zwischen Konjugaten mit variierendem Konjugationsgrad und eine hohe Sensitivität von bis zu 0,1 mg/mL PEGyliertem Protein aus. Durch diese Vorteile erwies sie sich als sehr effektiv für große Datensätze.

In der dritten Publikation³ wurde der Einfluss von kovalent gebundenem PEG auf das Phasenverhalten, die Löslichkeit und die Konformation von Lysozym untersucht. Hierfür wurde das automatisierte Hochdurchsatzverfahren zur Erstellung von Protein-Phasendiagrammen in Microbatch-Experimenten aus Publikation 1 für die Anwendung auf Proteinkonjugate adaptiert. Als Einflussgrößen wurden das PEG-Molekulargewicht (2 kDa, 5 kDa und 10 kDa) und die Anzahl der gebundenen PEG-Molekülen (PEGylierungsgrad) variiert. Höhere PEG-Molekulargewichte und PEGylierungsgrade resultierten in einer verstärkten Abschirmung der Proteineigenschaften. Daraus ergaben sich eine Erhöhung der konformellen Proteinstabilität sowie der Löslichkeit und eine gleichzeitige Abnahme der Restaktivität der Konjugate. Die vorgestellte Methodik eignet sich für die Feinab-

²Morgenstern et al., *J. Chrom. A*, 1462 (2016): 153-164.

³Morgenstern et al., *Int. J. Pharm.*, 519/1-2 (2017): 408-417.

stimmung von PEG-Molekulargewicht und PEGylierungsgrad hinsichtlich der Konjugat-Eigenschaften für spezifische Anwendungen.

Neben den vielen Vorteilen der Protein-PEGylierung treten in der klinischen Anwendung einige Nachteile wie allergische Reaktionen und Immunantworten auf, welche die Entwicklung von alternativen Polymeren vorantreiben. Darüber hinaus ist die Synthese von aktivierten PEGs mit geringer Dispersität komplex und daher teuer. Die Entwicklung von Proteinkonjugaten mit kosteneffizienteren Polymeren, welche die positiven Wirkungen von PEG reproduzieren, würde die Verfügbarkeit von stabilen Biopharmazeutika für die Masse der Bevölkerung erhöhen. Aus diesen Gründen wurde in Manuskript 4⁴ die Synthese zweier alternativer, biokompatibler Polymere (Poly-(4-acryloylmorpholin) = PNAM und Poly-(oligoethylenglykolmethacrylat) = POEGMA) und deren Wirkung auf die Lysozymstabilität untersucht. Durch beide Polymere konnte eine Erhöhung der Proteinlöslichkeit erzielt werden. Im Vergleich zu PEG mussten jedoch Polymere mit höherem Molekulargewicht oder Konjugationsgrade eingesetzt werden, um eine vergleichbare Wirkung auf die Löslichkeit zu erzielen. Dies hatte eine signifikante Reduzierung der Restaktivität zur Folge. Ein positives Ergebnis dieser Studie war jedoch die einfache Übertragbarkeit der mit PEG entwickelten Methoden zur Analyse, Reinigung und Stabilitätsbewertung. Dadurch wird die Suche nach effektiveren und kostengünstigeren Polymeren für die Proteinkonjugation vereinfacht.

Aufgrund der starken Unterschiede in den physikalisch-chemischen Eigenschaften von Proteinkonjugaten mit variierendem Konjugationsgrad ist deren Auftrennung sinnvoll. Ionenaustausch-Chromatographie (IEX) zählt zu den wichtigsten Aufreinigungsmethoden für Protein-Konjugate. Das Trennprinzip beruht dabei auf unterschiedlichen Transport- und Adsorptionseigenschaften der Konjugate innerhalb der chromatographischen Säule. Die Auslegung der Trennprozesse erfolgt noch immer hauptsächlich durch empirische Ansätze, die zeitaufwendig sind und mit einem hohen Verbrauch an Probenmaterial einhergehen. In Publikation 5⁵ wird ein alternativer Ansatz zur Prozessauslegung auf Basis der *in silico* Berechnung von Stoffübergangs- und Adsorptionsparametern anhand weniger Experimente vorgestellt.

Neben der Verwendung als Lösungsmitteladditiv und zur Proteinkonjugation kann PEG auch derartig funktionalisiert werden, dass seine Vernetzung zu dreidimensionalen Netzwerken möglich ist. In wässriger Umgebung quellen diese Netzwerke zu einem Vielfachen ihres Volumens auf und werden daher auch als Hydrogele bezeichnet. Aufgrund ihres

⁴in preparation: Stability Assessment of Protein-Polymer Conjugates: Alternative Polymers to Polyethylene Glycol.

⁵Morgenstern et al., *Biotechnology Journal*, accepted (2017), doi: 10.1002/biot.201700255.

hohen Wassergehaltes und ihrer porösen Struktur bieten Hydrogele eine physikalisch-chemische Ähnlichkeit zur natürlichen extrazellulären Matrix und bieten zusätzlich einen mechanischen Schutz für inkorporierte Proteine. Sowohl die Proteinstabilität als auch die -freisetzung aus Hydrogelen werden durch verschiedene Parameter beeinflusst. Dazu gehören die Art der Vernetzung, die Chemie und das Molekulargewicht des vernetzten Polymers, der pH-Wert und die Salzkonzentration der umgebenden Lösung und spezifische Proteineigenschaften wie Größe, dreidimensionale Struktur und Oberflächenbeschaffenheiten. Da die große Anzahl und die Interaktion dieser Parameter eine mechanistische Vorhersage der Protein-Hydrogel-Interaktionen kompliziert machen, wurde im letzten Manuskript⁶ ein Hochdurchsatzverfahren zu deren experimenteller Untersuchung etabliert. Die Hydrogele wurden mittels 3D-Druck zu hochdurchsatzkompatiblen Strukturen vernetzt und anschließend auf einer automatisierten Pipettierplattform prozessiert. Als Polymer wurde dabei Polyethylenglycol-diakrylat (PEG-DA) eingesetzt und zu einer weiterführenden Funktionalisierung des Hydrogels mit Acrylsäure copolymerisiert. In einer Fallstudie mit Lysozym waren die durch den demonstrierten Ansatz erzeugten Daten vergleichbar mit Literaturdaten. Im Vergleich zu herkömmlichen Methoden konnte der Screening-Prozess jedoch deutlich beschleunigt werden.

Zusammenfassend ist festzustellen, dass die Prozessentwicklung für die Stabilisierung pharmazeutischer Proteine und deren Verkapselung in polymeren Hydrogelen durch die Anwendung der vorgestellten Methoden deutlich beschleunigt und vereinfacht werden kann. Für die Entwicklung und Validierung dieser Methoden wurden in der vorliegenden Arbeit Modellproteine verwendet. Durch die Automatisierung der Methoden und die Reduzierung von benötigtem Probenmaterial ist eine Übertragung auf andere Moleküle jedoch ohne weiteres möglich.

⁶in preparation: Assessment of Hydrogels for Biopharmaceutical Purposes Using a Combination of 3D Printing and High-Throughput Screening.

Introduction

Proteins are organic macromolecules, which perform numerous functions in the human body. For example, they are part of the immune system and help defend the body from foreign molecules (antibodies), they catalyze and regulate biochemical reactions (enzymes), and form membrane receptors and channels, thus facilitating the transport of molecules within a cell or between separate biochemical reaction compartments. Due to their complex three-dimensional structure, proteins exhibit a high specificity for their respective target [1]. An insufficient, excessive or defective production of endogenous proteins may cause serious diseases such as diabetes [2], Gaucher's disease [3], haemophilia [4], Alzheimer's disease or Parkinson [5, 6]. The administration of proteins as drug substance has the potential to cure many human diseases with minimal side effects which can hardly be achieved by chemically synthesized small molecules [1].

Due to their high significance, it has always been of interest to produce proteins as active pharmaceutical ingredients (APIs). Initially, proteins were extracted from natural sources such as the human blood stream or specific cell tissues and organs. There have been serious issues with this type of production, including the transmission of infectious diseases and the limited availability of the natural sources. [7] The groundbreaking decipheration of the DNA molecule by Watson and Crick in 1953 [8] and the creation of the world's first recombinant organism by Cohen and Boyer in 1973 [9] marked milestones for the technical production of protein molecules as APIs. Advances in the process technologies for cell cultivation and protein purification have enabled the large-scale production of proteins [10, 11]. In 1982, recombinant human insulin was approved by the U.S. Food and Drug Administration (FDA) as the world's first recombinant drug [12]. Nowadays, protein drugs are an integral part of conventional therapy and it is estimated that in 2020 about 46 % of the sales volume of the 100 highest-selling pharmaceutical products will be achieved by biopharmaceuticals [13]. According to Strohl and Knight [14], the currently approved biopharmaceuticals can be categorized into four major groups: (1) protein

therapeutics with enzymatic or regulatory activity (e.g. insulin, growth hormones, blood factor replacement therapies), (2) protein therapeutics with special targeting activity (e.g. monoclonal antibodies, mAbs), (3) protein vaccines, and (4) protein diagnostics. The production of therapeutic proteins, however, is very demanding due to their size, complex structure, and biological origin [15]. The development of a manufacturing process for recombinant proteins usually follows a well-established scheme. At first, the recombinant gene with the necessary transcriptional regulatory elements is transferred into cells forcing them to synthesize the desired protein in large amounts [16]. Nowadays, about 60-70 % of all recombinant protein drugs are produced in mammalian cells due to their capacity for proper protein folding, assembly and post-translational glycosylation [16]. Successfully modified cells are cultivated under growth conditions optimized regarding production needs (upstream processing, USP). From the resulting crude fermentation broth, the target product is isolated and concentrated in a series of purification steps (downstream processing, DSP) which can be highly challenging. The highly pure drug substance resulting from this process is formulated to the final drug product with regard to storage stability and application in the human body. For reasons of patient safety and drug efficacy, the development, testing, production, and admission/licensing of biopharmaceutical products are subject to strict regulations by authorities such as the FDA. In order to gain regulatory approval, biopharmaceutical process development is nowadays based on the ‘Quality by Design’ (QbD) approach that aims for an efficient identification and reduction of errors during the production of biopharmaceuticals [17]. This approach involves the identification and monitoring of critical quality attributes (CQAs) such as size, molecular properties, structural and biological integrity and impurity profiles. Even slight changes in the manufacturing process can influence the CQAs [17, 18]. Therefore, critical process parameters and a tolerance range in which they can be varied need to be defined in order to consistently produce a drug product with the desired effect [19]. The investigation of the influencing parameters on protein properties and the associated analytical techniques are therefore of great importance to the production of biopharmaceuticals. The enormous expenditure for process development, approval, production, and quality control of therapeutic proteins leads to extensive costs for biopharmaceutical products.

1.1 Protein Structure and Properties

Proteins are (bio-)polymers composed of monomeric units called amino acids. The individual amino acids are linked by a peptide bond formed by a condensation reaction between the α -carboxyl group of one amino acid and the α -amino group of an adjacent amino acid. The linear amino acid sequence of a protein is also referred to as a primary sequence. Depending on the number of amino acids, the molecular weights for pharmaceutical blockbuster proteins are in the range of approximately 5 kDa (insulin) to 150 kDa (mAbs). Each amino acid carries specific properties due to the chemical composition of its side chain. These side chains are either basic, acidic, non-polar (hydrophobic) or polar. [20, 21]. Therefore, the physicochemical properties of a protein strongly depend on number, identity, and sequential order of amino acids. Under natural conditions, a protein is not present in its primary sequence but folds into a three-dimensional structure which is decisive for the specific interactions and thus the protein's biological functions [22]. This natural three-dimensional (3D) structure is unique for every protein and is referred to as native protein conformation [23, 24]. Non-native protein conformations cover incorrectly folded protein molecules as well as partially unfolded or completely denatured ones [25]. The folding process can be described more specifically by a subdivision into three further structure hierarchies. The secondary structure defines highly regular local sub-structures between the polypeptide backbone of nearby amino acids due to regular hydrogen-bonding. The most common secondary structures are α -helix, β -sheet, coil regions and random structures [26, 27]. The tertiary protein structure describes the 3D structure of the entire protein and thus also takes into account interactions between amino acids that are further apart in the primary sequence.

The main driving force for protein folding in aqueous environments is to reduce the interactions between water and the hydrophobic amino acids [28]. This leads to an accumulation of the hydrophobic amino acids in the interior of the protein molecule, which is also referred to as hydrophobic core [7, 20]. Additionally, due to the accumulation in the core and the resulting small distances between these amino acids, attractive van-der-Waals forces contribute to the stabilization of the protein structure. However, the hydrophobic amino acids cannot partition independently, since they are covalently linked to their chain neighbors of the primary sequence [29]. This leads to the existence of surface exposed hydrophobic amino acids as displayed in Fig. 1.1A. In contrast, the basic and acidic amino acids are ionizable. Their charge is strongly dependent on their logarithm-

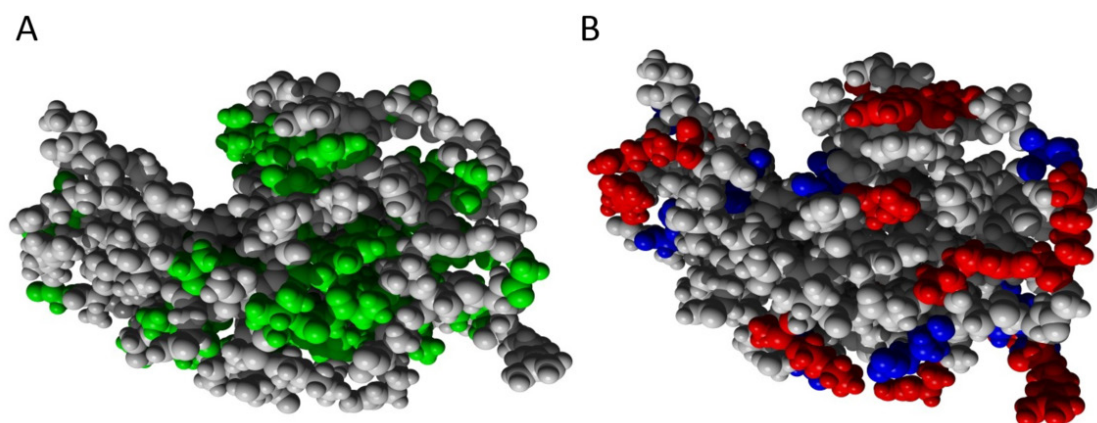


Figure 1.1: Representation of the 3D structure of lysozyme from chicken egg white at pH 7 (amino acid sequence from the pdb file 1LYZ of the RCSB protein database, edited with Yasara software). Left: Surface charges due to the amino acids lysine, arginine, histidine, aspartic acid and glutamic acid (blue = negative, red = positive). Right: Hydrophobic surface areas due to the hydrophobic amino acids alanine, isoleucine, leucine, methionine, phenylalanine, proline, tryptophan and valine.

mic acid dissociation constant pK_a and the pH value of the surrounding solution. The titratable side group is deprotonated for $pH > pK_a$ and protonated for $pH < pK_a$. Charged amino acids are predominantly oriented towards the surface of the protein molecules (see Fig. 1.1B) and ensure electrostatic interactions with the water molecules. This results in a stabilization of the protein in solution by the formation of a solvation or hydrate shell. The sum of charges of the individual amino acids at a specific pH value results in the net charge of the entire protein. The pH value where the net charge of the protein equals zero is defined as isoelectric point (pI) [30]. At this pH, there are still negative and positive charges, but their number is equal. There are also intrinsic charged amino acids, which contribute to the protein structure by the formation of salt bridges [31].

The spatial assembly of several tertiary structure monomers to a protein multimer is referred to as quaternary structure. This is often the case when complex functions in the human body cannot be fulfilled by a single amino acid chain. For example, a tetrameric hemoglobin complex is responsible for the transport of oxygen. [32, 33] The described protein structures are not rigid, but highly dynamic and in constant motion between different conformational states with similar energy [32, 34]. The fastest motions, vibrations and librations around covalent bonds, result in atoms moving only a fraction of an Ångström on the picosecond to nanosecond timescale. Ligand binding may involve subtle

motions like rearrangement of amino-acid residues in the binding site. This molecular flexibility allows the protein to respond to the presence of other molecules and/or to variations in the environment.[35]

1.2 Intermolecular Protein Interactions

The previously described protein structure and the formation of charged and hydrophobic surface regions are decisive for molecular interactions with other molecules in solution. Interactions between a protein molecule and molecules in its environment determine protein function, adsorption to surfaces and physicochemical properties such as solubility and protein stability. For the description of intermolecular interactions between two spherical particles in a liquid medium Derjaguin, Landau, Verwey, and Overbeek developed the DLVO theory in the 1940s [36–38]. According to the classical DLVO theory, interactions between dispersed particles in a liquid environment result from a superposition of van-der-Waals (dispersion) attraction and electrostatic repulsion [39]. Van-der-Waals interactions are short-range, non-covalent interactions between atomic or molecular dipoles [40]. Those dipoles may be permanent or induced due to rapid intramolecular fluctuations of the electron clouds of non-polar molecules. In larger molecules the electron clouds are subject to greater fluctuations so that the van-der-Waals forces are more pronounced than for small molecules. For the calculation of the van-der-Waals forces F_{vdW} between two spherical particles, the simple approximation formula

$$F_{vdW} = -\frac{H_a \cdot d}{24 \cdot x^2} \quad (1.1)$$

according to the Hamaker theory is often used with H_a being the Hamaker constant, x the distance between the spheres and d the sphere diameter [41, 42]. In case the spheres do not have the same diameter, d is further defined by

$$d = \frac{2 \cdot d_1 \cdot d_2}{d_1 + d_2} \quad (1.2)$$

for the two diameters d_1 and d_2 [41, 42]. According to Israelachvili et al. [43], the Hamaker constant H_a is primarily a function of particle density. Since most globular proteins have roughly the same density, it is expected that they have similar values of H_a [44]. For proteins in water, H_a is approximately 3-10 kT ($1 \text{ kT} = 4.11 \cdot 10^{-27} \text{ J}$ at 298.15 K) [45].

Electrostatic interactions occur due to the presence of electric charges and can be described quantitatively by Coulomb's law

$$F_{Coulomb} = k_e \cdot \frac{Q_1 \cdot Q_2}{x^2} \quad (1.3)$$

for two point charges Q_1 and Q_2 separated by the distance x . k_e is the Coulomb's constant ($k_e = 8.99 \cdot 109 \text{ Nm}^2\text{C}^{-2}$). A charged surface thus creates an electrostatic field which attracts opposing charges ($F_{Coulomb}$ is negative) and repels equal charges ($F_{Coulomb}$ is positive) [40]. Electrostatic interactions of proteins in an aqueous environment are influenced by the presence of salts. In the biopharmaceutical industry, salts are ubiquitously used to control ionic strength and osmolality. Dissociated ions form of a diffuse ionic layer (electrochemical double layer) shielding the charges on the surface. The concentration of the counter-ions decreases exponentially from a maximum value at the surface to the surrounding medium. Therefore, the electrostatic potential and thus the electrostatic interactions drop with the increase of distance between two molecules and reaches zero at the boundary of the electrochemical double layer. A measure of the thickness of the electrochemical double layer is the Debye-Hückel length, which is also referred to as decay length. Electrostatic forces are very long range in comparison to the forces associated with other interactions. [39, 46]

In principle, the molecular interactions discussed in this model are relevant for proteins. However, the classical DLVO theory neglects additional interaction mechanisms such as solvation, hydrogen bonds, hydrophobic interactions, and steric interactions; all of which are of major importance for protein solution behavior and function [44, 47, 48]. In addition, the size and complexity of proteins and the non-uniform distribution of functional groups on the molecular surface lead to a simultaneous existence of several interaction forces and thus to a total resulting interaction force (potential of mean force) [49].

Hydrophobic interactions are of particular importance for proteins. Non-polar surface groups are poorly solvated since they cannot form hydrogen bonds with the surrounding water molecules. Instead, hydrophobic structures induce ordered structures of the water molecules resulting in entropy loss. Surface-exposed hydrophobic amino acids generate attractive protein-protein interactions in an aqueous environment since the fusion of these hydrophobic surface areas reduces the overall surface exposed hydrophobic area and thus minimizes free energy. [28] Israelachvili et al. [50] observed that hydrophobic interaction forces increase exponentially at separation distances of less than 10 nm and are therefore more short-range than electrostatic interactions. In consequence, hydrophobic interactions become increasingly important at increased ionic strength since repulsive

electrostatic interaction and thus the distance between molecules are reduced under these conditions [51].

Experimental decomposition of protein interactions into their individual contribution is not feasible. Therefore, a solid platform for their theoretical prediction is highly demanded [52]. Until now, the complexity of protein interactions has hindered the establishment of a unified theoretical framework to calculate the potential of mean force. However, several empirical approaches have been developed to characterize protein interactions. These include thermodynamic equation as free energy minimization [44] and molecular dynamic (MD) simulations incorporating each atom of the protein explicitly [53]. However, the number of atoms in a protein molecule renders the computational burden prohibitively making these methods highly time consuming and expensive. [54, 55].

1.3 Protein Instabilities

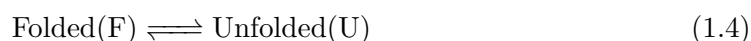
According to Remington [56], the stability of a pharmaceutical product may be defined as the capability to remain within its physical, chemical, microbiological, therapeutic, and toxicological specifications. To ensure patient safety, the drug stability needs to be investigated throughout the various processing steps and for the anticipated time period of storage (shelf life) [57]. Biomolecules are generally very sensitive to their microenvironment due to their complex and fragile structure [7]. Most recombinant proteins are prone to instabilities at elevated temperatures (e.g. cell cultivation), extreme pH values (e.g. virus inactivation), shear stress (e.g. pumping and stirring), and non-physiological salt concentrations (e.g. binding or elution in chromatography steps). Following the systemic administration, recombinant proteins are susceptible to degradation by endogenous proteases. [58]. Protein instabilities may result in a loss of function, changes in protein pharmacokinetics, and immunogenicity [10, 47, 59]. Manning et al. [60] subdivided protein instabilities further into chemical and physical instabilities. Chemical instabilities comprise processes in which covalent bonds are formed or broken resulting in new chemical entities. Protein-relevant chemical instabilities include proteolysis (peptide bond hydrolysis), deamidation, oxidation, and aspartate isomerization [7]. Physical instabilities are related to a change in the physical state of the protein without involving an alteration of the chemical protein composition and thus comprise conformational changes of the protein structure and colloidal changes (e.g. aggregation). [60] These physical changes are caused by the perturbation of intramolecular and intermolecular interactions forces. The

identification and assessment of suitable analytical tools for the detection and characterization of protein instabilities are of great importance for process control and formulation development. [61]

1.3.1 Conformational Stability

Thermodynamic Description of Protein Unfolding and Melting Point Determination

According to the thermodynamic hypothesis by Anfinsen [62], the native structure of a protein is stable under physiological conditions since it is in a global minimum of Gibbs free energy G [7]. Under non-physiological conditions, the folding is disturbed by changing molecular interactions favoring a transition from the native and biologically active 3D structure to an unfolded state. The physicochemical description of this transition is often based on the simplified two-state model



which assumes an equilibrium between these two distinct states and neglects any intermediate state of unfolding [63]. The Gibbs free energy G is defined as a function of the enthalpy H , the entropy S and the temperature T :

$$G = H - T \cdot S . \quad (1.5)$$

The change in in Gibbs free energy ΔG is described by

$$\Delta G = \Delta H - T \cdot \Delta S . \quad (1.6)$$

For the reaction 1.4 at 25°C in water, $\Delta G(H_2O)$ is defined as the conformational stability of the protein. Colloquially, the conformational stability describes how much more stable the folded conformation of a protein is relative to its unfolded state. [64]

The overall change in entropy S upon unfolding is due to the combined effect of the changing protein conformation and the resulting interactions with the surrounding water molecules. The native, folded state, is characterized by a low entropy, since all protein atoms are held in a well defined geometry by attractive intramolecular interactions. Upon unfolding, the conformational entropy of the protein increases since native interactions are lost and each amino acid residue can assume more degrees of freedom. The large

increase in entropy of the protein is, however, compensated by a decrease in entropy of the water in the system due to the hydrophobic effect. This effect causes water molecules to assume more ordered conformations in order to maximize their hydrogen bonds and to minimize the contact with non-polar side chains. This results in an entropy reduction of the solvent relatively to the folded state. [65] ΔH reflects the changes of energy due to the disruption of internal interactions within the protein molecule (hydrogen bonds, ionic salt bridges, and van-der-Waals interactions) and the hydration of the groups that are buried in the native state and become exposed to the solvent upon unfolding [66]. According to Eq. 1.6, ΔG depends on temperature. A temperature increase results in an increase of the entropy term. If T is sufficiently high, the entropy term becomes greater than the enthalpy term, resulting in a negative ΔG , and thus to a shift of the equilibrium to the unfolded state. The melting temperature T_m is described thermodynamically as the temperature at the equilibrium between the folded and the unfolded state and is hence the temperature at which $\Delta G=0$. T_m can therefore be mathematically described as

$$T_m = \frac{\Delta H(T_m)}{\Delta S(T_m)} . \quad (1.7)$$

Proteins with a higher melting point T_m are evaluated as conformationally more stable, since unfolding at higher temperatures suggests greater free energies of the native state [67].

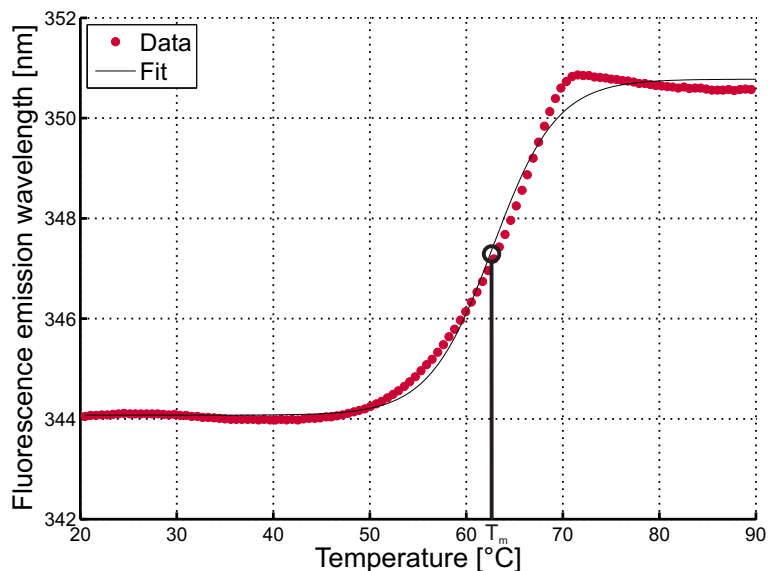


Figure 1.2: Melting curve of the serine protease Savinase[®] at pH 5.7.

Experimental approaches for the determination of T_m are based on the measurement of changes in different protein properties upon thermal unfolding. In this work, the change in intrinsic protein fluorescence is measured as observable variable. This analytical technique is based on the emission of light, occurring at wavelengths between 300 and 360 nm, when the delocalized electrons of aromatic amino acid residues (e.g. tryptophan) drop back to their initial state after being stimulated by laser light at 266 nm. Upon protein unfolding, the fluorescence spectrum shifts to red wavelengths due to a change in the vicinity of the hydrophobic tryptophan residues from the non-polar protein core to the polar environment [68, 69]. The plot of fluorescence emission wavelength against temperature results in a sigmoidal curve referred to as melting curve. The melting point T_m of the protein is defined as the inflection point of the melting curve. In Fig. 1.2, a sample melting curve is displayed for the serine protease Savinase[®] at pH 5.7.

FT-IR Spectroscopy for Secondary Structure Analysis

In order to further investigate conformational changes at the level of the secondary structure, Fourier transform infrared (FT-IR) spectroscopy is used in this thesis. In the 1960s Elliot and Ambrose showed that IR spectroscopy can be used to detect changes in the conformation of polypeptides and proteins [70, 71]. The absorption of infrared radiation

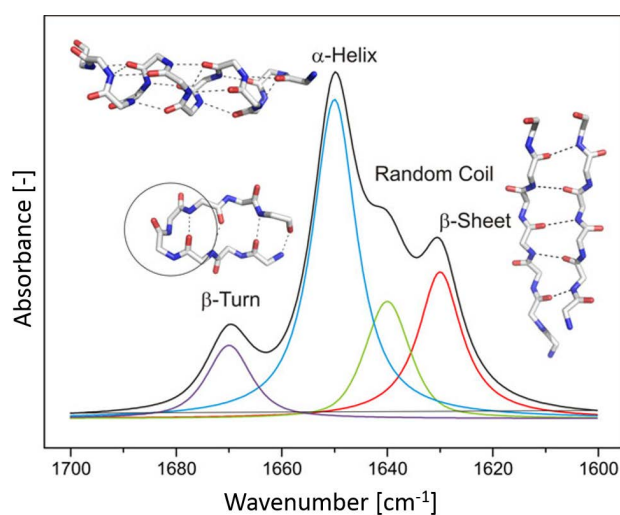


Figure 1.3: Illustration of the amide I band as superposition from overlapping secondary structure element bands [72].

excites vibrational transitions of molecules (primarily stretching and bending motions). The vibrational frequency and the absorption probability of covalent bonds depend on the polarity of the binding partners involved. In an FT-IR spectrum of proteins, there are nine characteristic absorption bands of which the amide I band is the most important one for secondary structure analysis. [26, 73] The amide I band appears in the wavenumber range of 1600 to 1700 cm^{-1} and is caused up to 80 % by the stretching vibrations of the carbonyl group (C=O) of the peptide bond [74, 75]. As already explained in section 1.1, the secondary structure of proteins is determined especially by hydrogen bonds between the functional groups of the peptide backbone. The carbonyl group functions as an acceptor for hydrogen bonding. The hydrogen bond involved in different secondary structure elements differ in length and thus in the strength. A change in the strength of a hydrogen bond leads to a change in the electron density of the C=O double bond. An increasing electron density of the C=O bond is associated with an increase in the vibrational frequency. The characteristic electron densities for the different secondary structural elements lead to characteristic absorption frequencies within the amide I band as displayed in Fig. 1.3. For this reason, changes in the secondary structure of a protein result in changes of the FT-IR spectrum. [74]

1.3.2 Colloidal Stability - Protein Solubility and Phase Behavior

Besides the conformational instabilities which indicate changes of native protein structure, undesired phase transitions may adversely affect the activity of a protein drug. The term phase refers to matter with a homogeneous chemical composition and spatially constant physical properties. The phase state of a protein depends on the surrounding system parameters and may change abruptly in case of variations. [76] Both in industrial purification and formulation process design, knowledge of the phase behavior of proteins is indispensable to avoid unwanted phase transitions as well as to exploit the potential of phase transitions as purification operation [77]. Commonly, protein phase behavior is determined and visualized by the generation of phase diagrams. Protein phase behavior is determined as a function of various parameters, e.g. protein concentration, precipitant (substance capable of inducing a phase transition) type and concentration, additional solutes, pH, and temperature. [78, 79] In Fig. 1.4, a schematic diagram of the phase states of a protein is displayed as a function of the protein concentration and the concentration of a precipitant. All other parameters, such as pH, temperature or the presence of addi-

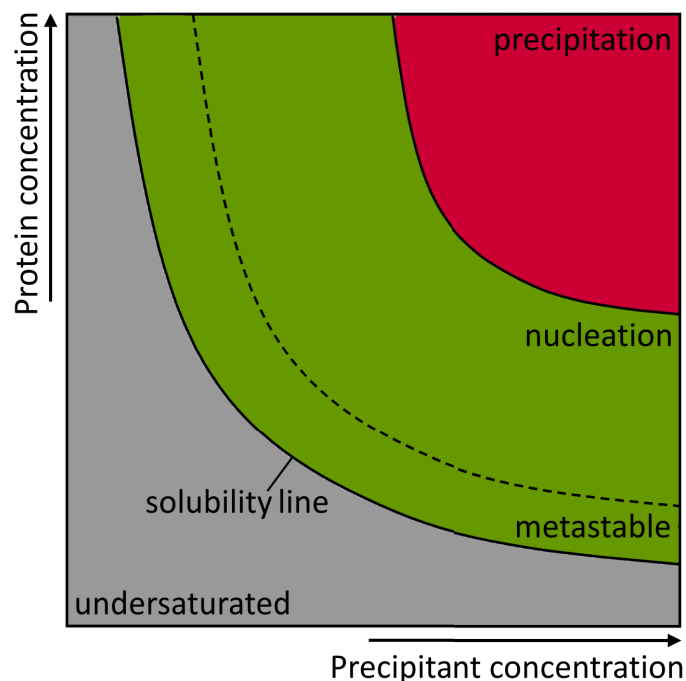


Figure 1.4: Schematic illustration of a protein phase diagram in dependency of protein and precipitant concentration according to [78, 80]. The solubility line separates the undersaturated zone (protein is completely dissolved) from the supersaturated zone where phase transitions (crystallization, precipitation, gelation) occur.

tives are kept constant. At low protein and precipitant concentrations, the protein is completely dissolved in the solvent forming a homogeneous liquid phase. This area is referred to as the undersaturated zone. The solubility line describes the amount of protein which can be dissolved at a given precipitant concentration until a thermodynamic equilibrium is reached [44]. System compositions above the equilibrium solubility result in protein aggregation. The term protein aggregation describes the assembly of native or non-native protein monomers to protein multimers, i.e. aggregation describes the formation of protein crystals, amorphous precipitates and gel-like structures [81, 82]. The driving force for this phase transition is a thermodynamic imbalance, which is also referred to as supersaturation. Depending on the kinetics of phase transition, the supersaturated area can be further divided into the metastable zone where no crystals are formed but existing crystals will grow, the nucleation zone which leads to crystal formation and growth and the precipitation zone [83].

1.3.2.1 Thermodynamic Description of Supersaturation

The thermodynamic parameter for the description of phase transitions is the chemical potential μ . The molar chemical potential $\tilde{\mu}$ of a component i in a real mixture is defined by

$$\tilde{\mu}_i = \tilde{\mu}_i^0 + RT \ln a_i \quad (1.8)$$

where $\tilde{\mu}_i^0$ is the molar chemical potential of component i in the standard state ($T=298.15$ K, $p=101.325$ kPa), R the universal gas constant, T the temperature and a_i is the activity (or effective concentration [47]) of component i [76, 84]. In contrast to the theory of an ideal mixture, the activity a_i takes into account interactions between the molecules of the different components in a real mixture. The activity is calculated according to

$$a_i = \tilde{c}_i \cdot \gamma_i \quad (1.9)$$

as the product of the molar concentration \tilde{c}_i of the component i and its activity coefficient γ_i [76, 85]. In ideal dilute solutions, the activity coefficient γ_i of the protein is unity and its effective concentration a_i is the actual concentration \tilde{c}_i [47].

As explained in section 1.3.2, the driving force for the formation of protein aggregates is the supersaturation. Thermodynamically, this is expressed by the difference between the chemical potentials of the component i in a supersaturated solution $\tilde{\mu}_i$ and the chemical potential of the component i in the saturated state $\tilde{\mu}_i^*$ [86]:

$$\Delta\tilde{\mu} = \tilde{\mu}_i - \tilde{\mu}_i^* = R \cdot T \cdot \ln \left(\frac{a_i}{a_i^*} \right) . \quad (1.10)$$

The supersaturation S_a is defined as the ratio of the actual activity of the solution divided by the activity at equilibrium. Using Eq. 1.9 S_a is defined as:

$$S_a \equiv \frac{a_i}{a_i^*} = \frac{\tilde{c}_i \cdot \gamma_i}{\tilde{c}_i^* \cdot \gamma_i^*} = \frac{c_i \cdot \gamma_i}{c_i^* \cdot \gamma_i^*} . \quad (1.11)$$

The measurement of activity coefficients for proteins poses a great problem because of their complex interactions in aqueous solutions [87]. Therefore, activity coefficients are often assumed to be the same resulting in a concentration-related supersaturation degree S_c [80]:

$$S_c = \frac{c_i}{c_i^*} . \quad (1.12)$$

1.3.2.2 Factors Influencing Protein Aggregation

Protein aggregation mechanisms depend on protein-protein interactions which are influenced by properties of the proteins themselves (e.g. conformation, surface charge distribution, hydrophobicity, and concentration), solution conditions (e.g. pH value, presence of additional solutes like salt ions, polymers, or additives) and physical processing parameters (e.g. temperature and mechanical stress due to shaking, pumping, stirring, freezing, and thawing). [25, 81, 88] A selection of these influencing parameters will be discussed in the following section.

Protein Conformation

Due to the presence of different folding states, the initial state of a protein monomer susceptible to aggregation may differ. Aggregation is either induced by natively folded protein monomers or by partially or completely unfolded protein monomers referred to as native and non-native aggregation, respectively [27, 89, 90]. For formulated protein therapeutics, in particular non-native aggregates were found to evoke immunogenic reaction as the formation of neutralizing antibodies or hypersensitivity responses such as anaphylaxis [59]. In aqueous solutions, non-native aggregates are induced mainly by hydrophobic interactions since hydrophobic amino acids are exposed upon protein unfolding [88].

Protein Concentration

Protein-protein interactions require some spatial proximity between protein molecules. In dilute protein solutions, intermolecular distances between molecules are comparably large. With increasing concentrations, the separation distance between the protein molecules decreases and the frequency of molecular collisions increases. [47, 91, 92] Due to smaller distances between the protein molecules, aggregation propensity increases due to electrostatic interactions, van-der-Waals interactions, hydrophobic interactions, hydrogen bonding [93, 94], and excluded volume effects [95]. The excluded volume originates from protein molecules occupying space and thereby excluding other molecules from their proximity. In solutions with increasing concentrations, the volume of solution available to added molecules is hence restricted. As a result, the effective concentration of macromolecules and thus macromolecular thermodynamic activities increase by several orders of magnitude favoring aggregation. [95, 96]

Solution pH

As illustrated in Fig. 1.5, the solubility of proteins strongly depends on the surrounding pH as the protein surface charges are altered. As displayed in Fig. 1.5A, the protonatable amino acids are predominantly charged alike (positively or negatively) for solution pH values in distance from the pI of the protein and therefore repel each other. Aggregation is prevented by the repulsion of the molecules and the protein remains in solution. Despite a net charge of zero, both positive and negative charges are present on the protein surface at the pI. The spatial orientation of the protein molecules is driven by the approximation of differently charged areas. Consequently, the level of electrostatic repulsion is minimal, while electrostatic attractions and hydrophobic interactions are favored enhancing protein aggregation. As a result, the solubility of a protein is minimal at its pI (Fig. 1.5B).

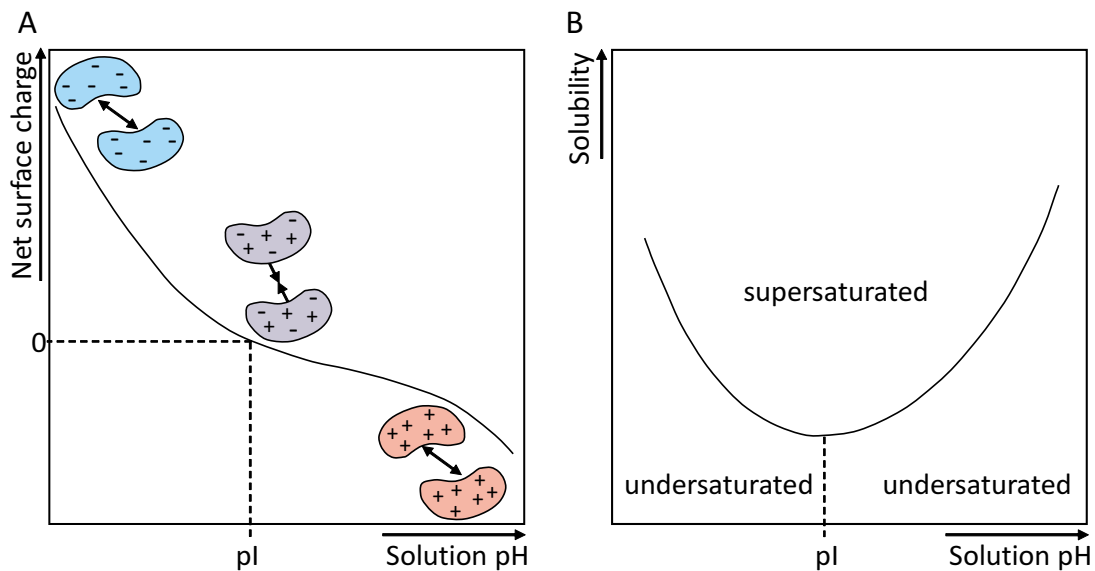


Figure 1.5: Surface net charge of a protein in dependence of the pH value (A). At the isoelectric point (pI) the surface net charge is zero resulting in a solubility minimum (B).

Salts

The effects of salt ions on the aggregation behavior of proteins can be classified into two types, that are non-specific and specific effects. The non-specific salt effects are simply due to their ionic properties leading to charge shielding by the formation of an electrochemical double layer. At higher salt concentrations (>0.1 M [97, 98]), salts exert specific effects depending on the type of salt. [25, 99] Salt ions have different sizes, hydration properties,

and polarizabilities and thus have different effects on protein-interactions. In 1888, Franz Hofmeister ordered salts empirically according to their ability to precipitate proteins. The resulting Hofmeister series can be divided into kosmotropic ions which decrease the protein solubility (salting-out) and chaotropic ions enhancing protein solubility (salting-in). [100] Several theories have been developed to understand the Hofmeister series, including preferential interaction theory introduced by Arakawa et al. [101, 102]. This theory, describes intermolecular interactions between proteins, co-solutes and the solvent. In a ternary system of protein molecules, water molecules and salt ions, water molecules and salt ions compete for the surface of the protein with the protein being preferably surrounded by one molecular species. Salt ions are classified into ions preferential binding to proteins and ions preferential excluded from the protein surface [102]. Polar and strongly hydrated ions tend to interact strongly with water molecules and are preferentially excluded from the protein surface. As a result, the ‘structuring of water’ is increased and the protein solvation shell is stabilized. For high salt concentrations, however, the salt competes with the protein for water molecules favoring the exposure of hydrophobic surface areas and thus aggregation. Non-polar and weakly hydrated ions tend to preferentially interact with the protein thereby partially replacing the water molecules in the solvation shell of the protein. These ions exert weak interactions with surrounding water molecules and reduce the ‘structuring of water’ resulting in a solubility increase [98, 103].

1.3.2.3 Experimental Methods to Determine Protein Solubility and Phase Behavior

There are various approaches described in literature to experimentally determine the protein phase behavior. In Fig. 1.6, the most frequently used approaches are displayed schematically. The equilibrium solubility may either be approached from an undersaturated or a supersaturated protein solution [80]. Starting from an undersaturated solution, the protein concentration is increased by the addition of pure, lyophilized protein until the solubility limit is reached (see Fig. 1.6 A) . This technique often requires large amounts of highly pure protein. [80, 104] Instead of dissolving more protein, the protein concentration can also be increased by the reduction of solvent (see Fig. 1.6 B) [105]. In this case, the solution reaches the equilibrium by forming a second phase, whereas the protein concentration in the supernatant converges to the solubility value. For this experimental approach, the protein concentration must reach at least the crystallization range since no spontaneous phase transition occurs in the metastable region. A popular method for

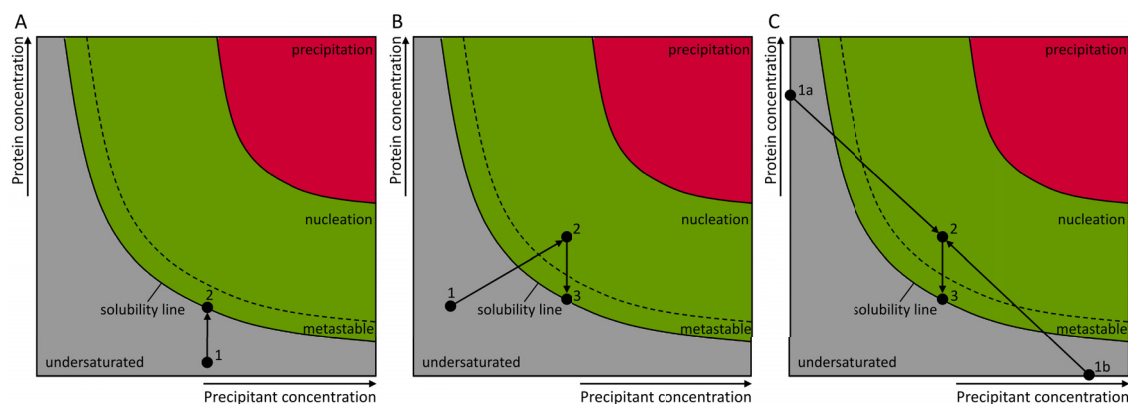


Figure 1.6: Experimental approaches to determine protein solubility and phase behavior.

concentrating protein solutions for solubility determination is the vapor diffusion technique using either sitting or hanging drops. The drop is equilibrated against a reservoir that contains a higher concentration of precipitant than the protein solution. The two solutions are connected by a gas phase, but sealed from the environment. Due to the resulting vapor pressure gradient, water diffuses from the drop to the reservoir leading to a volume decrease of the protein drop. As a consequence, protein and precipitant concentration in the drop increase until the phase transition occurs. In vapor diffusion experiments, conditions in the protein solution change throughout the equilibration process and protein as well as precipitant concentration where phase transition occurs cannot exactly be determined. A better control over the phase transition conditions can be achieved in batch experiments (see Fig. 1.6 C). An undersaturated protein solution is mixed with a protein-free precipitant solution and sealed from the environment. If the mixing point is in the two-phase region, a phase transition occurs and the concentration in the supernatant approaches the equilibrium concentration. [78, 106, 107] Baumgartner et al. [79] developed an experimental high-throughput approach to generate protein phase diagrams and determine protein solubilities on an automated liquid handling station. This method is characterized by its low sample consumption and high accuracy and is therefore used in this thesis.

1.4 Stabilization Strategies for Biopharmaceutical Proteins

Due to the previously described protein instabilities, enhancing the robustness of functional biomacromolecules is of major importance in biotechnology [108]. Stabilization of

proteins can be accomplished either by modifying the environmental conditions or by modifying the protein itself. Influencing the environment is realized by the adjustment of process and formulation parameters such as pH value, ionic strength and the addition of formulation additives. Moreover, polymeric drug-delivery vehicles are used to incorporate the protein in a favorable environment. The chemical modification of the product itself may be carried out prior to expression, cultivation and purification by alteration of the amino acid sequence (direct evolution/mutagenesis) [109] or subsequent to production and purification by post-translational modifications.

1.4.1 Additives

Solution additives are applied in the biopharmaceutical industry to control protein folding, stabilize proteins against unfolding and aggregation, increase solubility, reduce surface adsorption or to simply provide physiological osmolality [110, 111]. The stabilizers encompass a wide variety of molecules, of which osmolytes and the polymer polyethylene glycol (PEG) are studied in this work. Osmolytes are low molecular weight substances, which have been found to regulate the osmotic pressure and form part of the milieu for the biochemical reactions in all cells of bacteria, plants and animals. [107, 112–114] Some of these substances were found to stabilize the native protein structures in the bacterial cells upon environmental stress [114]. Among them are, for example, polyols such as glycerol, polysaccharides such as dextrans, sugars such as trehalose and sucrose, or amino acids such as arginine, glycine and L-glutamic acid [115–117]. Steric effects and a reduction of attractive intermolecular protein-protein interactions due to preferential interaction of the protein by either water or osmolyte are the two most common explanations for the effect of these molecules [111, 117, 118]. Due to their stabilizing effects, many of these osmolytes are used for the production of biopharmaceuticals [25, 119, 120]. For PEG, the mode of action is strongly influenced by its molecular weight [121] and concentration [122]. At low PEG molecular weights and concentrations, protein stabilization may be induced by steric shielding of attractive protein-protein interactions. At high PEG molecular weights and concentrations, however, protein destabilization occurs. This phenomena is due to the steric exclusion of the protein molecules from the regions of the solvent occupied by PEG molecules. As a result, the proteins are concentrated and precipitate as soon as the solubility limit in the non-excluded volume is exceeded. [95, 120, 122, 123]

Despite their diverse use in the biopharmaceutical industry, the underlying mechanisms

by which solution additives stabilize proteins are not yet fully understood. It is therefore of great interest to investigate the causes of their effect more closely. Moreover, the development of a fast, automated and reproducible strategy for the identification of suitable additives is indispensable for the formulation development [7]. Along with an estimation of protein stabilization, a careful consideration is needed regarding local toxicity and potential immunogenicity of these additives [120].

1.4.2 Protein Conjugation

Besides altering the chemical environment of a protein, the modification of the product itself is another approach to protein stabilization. One form of protein modification involves the covalent attachment of non-protein molecules to the protein. This process is referred to as protein conjugation. For biopharmaceutical proteins, the covalent attachment of biocompatible and water-soluble polymers has been found to increase the stability and extend the in vivo half-life [124, 125]. The aim of protein conjugation is to create hybrid molecules with a unique combination of properties derived from both biological and synthetic materials [58, 126]. The protein gives the hybrid molecule the biological activity with a high specificity for a reaction at low temperatures and concentrations. Synthetic polymers exhibit higher stabilities against thermal and chemical influences. Furthermore, polymer chemistry allows the incorporation of desired functional groups and thus enables the hybrid molecule to react to biological and non-biological stimuli. [126, 127]

The creation of such hybrid materials requires efficient chemical pathways to specifically couple proteins to polymers. The functional side groups of the amino acids cysteine (Cys), lysine (Lys), tyrosine (Tyr) and glutamine (Gln) as well as the N-terminus of the peptide backbone offer naturally occurring reaction partners for the chemical modifications [127, 128]. For the covalent binding to these amino acids, various reactive groups may be introduced into the polymer. The most frequent conjugation strategies are shown schematically in Fig. 1.7.

In this thesis, the very efficient reaction of polymer-aldehydes and N-hydroxysuccinimide (NHS) activated polymers to the ϵ -amine group of lysine (Lys) is exploited. Both of these amine-modifying methods result in multi-conjugation as many proteins have several surface-available lysine residues. For conjugated proteins, a distinction is made between the degree of conjugation (indicating the number of bound polymer molecules) and diffe-

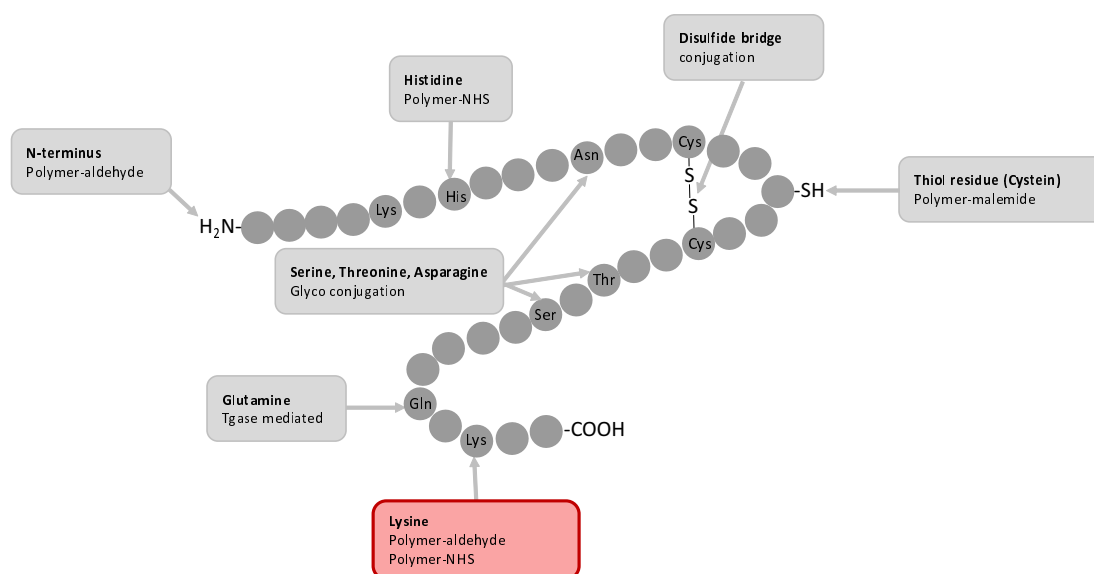


Figure 1.7: Natural occurring attachment sites for protein conjugation. Illustration adapted from [129].

rent isoforms (specifying the binding site). Both conjugation degree and isoform distribution influence the physicochemical and biological properties of the resulting mixture. For this reason, separation of the differently conjugated species is necessary after the reaction. [130] The desire to circumvent this additional process step raised considerable research efforts on side-specific conjugation reactions in order to install a single polymer chain at a defined protein site [131, 132].

1.4.2.1 PEGylation

First attempts to protein conjugation were undertaken in the 1970s by Davis and Abuchowski [133, 134] using the polymer polyethylene glycol (PEG). PEG consists of covalently linked ethylene oxide (EO) monomers having a molecular weight of 44 Da per monomer [58]. In their studies, Davis and Abuchowski observed a prolonged half-life in the circulatory system and a reduced immunogenicity of PEG-modified proteins compared to the native form. Since then, coupling of PEG chains to a therapeutic molecule (PEGylation) has emerged to a well-established technology with significant therapeutic value [126, 135]. In 1990, a PEGylated form of adenosine deaminase, Adagen[®] (Enzon Pharmaceuticals, USA), was the first conjugated protein to be approved by the FDA [136]. By now, a total of 12 PEGylated products are in clinical practice [137], includ-

ing the blockbuster drugs PegIntron[®] (Schering-Plough, USA), Pegasys[®] (Hoffman-La Roche, USA), Neulasta[®] (Amgen, USA), and Mircera[®] (Hoffman-La Roche, USA) [136, 138].

The overwhelming gain from PEGylated biopharmaceuticals arises from their altered physicochemical properties [58]. Due to the high hydration of PEG, PEGylated proteins have a significantly greater hydrodynamic radius than unmodified proteins with a comparable molecular weight [139, 140] resulting in a reduced systemic clearance [129]. An enhanced in vivo half-life leads to less frequent administrations thus increasing patient's convenience. Furthermore, the polymer modification provides steric shielding of protein surface properties and thus changes molecule interactions. As a result, recognition by the patient's immune system, digestion by endogenous enzymes [141], and toxicity of the drug are reduced. Another positive aspect of PEGylation may comprise a reduced aggregation propensity which is explained with masked hydrophobic patches on the protein surface by attached hydrophilic PEG. In contrast to these improvements, the conjugation may evoke changes in the drug activity by changing the native conformation, sterically interfering or altering binding properties [142]. Parameters influencing the properties of the conjugate include the type of polymer (chemistry, linear vs. branched [140]), the molecular weight of the polymer and the conjugation degree as well as the isoform distribution. A careful consideration and combination of these parameters allows for fine-tuning the properties of the conjugated drug product.

From the perspective of process development, despite almost 40 years of research and application of PEGylated proteins, there are still issues concerning purification, process control and characterization of protein conjugates. The attachment of the PEG molecules increases the heterogeneity of the resulting drug product increasing the need for sophisticated analytical techniques [125]. The analytical tasks to be fulfilled include, identification and quantification of conjugated species with different number of bound polymer molecules and their characterization with regard to their physical stabilities under process-relevant conditions. In order to reduce material consumption and shorten development times, those methods require automated processing of low sample volumes. In addition, computer-based (*in silico*) methods are a helpful tool for the cost-effective development of purification processes as well as for understanding of the underlying physical principles [143]. The parameters estimated by experimental and *in silico* approaches can be used for process up-scaling, process optimization, and process control.

1.4.2.2 Alternative Polymers for Protein Conjugation

While PEG remains useful for the modification of therapeutic proteins, some limitations in its clinical use have begun to emerge driving the development of alternatives. Discussions about these potential drawbacks include antibody formation against PEG (anti-PEG), hypersensitivity to PEG and vacuolation in various tissues upon repeated exposure [126, 144]. From a processing point of view, standard linear PEG is commonly prepared by anionic polymerization of EO, a sensitive and expensive process [145]. Novel monomers and new controlled polymerization techniques permit to extend the therapeutic use of protein-polymer conjugates. Controlled radical polymerization techniques such as reversible addition-fragmentation chain transfer (RAFT) polymerization [146] are the means of choice as they allow for the introduction of various functional endgroups, the strict control over polymer molecular weight and a narrow molecular weight distribution [126]. Since PEG is up to now the only FDA-approved polymer for bio-conjugation, these alternative polymers must be thoroughly investigated from a process-based, clinical, and regulatory perspective before being approved for use in humans.[147] Moving beyond therapeutical applications, the coupling of novel polymers to proteins opens up new application fields for technical hybrid systems including biosensing and diagnostics as well as biocatalysis [148].

1.5 Mechanistic Chromatography Modeling

In case of random conjugation, the existence of multiple binding-sites and the resulting heterogeneous product mixture necessitates a post-modificational purification of the resulting conjugate species. Ion-exchange chromatography (IEX) is one of the most frequently used purification methods for conjugated proteins [129, 130]. In case of IEX, the surface of the adsorber particles is functionalized with charged ligands facilitating the separation of protein molecules according to differences in charge. For protein conjugates, Seely and Richey [149] proposed the ‘charge-shielding effect’ which explains a decrease in binding strength and thus retention time [150] with increasing conjugation degree due to weakened electrostatic interactions.

The development and optimization of chromatographic separation processes is nowadays either based on experimental or model-based approaches. Mechanistic modeling and numerical simulations permit to reduce the number of experiments and thus costs during

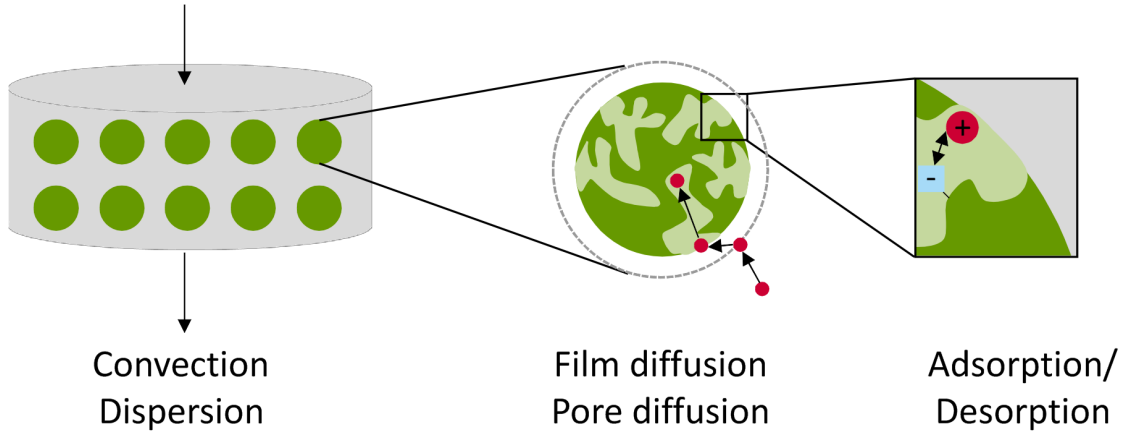


Figure 1.8: Mass transfer and adsorption/mechanisms determining chromatographic separation of proteins. Illustration adapted from [151].

process optimization by *in silico* predictions [143, 151]. Based on the mathematical description of the underlying physical processes, mechanistic modeling additionally allows to estimate experimentally inaccessible parameters. In order to quantitatively describe the behavior of protein species during the separation process by mathematical equations, an understanding of the underlying physical processes in the column is necessary [152]. Those physical effects are schematically displayed in Fig. 1.8. During chromatographic separation, a solution containing a mixture of proteins that are to be separated (mobile phase) is pumped through a packed bed of porous adsorber particles (stationary phase). The relevant mass transfer processes on the macroscopic column level are convection due to the forced fluid flow and dispersion. The environment surrounding a single particle in the packed bed is thought to be a film in which the mobile phase is stagnant. The mass transfer from the bulk phase through the film layer to the outermost edge of the particle is purely diffusive and is denoted as film diffusion. The actual separation takes place on the surface of the adsorber particles where the protein molecules interact with the ligands. To improve the performance of adsorbers, the particles have a high porosity increasing the total available surface area. Inside the pores, the proteins are transported via pore diffusion. This process is frequently the rate-determining process of a chromatographic separation.

In literature, several models to describe fluid dynamics, mass transfer and adsorption/desorption phenomena have been suggested, of which a comprehensive summary is provided in the text books by Schmidt-Traub et al. [151] and Guiochon et al. [153]. In this thesis, the general rate model (GRM) is used to describe fluid dynamics and mass transfer phe-

nomena as it includes axial dispersion as well as resistance to external and internal mass transport [152]. The GRM includes two mass balance equations for a component i , one for the inter-particle phase (Eq. 1.13) and one for the inner-pore phase (Eq. 1.14):

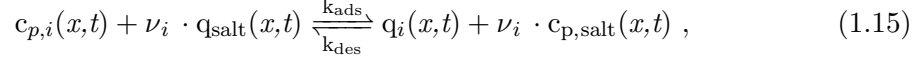
$$\underbrace{\frac{\partial c_i(x, t)}{\partial t}}_{\text{change of bulk concentration}} = \underbrace{-u(t) \frac{\partial c_i(x, t)}{\partial x}}_{\text{convective transport term}} + \underbrace{D_{ax} \frac{\partial^2 c(x, t)}{\partial x^2}}_{\text{axial dispersion term}} - \underbrace{\frac{1 - \varepsilon_b}{\varepsilon_b} k_{film, i} \frac{3}{r_p} (c_i(x, t) - c_{p, i}(x, t))}_{\text{mass transfer term}} \quad (1.13)$$

$$\frac{\partial c_{p, i}(x, t)}{\partial t} = \begin{cases} \frac{1}{r^2} \frac{\partial}{\partial r} (r^2 D_{p, i} \frac{\partial c_{p, i}(x, t)}{\partial r}) - \frac{1 - \varepsilon_p}{\varepsilon_p} \frac{\partial q_i(x, t)}{\partial t} & \text{for } r \in (0, r_p), \\ \frac{k_{film, i}}{\varepsilon_p D_{p, i}} (c_i(x, t) - c_{p, i}(x, t)) & \text{for } r = r_p, \\ 0 & \text{for } r = 0. \end{cases} \quad (1.14)$$

Eq. 1.13 describes the change of the bulk concentration $c_i(x, t)$ of a component i in the inter-particle phase at a position x in a column of length L dependent on the time t . Term 1 in Eq. 1.13 describes the convective transport influenced by the flow velocity of the mobile phase u in the inter-particle phase. The middle term describes hydrodynamic dispersion in axial direction by the axial dispersion coefficient D_{ax} . Hydrodynamic dispersion is mainly influenced by the quality of column packing. The last term describes the transition of molecules from the bulk phase having the concentration c_i to the pore phase having the concentration $c_{p, i}$. In Eq. 1.13, ε_b is the bed porosity, $k_{film, i}$ the film diffusion coefficient referring to the mass transfer over the film layer and r_p the particle radius. Eq. 1.14 describes the exchange between the pore volume concentration $c_{p, i}(x, t)$ and the stationary phase q_i depending on the particle porosity ε_p and the component-specific pore diffusion coefficient D_p along the radial pore position r within the particle. [154]

A thermodynamic adsorption model is used to describe the mass transition from the pore phase to the surface of the adsorber. In this thesis, the semi-mechanistic steric mass action (SMA) isotherm introduced by Brooks and Cramer [155] is used. The underlying assumption is that in IEX the proteins and the salt ions compete for the available ligands on the stationary phase. The adsorber is characterized by the total ionic capacity Λ which is the total ligand concentration on the adsorber surface. Proteins are charac-

terized by a specific number of characteristic binding charges ν_i which are involved in binding. According to the reaction



a protein displaces an equal amount of counter ions from the adsorber surface upon adsorbing to the ion exchange resin. In Eq. 1.15, q_{salt} and $c_{p,\text{salt}}$ are the concentration of the salt ions adsorbed and in solution inside the pore, respectively and k_{ads} and k_{des} the rate coefficients of adsorption and desorption, respectively. In addition, proteins cover binding sites without direct electrostatic interactions by steric shielding due to their molecular size. Therefore, the SMA model includes the steric shielding factor σ_i . For protein conjugates, this phenomenon is important because of the dynamic polymer layer and the resulting increased hydrodynamic radius [130, 139] reducing the apparent binding capacity in the non-linear range of the isotherm (overloaded state). According to Nilsson et al. [156], the kinetic formulation of the SMA isotherm for k protein species is:

$$k_{\text{kin},i} \frac{\partial q_i(x,t)}{\partial t} = \underbrace{k_{\text{eq},i} \left(\Lambda - \sum_{j=1}^k (\nu_j + \sigma_j) q_j(x,t) \right)^{\nu_i} c_{p,i}(x,t)}_{\text{adsorption-promoting}} - \underbrace{c_{p,\text{salt}}(x,t)^{\nu_i} q_i(x,t)}_{\text{desorption-promoting}} \quad (1.16)$$

Eq. 1.16 reproduces the influence of the counter-ion concentration $c_{p,\text{salt}}$ on the adsorption/desorption kinetics of the proteins. The equilibrium of adsorption/desorption is described by the adsorption equilibrium coefficient $k_{\text{eq},i} = k_{\text{ads},i}/k_{\text{des},i}$ and the velocity of the reaction by the coefficient $k_{\text{kin},i} = 1/k_{\text{des},i}$. The salt concentration in the stationary phase is described by

$$q_{\text{salt}}(x,t) = \Lambda - \sum_{j=1}^k \nu_j q_j(x,t) \quad (1.17)$$

as a function of proteins bound to the adsorber surface. $q_{\text{salt}}(x,t)$ equals the number of salt ions still attached to the adsorbent surface.

In this thesis, the resulting system of differential equations is solved numerically using the simulation software ChromX (GoSilico, Germany). The system parameters required for a numerical solution are accessible experimentally. This involves the determination of

the bed porosity ε_b and the axial dispersion coefficient D_{ax} by the injections of non-pore-penetrating tracer solutions, the particle porosity ε_p by the injection of pore-penetrating tracer solutions as well as the total ionic capacity Λ by acid-base titration [157]. For proteins, the individual parameters are estimated in calibration runs by minimizing the discrepancy between measurement and the simulation. This approach is called inverse modeling. Finally, the parameters are verified by an external set of validation runs. [158]

1.6 Hydrogels as Drug Delivery Systems

According to Webster et al. [159], a drug delivery system (DDS) is defined as device to introduce an API into the body. The main goal in the development of DDSs is to deliver the intact drug at the intended site of action in cells and tissues at a controlled rate. It is desirable to develop controlled release formulations and devices that can maintain a desired blood plasma level of the drug over an extended period of time avoiding frequent administration [1]. In this context, polymeric carrier materials have developed as a basis for the accommodation and delivery of a variety of drugs [160–163]. Particularly three-dimensional crosslinked networks of hydrophilic polymers are suitable for the use in DDSs since they swell without dissolving to a multiple of their volume in an aqueous environment forming a so called hydrogel [164]. Due to their high water content and porous structure, hydrogels provide a physiochemical similarity to the native extracellular matrix and thus a favorable and mechanically supportive environment for proteins [161, 165]. Hydrogels can be synthesized from a single species of monomers (homopolymers) or from a mixture of two or more different monomer species (copolymers) [166]. The applied polymeric materials need to be biocompatible and cannot cause any immunological reaction [163, 167]. Synthetic polymers often used for the synthesis of hydrogels for protein delivery include polyethylene glycol-diacrylate (PEG-DA), poly(vinyl alcohol) (PVA), polylactic acid (PLA), polyacrylamide, (meth)acrylic acid, and polyvinylpyrrolidone (PVP) [168, 169]. In addition to the choice of polymer, the hydrogel will be defined by the mode of crosslinking, the molecular weight of the polymer, the initial monomeric content and the presence of crosslinkers. The chemical composition of the hydrogel defines the physiochemical properties such as porosity, swelling behavior, mass transport profiles, and mechanical stability. [161, 170] DDSs can be classified according to the mechanism that controls the release of the therapeutic ingredient. The release is either diffusion controlled (reservoir systems and matrices, e.g. transdermal patches or drug-loaded stents [171]), chemically controlled (bioerosion or biodegradation) or responsive/-

solvent controlled (swelling, osmosis, change of intermolecular interactions) [1, 164, 172]. The multiplicity of factors affecting the drug delivery result renders the engineering of hydrogel-based drug delivery system with specified responses to particular stimuli challenging.

1.7 3D Printing to Synthesize Photopolymerized Hydrogels

Three-dimensional (3D) printing is an additive manufacturing technique in which three-dimensional objects are created by applying material in thin layers. For this purpose, 3D models are first designed with a computer-aided design (CAD) software and then converted into a vector-based machine code (G-code). This technique enables precise manufacturing of highly complex components with an arbitrary design and sophisticated internal features that are impossible to fabricate by conventional manufacturing processes. Moreover, it is an automated approach that offers a pathway for scalable and reproducible production. [83, 173, 174] Bioprinting is a subset of 3D printing in which 3D objects are built up from biological or biocompatible materials [175]. For biopharmaceutical applications, 3D printing represents an elegant tool to fabricate custom-tailored protein delivery systems with individualized dosage and accurate control of the desired release profile [176, 177]. In the field of medicine, 3D printing enables the production of personalized applications ranging from medical devices to implants and prostheses [178]. Previous printing successes for various types of human tissue nourish the vision of artificial human organs [175].

There are different 3D bioprinting techniques, which can be grouped into extrusion-based printing, inkjet-based printing and laser-based printing [173, 179]. In this thesis, a 3D printing technology called digital light processing (DLP) is used. This process is related to the laser-based stereolithography (SLA) patented by Charles W. Hull in 1986. The basis of both techniques is photopolymerization in which a light-sensitive photoinitiator is cleaved into free radicals by irradiation with light of a certain wavelength leading to the crosslinking of the monomer precursor [180]. In the case of SLA, only the area which forms the cross-sectional area of the 3D object in this specific layer is selectively exposed by a focused laser beam leading to a spatially defined curing of the monomer precursor. After one layer is finished, the printing object is coated with a fresh layer of uncured precursor and the process is repeated until the 3D object is built [181]. DLP uses a conventional light source to project an entire layer of the model to be printed, which makes

it faster than the laser-based SLA [182].

In this work, DLP is used to crosslink PEG-DA-based hydrogels to 3D objects. The reaction mechanism of the radical polymerization is displayed in Fig. 1.9. At first, the reaction is initiated by the formation of a free methyl radical due to the irradiation of the photoinitiator. The resulting radical attacks the carbon-carbon double bond of PEG-DA thus creating a PEG-DA radical. During the propagation step, the chain length and crosslinking density increases by reactions of a radical with a carbon-carbon double bond of the forming network. The chain propagation is terminated by the reaction of two radicals.

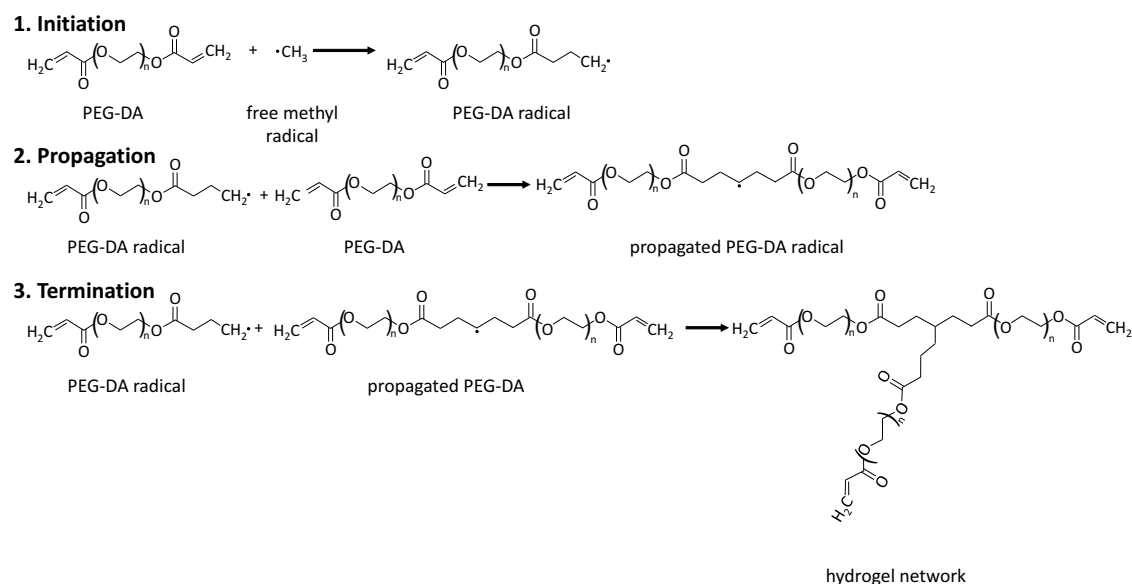


Figure 1.9: Reaction mechanism of photopolymerization of PEG-DA for the formation of a crosslinked hydrogel network. Illustration adapted from [167, 183].

Research Proposal

Protein drugs (biopharmaceuticals) offer unique opportunities and give hope for treating and healing severe diseases. The functionality and high selectivity of proteins for molecular targets in the human body is due to their complex three-dimensional structure. As previously described, the structure of proteins depends on various intra- and inter-molecular interactions. Both technical production of proteins and their integration into polymeric drug delivery systems may require conditions which influence molecular interactions and thus promote protein instabilities and functional loss. In addition to structural instabilities [184], the low solubility and the unwanted formation of protein aggregates are identified as a key challenge [185, 186]. Methods to stabilize the native protein structure as well as to selectively manipulate protein aggregation behavior are crucial to the development and manufacturing of safe and efficient drug products. Accordingly, the question arises of suitable stabilization strategies and their implementation in development and production of therapeutic proteins.

In recent years, various strategies have been studied to overcome the protein stability issue. Manipulation of protein-protein interactions through the addition of additives is reported as effective [110]. Especially, some uncharged sugars, polyols, and free amino acids as well as biocompatible polymers have shown to stabilize the proteins' native state and to reduce aggregation propensity [113, 116]. The addition of solution additives offers the advantage of simplicity since the components solely need to be dissolved and no additional process step is required. In addition, different additives can be combined in any ratio. However, the mechanisms underlying stabilization are not yet fully understood. Therefore, suitable solution additives are often identified in trial and error experiments, which are time and material consuming. Against this background, the first subsection of this work is devoted to the development and implementation of an automated, reproducible and efficient methodology for assessing the effect of solution additives on protein

stability. In order to gain a deeper understanding of how the investigated additives stabilize proteins, this study focuses on an integrated examination of protein conformation and aggregation.

The success of solution additives as protein stabilizers have led to the idea of covalently binding those stabilizers to the protein. The resulting stabilization strategy is entitled protein conjugation. Protein conjugation has the benefit that the stabilization is not solely based on interactions and can thus be maintained under changing process conditions. Moreover, the covalently bound molecule can be functionalized imparting additional properties to the protein molecule. In the pharmaceutical industry, the most prominent example is the covalent attachment of polyethylene glycol (PEGylation) [187]. In order to avoid additional and complex modifications of the target protein, polyethylene glycol (PEG) is most commonly attached to the naturally occurring surface amino acids in random conjugation reactions. Since the individual amino acids occur repeatedly in a protein, this approach results in a heterogeneous product mixture of molecules with different number (conjugation degree) and position of bound polymers. For the regulatory approval of conjugated protein drugs, the authorities require an extensive characterization concerning the distribution of different conjugate species. The second part of this work hence deals with the development of a fast analytical method to investigate the conjugate distribution in PEG-protein mixtures with low sample consumption. The distribution of different conjugate species is mainly influenced by reaction conditions. The developed analytical method is used to optimize the latter.

The different conjugate species have shown to differ significantly in their physicochemical properties [133, 139]. The third part of this study aims to investigate the potential of PEGylation for the stabilization of the protein conformation and for enhancing solubility. Increasing protein solubility is of great interest to the biopharmaceutical industry as it allows the development of highly concentrated protein formulations. In a systematic study, the influence of PEG molecular weight and conjugation degree is examined. In the fourth part, the method developed for PEGylated proteins are applied to alternative polymers. The desire for alternative polymers for protein conjugation is driven by several ideas. On the one hand, clinical limitation of PEGylated proteins emerged including antibody formation against PEG (anti-PEG), hypersensitivity and vacuolation in various tissues upon repeated exposure. On the other hand, the synthesis of activated PEGs with narrow dispersity is complex and therefore expensive. The development of protein conjugates with lower-cost polymers having similar advantages as PEG would increase the availability of stable biopharmaceuticals to a broader mass of the population. Finally, the use of different monomers allows for a variation in protein functionalization with regard

to specific applications.

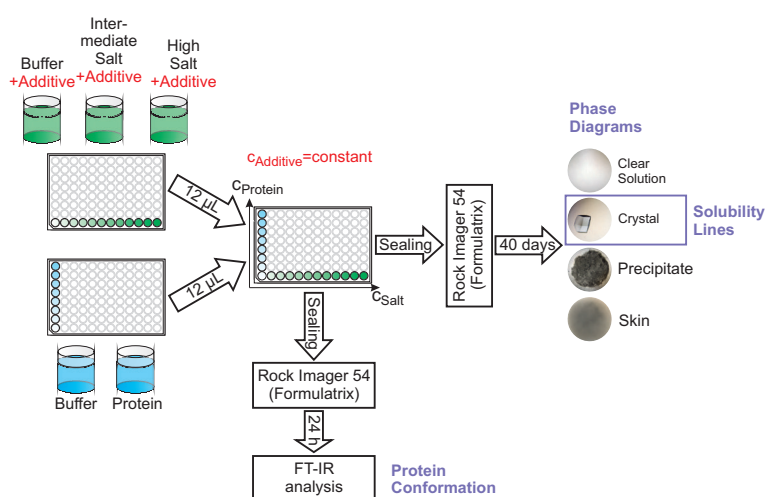
Due to the different properties of the conjugates, methods for the separation of the individual molecules on a production scale are required. Ion-exchange chromatography (IEX) is among the most frequently used purification methods for conjugated proteins. Purification processes are typically developed and optimized in small-scale experiments. However, transfer of laboratory methods to the production level (scale-up) is not straightforward and remains largely empirical [188]. To address this issue, the purification process must be characterized by key parameters which are independent of the equipment used. For a chromatographic separation, this can be realized by determining mass transfer and adsorption parameters. In this context, mechanistic chromatography modeling provides an excellent tool to obtain these parameters with a low number of experiments and is hence applied in the fifth part of this thesis to describe PEGylated proteins in IEX.

In addition to the use as solution additive and for protein conjugation, PEG can also be functionalized to form three-dimensional, highly crosslinked and biocompatible networks. Due to their high water content and the porous support structure, these networks (hydrogels) provide a protective environment for proteins. Protein-hydrogel interactions are influenced by the highly complex physical and chemical properties of the hydrogel, the surrounding solution conditions and the protein itself. In the last section of this thesis, an automated, reproducible and efficient methods for the evaluation of hydrogels for biopharmaceutical purposes is presented. This method involves crosslinking the hydrogel precursor with a 3D printer. The results of this study are intended to provide an insight into whether hydrogels are applicable in the context of the emerging field of 3D bioprinting. The long-term goal is to produce three-dimensional objects with arbitrary geometries from functional and technically relevant hybrid materials having both biological and polymer properties.

Comprehensive Overview of Publications & Manuscripts

1. Manipulation of Lysozyme Phase Behavior by Additives as Function of Conformational Stability

Lara Galm, Josefine Morgenstern and Jürgen Hubbuch



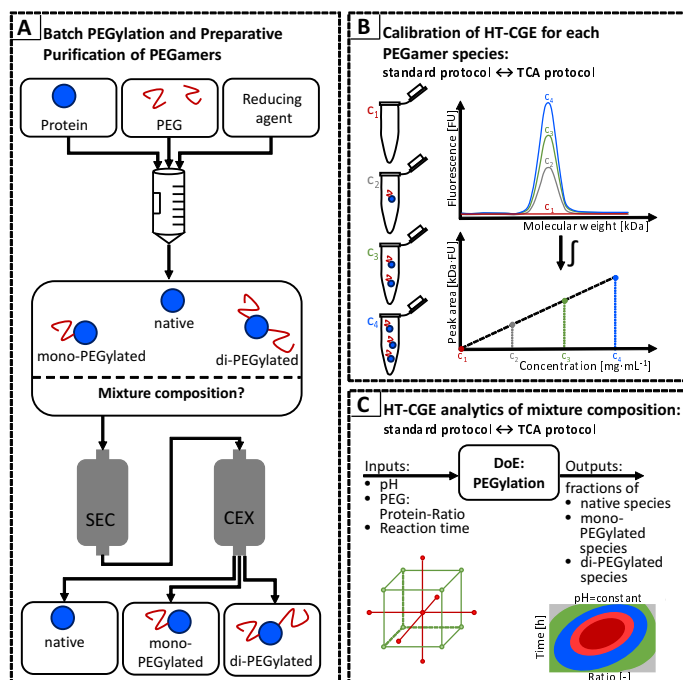
The potential of selected solution additives, namely glycerol, PEG 1000 and glycine for the stabilization of lysozyme from chicken egg white was investigated in this study. For this purpose, a combination of automated generation of protein phase diagrams on a liquid handling station and sec-

ondary structure analysis using Fourier transform infrared spectroscopy (FT-IR) was used. The effect of the additives on solubility as well as crystal size and morphology was investigated by the protein phase diagrams. It was shown that the influence of the additives on the lysozyme phase behavior and the equilibrium solubility depends on the solution pH. The pH dependent impact was explained by differences in the conformational stability of lysozyme. Of the investigated additives, glycerol and PEG 1000 stabilized the native protein conformation while glycine destabilized it.

International Journal of Pharmaceutics 494/1 (2015): 370-380.

2. Quantification of PEGylated Proteases with Varying Degree of Conjugation in Mixtures: An Analytical Protocol Combining Protein Precipitation and Capillary Gel Electrophoresis

Josefine Morgenstern, Markus Busch, Pascal Baumann and Jürgen Hubbuch



In this article, the development of a fast and reproducible analysis for the quantification of protein-PEG conjugates with varying degree of conjugation (PEGamers) is presented for both stable and unstable proteins. As an example for structurally unstable proteins, proteases were examined being prone to autocatalysis. An increase in sample throughput was achieved by using a microchip-based capillary gel electrophoresis (HT-CGE) enabling an implementation in high-throughput screenings. An increase in appar-

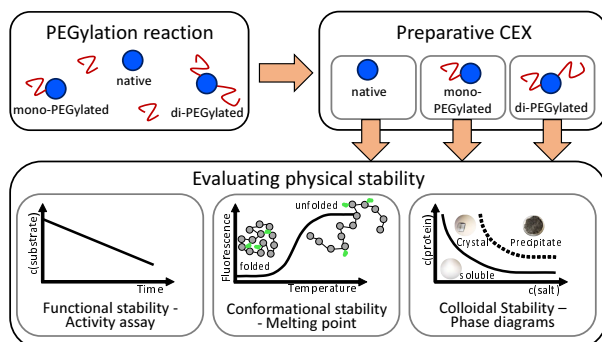
ent molecular weight of the conjugates as well as band broadening effects were considered by calibrating the HT-CGE system with purified PEGamer samples. For structurally unstable proteins, a conservation of the sample composition was established by protein precipitation and redissolution prior to analysis. The potential of the presented method is demonstrated by a case study on the optimization of the reaction conditions for protein conjugation with respect to the distribution of PEGamers.

Journal of Chromatography A 1462 (2016): 153-164.

3. Effect of PEG Molecular Weight and PEGylation Degree on the Physical Stability of PEGylated Lysozyme

Josefine Morgenstern, Pascal Baumann, Carina Brunner and Jürgen Hubbuch

This article presents a systematic, high-throughput study investigating the influence of PEG molecular weight and PEGylation degree on the phase behavior, equilibrium solubility, melting point and residual activity of lysozyme conjugates. The physico-chemical



properties of the conjugates have shown to result form a superposition of protein and polymer characteristics. Higher PEG molecular weights and PEGylation degrees resulted in an amplified shielding of the protein properties yielding an increase in conformational and colloidal stability. However,

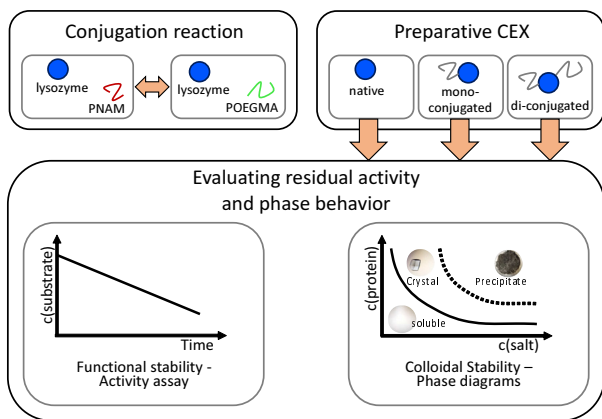
the residual activities of the conjugates decreased simultaneously. The origin of the resulting conjugate activities is discussed as a combination of steric hindrance and molecular flexibility. The methodology employed is extremely useful for the selection of suitable polymers and the fine tuning of the conjugate properties for particular applications.

International Journal of Pharmaceutics 519/1-2 (2017): 408-417.

4. Stability Assessment of Protein-Polymer Conjugates: Alternative Polymers to Polyethylene Glycol

Josefine Morgenstern*, Gabriela Gil Alvaradejo*, Nicolai Bluthardt, Guillaume Delaittre and Jürgen Hubbuch

* *These authors contributed equally to this work*



In this manuscript, alternatives to the current gold standard (PEG) are investigated for their potential use in protein-polymer conjugation. The alternative, biocompatible polymers PNAM and POEGMA are synthesized by reversible addition-fragmentation chain transfer (RAFT) polymerization and randomly coupled to lysozyme from chicken egg. After chromatographic purification, the conjugate species are screened for phase behavior and residual activity.

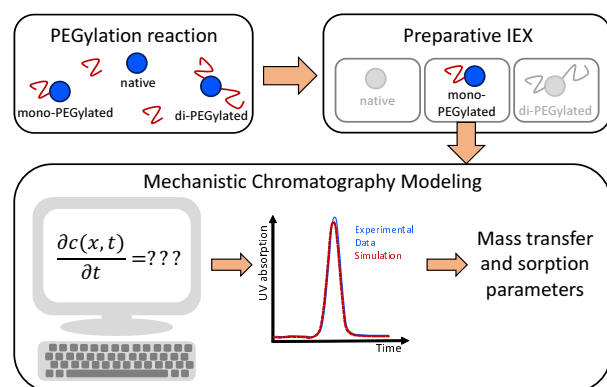
Compared to the unmodified protein an increase in equilibrium solubility was achieved for all investigated conjugate species. Compared to PEG conjugates, however, a higher polymer molecular weight was necessary for a comparable increase in the solubility. The decrease in residual enzyme activity due to steric hindrance was comparable to that observed in case of PEGylation.

Manuscript in preparation.

5. Model-based Investigation on the Mass Transfer and Adsorption Mechanisms of Mono-PEGylated Lysozyme in Ion-Exchange Chromatography

Josefine Morgenstern*, Gang Wang*, Pascal Baumann and Jürgen Hubbuch

* These authors contributed equally to this work.



In this study, mechanistic chromatography modeling was used for the *in silico* determination of mass transfer and sorption parameters for PEGylated lysozyme conjugates in IEX. For parameter estimation, a system of differential equations describing fluid dynamics, mass transfer and adsorption/desorption phenomena in the chromatography column was solved

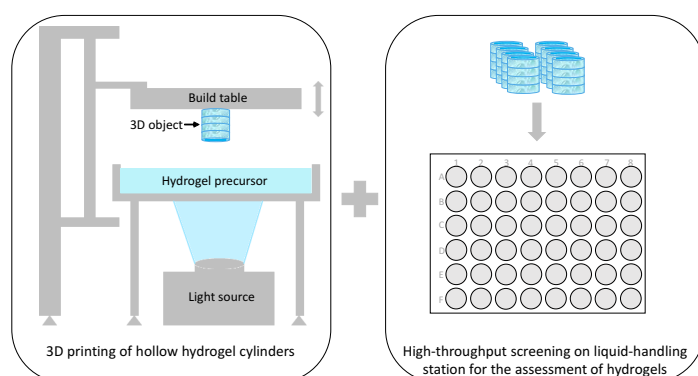
numerically and validated experimentally. Since both molecular weight and surface properties influence the separation result in IEX, the PEG molecular weight has been varied. Changes in mass transfer and sorption processes are discussed with regard to chromatographically relevant parameters such as retention time, peak shape and binding capacity.

Accepted manuscript: to appear in Biotechnology Journal, doi: 10.1002/biot.201700255.

6. Assessment of Hydrogels for Biopharmaceutical Purposes Using a Combination of 3D Printing and High-Throughput Screening

Josefine Morgenstern*, Carsten Philipp Radtke*, Cathrin Dürr and Jürgen Hubbuch

* These authors contributed equally to this work.



Both protein stabilization and release by hydrogels are influenced by various parameters, including the type and molecular weight of the crosslinked polymer, pH and salt strength of the surrounding solution and protein-specific properties. This study presents the development

of a rapid and cost-effective screening-tool for the investigation of protein-hydrogel interactions. The hydrogels are crosslinked to high-throughput compatible structures using

3D printing and subsequently processed on a liquid handling station. By comparing the obtained results with literature data generated by conventional methods, a high data consistency is demonstrated.

Manuscript in preparation.

Manipulation of Lysozyme Phase Behavior by Additives as Function of Conformational Stability

Lara Galm, Josefine Morgenstern and Jürgen Hubbuch

*Institute of Engineering in Life Sciences, Section IV: Biomolecular Separation Science,
Karlsruhe Institute of Technology (KIT), 76131 Karlsruhe, Germany*

International Journal of Pharmaceutics 494/1 (2015): 370–380.

Abstract

Undesired protein aggregation in general and non-native protein aggregation in particular need to be inhibited during bio-pharmaceutical processing to ensure patient safety and to maintain product activity. In this work the potency of different additives, namely glycerol, PEG 1000, and glycine, to prevent lysozyme aggregation and selectively manipulate lysozyme phase behavior was investigated. The results revealed a strong pH dependency of the additive impact on lysozyme phase behavior, lysozyme solubility, crystal size and morphology. This work aims to link this pH dependent impact to a protein-specific parameter, the conformational stability of lysozyme. At pH 3 the addition of 10 %(w/v) glycerol, 10 %(w/v) PEG 1000, and 1 M glycine stabilized or destabilized lysozymes' native conformation resulting in a modified size of the crystallization area without influencing lysozyme solubility, crystal size and morphology. Addition of 1 M glycine even promoted non-native aggregation at pH 3 whereas addition of PEG 1000 completely inhibited non-native aggregation. At pH 5 the addition of 10 %(w/v) glycerol, 10 %(w/v) PEG 1000, and 1 M glycine did not influence lysozymes' native conformation, but strongly influenced the position of the crystallization area, lysozyme solubility, crystal size and morphology. The observed pH dependent impact of the additives could be linked to a differing lysozyme conformational stability in the binary systems without additives at pH 3 and pH 5. However, in any case lysozyme phase behavior could selectively be manipulated by addition of glycerol, PEG 1000 and glycine. Furthermore, at pH 5 crystal size and morphology could selectively be manipulated.

Keywords: *Osmolytes; solubility line; crystallization area; non-native aggregation; FT-IR*

4.1 Introduction

The term protein aggregation describes the assembly of native or non-native protein monomers to protein multimers, i.e. aggregation characterizes both the formation of protein crystals and amorphous precipitates and includes native and non-native aggregation forms. Protein aggregation can occur through different mechanisms [82] and during different steps of a production process [88]. However, crystallization and precipitation are also acknowledged process steps in biopharmaceutical industries either for formulation or purification purposes [189]. Crystalline drug formulations for example have shown significant benefits in the delivery of protein therapeutics to achieve high-concentration, high-stability, low-viscosity and controlled-release formulations [190, 191]. Crystalline insulin formulations are market approved [190, 192, 193] and crystalline antibody formulations are studied, too [194]. For formulated protein therapeutics, the presence of precipitates is typically considered to be undesirable because of the concern that especially non-native precipitates may lead to immunogenic reactions [88]. The widespread opinion exists that aggregation processes are usually associated with a conformational change, i.e. partial unfolding of the proteins [25, 89] and aggregation processes that resulted in non-native protein conformations have been observed [26, 195–198]. Moreover, aggregation processes might influence biological activity of protein therapeutics. Thus, in either case it is essential to ensure that the target protein remains in its native conformation and that biological activity is preserved despite aggregation. Thus, in cases where non-native aggregation is likely to occur aggregation needs to be prevented completely unless there are possibilities to stabilize the native conformational state. In cases where native aggregation occurs, the selective control of phase states is considered to be beneficial as sometimes either crystalline or precipitated forms are preferred e.g. due to a better bioavailability in the respective aggregate state [193]. Particular additives are thought to stabilize the proteins' native state, for example stabilize the protein against thermal denaturation, and thus might be used to prevent non-native aggregation processes. According to Harris and Rösigen [199] particular additives influence protein solubility as well, resulting in a manipulation of the protein phase behavior, i.e. protein aggregation might be completely inhibited or protein phase states (e.g. crystallization, precipitation) might be selectively changed. Frequently used additives are polymers (polyethylene glycol, PEG) and osmolytes. Osmolytes are low molecular weight additives, that can be grouped into the major categories of free amino acids and derivatives (e.g. glycine), polyols and uncharged sugars (e.g. glycerol), methylamines, and urea [113]. The impact of these additives on

protein stability is described to be due to a preferential binding or a preferential exclusion of the additives from the proteins' local domain. In cases where they are preferentially excluded from the proteins' local domain they are known to stabilize the proteins' native state [115, 116, 200–204]. The impact of additives on protein solubility is according to Harris and Rösigen [199] not as easy as predicting protein stability and no general models exist. Though, the mode of action of osmolytes and PEG on protein stability is as well not as easy as it might sound since for some additives stabilizing as well as destabilizing effects have been observed. Parameters that strongly influence the stabilizing or destabilizing character of additives are the additive concentration, the molecular weight of the additive, and the solvent pH. PEG, dimethylglycine, and betaine for example have been found to stabilize proteins up to a certain concentration and destabilize them for higher concentrations [201, 205]. High molecular weights of PEG have been found to be destabilizing as well [202], whereas high molecular weight polyols stabilize proteins better than their low molecular weight counterparts [206]. Additive impact as function of solvent pH is even harder to generalize. According to Singh et al. [207], polyols have a higher potency to stabilize the proteins' native state at low pH, whereas methylamines are described to act most stabilizing at neutral pH and destabilizing at low pH and amino acids were found to stabilize the native state of proteins almost independent of the pH [208]. This pH dependent osmolyte action has been related to the chemical nature of the osmolytes, e.g. the pK_a values [209–211], but could not explain all pH dependent observations [212]. In contrast, there are indications that the pH dependent mode of action of additives might have its origin in the nature of the proteins instead [208, 212]. It is for example known that proteins at extreme pH values are conformationally unstable, i.e. prone to at least partial unfolding [27]. Thus, our work aims to find a link between the pH dependent mode of action of additives and the conformational stability of a model protein in its initial state without additive. To the best of our knowledge up to now there are no investigations on the pH dependent mode of action as a function of conformational stability of proteins in their initial state without additive. Furthermore, this publication examines if the additives impact protein solubility and thus protein phase behavior. Lysozyme from chicken egg white was studied as a model protein, but the presented approaches can easily be transferred to other biopharmaceutical proteins. Lysozyme was investigated at pH 3 and pH 5. Sodium chloride was added as precipitant to induce phase transitions of lysozyme (e.g. crystallization and precipitation) in order to study the phase behavior of lysozyme. In the following the term binary describes lysozyme in aqueous sodium chloride solutions ranging from 0 M to 2.5 M sodium chloride. This was also referred to as the initial state of lysozyme above. The term ternary in the follow-

ing describes lysozyme in aqueous sodium chloride solutions ranging from 0 M to 2.5 M sodium chloride and with a constant additive concentration. Lysozyme conformational stability, solubility, and phase behavior in these ternary systems (with additive) will be compared to lysozyme conformational stability, solubility, and phase behavior in the binary systems (without additive), i.e. to lysozymes' initial state. Glycerol and glycine as additives were chosen as representatives of two osmolyte classes and PEG 1000 as additive beyond the osmolyte class. Fourier-Transformed-Infrared (FT-IR) spectroscopy was applied to monitor lysozyme conformation and to account for non-native conformational changes. This allows to evaluate the impact of the additives on conformational stability and their potency to stabilize or destabilize the proteins' native state. Ternary phase diagrams, consisting of lysozyme, sodium chloride and the respective additive as solution components, were generated and compared to binary ones, consisting of lysozyme and sodium chloride. The comparison of the phase diagrams reveals information about how strong the additives manipulate lysozyme phase behavior, i.e. if they completely prevent aggregation, delay it or if they can be used to selectively control phase states, e.g. transfer former precipitated to crystalline phase states. The phase diagrams additionally allow to experimentally determine lysozyme solubility in cases where crystallization occurs as the supernatant of a crystalline solution is saturated and the lysozyme concentration in the supernatant thus reflects lysozyme solubility [78, 213, 214]. Experimentally determined solubility data points are fitted to an empirically found equation, resulting in continuous solubility lines. Comparison between the binary and ternary systems gives the additive impact on lysozyme solubility lines.

Altogether this publication aims to elucidate the potential origin of pH dependent additive action and tries to expand the basic knowledge on additive impact on protein solubility and phase behavior.

4.2 Materials and Methods

4.2.1 Materials

The used buffer substances were citric acid (Merck, Darmstadt, Germany) and sodium citrate (Sigma-Aldrich, St. Louis, MO, USA) for pH 3 and sodium acetate (Sigma-Aldrich, St. Louis, MO, USA) and acetic acid (Merck, Darmstadt, Germany) for pH 5. PEG 300 and PEG 1000 were obtained from Sigma-Aldrich (St. Louis, MO, USA). Sodium chloride as well as glycine were purchased from Merck (Darmstadt, Germany), glycerol was

from Alfa Aesar (Ward Hill, MA, USA) and lactose from Carl Roth GmbH & Co. KG (Karlsruhe, Germany). Hydrochloric acid and sodium hydroxide for pH adjustment were obtained from Merck (Darmstadt, Germany). pH adjustment was performed using a five-point calibrated pH-meter (HI-3220, Hanna Instruments, Woonsocket, RI, USA). All buffers were filtered through 0.2 μm cellulose acetate filters (Sartorius, Goettingen, Germany).

Lysozyme from chicken egg white was purchased from Hampton Research (Aliso Viejo, CA, USA). The lysozyme solutions were filtered through 0.2 μm syringe filters with cellulose acetate membranes (VWR, Radnor, PA, USA) previous to further desalting via size exclusion chromatography. Size exclusion chromatography was conducted using a HiTrap Desalting Column (GE Healthcare, Uppsala, Sweden) on an AEKTAprime plus system (GE Healthcare, Uppsala, Sweden). A subsequent protein concentration step was performed using Vivaspin[®] centrifugal concentrators (Sartorius, Goettingen, Germany) with PES membranes and molecular weight cutoffs of 3 kDa.

Binary and ternary protein phase diagrams, consisting of lysozyme and sodium chloride or lysozyme, sodium chloride and additive as solution components, were prepared on MRC Under Oil 96 Well Crystallization Plates (Swissci, Neuheim, Switzerland) in 24 μL scale microbatch experiments with a Freedom EVO[®] 100 (Tecan, Maennedorf, Switzerland) automated liquid handling station. The MRC Under Oil 96 Crystallization Plates were covered with HDclear sealing tape (ShurTech Brands, Avon, OH, USA) to prevent evaporation. The sealed plates were stored at 20°C and for 40 days in a Rock Imager 182/54 (Formulatrix, Waltham, MA, USA) automated imaging system.

Lysozyme concentration in the supernatant of crystalline phase states was determined using a NanoDrop 2000c UV-Vis spectroscopic device (Thermo Fisher Scientific, Waltham, MA, USA). An extinction coefficient of $\epsilon_{280\text{ nm}, \text{Savinase}}^{1\%} = 22.00$ was used.

Fourier-Transformed-Infrared (FT-IR) spectra of selected binary and ternary lysozyme systems were measured with a Bruker Tensor 27 (Bruker Corporation, Billerica, MA, USA) Fourier-Transformed-Infrared (FT-IR) spectrophotometer with CONFOCHECK configuration at 20°C. Infrared analysis was conducted using the attenuated total reflection technique in a Bio-ATR II cell (Bruker Corporation, Billerica, MA, USA).

4.2.2 Methods

4.2.2.1 Preparation of Stock Solutions

To set up the buffers all substances were weighed in and dissolved in ultrapure water of approximately 90 % of the final buffer volume. Buffer capacity was 100 mM for all buffers. pH was adjusted with the appropriate titrant with an accuracy of ± 0.05 pH units. After pH adjustment the buffers were brought to their final volume using ultrapure water. All buffers were filtered through $0.2 \mu\text{m}$ cellulose acetate filters. Buffers were used at the earliest one day after preparation and after repeated pH verification.

To set up the protein stock solutions, protein was weighed in and dissolved in the appropriate buffer. The protein solution then was filtered through a $0.2 \mu\text{m}$ syringe filter, and further desalted using size exclusion chromatography. Protein concentration was adjusted to 65.25 ± 1 mg/mL via centrifugal concentrators. A volume of 1 mL of protein stock solution was required for generation of one ternary phase diagram.

4.2.2.2 Generation of Phase Diagrams

Binary protein phase diagrams for lysozyme from chicken egg white were generated earlier [79]. Binary phase diagrams of lysozyme from chicken egg white at pH 3 and pH 5 using sodium chloride as precipitant showed multiple phase transitions. Therefore, lysozyme in aqueous sodium chloride solutions at pH 3 and pH 5 was selected for further investigation in ternary phase diagrams using 1 M glycine, 10 % (m/v) glycerol and 10 % (m/v) PEG 1000 as additives. In total six ternary phase diagrams were generated. Additive concentration was constant in any of the 96 wells on the crystallization plates for the respective pH and additive type. Only lysozyme and sodium chloride concentrations were varied in exactly the same way as in the binary phase diagrams. The resulting protein and sodium chloride concentrations on the crystallization plates thus ranged between 2.5 and 21.75 mg/mL lysozyme and between 0 and 2.5 M sodium chloride. For generation of 96 different ternary system points on the crystallization plates $8 \mu\text{L}$ of solutions with varying sodium chloride concentration and a fixed concentration of additive were mixed with $16 \mu\text{L}$ of solutions with varying lysozyme concentrations in the respective buffer without sodium chloride and additive. After mixing crystallization plates were treated as described by Baumgartner et al. [79]. The images after 40 days were visually examined

to distinguish between the following phase states: soluble, crystalline, precipitated, skin formation, gelation, liquid-liquid phase separation.

4.2.2.3 Determination of Solubility Lines

After 40 days and after scoring of the phase states the plates were removed from the Rock Imager. In cases where crystalline phase states occurred, lysozyme concentration in the supernatant of these crystalline solutions was determined. The supernatant of a crystalline solution is saturated and the lysozyme concentration in the supernatant thus reflects lysozyme solubility [78, 213, 214]. Therefore, experimental data points for lysozyme concentration in the supernatant of crystalline solutions will be referred to as solubility hereafter and were used to fit solubility lines. For determination of lysozyme solubility 3 μL of the supernatant of crystalline solutions were transferred to a Nanodrop 2000c UV-Vis spectroscopic device to determine the lysozyme concentration in the supernatant. This was conducted two- or threefold depending on the available supernatant volume. Values were averaged and solubility lines were fitted using Eq. 4.1 resulting from a Box Lucas 1 model with S being the protein solubility, S_0 the theoretical protein solubility for a sodium chloride concentration of 0 M. A and $R_0 < 0$ are adaptable parameters and c_{NaCl} the sodium chloride concentration.

$$S = S_0 + A \cdot e^{(R_0 \cdot c_{\text{NaCl}})} \quad (4.1)$$

4.2.2.4 FT-IR Analysis

Lysozyme solutions were scanned 24 h after preparation in absorbance mode with 700 scans at a spectral resolution of 2 cm^{-1} . Spectra were recorded from 4000 to 1000 cm^{-1} . Background spectra were recorded for the respective solution the protein was dissolved in also with 700 scans at a spectral resolution of 2 cm^{-1} . Sample volume was 20 μL . All measurements were conducted in duplicate. The OPUS 6.5 spectroscopy software was used for recording and data processing of the recorded FT-IR spectra. Data pre-processing was performed as follows: atmospheric compensation and vector normalization (Euclidean norm) were carried out to delete the influence of water vapor bands on the spectra and to delete protein concentration dependent effects. After data pre-processing second derivative spectra were calculated. Calculation of second derivative spectra was conducted in

a wavenumber region from 1700 to 1600 μL and with 25 smoothing points. Changes in the second derivative spectra correlate to conformational changes of lysozyme.

4.3 Results

4.3.1 FT-IR Spectra of Binary Lysozyme Systems at pH 3 and pH 5

The upper left section of Fig. 4.1 shows results from FT-IR spectroscopic measurements of lysozyme at pH 3 in different binary systems (without additive). FT-IR second derivative spectra of soluble, crystalline, crystalline and coexisting precipitated phase states of lysozyme and for phase states where skin formation occurred are shown. The different

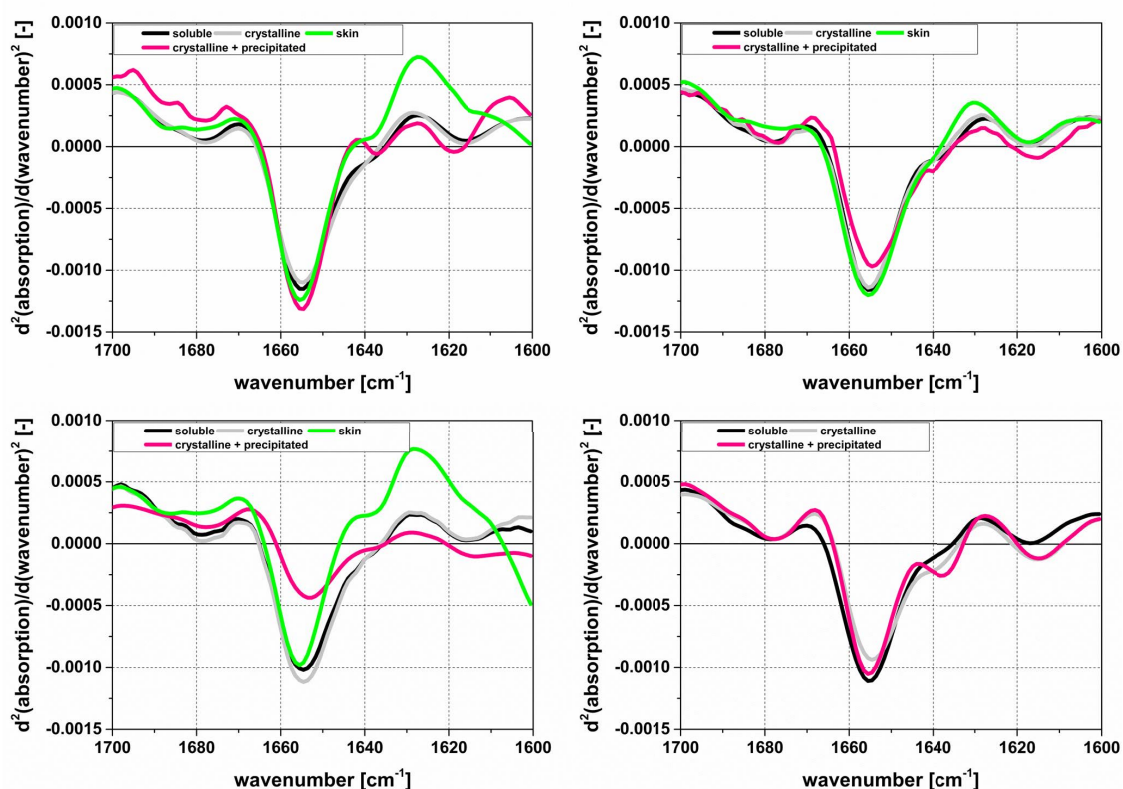


Figure 4.1: Second derivative spectra from FT-IR measurements of lysozyme at pH 3 with different sodium chloride concentrations and without additive (upper left), with 10 % (m/v) glycerol (upper right), with 1 M glycine (lower left), with 10 % (m/v) PEG 1000 (lower right).

phase states were induced by addition of different concentrations of sodium chloride following the conditions from the phase diagrams. For the binary systems at pH 3 the spectrum of crystalline lysozyme was very similar to the native soluble one. The sample with lysozyme in coexisting crystalline and precipitated states deviated slightly from the native soluble spectrum but the most evident deviation occurred for the sample with skin formation. Here, a significant deviation occurred in a wavenumber region between 1640 and 1620 cm^{-1} , which corresponds to the β -sheet region.

The upper left section of Fig. 4.2 shows results from FT-IR spectroscopic measurements of lysozyme at pH 5 in different binary systems (without additive). FT-IR second derivative spectra of soluble, crystalline, precipitated phase states of lysozyme are shown. At pH 5 the second derivative spectra of the investigated phase states in the binary systems were very similar, even the precipitated state showed only small deviations from the native soluble state.

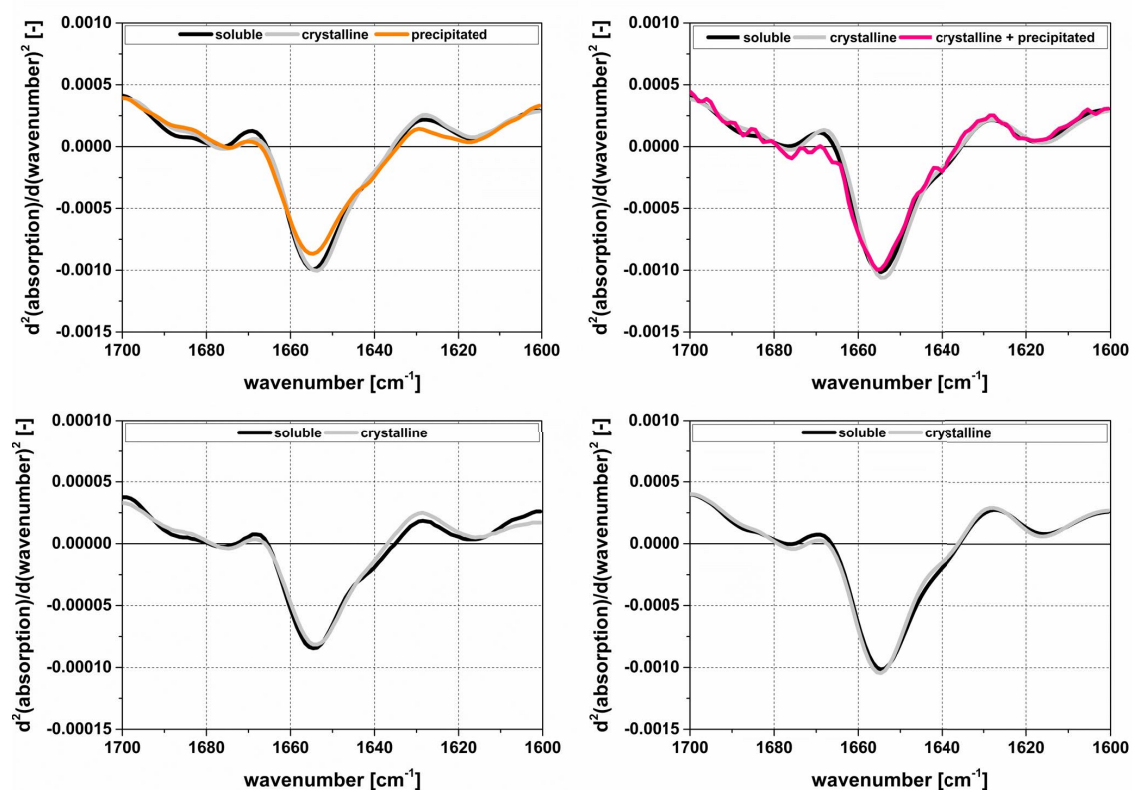


Figure 4.2: Second derivative spectra from FT-IR measurements of lysozyme at pH 5 with different sodium chloride concentrations and without additive (upper left), with 10 %(m/v) glycerol (upper right), with 1 M glycine (lower left), with 10 %(m/v) PEG 1000 (lower right).

4.3.2 Impact of Investigated Additives on Lysozyme Conformation as Function of pH

4.3.2.1 Impact on Lysozyme Conformation at pH 3

The upper right and the lower sections of Fig. 4.1 show the second derivative spectra of the FT-IR spectroscopic measurements of lysozyme at pH 3 in different ternary systems (with additives). Addition of 10 %(m/v) glycerol (Fig. 4.1, upper right) smoothed the deviation between the second derivative spectra of different phase states in comparison to the spectra of different phase states in binary systems (Fig. 4.1, upper left). The spectrum for coexisting crystallization and precipitation was much more similar to the native soluble one than in the binary case. Even the spectrum for the sample with skin formation was more similar to the soluble, native spectrum than in the binary case. The same accounted for the addition of 10 %(m/v) PEG 1000 (Fig. 4.1, lower right). Deviation between the second derivative spectra of different phase states was smoothed by addition of PEG 1000. In contrast, addition of 1 M glycine (Fig. 4.1, lower left) increased deviation between the second derivative spectra of the different phase states. The spectrum of the sample with coexisting crystalline and precipitated lysozyme deviated stronger from soluble, native spectrum than in the binary case, especially in a wavenumber region between 1660 and 1640 cm^{-1} . A decrease of the peak depth in this region corresponds to a dissipation of α -helix structures. The spectrum of the sample with skin formation again deviated strongest in the wavenumber region between 1640 and 1620 cm^{-1} . The FT-IR analysis results for pH 3 showed that addition of glycerol and PEG 1000 reduced deviations between the second derivative FT-IR spectra of different phase states. Glycine in contrast increased deviations between the second derivative FT-IR spectra compared to the samples without additive.

4.3.2.2 Impact on Lysozyme Conformation at pH 5

The upper right and the lower sections of Fig. 4.2 show the second derivative spectra of the FT-IR spectroscopic measurements of lysozyme at pH 5 in different ternary systems (with additives). The addition of 10 %(m/v) glycerol, 10 %(m/v) PEG 1000 and 1 M glycine hardly influenced the second derivative FT-IR spectra of lysozyme in different phase states. Even for addition of glycine the spectra hardly deviated.

4.3.3 Impact of Investigated Additives on Lysozyme Phase Behavior as Function of pH

For examination of the impact of selected additives on lysozyme phase behavior ternary phase diagrams with lysozyme, sodium chloride and additive as solution components were compared to binary phase diagrams, consisting of lysozyme and sodium chloride, at pH 3 and pH 5. In particular, the sodium chloride concentration for initiation of crystallization, the size of the crystallization area and the crystal size and morphology were compared.

4.3.3.1 Impact on Lysozyme Phase Behavior at pH 3

Fig. 4.3 shows the binary (upper left) and ternary (upper right, lower right, and lower left) phase diagrams of lysozyme at pH 3. The sodium chloride concentration for initiation

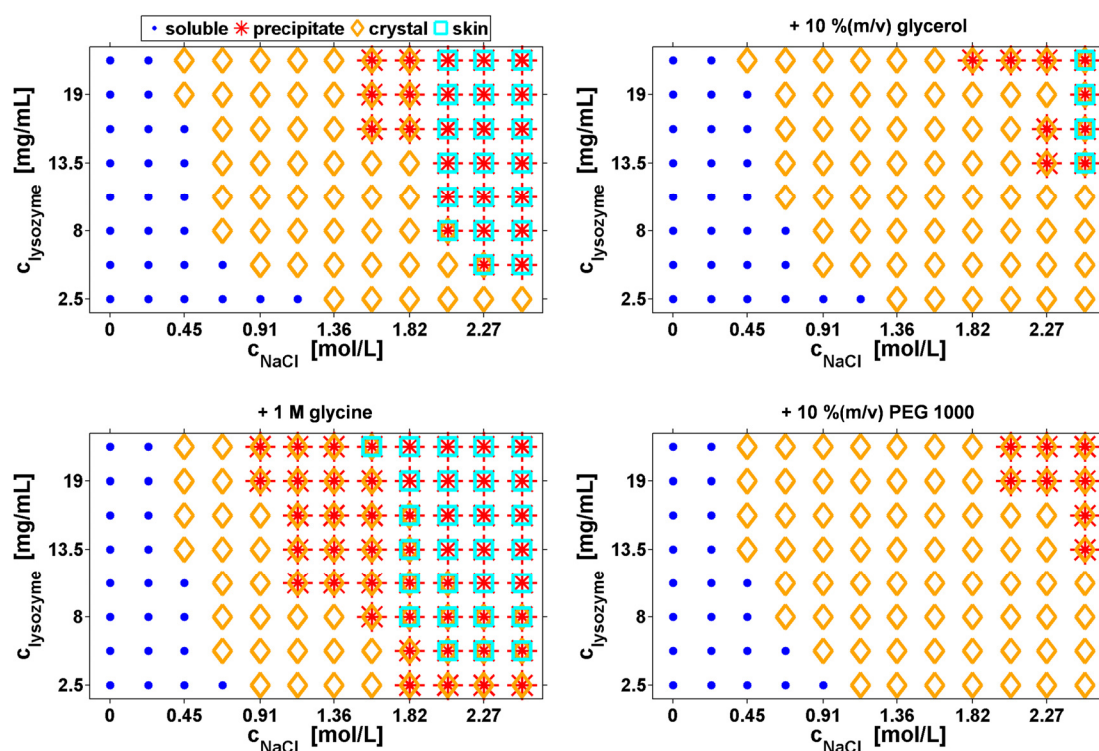


Figure 4.3: Phase diagrams of lysozyme at pH 3 depending on sodium chloride concentration without additive (upper left), with 10 %(m/v) glycerol (upper right), with 1 M glycine (lower left), and with 10 %(m/v) PEG 1000 (lower right).

of lysozyme crystallization did not change by addition of glycerol, PEG 1000 or glycine. In any case lysozyme crystallization started at 0.45 M sodium chloride. This said, the lysozyme concentration for crystallization was influenced and was higher than in the binary case for addition of 10 % (m/v) glycerol (upper right) and lower than in the binary case for addition of 10 % (m/v) PEG 1000 and 1 M glycine (lower right and left). Adding 10 % (m/v) glycerol to the solutions resulted in a wider crystallization area, a smaller precipitation area and reduced skin formation. Glycerol reduced the number of conditions where skin formation occurred to 4 in contrast to 20 in the binary phase diagram. Addition of 10 % (m/v) PEG 1000 enlarged the size of the crystallization area and delayed precipitation even further than glycerol. The most remarkable difference was that the addition of PEG 1000 completely inhibited skin formation. The addition of 1 M glycine decreased the size of the crystallization area dramatically and enlarged the precipitation area as well as the area where skin formation occurred. The number of conditions where skin formation occurred was increased to 28.

In summary, at pH 3 the additives did not strongly affect the sodium chloride concentration needed for initiation of aggregation (crystallization) but they did influence the size of the crystallization and precipitation area, and the size of the area where skin formation occurred. Thus, the phase states or rather the aggregate states could be successfully selectively manipulated, for example from former precipitated states to crystalline ones.

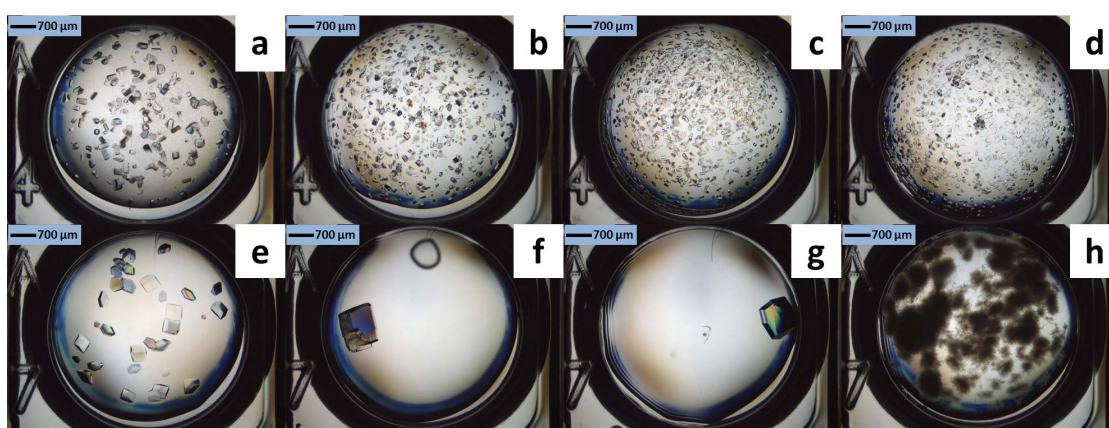


Figure 4.4: Phase states of 21.75 mg/mL lysozyme after 40 days at pH 3 with 0.68 M sodium chloride (upper row) and pH 5 with 1.36 M sodium chloride (lower row). Additive concentrations: without additive (a), 10 % (m/v) glycerol (b), 10 % (m/v) PEG 1000 (c), 1 M glycine (d), without additive (e), 10 % (m/v) glycerol (f), 10 % (m/v) PEG 1000 (g), 1 M glycine (h).

No significant influence on crystal size and morphology was observed for addition of glycerol, PEG 1000 or glycine as can be seen in Fig. 4.4(a-d).

4.3.3.2 Impact on Lysozyme Phase Behavior at pH 5

Fig. 4.5 shows the binary (upper left) and ternary (upper right, lower right, and lower left) phase diagrams of lysozyme at pH 5. In contrast to pH 3 the sodium chloride concentration for initiation of lysozyme crystallization was influenced by addition of glycerol and glycine. The addition of 10 % (m/v) glycerol at pH 5 caused a shift of the crystallization area to higher sodium chloride concentrations. The addition of 1 M glycine shifted the crystallization area slightly towards lower sodium chloride concentrations. PEG 1000 did not shift the sodium chloride concentration for initiation of lysozyme crystallization but shifted the crystallization area to higher lysozyme concentrations. Moreover, addition of PEG 1000 caused a crystallization area that was interspersed with

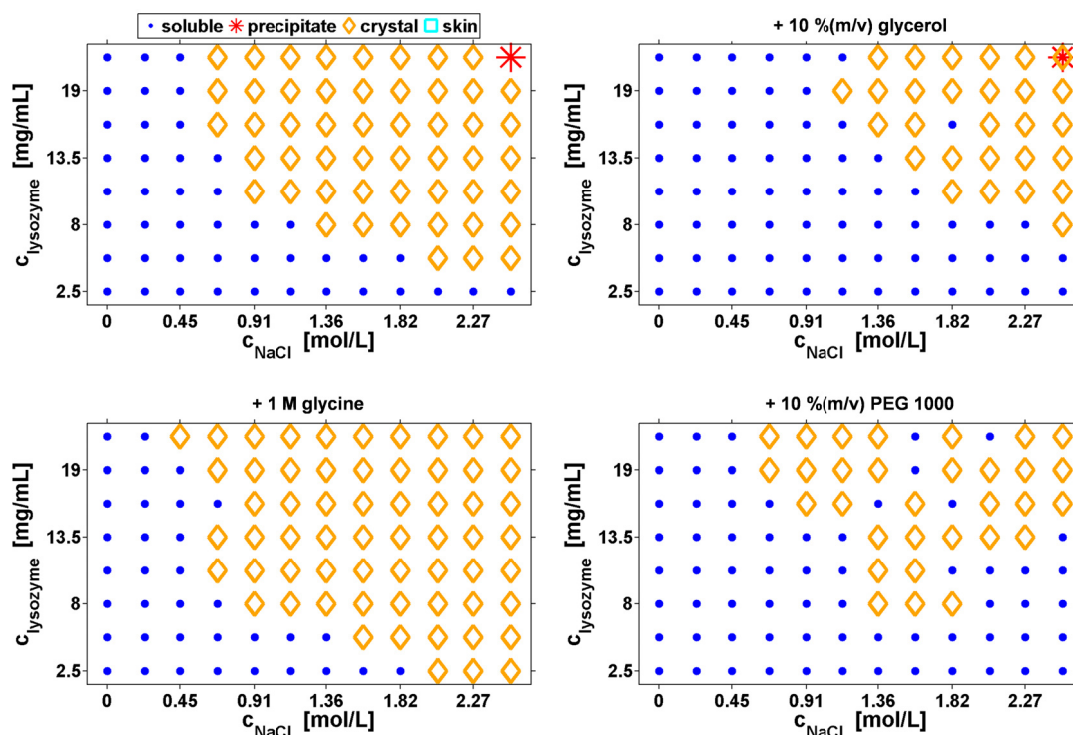


Figure 4.5: Phase diagrams of lysozyme at pH 5 depending on sodium chloride concentration without additive (upper left), with 10 % (m/v) glycerol (upper right), with 1 M glycine (lower left), and with 10 % (m/v) PEG 1000 (lower right).

soluble conditions. These shifts of the crystallization areas caused a decrease of the size of the crystallization areas by addition of 10 % (m/v) glycerol and 10 % (m/v) PEG 1000 and an increase by addition of 1 M glycine. Addition of 10 % (m/v) glycerol and 10 % (m/v) PEG 1000 turned some former crystalline phase states to soluble phase states, i.e. inhibited aggregation. Compared to the binary phase diagram with 51 crystalline phase states and one precipitated phase state, addition of 10 % (m/v) glycerol reduced the number of crystalline phase states to 27 and one phase state with coexisting crystallization and precipitation. Addition of 10 % (m/v) PEG 1000 reduced the number of crystalline phase states to 31 and completely inhibited precipitation. Addition of 1 M glycine increased the number of crystalline phase states to 61 but also completely inhibited precipitation. The influence of the investigated additives on crystal size and morphology was strong as can be seen in Fig. 4.4(e-h). In the binary systems three-dimensional crystals with a size of averagely 400 μm occurred up to sodium chloride concentrations of 2.05 M (exemplarily shown in Fig. 4.4e). For higher sodium chloride concentrations small, sea-urchin shaped two-dimensional crystals evolved instead. Addition of 10 % (m/v) glycerol and PEG 1000 (Fig. 4.4f and g) caused the formation of single, three-dimensional crystals with averagely twice the size of the crystals in the binary case over the whole sodium chloride concentration range. Glycine in contrast inhibited the formation of three-dimensional crystals from 1.36 M sodium chloride (Fig. 4.4h) and small, sea-urchin shaped two-dimensional crystals evolved instead.

In summary, at pH 5 the additives strongly affected either the sodium chloride concentration and/or the lysozyme concentration for initiation of aggregation (crystallization), i.e. caused a shift of the crystallization area. This as well influenced the size of the crystallization area. Thus, aggregation could be successfully inhibited or accelerated. Furthermore, a striking influence on lysozyme crystal size and morphology was observed.

4.3.4 Effect of Investigated Additives on Lysozyme Solubility

4.3.4.1 Determination of Lysozyme Solubility and Fit of Solubility Lines

Lysozyme concentration in the supernatant of crystalline solutions at pH 3 could be determined with a maximum relative deviation of 6.4 % for the binary system and 13 % for the ternary systems. Lysozyme concentration in the supernatant of crystalline solutions at pH 5 could be determined with a maximum relative deviation of 16.9 % for the binary system and 24.9 % for the ternary systems. Inaccuracies could have been due

to development of incomplete equilibria in the ternary systems as described by Asherie [78]. There, the presented approach to determine protein solubility starting with a supersaturated solution is described to be more difficult and less accurate than to dissolve a protein crystal in an undersaturated protein solution. This is however not possible with the experimental approach described in this study. Nevertheless, solubility lines could be fitted to these experimental solubility data points with a high accuracy using Eq. 4.1 which arised from a Box Lucas 1 fit model. This fit model was found to give the best approximation to the solubility data points, but exponential correlations between protein solubility and salt concentration as described in Eq. 4.1 were empirically found earlier, too, employed for example in the Cohn equation [215]. Eq. 4.1 though could even fit the ternary systems with a high accuracy as can be seen in Table 4.1 , i.e. the addition of additives did not influence the validity of the used exponential correlation. The only exception from this was the solubility line for the ternary system consisting of lysozyme, sodium chloride and 10 %(m/v) glycerol at pH 5. In this case no correlation between the experimental solubility data points and Eq. 4.1 could be found. In the other cases the coefficient of correlation was above 0.98. The fit parameters as well as the coefficients of correlation for the individual binary and ternary systems are listed in Table 4.1. The calculated lysozyme solubility lines as well as the experimental data points are shown in Fig. 4.6.

Table 4.1: Fit parameters and coefficients of correlation for fit of the experimental data to Eq. 4.1

	pH	S_0	A	R_0	R^2
without additive	3	0.95617	115.70692	-4.77088	0.98775
+ 10 %(m/v) glycerol	3	1.27213	48.94989	-2.94109	0.9909
+ 1 M glycine	3	0.83462	61.11589	-3.98231	0.99325
+ 10 %(m/v) PEG 1000	3	1.42829	199.84551	-5.64349	0.99394
without additive	5	3.29623	42.61535	-3.40082	0.98851
+ 10 %(m/v) glycerol	5	-	-	-	-
+ 1 M glycine	5	2.07977	125.1018	-4.41318	0.99529
+ 10 %(m/v) PEG 1000	5	5.89109	88.6513	-3.71137	0.98821

4.3.4.2 Impact on Lysozyme Solubility at pH 3

At pH 3 (Fig. 4.6, left) the addition of glycerol, PEG 1000 and glycine did not significantly influence lysozyme solubility in comparison to the binary system. The addition of 10 % (m/v) glycerol slightly enhanced lysozyme solubility in a sodium chloride concentration range between 0.68 and 1.82 M. The addition of 1 M glycine slightly decreased the lysozyme solubility below 0.68 M sodium chloride. The experimental data points as well as the fitted solubility line for the ternary system with PEG 1000 are almost identical to the binary system.

4.3.4.3 Impact on Lysozyme Solubility at pH 5

At pH 5 (Fig. 4.6, right) the addition of glycerol, PEG 1000 and glycine significantly influenced the lysozyme solubility. The addition of 10 % (m/v) glycerol caused an enhancement of the lysozyme solubility for sodium chloride concentrations from 1.14 M to 2.5 M. The addition of 10 % (m/v) PEG 1000 enhanced lysozyme solubility in the whole investigated sodium chloride concentration range: The addition of glycine increased lysozyme solubility up to 0.68 M sodium chloride and decreased lysozyme solubility for sodium chloride concentrations from 0.91 M to 2.5 M. Thus, the effect of glycine on lysozyme solubility at pH 5 depended on the sodium chloride concentration.

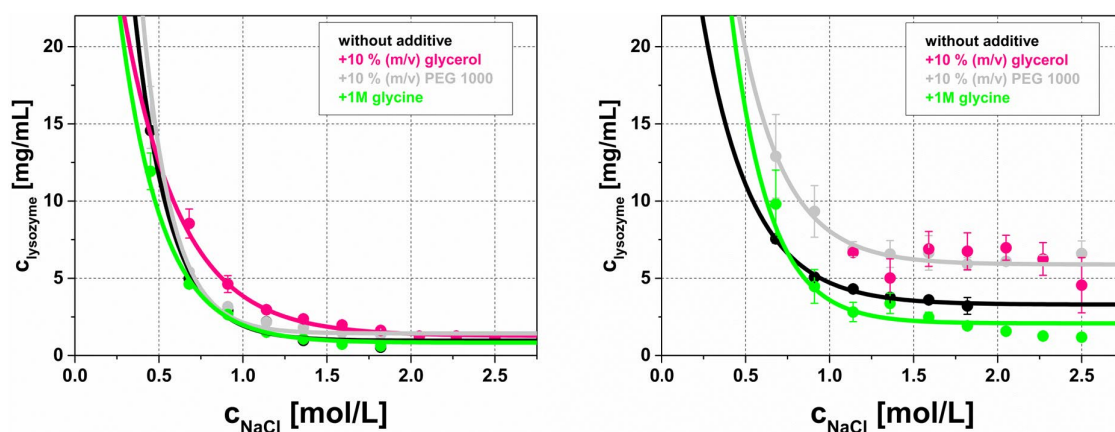


Figure 4.6: Solubility lines of lysozyme at pH 3 (left) and pH 5 (right) depending on sodium chloride concentration without additive and with 10 % (m/v) glycerol, 1 M glycine and 10 % (m/v) PEG 1000. The solid lines depict the solubility lines fitted using Eq. 4.1 with fit parameters as provided in Table 4.1.

4.4 Discussion

4.4.1 Impact of Investigated Additives on Lysozyme Phase Behavior, Conformation and Solubility at pH 3

Deviation between the FT-IR spectra of different phase states of lysozyme in the binary systems at pH 3 is high, i.e. conformational instability of lysozyme at pH 3 in different phase states is high. Even non-native changes in lysozyme conformation during aggregation could be observed in the binary system as the spectrum of the sample with skin formation showed a significant deviation and according to Zeelen [216] this skin is a layer of denatured protein. Addition of glycerol and PEG 1000 reduced the deviation between the FT-IR spectra of different phase states of lysozyme in the ternary systems, i.e. glycerol and PEG 1000 increase conformational stability of lysozyme. In contrast, addition of glycine increased the deviation between the FT-IR spectra, i.e. glycine further increased conformational instability. The differing impact of glycerol, PEG 1000 and glycine on conformational stability was also reflected in a differing impact on lysozyme phase behavior in the ternary phase diagrams compared to the binary ones. Addition of glycerol and PEG 1000 enlarged the size of the crystallization area, whereas addition of glycine reduced the size of the crystallization area. Under the assumption that crystallization is a oligomerization of native protein molecules [82, 217] the above further supports the results from the FT-IR experiments and indicates that glycerol as well as PEG 1000 stabilized the native state of lysozyme whereas glycine destabilized the native state of lysozyme. Additionally, skin formation could be reduced or completely inhibited by addition of glycerol and PEG 1000 at pH 3 and was enhanced by addition of glycine. As this skin represents a non-native phase state [216], reduction or inhibition of skin formation shows the potency of glycerol and PEG 1000 to delay or completely inhibit non-native aggregation. In contrast, addition of glycine promoted non-native aggregation. This again further supports the results from the FT-IR experiments. The impact of glycerol, PEG 1000 and glycine on conformational stability was not reflected in a significant influence on lysozyme solubility lines at pH 3. Lysozyme solubility lines were hardly influenced by the addition of glycerol, PEG 1000 and glycine. As protein solubility in many cases is described as directly related to protein-protein interactions [218–221], no influence on the solubility lines implies no influence on protein-protein interactions by addition of glycerol, PEG 1000 and glycine. Fig. 4.4(a-d) shows that glycerol, PEG 1000 and glycine did not significantly influence lysozyme crystal size and morphology. This

indicates that they as well did not influence aggregation kinetics [222–224]. This is further supported by the fact that both, lysozyme solubility lines and the initiation of crystallization, were not significantly influenced by addition of glycerol, PEG 1000 and glycine. However, lysozyme phase states could be selectively controlled by addition of glycerol, PEG 1000 and glycine. For example, precipitation and skin formation could be transformed to crystallization or the other way around.

Altogether, additive action at pH 3 was identified to be simply driven by structure stabilizing or destabilizing tasks. This is in agreement with the preferential interaction theory. Addition of glycerol and PEG 1000 stabilized the native lysozyme conformation and thus seem to cause a preferential hydration of lysozyme, i.e. glycerol and PEG 1000 are preferentially excluded from lysozymes' local domain. Addition of glycine destabilized the native state, i.e. it is preferentially bound to or enriched at the lysozyme surface. The destabilizing properties of glycine were surprising, though. Glycine was earlier described as stabilizing osmolyte even for concentrations up to 5 M [205, 225]. However, it has to be mentioned that according to Singh et al. [207] osmolyte action is extremely pH dependent and the above named investigations with lysozyme and glycine whose results are in opposition to ours were conducted at pH 5.8–6.5.

In summary, at pH 3, glycerol and glycine exhibited typical osmolyte character that could be explained by the preferential interaction theory. PEG 1000 action could also be explained using the preferential interaction theory, but its stabilizing impact was stronger compared to glycerol as it could even completely inhibit non-native aggregation. Protein-protein interactions and aggregation kinetics were not only or only weakly influenced by addition of glycerol, glycine, and PEG 1000 as far as could be evaluated here.

4.4.2 Impact of Investigated Additives on Lysozyme Phase Behavior, Conformation and Solubility at pH 5

Deviation between the FT-IR spectra of different phase states of lysozyme in the binary systems at pH 5 is low. Thus, conformational stability of lysozyme at pH 5 is high, even during precipitation. The additives investigated did have no apparent influence on the FT-IR spectra, i.e. conformational stability of lysozyme seems to be untouched by addition of glycerol, PEG 1000 and glycine. In contrast to the impact of the additives on lysozyme phase behavior at pH 3, where only the size of the crystallization area was changed, at pH 5 the investigated additives caused a shift of the crystallization area to

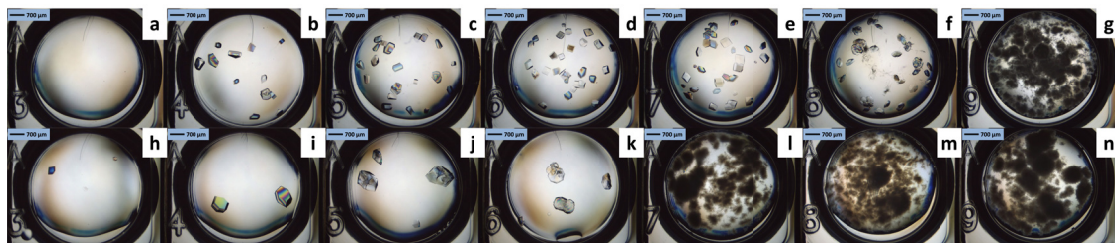


Figure 4.7: Phase states of 21.75 mg/mL lysozyme after 40 days at pH 5 with varying sodium chloride concentrations. The upper row shows the phase states for binary systems without additive, the lower row the phase states for ternary systems with 1 M glycine. Sodium chloride concentrations are 0.45 M (a and h), 0.68 M (b and i), 0.91 M (c and j), 1.14 M (d and k), 1.36 M (e and l), 1.59 M (f and m), and 1.82 M (g and n).

higher or lower sodium chloride and/or lysozyme concentrations. The addition of 10 % (m/v) glycerol significantly shifted the crystallization area to higher sodium chloride and lysozyme concentrations. The addition of PEG 1000 caused a shift of the crystallization area to higher lysozyme concentrations and the ternary crystallization area is interspersed with soluble conditions. Therefore, glycerol and PEG 1000 successfully completely inhibited aggregation in some cases compared to the binary system. Glycine shifted the crystallization area to lower sodium chloride concentrations and thus promoted aggregation in comparison to the binary system. This shift of the crystallization area caused by the additives at pH 5 is not due to an impact of glycerol, PEG 1000 and glycine on lysozyme conformational stability. Furthermore, in contrast to pH 3 glycine at pH 5 did not induce or promote non-native aggregation. However, at pH 5 lysozyme solubility lines were significantly changed by addition of glycerol, PEG 1000 and glycine. Addition of glycerol and PEG 1000 enhanced lysozyme solubility at pH 5, whereas glycine enhanced lysozyme solubility up to 0.68 M sodium chloride and decreased solubility for higher sodium chloride concentrations. Thus, instead of affecting lysozyme conformational stability glycerol, PEG 1000 and glycine seem to strongly influence protein-protein interactions. Addition of glycerol and PEG 1000 probably reduced attractive protein-protein interactions in comparison to the binary system over the whole sodium chloride concentration range. Attractive protein-protein interactions were either reduced or enhanced by addition of glycine dependent on sodium chloride concentration, yielding in increased or decreased solubility. The impact of the additives on lysozyme solubility and intermolecular interactions was also reflected in crystal size and morphology, i.e. in aggregation or crystallization kinetics. Much bigger lysozyme crystals than in the binary system at pH 5 evolved in

presence of 10 % (m/v) glycerol and PEG 1000, i.e. glycerol and PEG 1000 slowed aggregation or crystallization kinetics. The diverse impact of glycine on lysozyme solubility and intermolecular interactions is also reflected in the crystal size and morphology for the ternary systems as can be seen in Fig. 4.7. Up to 1.14 M sodium chloride crystal size was increased, i.e. aggregation or crystallization kinetics slowed in comparison to the binary system, whereas for higher sodium chloride concentrations small, two-dimensional, sea-urchin shaped crystals occurred, i.e. aggregation or crystallization kinetics were accelerated.

In summary, the presented results for pH 5 indicate that additives that do not influence lysozyme conformational stability mainly act on lysozyme solubility, i.e. protein-protein interactions, and on crystal size and morphology, i.e. aggregation or crystallization kinetics. The mode of action of the additives at pH 5 could not be correlated to the preferential interaction theory as no influence on lysozyme conformation could be detected and lysozymes' native conformational state was very stable.

4.4.3 Impact of Investigated Additives as Function of pH

Generally a pH dependency of osmolyte action was described earlier [207, 208]. So far, pH dependent osmolyte action was connected to the chemical nature of the osmolyte, e.g. the pK_a value [209–211]. This could be excluded in our case as no pK_a is exceeded between pH 3 and pH 5 for the investigated additives. More likely the differences between pH 3 and pH 5 are associated with the conformational stability of lysozyme in the binary systems. At pH 3 FT-IR investigations of the binary system showed that lysozyme is conformationally unstable. Here, glycerol, PEG 1000 and glycine exhibited no impact on lysozyme solubility lines, crystal size and crystal morphology. At pH 3 the additives however stabilized (glycerol and PEG 1000) or destabilized (glycine) the native conformation of lysozyme and reduced (glycerol), completely inhibited (PEG 1000) or promoted (glycine) non-native aggregation. Stabilization or destabilization of lysozymes' native conformation resulted in modified sizes of the crystallization area, the precipitation area and the area where skin formation occurred. Thus, a selective control of lysozyme phase states is possible.

At pH 5 FT-IR investigations of the binary system showed that lysozyme is conformationally stable. Here, glycerol, PEG 1000 and glycine exhibited a significant impact on lysozyme solubility lines, the initiation of crystallization, crystal size and morphology, but no impact on lysozyme conformation could be identified. Aggregation or crystallization

in particular could be selectively inhibited or promoted and crystal size and morphology could be selectively manipulated.

This in summary indicates that in cases where protein conformational stability is threatened additives adopt stabilization tasks. Their mode of action in these cases can be described following the preferential interaction theory [115, 116, 200–204]. In cases where protein conformational stability is not threatened the ability of the additives to stabilize proteins is not needed, but their ability to increase the solubility of native proteins is essential. This was described earlier by Auton et al. [226] and is further supported by Bolen and Baskakov [227] who stated that stabilizing osmolytes act mainly on the denatured state leaving the native state largely unperturbed.

4.5 Conclusion

The impact of the additives on lysozyme phase behavior and solubility lines was observed to be pH dependent. The pH dependent impact could be explained by differences in the conformational stability of lysozyme at pH 3 and pH 5 in presence of sodium chloride. pH dependent additive impact was described earlier but the presented work allowed to reduce this to lysozyme conformational stability. This publication additionally expanded the basic knowledge about additive impact on protein solubility and could present a mathematical description for a solubility line that could capture lysozyme solubility in binary and ternary systems. For conditions where the native conformational state of lysozyme was unstable in the binary system the impact caused by the investigated additives could be explained by the preferential interaction theory. Native conformation was stabilized by glycerol and PEG 1000 and destabilized by addition of glycine. PEG 1000 in particular even completely inhibited non-native aggregation, whereas glycine even promoted non-native aggregation. Stabilization or destabilization of the native conformational state resulted in a modified lysozyme phase behavior without affecting solubility lines and crystal size and morphology. Phase states could be successfully selectively controlled. For conditions where the native conformational state of lysozyme was stable in the binary system no impact of the additives on lysozymes' native conformation could be observed. Though, the additives exhibited a significant impact on lysozyme solubility lines, the initiation of crystallization, crystal size and morphology. Glycerol and PEG 1000 increased lysozyme solubility and crystal size. Glycine increased or decreased lysozyme solubility and crystal size depending on sodium chloride concentration in the ternary systems. All

of the three additives showed characteristics that could be of interest for biopharmaceutical industries: aggregation processes could be successfully manipulated with or without effects on solution characteristics like solubility or aggregate characteristics like crystal size and morphology.

4.6 Acknowledgments

We gratefully acknowledge the financial support by the Federal Ministry of Education and Research (BMBF) (0315342B).

4.7 References

25. Chi, E. Y., Krishnan, S., Randolph, T. W. & Carpenter, J. F. Physical stability of proteins in aqueous solution: Mechanism and driving forces in nonnative protein aggregation. *Pharm. Res.* **20**, 1325–1336 (2003).
26. Dong, A., Prestrelski, S. J., Allison, S. D. & Carpenter, J. F. Infrared spectroscopic studies of lyophilization-and temperature-induced protein aggregation. *J. Pharm. Sci.* **84**, 415–424 (1995).
27. Wang, W. & Roberts, C. J. *Aggregation of therapeutic proteins* (John Wiley & Sons, 2010).
78. Asherie, N. Protein crystallization and phase diagrams. *Methods* **34**, 266–272 (2004).
79. Baumgartner, K., Galm, L., Nötzold, J., Sigloch, H., Morgenstern, J., Schleining, K., Suhm, S., Oelmeier, S. A. & Hubbuch, J. Determination of protein phase diagrams by microbatch experiments: Exploring the influence of precipitants and pH. *Int. J. Pharm.* **479**, 28–40 (2015).
82. Philo, J. S. & Arakawa, T. Mechanisms of protein aggregation. *Current pharmaceutical biotechnology* **10**, 348–351 (2009).
88. Cromwell, M., Hilario, E. & Jacobson, F. Protein aggregation and bioprocessing. *The AAPS journal* **8**, E572–E579 (2006).
89. Fink, A. L. Protein aggregation: Folding aggregates, inclusion bodies and amyloid. *Folding and design* **3**, R9–R23 (1998).

113. Yancey, P. H. Water Stress, Osmolytes and Proteins. *American Zoologist* **41**, 699–709 (2001).
115. Arakawa, T. & Timasheff, S. Stabilization of protein structure by sugars. *Biochemistry* **21**, 6536–6544 (1982).
116. Arakawa, T. & Timasheff, S. The stabilization of proteins by osmolytes. *Biophys. J.* **47**, 411–414 (1985).
189. Scopes, R. K. in *Protein Purification* 41–71 (Springer, 1987).
190. Basu, S. K., Govardhan, C. P., Jung, C. W. & Margolin, A. L. Protein crystals for the delivery of biopharmaceuticals. *Expert. Opin. Biol. Ther.* **4**, 301–317 (2004).
191. Jen, A. & Merkle, H. P. Diamonds in the rough: Protein crystals from a formulation perspective. *Pharm. Res.* **18**, 1483–1488 (2001).
192. Brange, J. & Vølund, A. Insulin analogs with improved pharmacokinetic profiles. *Advanced drug delivery reviews* **35**, 307–335 (1999).
193. Vajo, Z., Fawcett, J. & Duckworth, W. C. Recombinant DNA technology in the treatment of diabetes: Insulin analogs. *Endocrine reviews* **22**, 706–717 (2001).
194. Yang, M. X., Shenoy, B., Disttler, M., Patel, R., McGrath, M., Pechenov, S. & Margolin, A. L. Crystalline monoclonal antibodies for subcutaneous delivery. *PNAS* **100**, 6934–6939 (2003).
195. Dzwolak, W., Ravindra, R., Lendermann, J. & Winter, R. Aggregation of bovine insulin probed by DSC/PPC calorimetry and FTIR spectroscopy. *Biochemistry* **42**, 11347–11355 (2003).
196. Feng, Y. W., Ooishi, A. & Honda, S. Aggregation factor analysis for protein formulation by a systematic approach using FTIR, SEC and design of experiments techniques. *Journal of pharmaceutical and biomedical analysis* **57**, 143–152 (2012).
197. Kendrick, B. S., Cleland, J. L., Lam, X., Nguyen, T., Randolph, T. W., Manning, M. C. & Carpenter, J. F. Aggregation of recombinant human interferon gamma: Kinetics and structural transitions. *J. Pharm. Sci.* **87**, 1069–1076 (1998).
198. Matheus, S., Friess, W., Schwartz, D. & Mahler, H.-C. Liquid high concentration IgG1 antibody formulations by precipitation. *J. Pharm. Sci.* **98**, 3043–3057 (2009).
199. Harries, D. & Rösgen, J. A practical guide on how osmolytes modulate macromolecular properties. *Methods in cell biology* **84**, 679–735 (2008).

-
200. Arakawa, T. & Timasheff, S. N. Preferential interactions of proteins with solvent components in aqueous amino acid solutions. *Arch. Biochem. Biophys.* **224**, 169–177 (1983).
 201. Arakawa, T. & Timasheff, S. N. Mechanism of polyethylene glycol interaction with proteins. *Biochemistry* **24**, 6756–6762 (1985).
 202. Lee, J. & Lee, L. Preferential solvent interactions between proteins and polyethylene glycols. *Journal of Biological Chemistry* **256**, 625–631 (1981).
 203. Timasheff, S. N. & Arakawa, T. Mechanism of protein precipitation and stabilization by co-solvents. *Journal of Crystal Growth* **90**, 39–46 (1988).
 204. Webb, J. N., Webb, S. D., Cleland, J. L., Carpenter, J. F. & Randolph, T. W. Partial molar volume, surface area, and hydration changes for equilibrium unfolding and formation of aggregation transition state: High-pressure and cosolute studies on recombinant human IFN-gamma. *PNAS* **98**, 7259–7264 (2001).
 205. Santoro, M. M., Liu, Y., Khan, S. M., Hou, L. X. & Bolen, D. Increased thermal stability of proteins in the presence of naturally occurring osmolytes. *Biochemistry* **31**, 5278–5283 (1992).
 206. Poddar, N., Ansari, Z., Singh, R., Moosavi-Movahedi, A. & Ahmad, F. Effect of monomeric and oligomeric sugar osmolytes on ΔG_D , the Gibbs energy of stabilization of the protein at different pH values: Is the sum effect of monosaccharide individually additive in a mixture? *Biophys. Chem.* **138**, 120–129 (2008).
 207. Singh, L. R., Poddar, N. K., Dar, T., Kumar, R. & Ahmad, F. Protein and DNA destabilization by osmolytes: The other side of the coin. *Life sciences* **88**, 117–125 (2011).
 208. Macchi, F., Eisenkolb, M., Kiefer, H. & Otzen, D. E. The effect of osmolytes on protein fibrillation. *International journal of molecular sciences* **13**, 3801–3819 (2012).
 209. Granata, V., Palladino, P., Tizzano, B., Negro, A., Berisio, R. & Zagari, A. The effect of the osmolyte trimethylamine N-oxide on the stability of the prion protein at low pH. *Biopolymers* **82**, 234–240 (2006).
 210. Natalello, A., Liu, J., Ami, D., Doglia, S. M. & de Marco, A. The osmolyte betaine promotes protein misfolding and disruption of protein aggregates. *Proteins: Structure, Function, and Bioinformatics* **75**, 509–517 (2009).

211. Singh, L. R., Dar, T. A., Rahman, S., Jamal, S. & Ahmad, F. Glycine betaine may have opposite effects on protein stability at high and low pH values. *Biochimica et Biophysica Acta (BBA)-Proteins and Proteomics* **1794**, 929–935 (2009).
212. Kaushik, J. K. & Bhat, R. Why is trehalose an exceptional protein stabilizer? An analysis of the thermal stability of proteins in the presence of the compatible osmolyte trehalose. *Journal of Biological Chemistry* **278**, 26458–26465 (2003).
213. Howard, S. B., Twigg, P. J., Baird, J. K. & Meehan, E. J. The solubility of hen egg-white lysozyme. *Journal of Crystal Growth* **90**, 94–104 (1988).
214. Retailleau, P., Ries-Kautt, M. & Ducruix, A. No salting-in of lysozyme chloride observed at low ionic strength over a large range of pH. *Biophys. J.* **73**, 2156–2163 (1997).
215. Cohn, E. The physical chemistry of proteins. *Physiological Reviews* **5**, 349–437 (1925).
216. Zeelen, J. P. Interpretation of the crystallization drop results. *Protein Crystallization Techniques, Strategies, and Tips, TM Bergfors, Ed. (International University Line, CA, 1999)*, 131 (2009).
217. McPherson, A. Introduction to protein crystallization. *Methods* **34**, 254–265 (2004).
218. Curtis, R., Prausnitz, J. & Blanch, H. Protein-protein and protein-salt interactions in aqueous protein solutions containing concentrated electrolytes. *Biotechnol. Bioeng.* **57**, 11–21 (1998).
219. Guo, B., Kao, S., McDonald, H., Asanov, A., Combs, L. L. & Wilson, W. W. Correlation of second virial coefficients and solubilities useful in protein crystal growth. *Journal of crystal growth* **196**, 424–433 (1999).
220. Haas, C., Drenth, J. & Wilson, W. W. Relation between the solubility of proteins in aqueous solutions and the second virial coefficient of the solution. *The Journal of Physical Chemistry B* **103**, 2808–2811 (1999).
221. Ruppert, S., Sandler, S. & Lenhoff, A. Correlation between the osmotic second virial coefficient and the solubility of proteins. *Biotechnology progress* **17**, 182–187 (2001).
222. Durbin, S. & Feher, G. Crystal growth studies of lysozyme as a model for protein crystallization. *Journal of Crystal Growth* **76**, 583–592 (1986).

223. Heidner, E. Protein crystallizations: The functional dependence of the nucleation rate on the protein concentration and the solubility. *Journal of Crystal Growth* **44**, 139–144 (1978).
224. Kam, Z., Shore, H. & Feher, G. On the crystallization of proteins. *Journal of molecular biology* **123**, 539–555 (1978).
225. Bruzzdziak, P., Panuszko, A. & Stangret, J. Influence of osmolytes on protein and water structure: A step to understanding the mechanism of protein stabilization. *The Journal of Physical Chemistry B* **117**, 11502–11508 (2013).
226. Auton, M., Rösgen, J., Sinev, M., Holthauzen, L. M. F. & Bolen, D. W. Osmolyte effects on protein stability and solubility: A balancing act between backbone and side-chains. *Biophys. Chem.* **159**, 90–99 (2011).
227. Bolen, D. & Baskakov, I. V. The osmophobic effect: Natural selection of a thermodynamic force in protein folding. *Journal of molecular biology* **310**, 955–963 (2001).

Quantification of PEGylated Proteases with Varying Degree
of Conjugation in Mixtures: An Analytical Protocol
Combining Protein Precipitation and Capillary Gel
Electrophoresis

Josefine Morgenstern, Markus Busch, Pascal Baumann and Jürgen Hubbuch

*Institute of Engineering in Life Sciences, Section IV: Biomolecular Separation Science,
Karlsruhe Institute of Technology (KIT), 76131 Karlsruhe, Germany*

Journal of Chromatography A 1462 (2016): 153–164.

Abstract

PEGylation, i.e. the covalent attachment of chemically activated polyethylene glycol (PEG) to proteins, is a technique commonly used in biopharmaceutical industry to improve protein stability, pharmacokinetics and resistance to proteolytic degradation. Therefore, PEGylation represents a valuable strategy to reduce autocatalysis of biopharmaceutical relevant proteases during production, purification and storage. In case of non-specific random conjugation the existence of more than one accessible binding site results in conjugates which vary in position and number of attached PEG molecules. These conjugates may differ considerably in their physicochemical properties. Optimizing the reaction conditions with respect to the degree of PEGylation (number of linked PEG molecules) using high-throughput screening (HTS) technologies requires a fast and reliable analytical method which allows stopping the reaction at defined times.

In this study an analytical protocol for PEGylated proteases is proposed combining preservation of sample composition by trichloroacetic acid (TCA) precipitation with high-throughput capillary gel electrophoresis (HT-CGE). The well-studied protein hen egg-white lysozyme served as a model system for validating the newly developed analytical protocol for 10 kDa mPEG-aldehyde conjugates. PEGamer species were purified by chromatographic separation for calibrating the HT-CGE system. In a case study, the serine protease Savinase[®] which is highly sensitive to autocatalysis was randomly modified with 5 kDa and 10 kDa mPEG-aldehyde and analyzed. Using the presented TCA protocol baseline separation between PEGamer species was achieved allowing for the analysis of heterogeneous PEGamer mixtures while preventing protease autocatalysis.

Keywords: *Autocatalysis; Protease PEGylation; TCA precipitation; PEGamer quantification; High-throughput capillary gel electrophoresis*

5.1 Introduction

Proteases already are widely applied as industrial catalysts in food processing (e.g. manufacturing of cheese in dairy industry), in the leather industry and as laundry detergents [228]. The rapid technological progress in the field of biotechnology enables the production of proteases with novel properties and substrates causing an increased interest in proteases for diagnostic and therapeutic applications in the pharmaceutical industry [228]. The global pharmaceutical market benefits from proteases as a growing class of drugs. In 2011 twelve protease therapies had been approved by the Food and Drug Administration (FDA) [229]. For instance, the recombinant extracellular serine proteases plasmin and tissue plasminogen activator (tPA) are applied in thrombolytic therapy as a treatment of heart attacks and ischemic stroke [230]. Both cardiovascular diseases represent the major causes of death in the western world [231]. They are both caused by circulatory blockages of blood vessels consisting mainly of insoluble fibrin. Plasmin directly degrades fibrin initiating clot breakdown whereas tPA catalyzes the reaction of the precursor plasminogen to the active plasmin by cleavage of a single bond [232, 233]. In the case of tPA the therapeutic application is aggravated due to a fast clearance from the blood stream resulting in an extremely short half-life of only two to six minutes [234, 235].

Moreover, proteases such as enterokinase, thrombin and factor Xa are used during the production of recombinant proteins for the removal of fusion tags [236–238]. Those tags are often attached to different peptides and proteins in order to simplify their expression, purification and analytics as well as to improve their solubility [238–240]. Fusion tags often need to be cleaved from protein drugs for meeting the regulatory standards since the tag may potentially modify the biological activity of the target protein or induce an immune response in the patient [241].

Modern biotechnology is capable of producing recombinant proteases to an industrial scale with high production efficiencies. However, a high loss of protease activity due to autoproteolytic degradation during production, purification and storage represent a major challenge [239, 242]. Different approaches to solve both short serum half-life of therapeutic proteins and autoproteolytic degradation include mutagenic variations of the amino-acid sequence [242], incorporating proteins into drug-delivery vehicles such as liposomes [235, 243] or microspheres of biodegradable polymers [244] and protein conjugation [142].

Protein conjugation denotes the linkage of synthetic polymers to a native protein in order to alter its physicochemical properties [245]. The attached molecules shield the protein surface which results in an enhanced stability towards proteases and a reduced recognition of the protein by the immune system [142], [246], [187]. The covalent attachment of chemically activated polyethylene glycol (PEG) to proteins is by this means one of the most commonly used technique in biopharmaceutical industry. PEG is especially interesting as a modifier for biopharmaceuticals since it is approved by the FDA for use in pharmaceuticals. It proved to show little toxicity and immunogenicity and it is eliminated from the body by the kidneys or in the feces [142]. The use of the hydrophilic polymer PEG as modifier results in an increased hydrodynamic radius of the protein in solution [247]. This effect engenders both an increased protein solubility and a decreased clearance from the blood stream. Several proteins, reaction mechanisms and conditions have been studied following first pioneering studies on PEGylated albumin and bovine liver catalase in the 1970s by the group of Abuchowski [133, 134]. Most commonly amino coupling PEG reagents binding to the N-terminus or to surface lysines, such as PEG-aldehyde are used [187]. The existence of more than one accessible binding site results in conjugates varying in position and number of attached PEG molecules. Those conjugates can significantly differ in their physicochemical properties [248]. The PEGylation reaction and thereby the conjugate mixture can be controlled through reaction conditions like the PEG to protein ratio, reaction time, temperature and solution pH. The interactions between these factors, however, make it difficult to reproduce protein batches in terms of Quality by Design (QbD) [19]. One of the key tools within the QbD-framework to gain a deeper process understanding are high-throughput screenings (HTS) coupled with Design of Experiments (DoE). Since speed and throughput of experimental facilities are constantly increasing appropriate high-throughput compatible analysis techniques of high resolution are crucial to determine the experimental outcome. The quantification of PEGylation processes remains a challenge due to poor spectrophotometric properties of PEG [249]. The increased molecular mass of protein conjugates promotes size exclusion chromatography (SEC) for quantitative separation of protein PEGamers. However, most SEC-based assays are limited by a maximum throughput of a few samples per hour. Approaches to increase the throughput of SEC include interlaced injection of samples, the parallel operation of two columns and multivariate evaluation of chromatographic data with poor resolution [250]. Especially protein conjugation with low molecular weight PEG molecules lead to poor separation of individual PEGamers by SEC. Capillary gel electrophoresis (CGE) represents an alternative to SEC with a reduced processing time of approximately 60 s per sample [125]. Due to the microfluidic measurement principle,

CGE provides a high peak resolution. As SEC, CGE separates proteins by molecular weight and therefore the conjugates by the number of attached PEG molecules [251]. This work demonstrates the potential of high-throughput capillary gel electrophoresis (HT-CGE) for the quantification of PEGylated proteins with varying degrees of conjugation. In the first part of this study the applicability of the standard HT-CGE protocol is shown for structural stable proteins using the model protein lysozyme from hen egg-white. For proteins that are subject to structural degradation an improved analytical protocol is presented which combines TCA (trichloroacetic acid) precipitation and high-throughput capillary gel electrophoresis. As an example the model serine protease Savinase[®] was chosen which could not be analyzed with the standard protocol due to high autocatalysis rates triggered by high temperatures used for denaturation during HT-CGE sample preparation. The benefit of integrating TCA precipitation into the analytical protocol is the immediate inactivation of the proteases and the resulting preservation of the sample composition. Moreover, TCA is assumed to precipitate all proteins in solution whereas salts and other buffer components remain in solution. TCA precipitation hence reduces the concentration of critical components from the sample [252] which otherwise may alter electrophoretic mobility of proteins in HT-CGE. The validated analytical method was subsequently used to determine the PEGamer composition for PEGylated Savinase[®] mixtures.

5.2 Materials and Methods

5.2.1 Overview of Workflow

The methods applied in this work are summarized schematically in Fig. 5.1. After producing PEGylated proteins via batch reactions a chromatographic purification was performed to isolate pure PEGamer (molecules with a varying number of attached PEG molecules) fractions. The purification of PEGylated lysozyme was performed by a two-step chromatography process of SEC followed by CEX. Savinase[®] was purified by a single CEX step (Fig. 5.1A). In this study a distinction is made between native proteins (non-PEGylated), proteins with one attached PEG molecule (mono-PEGylated) and proteins with two attached PEG molecules (di-PEGylated). Proteins with more than two attached PEG molecules (poly-PEGylated) are taken into consideration using a mass balance only. Each purified PEGamer fraction was subsequently used to determine a linear calibration curve for HT-CGE by linking the fluorescence signal to the PEGamer

concentration (Fig. 5.1B). For the standard protocol the PEGamer fractions were thereby used without further treatment. For the TCA protocol samples were precipitated with trichloroacetic acid before HT-CGE analysis. The described HT analytic was then applied to PEGylated protein samples with an unknown mixture composition (Fig. 5.1C).

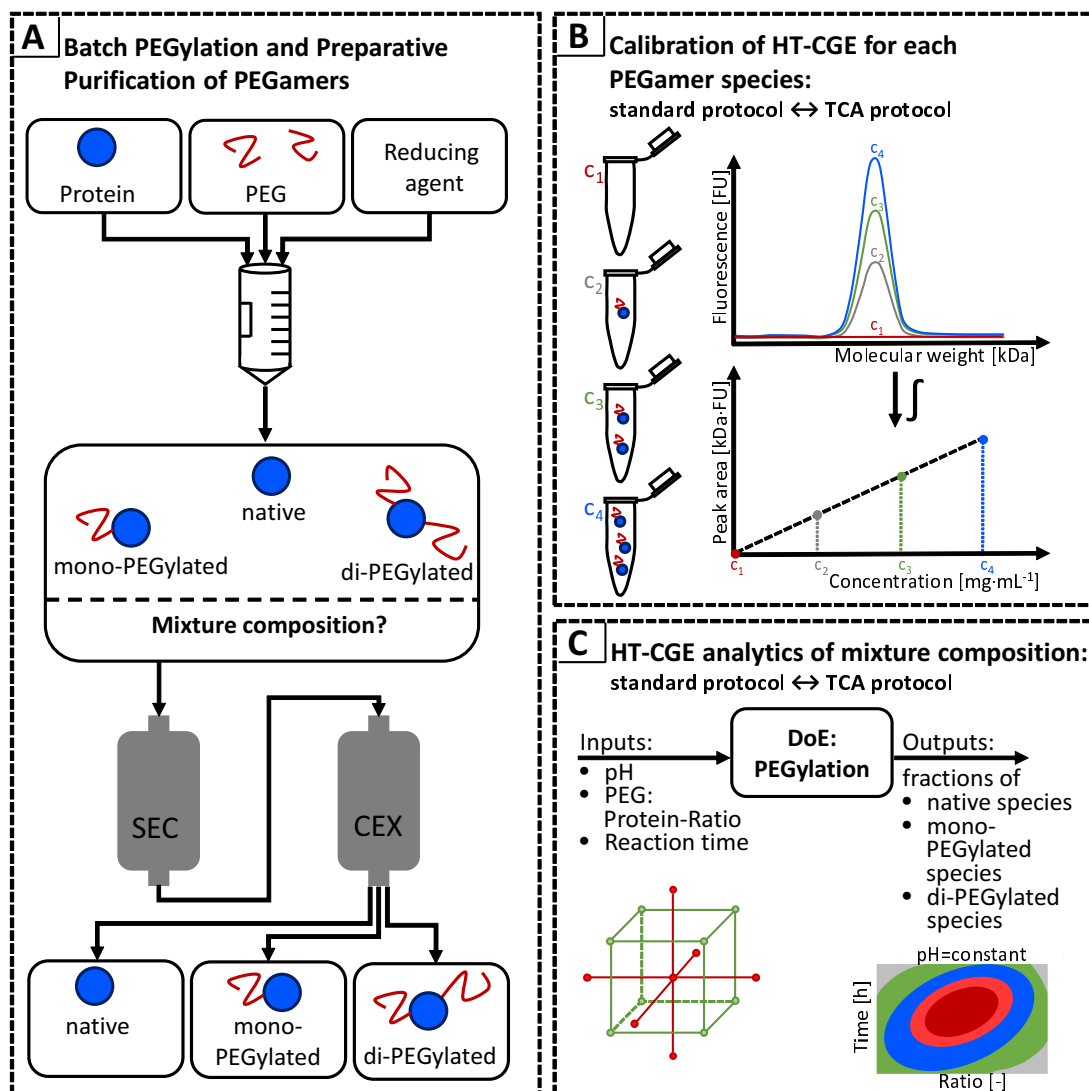


Figure 5.1: Schematic overview of the workflow for the development of a new analytical protocol for PEGylated proteins.

5.2.2 Preparation of Buffer and Protein Solutions

All solutions were prepared with ultrapure water provided by a PURELAB Ultra water purification system (ELGA Labwater, Germany). The used buffer substances were sodium acetate trihydrate (Sigma–Aldrich, St. Louis, MO, USA) and acetic acid (Merck, Germany) for pH 5 and sodium phosphate monobasic dihydrate (Sigma-Aldrich, USA) as well as di-sodium hydrogen phosphate dihydrate (Merck, Germany) for pH 6.2, pH 7.2 and pH 8.2. The buffer capacity was set to 25 mM for all buffers. Sodium chloride (NaCl) included in the SEC running buffer and the CEX elution buffer was purchased from Merck (Germany). pH adjustment within a range of ± 0.05 units was performed using a five-point calibrated pH-meter HI-3220 (Hanna Instruments, USA) with a SenTix[®] 62 pH electrode (Xylem Inc., USA). For pH correction hydrochloric acid and sodium hydroxide were obtained from Merck (Germany). Buffers were used at the earliest one day after preparation and repeated pH verification. All buffers were filtered using a 2 μ m cellulose-acetate filter (Sartorius, Germany) and degassed for chromatographic purposes. Protein solutions were prepared using Savinase[®] (Protease from *Bacillus* sp. liquid, ≥ 16 U/g) from Sigma-Aldrich (USA) and hen egg-white lysozyme (subsequently referred to as lysozyme) from Hampton Research (USA). Methoxy-PEG-propionaldehyde (mPEG-aldehyde) with an average molecular weight of 5 kDa (Sunbright ME-050 AL) and 10 kDa (Sunbright ME-100 AL) was obtained from NOF Corporation (Japan). Sodium cyanoborohydride (NaCNBH₃) as reducing agent for PEGylation and L-lysine for terminating the reaction were purchased from Sigma-Aldrich (USA). The Trichloroacetic acid (TCA) stock solution consisted of 50% (w/w) TCA (AppliChem, Germany) in ultrapure water.

5.2.3 Batch PEGylation

For the PEGamer isolation, PEGylation experiments were performed batch-wise in 15 mL Falcon Tubes (BD Biosciences, USA). 25 mM sodium phosphate buffer (pH 7.2) containing 20 mM NaCNBH₃ for lysozyme and 60 mM for Savinase[®] was used to dissolve mPEG-aldehyde. Protein was then added based on the desired molar PEG to protein ratio ($r = N_{PEG}/N_{protein}$ with N being the concentration of moles per volume). In case of lysozyme PEGamer isolation was performed with $r=6.67$ and $r=15$ for Savinase[®], respectively. The set protein concentration was 5 mg/mL for lysozyme and 10 mg/mL for Savinase[®]. For the PEGylation reaction the tube was continuously shaken in an overhead

shaker (Labinco LD79, Labinco BV, Brade, Netherlands) for 3.5 h in case of lysozyme and 24 h for Savinase[®]. The PEGylation reaction was stopped by adding 200 mM of L-lysine according to Ottow et al. [253].

5.2.4 Preparative Purification of PEGamers

Preparative separation of PEGamers was performed on an ÄKTA[™] purifier system equipped with an Autosampler A-905 and a Fraction Collector Frac-950 (GE Healthcare, Sweden). The purification of PEGylated lysozyme was performed by a two-step process involving a size exclusion (SEC) step followed by a cation exchange (CEX) step. A single CEX step was used to separate the different PEGylation degrees in case of Savinase[®].

5.2.4.1 Purification of Lysozyme PEGamers

The separation of lysozyme PEGamers was performed on a Superdex 200 Increase 10/300 GL (ID x L = 10 x 30 mm) (GE Healthcare, Uppsala, Sweden) SEC column using a 25 mM sodium phosphate buffer with 150 mM sodium chloride at pH 7.2. The column was loaded with 250 μ l of sample and the system was run at a flow rate of 0.8 mL/min. Fractions of 250 μ l were collected into a 96-well deep well plate (VWR, Radnor, PA, USA). The PEGamer containing fractions of multiple runs were pooled for each PEGamer species separately. As a desalting step for the subsequent cation exchange chromatography a buffer exchange to 25 mM sodium phosphate buffer (pH 7.2) was performed using Vivaspin[®] centrifugal concentrators (Sartorius, Germany) with PES membranes and a molecular weight cutoff of 5 kDa. The protein concentration was equally adjusted to approximately 3 mg/mL. Lysozyme concentrations were determined using a NanoDrop 2000c UV-Vis spectroscopic device (Thermo Fisher Scientific, USA) using an extinction coefficient of $\epsilon_{280\text{ nm, lysozyme}}^{1\%} = 22.00$ [254]. For PEGylated species the extinction coefficient of native lysozyme was assumed (Supplementary Figure A.1). Appropriate blanks were subtracted.

Polishing of lysozyme PEGamers was performed using cation exchange chromatography. Toyopearl GigaCap S-650M (mean particle diameter = 75 μ m) provided by Tosoh Bioscience (Germany) was used as stationary phase. The adsorber material was packed into an Omnitfit[®] column (0.34 $\text{cm}^2 * 10.5\text{ cm} = 3.6\text{ mL}$). For column loading, 25 mM sodium phosphate buffer at pH 7.2 was used and the injection volumes were set to 300 μ l. Elution was performed by applying an NaCl step gradient with an elution buffer containing 1 M

sodium chloride in 25 mM sodium phosphate buffer at pH 7.2. The elution steps were set to 0.045 M for di-PEGylated lysozyme and 0.1 M NaCl for mono-PEGylated lysozyme. The final elution step at 1 M NaCl for native lysozyme was followed by a 3.5 column volumes (CV) wash step at 1 M NaCl and a 2.5 CV reequilibration step with 25 mM sodium phosphate buffer (pH 7.2). The flowrate for binding, elution and equilibration was set to 1 mL/min. To obtain sufficient sample for HT-CGE calibration multiple chromatography runs were pooled. The pools were transferred into 25 mM sodium phosphate buffer (pH 7.2) and the protein concentrations were adjusted to 1 mg/mL using Vivaspin[®] centrifugal concentrators (Sartorius, Germany) with PES membranes and molecular weight cutoffs of 3 kDa for non-PEGylated species and 5 kDa for PEGylated species.

5.2.4.2 Purification of Savinase[®] PEGamers

Purification of Savinase[®] PEGamers was performed using a self-packed Omnifit[®] column with Toyopearl GigaCap S-650M as described in section 2.4.1. For column loading, 25 mM sodium acetate buffer at pH 5 was used. In order to reduce the influence of unreacted PEG on the binding behavior of the PEGamers to the cation exchange resin the PEGylation batch was diluted 1:50 in 25 mM sodium acetate buffer at pH 5. Injection of the diluted batch was performed using a 50 mL super loop purchased from GE Healthcare (Sweden). The flowrate for binding was set to 0.7 mL/min. Elution was performed by applying an NaCl step gradient with an elution buffer containing 1 M sodium chloride in 25 mM sodium acetate buffer at pH 5. The elution steps were 0.03 M for di-PEGylated Savinase[®] and 0.1 M NaCl for mono-PEGylated Savinase[®]. The final elution step at 1 M NaCl for native Savinase[®] was followed by a 2 CV wash step at 1 M NaCl and a 2 CV reequilibration step with 25 mM sodium acetate buffer (pH 5). The flowrate for elution, wash and equilibration was set to 1 mL/min. Again consecutive runs were pooled and transferred into 25 mM sodium acetate buffer (pH 5) using Slide-A-Lyzer[™] Dialysis Cassettes (Thermo Fisher Scientific, USA) with a molecular weight cut off of 10 kDa and a volume of 3-12 mL. Protein concentrations of the native Savinase[®] and the mono-PEGylated Savinase[®] pool were above 1 mg/mL. For HT-CGE analytics those pools were diluted to 1 mg/mL using 25 mM sodium acetate buffer (pH 5) in order to ensure a measurement in the linear range of the HT-CGE instrument. Di-PEG Savinase[®] needed to be concentrated to 1 mg/mL. Since di-PEGylated molecule species adsorbed to the PES membranes of the Vivaspin[®] centrifugal concentrators, concentrating was performed using a vacuum concentration unit RVC 2-33 CDplus (Martin

Christ Gefriertrocknungsanlagen GmbH, Germany). Savinase[®] concentrations were determined by a NanoDrop 2000c UV-Vis spectroscopic device using an extinction coefficient of $\epsilon_{280\text{ nm},\text{Savinase}}^{1\%} = 10.09$. The extinction coefficient was calculated with ExPASy ProtParam tool [255] using the UniProtKB-P29600 amino acid sequence. For PEGylated species the same extinction coefficient was assumed (Supplementary Figure A.1). Appropriate blanks were subtracted.

5.2.5 TCA Precipitation Protocol

In the TCA protocol, the samples first were precipitated with Trichloroacetic acid (TCA). 800 μL protein sample and 200 μL ice-cold TCA stock solution (50% (w/w)) were mixed in 2 mL Eppendorf tubes (Eppendorf, Germany). The mixtures were incubated for 30 minutes on ice. Subsequently, the precipitate was centrifuged for 15 minutes at 13300 rpm in a table-top Heraeus Pico 17 centrifuge (Thermo Fisher Scientific, USA). Then the pellet was washed twice with an equal volume of cold ultrapure water. After removing the water, 1000 μL of -20°C cold pure acetone (Merck, Germany) were added to the protein pellet and 800 μL of the acetone were directly removed. The sample was vortexed gently and centrifuged for 10 minutes at 13300 rpm on a table-top centrifuge. Remaining acetone evaporated overnight under a hood. The obtained protein pellets were redissolved in 800 μL ultrapure water for at least 1 h at 80°C in a Thermomixer Comfort (Eppendorf, Germany) for further analysis.

5.2.6 Protein Analysis Using HT-CGE

5.2.6.1 Analytical Procedure

For protein quantification an automated capillary gel electrophoresis device Caliper LabChip[®] GX II with an HT Protein Express LabChip[®] and an HT Protein Express Reagent Kit (Perkin Elmer, USA) were used. Experiments were carried out using the HT Protein Express 200 assay in the LabChip[®] GX 3.1 software. The LabChip[®] installation, sample preparation and analysis were performed according to the manufacturer's standard protocol. Sample preparation was performed in skirted 96-well polypropylene twin.tec[®] PCR plates from Eppendorf (Germany). Molecular weight determination was performed according to protein standards from the HT Protein Express Reagent Kit. Peak

area determination was conducted with MATLAB's (MathWorks, USA) trapezoidal numerical integration algorithm. To compensate for variations between different batches of the HT Protein Express Reagent Kit a scaling of the peak area to an external lysozyme protein standard of 1 mg/mL was performed for all protein measurements performed.

5.2.6.2 HT-CGE Calibration

For quantitative analysis of PEGamer concentrations in the Caliper LabChip® GX II HT-CGE system a calibration was required since PEG attached to the protein altered the retention behavior as well as the peak area of proteins. A ten point calibration between 0.1 mg/mL and 1 mg/mL was performed in 0.1 mg/mL steps as triplicates. Therefore, a serial dilution either of the concentrated PEGamer samples for the standard protocol or the redissolved TCA pellets for the TCA protocol were prepared.

5.2.7 HT-CGE Validation: Automated Batch PEGylation Screenings for Lysozyme

To validate the adapted TCA protocol, 29 samples with an unknown PEGamer composition were analyzed by the HT-CGE manufacturer's standard protocol and the TCA protocol for the model protein lysozyme. The 29 samples were prepared by PEGylation under varying reaction conditions in 300 μ L scale in 96-well UV-Star full-area plates (Greiner Bio-One, Austria) on a fully automated robotic liquid handling station (Freedom EVO® 200 from Tecan, Germany). The liquid handling station was operated using Evoware 2.5. Accurate liquid handling for a reproducible generation of PEGylated protein samples was assured by using custom liquid classes for buffers, PEG and protein solutions, respectively. The method to determine liquid classes, including important variables such as plunger volume, aspiration and dispense speed, was described earlier by Oelmeier et al. [256].

The 29 PEGylation experiments were selected according to an experimental design plan by MODDE 10.1 (Umetrics, Sweden). The design space was based on a D-optimal design with a quadratic model. pH values were varied in three steps covering 6.2, 7.2 and 8.2. In addition, the three different protein to PEG ratios $r=2.86$, $r=4$ and $r=6.67$ were screened resulting in nine different buffer conditions in total. To obtain kinetic PEGylation data, samples of the same buffer conditions were mixed with L-lysine for reaction termination according to Ottow et al. [23] after reaction times between 1.5 h and 12 h in 1.5 h intervals.

For $t=0$ it was assumed that the reaction mixture consisted of 100% native protein and no chemical reaction product was formed. This assumption was included as a boundary condition in the model although experiments for $t=0$ were not carried out. The lysozyme concentration was set to 4 mg/mL in all samples. During incubation, the plates were covered to avoid evaporation and mixed at 700 rpm on a Te-Shake orbital mixer (Tecan, Germany). The mixture composition of all samples was analyzed with HT-CGE using both the standard protocol and the adapted TCA protocol.

5.2.8 Application of the TCA Protocol to PEGamer Mixtures of Savinase[®]

The validated TCA protocol was consecutively applied to the serine protease Savinase[®]. First, four mixtures with a predetermined composition of the individual PEGamers (purified and quantified as described in section 2.4.2) were mixed in the concentration ratios displayed in Table 5.1. The prepared mixtures were precipitated according to the TCA protocol and analyzed using HT-CGE. Subsequently, the adapted TCA protocol was applied to a PEGylation sample with unknown composition. A PEGylation batch with $r=15$ at pH 7.2 (in 25 mM sodium phosphate) and a reaction time of 24 h was diluted to a total protein concentration of 1 mg/mL. 800 μ l of the diluted batch sample were precipitated by TCA and the resulting protein pellet was redissolved in 2000 μ l of ultra pure water. The resulting protein solution was analyzed with HT-CGE. The same procedure was applied for a modification of Savinase[®] with 5 kDa mPEG-aldehyde for comparing the applicability of the analytical procedure for other PEG molecules.

Table 5.1: Predefined composition of Savinase[®] PEGamers

	Mixture 1	Mixture 2	Mixture 3	Mixture 4
c(Native) [mg/mL]	0.34	0.11	0.26	0.81
c(mono-PEGylated) [mg/mL]	0.34	0.81	0.26	0.11
c(di-PEGylated) [mg/ml]	0.34	0.11	0.51	0.11

5.3 Results and Discussion

5.3.1 Preparative Purification of PEGamers

5.3.1.1 Purification of Lysozyme PEGamers

Since the PEGylation was performed using a PEG to protein excess, unreacted PEG remained in the mixture after the conjugation reaction. This weakened the interaction of native and PEGylated lysozyme with the cation-exchange media (results not shown). For lysozyme it was decided to use a SEC step to remove the excess PEG. SEC was performed using a Superdex 200 Increase 10/300 GL column with a bed volume of 23.6 mL. In Fig. 5.2 the SEC chromatogram of a PEGylation batch at pH 7.2 with $r=6.67$ after 3.5 h reaction time is displayed. The absorption signal at 280 nm is plotted against the retention volume. The chromatogram shows four peaks with maxima at retention volumes of 10.6 mL, 11.6 mL, 14.5 mL and 19.2 mL, respectively. Peak allocation for the PEG-

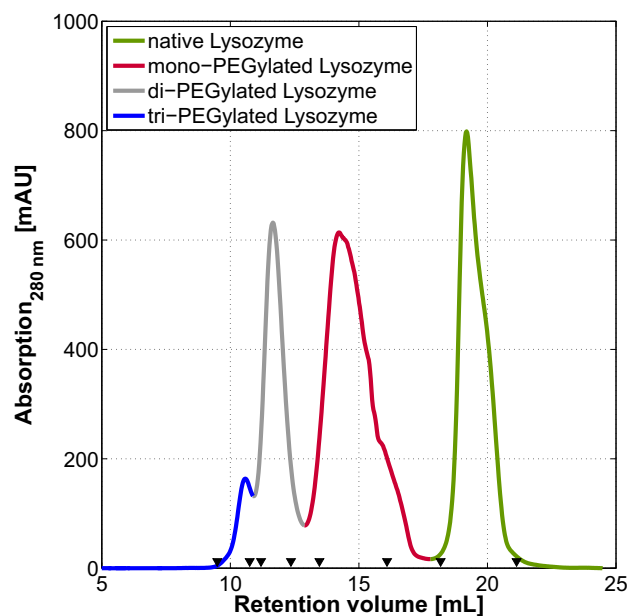


Figure 5.2: SEC chromatograms of a heterogeneous PEGamer mixture after batch PEGylation of lysozyme (pH 7.2, $r=6.67$ and $t=3.5$ h). The black triangles indicate the respective pooling limits for each PEGamer species.

amer species was performed on basis of the elution order in accordance with the results of Maiser et al. [257]. The peak eluting at 19.2 mL was assigned to native lysozyme by a reference sample. Baseline separation between the single species was not achieved applying SEC separation alone. From the chromatogram it is evident that under the selected reaction conditions only traces of tri-PEGylated lysozyme and no higher PEGylated species were formed. For this reason, PEGamer species with more than two attached PEG molecules were combined as poly-PEGylated in the further course of this study.

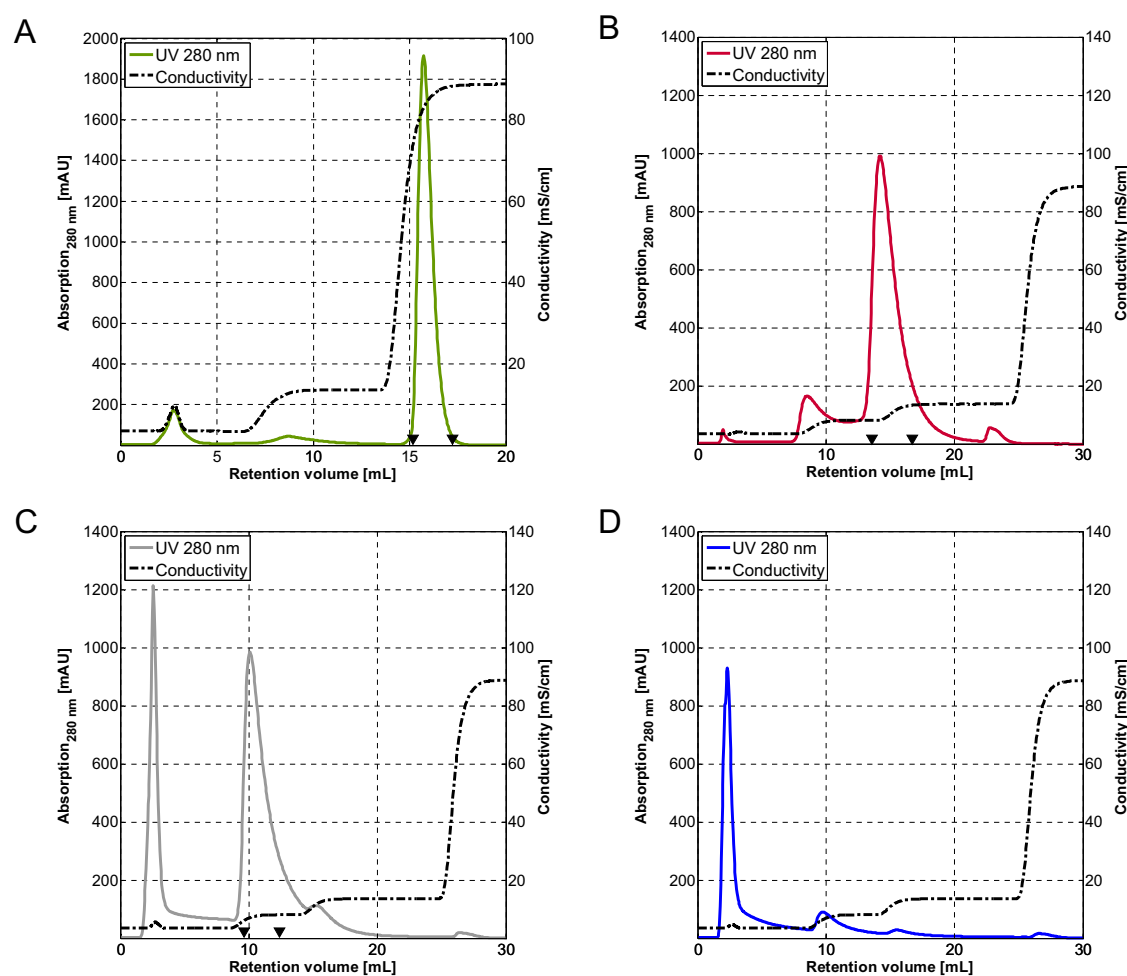


Figure 5.3: CEX chromatograms for pooled hen egg-white lysozyme fractions after SEC: A) native, B) mono-PEGylated, C) di-PEGylated, D) poly-PEGylated. The black triangles indicate the respective pooling limits for each PEGamer species.

After SEC separation of PEGamer species a cation exchange chromatography step was performed. In Fig. 5.3 the resulting CEX chromatograms with an NaCl gradient for the pooled PEGamer fractions after SEC are illustrated. The pooled fractions contained mainly the targeted PEGamer species. Impurities of the other species can be attributed to the wide pooling limits during SEC (illustrated by the black triangles in Fig. 5.2 for each PEGamer species). The comparison of Fig. 5.3A-D indicates that non-PEGylated lysozyme has the highest binding affinity to the adsorbent material of all PEGamers. The attachment of one PEG molecule already results in a significant decrease in binding strength, since mono-PEGylated lysozyme elutes at a conductivity of approximately 9 mS/cm (see Fig. 5.3B) whereas native lysozyme starts eluting at approximately 50 mS/cm (see Fig. 5.3A). All four sub-images show a flow-through which is especially pronounced for the di- and the poly-PEGylated SEC fractions. HT-CGE analysis of flow-through fractions showed a considerable amount of di- and poly-PEGylated species (data not shown) indicating a low binding affinity of di-PEGylated lysozyme to the GigaCapS 650M resin. These observations are described in literature inter alia by Yoshimoto et al. [258] and can be explained by PEG shielding the protein surface and respective surface charges necessary for protein-adsorbent-interactions. Fractions of 250 μ l were taken and pooled for the individual peaks in order to isolate pure protein samples for TCA precipitation and HT-CGE calibration (illustrated by the black triangles in Fig. 5.3A-C for native, mono-PEGylated and di-PEGylated lysozyme). PEGylated species that appeared as an impurity in one CEX run were added to the respective pure PEGamer sample pools and were not discarded. The purities of the individual PEGamer species were determined by HT-CGE and were above 98% for all PEGamers and pure lysozyme.

5.3.1.2 Purification of Savinase[®] PEGamers

SEC is a time consuming process step. In case of proteases long process times promote the formation of autocatalysis products. Therefore, the reduction of the purification process to a single cation exchange step was crucial for Savinase[®]. Initial experiments revealed that PEGylation of Savinase[®] requires a higher PEG to protein ratio compared to lysozyme (data not shown). With the aim to use a cation exchanger for PEGamer purification, the need for dilution of residual PEG increased analogously. The reduction of the negative influence of PEG during binding of proteins to the cation exchange resin was achieved by a 1:50 dilution of the reaction batch with cation exchange loading buffer

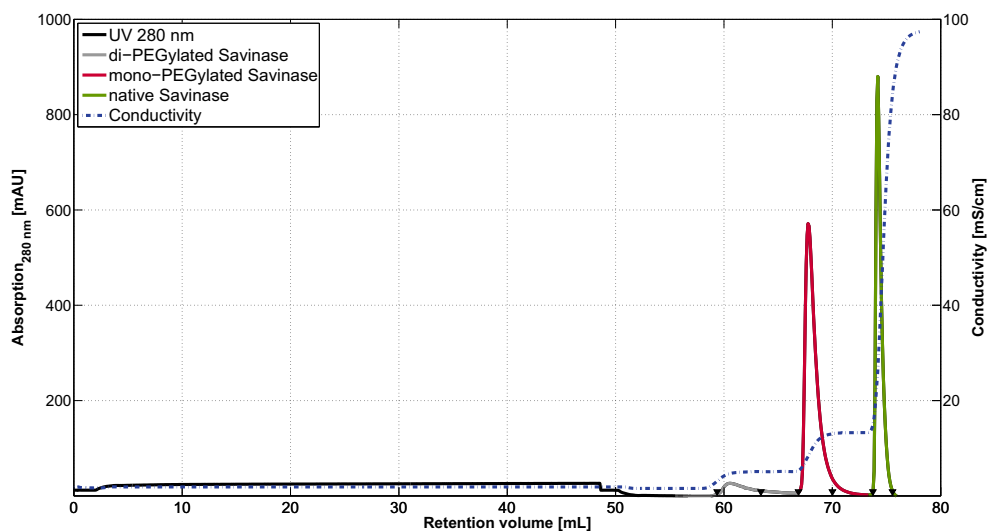


Figure 5.4: CEX chromatogram of a 1:50 diluted Savinase[®] PEGylation batch ($r=15$, pH 7.2, 24 h) loaded with a 50 mL loop. The black triangles indicate the respective pooling limits for each PEGamer species.

before binding. In Fig. 5.4 the resulting CEX chromatogram with an NaCl gradient is displayed. The first 48 mL of the chromatography run correspond to sample loading with a 50 mL loop. Through three salt steps 0.03 M, 0.1 M and 1.0 M NaCl baseline separated PEGamer peaks were generated. The allocation of the peaks for the PEGamer species was done by comparing the elution order to runs of PEGylated lysozyme (see Fig. 5.3). The electropherograms of PEGylated Savinase[®] species indicated similar molecular weights as those of the corresponding lysozyme species. The purities of the pooled PEGamer fractions (pooling limits are indicated in Fig. 5.4 by the black triangles) were determined by HT-CGE and were above 97% for all species.

5.3.2 Calibration of HT-CGE

Throughout HT-CGE analysis PEGylated species showed molecular masses which were higher than the expected total nominal weights of protein and polymer. For example, the mono-PEGylated Savinase[®] peak was correlated to a molecular weight of 69 kDa instead of the expected 37 kDa. Moreover, PEGylated species showed a distinct increase in peak area compared to the native protein. Both phenomena, the change in migration properties and the increase in peak area have been described in literature for sodium dodecyl sulfate

polyacrylamide gel electrophoresis (SDS-PAGE) [259, 260] as well as for CGE [125]. Both effects indicate that PEG attached to proteins hinders the electrophoretic mobility in the gel matrix of the microfluidic separation channel. The change in mobility is attributed to sample preparation and operating principle of HT-CGE. As the protein sample denatures, its tertiary structure resolves and the molecule is linearized. Linearized molecules follow the laminar flow profile in the microfluidic channel resulting in a narrow residence time distribution. Attached PEG molecules act as non-linearized side chains with an uncertain conformation. The nonlinearity deviates migration of PEGylated proteins from the ideal flow path and thereby slows down permeation through the gel matrix. Furthermore, a statistical distribution in residence time of single molecules within one PEGamer species is created which in turn results in peak broadening in the electropherogram of HT-CGE. This effect may be increased by the presence of different positional isoforms within one PEGamer species. Since in LabChip[®] GXII the internal molecular mass standard is used to allocate runtimes to molecular masses, a slowing effect not solely based on the molecular mass but also on the non-linearity of the molecule causes PEGylated species to appear heavier than they truly are [125].

A further effect is involved in the increase in peak area which is also described extensively in literature [261, 262]. Sodium dodecyl sulfate (SDS) binds at concentrations above the critical micelle concentration (CMC) to PEG molecules having a molecular weight above 4 kDa [261]. Since during HT-CGE analysis the CMC of SDS is exceeded, the attached PEG molecules act as an additional protein surface to which SDS adheres. Thus, the concentration of bound fluorescent marker increases and enhances the fluorescent peak area for PEGylated species. A higher fluorescence signal per PEGylated protein molecule in combination with the decelerated electrophoretic mobility explains higher peak areas. Since LabChip[®] GXII determines concentrations based on the peak area, the observed increase in peak area results in disproportional concentration results. A calibration of peak area with known protein concentrations was indispensable for PEGamers to compensate for such phenomena.

The calibration was performed by means of a serial dilution of each purified PEGamer species (see section 2.6.2) on the LabChip[®] GXII device. In Fig. 5.5 the resulting calibration curves are depicted for lysozyme analyzed by the standard protocol (A) and by the TCA protocol (B). In Fig. 5.5C the resulting electropherograms of a dilution series of mono-PEGylated Savinase[®] analyzed by the TCA protocol are exemplary shown for the calibrated concentration range between 0.1 mg/mL and 1 mg/mL. Through peak integration of the measured fluorescence signals for each PEGamer concentration and PEGamer species the calibration curves shown in Fig. 5.5D were calculated. As expected, for both

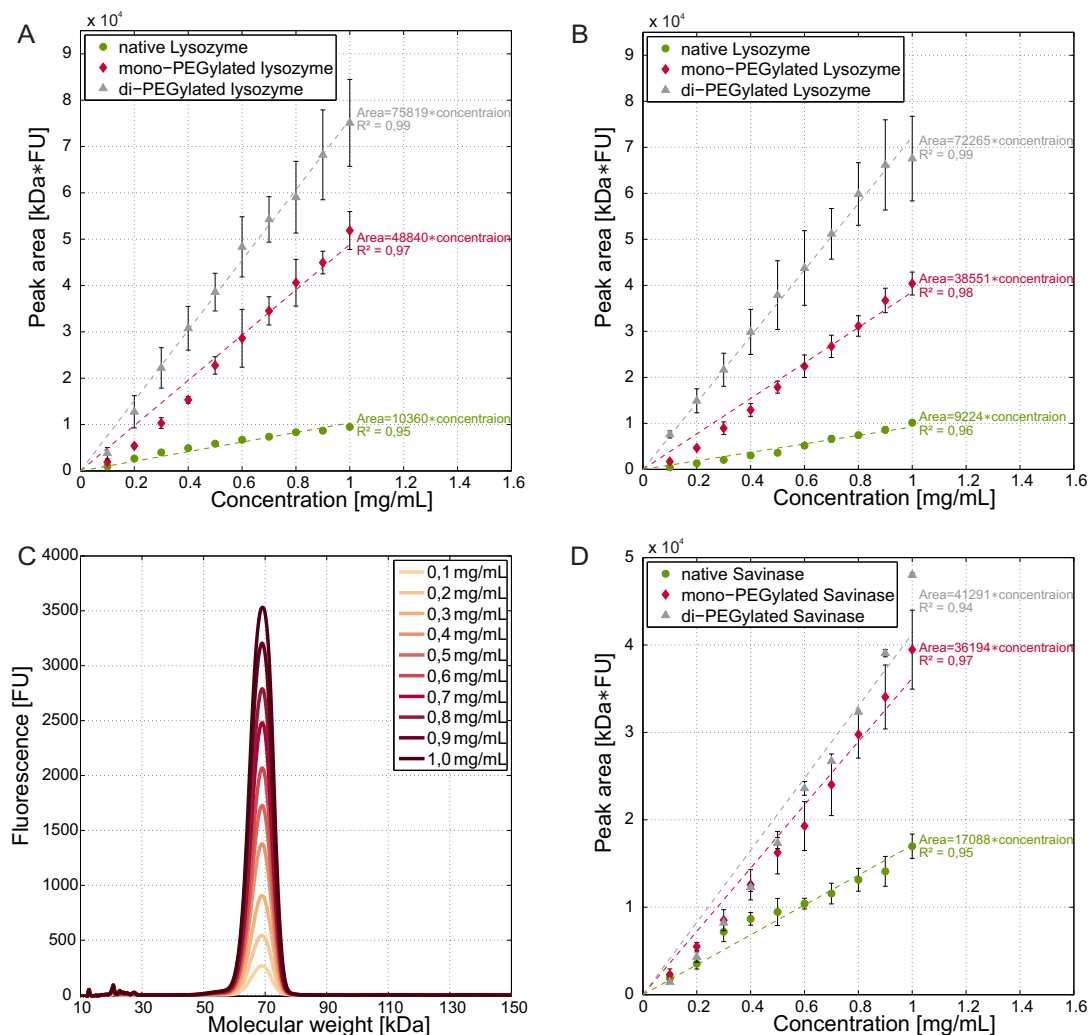


Figure 5.5: PEGamer concentration to peak area calibration for hen egg-white lysozyme analyzed by the standard HT-CGE protocol (A) and the TCA protocol (B), fluorescence signals of a linear dilution series of mono-PEGylated Savinase[®] gained using the TCA protocol (C) and the resulting calibration curves for all Savinase[®] species (D).

proteins the peak area increases with increasing PEGamer concentration for all species. A linear relationship (peak area = slope * concentration) between applied concentration and peak area was determined for all examined proteins and PEGamer species with adequate coefficients of determination. It becomes apparent that the slopes of the calibration curves increase with the number of bound PEG molecules. For lysozyme (Fig. 5.5A and

B) the two analytical protocols show similar progressions of calibration for the different PEGamer species within the measurement uncertainty. This indicates that in the case of lysozyme the TCA protocol and the standard protocol deliver equivalent analytical results. The TCA protocol could thus be used for Savinase[®]. For lysozyme, a linear increase of the slope of the calibration curve with an increasing number of bound PEG molecules was observed. For Savinase[®] a similar behavior of native and mono-PEGylated protein was observed as for lysozyme. However, the calibrations of mono-PEGylated and di-PEGylated Savinase[®] result in a comparable slope. The different behavior between lysozyme and Savinase[®] during the measurement of PEGylated species in HT-CGE might be explained by different interactions between the protein backbone and the bound PEG molecules in the denatured state. Attached PEG molecules with an uncertain conformation may result in a different electrophoretic mobility and SDS accessibility during the analysis. However, when performing adequate calibrations with purified PEGamers, such a behavior can be compensated for.

5.3.3 Validation of TCA Protocol

The establishment of a new analytical protocol requires the verification of obtained results in terms of accuracy and reproducibility. In this study the validation of the presented TCA protocol was performed using random batch PEGylation of the model protein lysozyme for which many reference values can be found in literature. By batch PEGylations at different reaction conditions PEGamer mixtures with unknown composition were produced. Those mixtures were analyzed by HT-CGE using both the standard protocol specified by the manufacturer and the adapted TCA protocol for determining non-PEGylated, mono-PEGylated and di-PEGylated lysozyme concentrations. The results were used to fit a response surface model investigating the influence of the parameters pH, reaction time and PEG to protein ratio r on the PEGylation behavior using MODDE. The model yielded an average value of 0.95 for R^2 and 0.91 for Q^2 for both analytical protocols and the three PEGamer species. These values indicate that the model formed by MODDE is valid and can therefore be used to predict the PEGamer fractions within the calibrated range for reaction conditions which were not investigated experimentally. In Fig. 5.6A the influence of the parameters pH value, reaction time and PEG to protein ratio r on the mixture composition is illustrated as analyzed by the standard protocol. The reproducibility of the automated PEGylation reactions was above 94% for all PEGamer species and the mass balances showed a recovery of total protein above 89% for all samples.

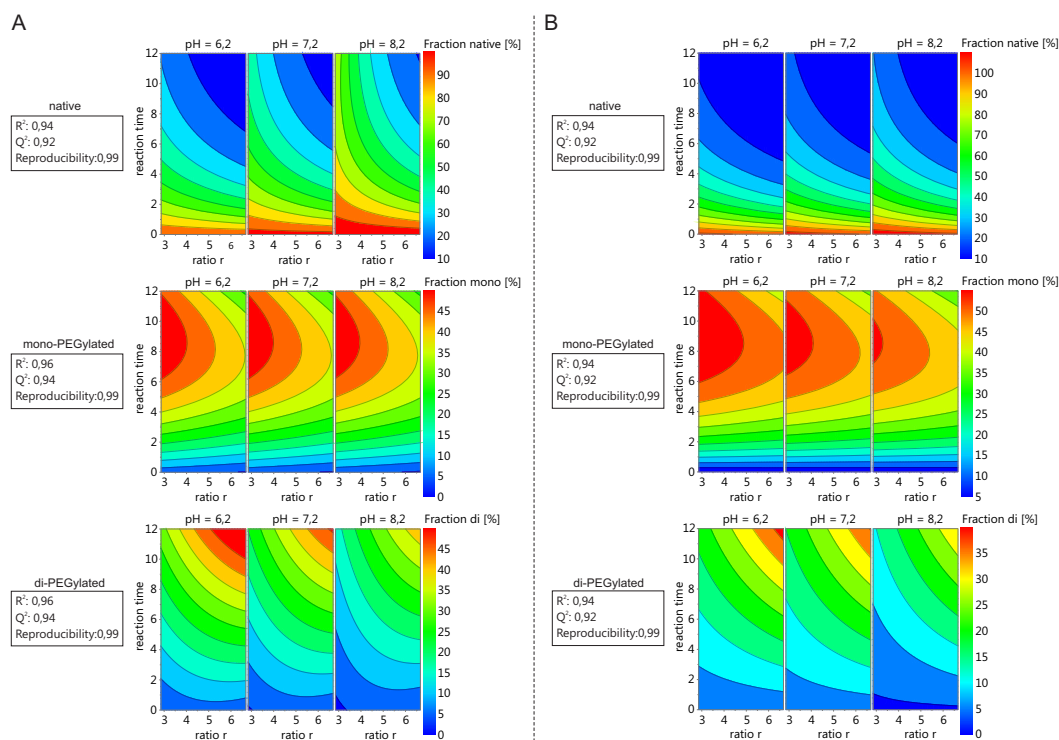


Figure 5.6: Design of experiments for investigating the PEGylation behavior of lysozyme for different reaction conditions: Comparison of the standard HT-CGE (A) and the TCA protocol (B) for the model protein hen egg-white lysozyme.

These results indicate precise liquid handling. It is obvious that a high PEG excess results in a decrease of native lysozyme for all pH values and reaction times. A simultaneous accumulation of PEG-protein conjugates can be observed as shown by [263] and [264]. Maximal concentrations of mono-PEGylated lysozyme were identified for PEG to protein ratios in a range of 3 to 4 and reaction times above 6 h. For higher PEG to protein ratios and reactions times a decrease of mono-PEGylated lysozyme is recorded which is accompanied by an increase in di-PEGylated lysozyme. In accordance with Maiser et. al [264] a lower buffer pH yields a faster PEGylation reaction as the maximal amount of di-PEGylated lysozyme was generated at pH 6.2. Comparing the results of the standard protocol to the adapted TCA protocol, differences in the fractions of each PEGamer are negligible. Thus, a comparable reaction behavior as a function of the investigated reaction parameters is detectable. The reproducibility and the consistency of the mass balance are in accordance with the standard protocol. As for the calibration of HT-CGE, this experimental set-up shows that the new TCA protocol provides results as the standard

protocol. The TCA protocol is therefore suitable for the analysis of proteins which cannot be analyzed by the standard protocol such as proteases of autocatalytic activity.

5.3.4 Analyzing Mixtures of PEGylated Savinase[®] Species Using the TCA Protocol

The described analytical method was tested within the calibrated concentration range with regard to linearity, reproducibility and accuracy for the used model protease Savinase[®] using four predefined samples of known composition. In Fig. 5.7 the PEGamer concentrations measured by the TCA protocol are plotted against the nominal concentration values for the four predefined mixtures. For all samples an evaluation of PEGamer concentrations in mixtures was achieved, which represents a major improvement compared

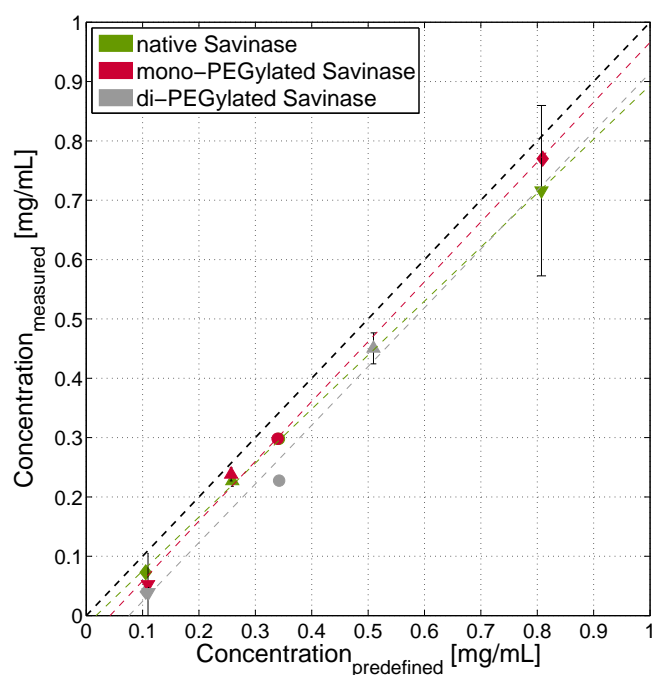


Figure 5.7: Comparison between predefined concentrations of Savinase[®] and the ones analyzed by the adapted TCA protocol for the model protease Savinase[®] in the PEGamers mixtures 1 (●), 2 (◆), 3 (▲) and 4 (▼).

to the HT-CGE measurements without the TCA precipitation step where the protease was entirely eliminated by autocatalysis (see Fig. 5.8A, black line). The linearity of gained results was shown both for the native protein as well as the PEGylated species with regression coefficients above 0.98. The multiple determinations of the individual PEGamer concentrations in the mixtures show a high reproducibility with the exception of native Savinase[®] at 0.8 mg/mL (mixture 4). All measured PEGamer concentrations are slightly undervalued compared to the nominal concentration value applied. The reduced measured values can be explained by protein losses during precipitation and redissolution of the denatured protein pellet. The largest deviations of up to 64% relative error between nominal and measured PEGamer concentration were observed for small protein concentrations of 0.1 mg/mL which corresponds to an absolute error of no more than 0.064 mg/mL. At this point the quantification limit was reached. With increasing protein concentration in the sample the relative error in the measurement decreases. For native and mono-PEGylated Savinase[®] the relative error was reduced to a range of 4.9% and 12.8% for protein concentrations above 0,1 mg/mL. Through an undervaluation of all absolute concentrations to a similar degree, however, the percentage composition of the different PEGamer species in mixtures are well displayed. Therefore, the introduced analytical protocol represents a valuable method to perform a high-throughput-based optimization of reaction conditions for the PEGylation of pharmaceutically relevant proteases.

After validating the adapted HT-CGE protocol for mixtures of known composition a PEGylated Savinase[®] batch with unknown PEGamer fractions was analyzed by HT-CGE. In Fig. 5.8A the resulting electropherogram is shown (red line). The peaks of the different PEGamer species are baseline-resolved so that integration and thus the quantification of the individual species in an unknown mixture is possible. The peak between 10 kDa and 25 kDa can be attributed to autocatalysis products formed during the 24 hours of PEGylation reaction. The peaks at 27 kDa, 70 kDa and 150 kDa correspond to native Savinase[®], mono-PEGylated Savinase[®] and di-PEGylated Savinase[®], respectively. Identical PEGylation conditions were used for the purification of PEGamer species (Fig. 5.4). In the chromatogram of the preparative purification and the electropherogram (Fig. 5.8, red line) similar fractions of the different protein species can be recognized but in a reverse order of runtimes. By integration of the peak area from the electropherogram and application of the calibration function PEGamer concentrations were calculated. The PEGylation of Savinase[®] with an initial protein concentration of 10 mg/mL at pH 7.2 with a PEG to protein ratio of $r=15$ yielded 3.77 mg/mL native Savinase[®], 4.22 mg/mL mono-PEGylated Savinase[®] and 0.56 mg/mL di-PEGylated Savinase[®] after 24 hours.

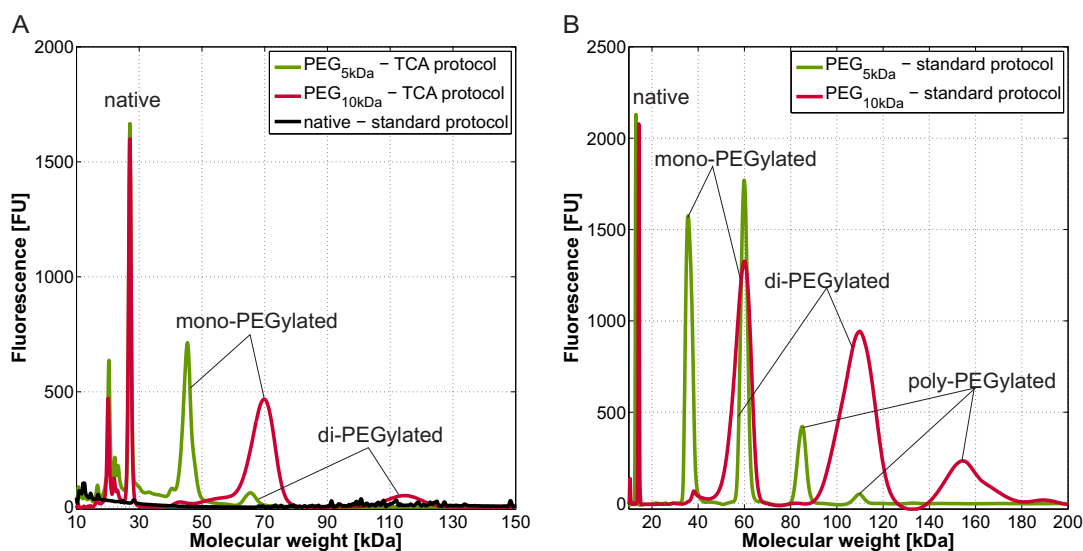


Figure 5.8: Comparison of 5 kDa and 10 kDa PEGylated Savinase[®] mixtures ($r=15$, pH 7.2 and $t=24$ h) analyzed by the TCA protocol and a native Savinase sample analyzed by the standard protocol (A) as well as comparison of 5 kDa and 10 kDa PEGylated lysozyme mixtures ($r=6,67$, pH 7.2 and $t=14.5$ h) analyzed by the standard protocol (B).

For comparison, the electropherogram of a native Savinase[®] sample ($c=1.5$ mg/mL) analyzed by the standard protocol is displayed in Fig. 5.8A (black line). An identification of individual protein species is not possible. Rather small protein fragments are detectable which may be aggregated partially. The decomposition of the sample is likely to be caused by high autocatalysis rates due to the elevated temperature used for denaturation during HT-CGE sample preparation.

The question which arises for a practical application of the presented PEGylation analytics is whether the method is applicable to other PEG molecular weights without a reduction of resolution. As an example, Savinase[®] was modified with a smaller molecular weight mPEG-aldehyde of 5 kDa as shown in Fig. 5.8A (green line). The individual PEGamer species remain baseline separated, but show lower molecular weights than the PEGamer species modified with 10 kDa mPEG-aldehyde (red line). As can be seen, the molecular weights of 5 kDa di-PEG and 10 kDa mono-PEG conjugates equal each other. They consequently have the same hydrodynamic radius. The increase in size upon PEGylation is therefore only dependent on the molecular weight of the bonded PEG molecules and regardless of their number. This observation has already been demonstrated by Fee and Van Alstine [139] for size exclusion chromatography. The same observation was

made for lysozyme as displayed in Fig. 5.8B. These results demonstrate that HT-CGE is a valuable tool to analyze both stable (with the standard protocol) and instable protein conjugates (with the TCA protocol) with respect to their degree of conjugation for variable polymer molecular weights within the studied parameter range.

5.4 Conclusion

In the presented work, purified samples of protein PEGamers were used for the calibration of high-throughput capillary gel electrophoresis (HT-CGE). A distinction was made between the standard protocol specified by the manufacturer and the newly applied TCA protocol. As shown for lysozyme, the standard protocol is applicable to monitor PEGylation reactions for structurally stable proteins. In this case, HT-CGE provides an analytical method with a low sample consumption of only 2 μL , an analysis time of 40 s per sample, a high resolution allowing for peak baseline separation and a high sensitivity down to 0.1 mg/mL of PEGylated species. In contrast, the TCA protocol includes a denaturing precipitation step by trichloroacetic acid. The main advantage of this approach is the preservation of the sample composition, which allows time-resolved measurements of proteins which are subject to degradation. In this study, the model protease Savinase[®] was examined as an example of a critical protein, since proteases are highly affected by autocatalysis. However, the method can be applied to all kinds of kinetic studies of protein reactions. The validation of the new protocol has successfully been carried out for mixtures of PEGylated lysozyme. The two protocols resulted in comparable PEGamer concentration ratios for a DoE of PEGylation experiments under distinct reaction conditions. The validated TCA protocol was successfully applied for the model protease Savinase[®]. The problem of autocatalysis resulting in irreproducible results during the analysis of PEGylated proteases can be overcome by applying a protein precipitation step. The presented combination of TCA precipitation and HT-CGE analytics was found to be a fast and reproducible tool for the tracking of PEGylated species for both stable and instable proteins.

5.5 Acknowledgments

The authors would like to acknowledge the financial support by the German Federal Ministry of Education and Research (BMBF). This research work is part of the project

”Molecular Interaction Engineering: From Nature’s Toolbox to Hybrid Technical Systems”, funding code 031A095B. We gratefully acknowledge Tosoh Bioscience GmbH (Griesheim, Germany) for providing chromatographic materials in the context of the Tosoh Chromatography Scholarship 2015. We want to thank Lara Galm and Kai Baumgartner, former scientist at the Institute of Engineering in Life Sciences (KIT), for the scientific support and Carina Brunner for her support in the laboratory.

5.6 References

19. Lawrence, X. Pharmaceutical quality by design: product and process development, understanding, and control. *Pharm. Res.* **25**, 781–791 (2008).
125. Seyfried, B. K., Marchetti-Deschmann, M., Siekmann, J., Bard, M. J., Scheiflinger, F., Turecek, P. L. & Allmaier, G. Microchip capillary gel electrophoresis of multiply PEGylated high-molecular-mass glycoproteins. *Biotechnol. J.* **7**, 635–641 (2012).
130. Fee, C. J. & Van Alstine, J. M. PEG-proteins: Reaction engineering and separation issues. *Chemical engineering science* **61**, 924–939 (2006).
133. Abuchowski, A., McCoy, J., Palczuk, N., van Es, T. & Davis, F. Effect of covalent attachment of polyethylene glycol on immunogenicity and circulating life of bovine liver catalase. *J. Biol. Chem.* **252**, 3582–3586 (1977).
134. Abuchowski, A., van Es, T., Palczuk, N. C. & Davis, F. F. Alteration of Immunological Properties of Bovine Serum Albumin by Covalent Attachment of Polyethylene Glycol. *Journal of Biological Chemistry* **252**, 3578–3581 (1977).
139. Fee, C. J. & Van Alstine, J. M. Prediction of the viscosity radius and the size exclusion chromatography behavior of PEGylated proteins. *Bioconjugate chemistry* **15**, 1304–1313 (2004).
142. Harris, J. M. & Chess, R. B. Effect of PEGylation on pharmaceuticals. *Nat. Rev. Drug Discov.* **2**, 214–221 (2003).
187. Veronese, F. M. & Pasut, G. PEGylation, successful approach to drug delivery. *Drug Discovery Today* **10**, 1451–1458 (2005).
228. Li, Q., Yi, L., Marek, P. & Iverson, B. L. Commercial proteases: Present and future. *FEBS Letters* **587**, 1155–1163 (2013).
229. Craik, C. S., Page, M. J. & Madison, E. L. Proteases as therapeutics. *Biochemical Journal* **435**, 1–16 (2011).

230. Sheehan, J. J. & Tsirka, S. E. Fibrin-modifying serine proteases thrombin, tPA, and plasmin in ischemic stroke: A review. *Glia* **50**, 340–350 (2005).
231. WorldHealthOrganization. *Media centre* <http://www.who.int/mediacentre/factsheets/fs310/en/>. [Online; accessed 07/2017].
232. Chen, W. T. Membrane proteases: Roles in tissue remodeling and tumour invasion. *Current Opinion in Cell Biology* **4**, 802–809 (1992).
233. Weidle, U. H., Buckel, P. & Wienberg, J. Amplified expression constructs for human tissue-type plasminogen activator in Chinese hamster ovary cells: Instability in the absence of selective pressure. *Gene* **66**, 193–203 (1988).
234. Rouf, S. A., Moo-Young, M. & Chisti, Y. Tissue-type plasminogen activator: Characteristics, applications and production technology. *Biotechnology advances* **14**, 239–266 (1996).
235. Kim, J. Y., Kim, J. K., Park, J. S., Byun, Y. & Kim, C. K. The use of PEGylated liposomes to prolong circulation lifetimes of tissue plasminogen activator. *Biomaterials* **30**, 5751–5756 (2009).
236. Terpe, K. Overview of bacterial expression systems for heterologous protein production: From molecular and biochemical fundamentals to commercial systems. *Applied Microbiology and Biotechnology* **72**, 211–222 (2006).
237. Li, Y. Self-cleaving fusion tags for recombinant protein production. *Biotechnology Letters* **33**, 869–881 (2011).
238. Baumann, P., Bluthardt, N., Renner, S., Burghardt, H., Osberghaus, A. & Hubbuch, J. Integrated development of up- and processes supported by the Cherry-Tag for real-time tracking of stability and solubility of proteins. *J. Biotech.* **200**, 27–37 (2015).
239. Kapust, R. B., Tözsér, J., Fox, J. D., Anderson, D. E., Cherry, S., Copeland, T. D. & Waugh, D. S. Tobacco etch virus protease: Mechanism of autolysis and rational design of stable mutants with wild-type catalytic proficiency. *Protein engineering* **14**, 993–1000 (2001).
240. Ohana, R. F., Encell, L. P., Zhao, K., Simpson, D., Slater, M. R., Urh, M. & Wood, K. V. HaloTag7: A genetically engineered tag that enhances bacterial expression of soluble proteins and improves protein purification. *Protein Expr. Purif.* **68**, 110–120 (2009).

-
241. Arnau, J., Lauritzen, C., Petersen, G. E. & Pedersen, J. Current strategies for the use of affinity tags and tag removal for the purification of recombinant proteins. *Protein Expr. Purif.* **48**, 1–13 (2006).
242. Rose, J. R., Salto, R. & Craik, C. S. Regulation of autoproteolysis of the HIV-1 and HIV-2 proteases with engineered amino acid substitutions. *Journal of Biological Chemistry* **268**, 11939–11945 (1993).
243. Tiukinhoy-Laing, S. D., Huang, S., Klegerman, M., Holland, C. K. & McPherson, D. D. Ultrasound-facilitated thrombolysis using tissue-plasminogen activator-loaded echogenic liposomes. *Thrombosis Research* **119**, 777–784 (2007).
244. Sinha, V. R. & Trehan, A. Biodegradable microspheres for protein delivery. *Journal of Controlled Release* **90**, 261–280 (2003).
245. Lutz, J. F. & Börner, H. G. Modern trends in polymer bioconjugates design. *Progress in Polymer Science* **33**, 1–39 (2008).
246. Mehvar, R. Modulation of the pharmacokinetics and pharmacodynamics of proteins by polyethylene glycol conjugation. *Journal of pharmacy and pharmaceutical sciences* **3**, 125–136 (2000).
247. Pfister, D. & Morbidelli, M. Process for protein PEGylation. *Journal of Controlled Release* **180**, 134–149 (2014).
248. Gaberc-Porekar, V., Zore, I., Podobnik, B. & Menart, V. Obstacles and pitfalls in the PEGylation of therapeutic proteins. *Current Opinion in Drug Discovery and Development* **11**, 242 (2008).
249. Zillies, J. C., Zwiorek, K., Winter, G. & Coester, C. Method for quantifying the PEGylation of gelatin nanoparticle drug carrier systems using asymmetrical flow field-flow fractionation and refractive index detection. *Anal. Chem.* **79**, 4574–4580 (2007).
250. Hansen, S. K., Maiser, B. & Hubbuch, J. Rapid quantification of protein–polyethylene glycol conjugates by multivariate evaluation of chromatographic data. *J. Chrom. A* **1257**, 41–47 (2012).
251. Roberts, M. J. & Harris, J. M. Attachment of degradable poly(ethylene glycol) to proteins has the potential to increase therapeutic efficacy. *J. Pharm. Sci.* **87**, 1440–1445 (1998).

252. Jiang, L., He, L. & Fountoulakis, M. Comparison of protein precipitation methods for sample preparation prior to proteomic analysis. *J. Chrom. A* **1023**, 317–320 (2004).
253. Ottow, K. E., Lund-Olesen, T., Maury, T. L., Hansen, M. F. & Hobley, T. J. A magnetic adsorbent-based process for semi-continuous PEGylation of proteins. *Biotechnol. J.* **6**, 396–409 (2011).
254. Galm, L., Morgenstern, J. & Hubbuch, J. Manipulation of lysozyme phase behavior by additives as function of conformational stability. *Int. J. Pharm.* **494**, 370–380 (2015).
255. Gasteiger, E., Hoogland, C., Gattiker, A., Duvaud, S., Wilkins, M. R., Appel, R. D. & Bairoch, A. *Protein identification and analysis tools on the ExPASy server* (Springer, 2005).
256. Oelmeier, S. A., Dismer, F. & Hubbuch, J. Application of an aqueous two-phase systems high-throughput screening method to mAb HCP separation. *Biotechnol. Bioeng.* **108**, 69–81 (2011).
257. Maiser, B., Kröner, F., Dismer, F., Brenner-Weiß, G. & Hubbuch, J. Isoform separation and binding site determination of mono-PEGylated lysozyme with pH gradient chromatography. *J. Chrom. A* **1268**, 102–108 (2012).
258. Yoshimoto, N. & Yamamoto, S. PEGylated protein separations: Challenges and opportunities. *Biotechnol. J.* **7**, 592–593 (2012).
259. Zheng, C. Y., Ma, G. & Su, Z. Native PAGE eliminates the problem of PEG-SDS interaction in SDS-PAGE and provides an alternative to HPLC in characterization of protein PEGylation. *Electrophoresis* **28**, 2801–2807 (2007).
260. Odom, O. W., Kudlicki, W., Kramer, G. & Hardesty, B. An effect of polyethylene glycol 8000 on protein mobility in sodium dodecyl sulfate-polyacrylamide gel electrophoresis and a method for eliminating this effect. *Anal. Biochem.* **245**, 249–252 (1997).
261. Dai, S. & Tam, K. C. Isothermal titration calorimetry studies of binding interactions between polyethylene glycol and ionic surfactants. *The Journal of Physical Chemistry B* **105**, 10759–10763 (2001).
262. Maltesh, C. & Somasundamn, P. Effect of Binding of Cations to Polyethylene Glycol on Its Interactions with Sodium Dodecyl Sulfate. *Langmuir* **8**, 1926–1930 (1992).

263. Moosmann, A., Blath, J., Lindner, R., Müller, E. & Böttinger, H. Aldehyde PEGylation kinetics: A standard protein versus a pharmaceutically relevant single chain variable fragment. *Bioconjugate chemistry* **22**, 1545–1558 (2011).
264. Maiser, B., Dimer, F. & Hubbuch, J. Optimization of random PEGylation reactions by means of high throughput screening. *Biotechnol. Bioeng.* **111**, 104–114 (2014).

Effect of PEG Molecular Weight and PEGylation Degree on the Physical Stability of PEGylated Lysozyme

Josefine Morgenstern, Pascal Baumann, Carina Brunner and Jürgen Hubbuch

Institute of Engineering in Life Sciences, Section IV: Biomolecular Separation Science, Karlsruhe Institute of Technology (KIT), 76131 Karlsruhe, Germany
International Journal of Pharmaceutics 519 (2017): 408–417.

Abstract

During production, purification, formulation, and storage proteins for pharmaceutical or biotechnological applications face solution conditions that are unfavorable for their stability. Such harmful conditions include extreme pH changes, high ionic strengths or elevated temperatures. The characterization of the main influencing factors promoting undesired changes of protein conformation and aggregation, as well as the manipulation and selective control of protein stabilities are crucially important to biopharmaceutical research and process development. In this context PEGylation, i.e. the covalent attachment of polyethylene glycol (PEG) to proteins, represents a valuable strategy to improve the physico-chemical properties of proteins.

In this work, the influence of PEG molecular weight and PEGylation degree on the physical stability of PEGylated lysozyme is investigated. Specifically, conformational and colloidal properties were studied by means of high-throughput melting point determination and automated generation of protein phase diagrams, respectively. Lysozyme from chicken egg-white as a model protein was randomly conjugated to 2 kDa, 5 kDa and 10 kDa mPEG-aldehyde and resulting PEGamer species were purified by chromatographic separation. Besides protein stability assessment, residual enzyme activities were evaluated employing a *Micrococcus lysodeikticus*-based activity assay. PEG molecules with lower molecular weights and lower PEGylation degrees resulted in higher residual activities. Changes in enzyme activities upon PEGylation have shown to result from a combination of steric hindrance and molecular flexibility. In contrast, higher PEG molecular weights and PEGylation degrees enhanced conformational and colloidal stability. By PEGylating lysozyme an increase of the protein solubility by more than 11 fold was achieved.

Keywords: *PEGylation; Protein phase diagram; Melting point determination; Molecular flexibility; Enzyme activity*

6.1 Introduction

The outstanding potential of proteins for industrially relevant applications is based on their highly specific interactions with a target molecule due to their individual amino acid sequence and three-dimensional structure. The high activity of proteins at moderate concentrations and temperatures renders them an extremely beneficial alternative to small molecule compounds [77]. The current state of knowledge of biotechnology enables the production of recombinant proteins for pharmaceutical or biotechnological applications with high production efficiencies. However, many recombinant proteins are prone to instabilities during cell cultivation, purification, formulation and storage, which manifest mostly in a loss of functionality. In terms of pharmaceutical proteins, instabilities may equally result in immune responses and serious side effects when applied to the patient [6].

Protein instabilities can be divided into two classes being of chemical and physical nature [60]. Chemical instabilities include processes in which covalent bonds are formed or broken [60]. On the other hand, physical instabilities are related to a change in the physical state of the protein without involving an alteration of the chemical protein composition [60]. Therefore, physical instabilities comprise conformational changes of the protein structure and colloidal changes (e.g. aggregation). Závodszy et al. [265] further divide the term conformational stability into macrostability and microstability. Macroscopically stable proteins maintain the integrity of their native state and are not subject to either partial or complete unfolding. Microstability is described as the flexibility of the protein molecule due to fluctuations of the internal energy. Furthermore, it is stated that the enzyme activity and conformational flexibility are closely correlated for a macroscopically stable protein. The term colloidal stability in the sense of protein aggregation describes the assembly of protein monomers to multimers and characterizes the formation of protein crystals, amorphous precipitates and also incorporates cross-linked structures such as protein gels.

The occurrence of protein instabilities is often caused by a complex and hardly predictable interplay of environmental conditions such as extreme pH values, presence of organic solvents, non-physiological salt concentrations, high protein concentrations and high temperatures influencing molecule interactions [81, 82]. Characterization and control of protein stabilities as critical quality attributes are essential to process development. In order to take a step towards predictability of protein stabilities, several analytical techniques have to be employed and interlinked [266].

Also, a thorough characterization of protein stabilization strategies for an enhanced robustness of functional biomolecules presents one of the critical challenges in biotechnology. Stabilization strategies are based either on modulation of properties of the surrounding aqueous solution or on modifications of the protein itself. For some therapeutic proteins such as the granulocyte colony stimulating factor (G-CSF) [25, 267] or the recombinant human tissue factor pathway inhibitor (rhTFPI) [268] moderate salt concentrations can already induce instabilities. In a review by Hansen et al. effects of buffer substances, pH levels, precipitating agents, surfactants are summarized for the enzyme Xylanase [269]. Besides adjusting the pH value and the salt concentration, a stabilization of proteins can be achieved by the addition of various excipients. Most commonly low molecular weight osmolytes such as polymers and polyols [254] are employed. Additional stabilizing candidates were determined to be cyclodextrins and surfactants [270], as well as sugars (e.g. sucrose), enzymatic co-factors, amino acids [271], and ampholytes such as Tween[®]20 [272].

Besides altering the chemical surroundings of the protein, protein modification is another approach for stabilization. The portfolio of modification includes site-directed mutagenesis, the addition of protein fusion tags and polymer conjugation. In case of site-directed mutagenesis specific and rational changes of the primary amino acid sequence are performed via recombinant DNA technologies [60]. When using fusion tags for engineering protein stability, additional amino acids are fused to the product which are mostly composed of an amino acid sequence from a highly stable or soluble peptide or protein. Such tags include the maltose-binding protein (MBP) [273], Thioredoxin (Trx), the phage T7 protein kinase (T7PK) [274], the Cherry-Tag [238, 275, 276], as well as synthetic solubility-enhancing tags (SETs) used by Zhang et al. [277]. Polymer conjugation denotes the linkage of synthetic polymers to a native protein in order to alter its physico-chemical properties. In contrast to protein and peptide fusion tags where the additional amino acids are already added to the genetic code of the host strain, the chemical modification of the protein is performed after product isolation and purification.

In this study, the potential of PEGylation, i.e. the covalent attachment of chemically activated polyethylene glycol (PEG), as an example of polymer conjugation for the stabilization of proteins is demonstrated. In order to understand stabilization mechanisms, several analytical methods are applied and their results compared. PEG is especially interesting as a modifier for biopharmaceuticals since it is approved by the FDA for the use in pharmaceuticals. It proved to show little toxicity and immunogenicity and it is eliminated from the body by the kidneys or in the feces [142]. Da Silva Freitas et al. [278] illustrated that PEGylation of lysozyme with a 5 kDa polymer entails a stable protein

conformation, an improved thermal stability, as well as resistance to enzymatic degradation. Further examples can be found in a study by Nie et al. for recombinant human endostatin modified with 5 kDa PEG [279] and by Basu et al. for interferon-beta using 40 kDa PEG [280].

Whereas the beneficial effect of PEG is widely proven in industry and academia, there is a lack of detailed and systematic studies on the influence of PEG molecular weight, as well as PEGylation degree on different types of protein stability. In particular, knowledge of the functional, conformational and colloidal stability of PEGylated proteins is missing. Therefore the aim of this study is to investigate systematically physical stability attributes using different PEG molecular weights and PEGylation degrees. To assess the influence of PEG molecular weight on the physico-chemical properties upon PEGylation, 2 kDa, 5 kDa and 10 kDa mPEG-aldehyde is conjugated to the model protein lysozyme (from chicken egg white). In order to evaluate the differences in stability in dependency of the PEGylation degree, protein species with different numbers of attached PEG molecules (PEGamers) are purified by chromatographic separation after random batch PEGylation. A distinction is made between native proteins (non-PEGylated), proteins with one attached PEG molecule (mono-PEGylated) and proteins with two attached PEG molecules (di-PEGylated).

Since PEGylation is known to evoke changes of the in vitro activity (resp. functional stability) of proteins [142], the residual enzyme activity after PEGylation is assessed and compared to the native protein using the lysozyme-specific activity assay based on the substrate *Micrococcus lysodeikticus*. Furthermore, the influence of PEGylation on the physical stability is investigated by evaluation of the macroscopic conformational stability by means of melting point determination using intrinsic protein fluorescence under an increased salt concentration. Additionally, the colloidal stability of PEGylated lysozyme is evaluated using an automated screening technique described by Baumgartner et al. [79]. Thereby, the combined influence of an extreme pH value (pH 3) and non-physiological salt concentrations are investigated.

6.2 Materials and Methods

6.2.1 Materials

All solutions were prepared with ultrapure water provided by a PURELAB Ultra water purification system (ELGA Labwater, Germany). The used buffer substances were

citric acid monohydrate (Merck, Germany) as well as sodium citrate tribasic dihydrate (Sigma-Aldrich, USA) for pH 3, sodium acetate trihydrate (Sigma-Aldrich, USA) for pH 5 and sodium phosphate monobasic dihydrate (Sigma-Aldrich, USA) as well as di-sodium hydrogen phosphate dihydrate (Merck, Germany) for pH 7.2. Sodium chloride (NaCl) included in the cation exchange chromatography (CEX) elution buffer and the precipitation buffers for phase diagrams were purchased from Merck (Germany). Sodium sulfate (Na_2SO_4) for the study of colloidal stability was purchased from Merck (Germany). pH adjustment of all buffers within a range of ± 0.05 units was performed using a five-point calibrated pH-meter HI-3220 (Hanna Instruments, USA) with a SenTix[®] 62 pH electrode (Xylem Inc., USA). For pH correction hydrochloric acid and sodium hydroxide were obtained from Merck (Germany). All buffers were filtered using a $0.2 \mu\text{m}$ cellulose-acetate filter (Sartorius, Germany) and degassed for chromatographic purposes.

Protein solutions were prepared using chicken egg-white lysozyme (subsequently referred to as lysozyme) from Hampton Research (USA). Methoxy-PEG-propionaldehyde (mPEG-aldehyde) with an average molecular weight of 2 kDa (Sunbright[®]ME-020 AL), 5 kDa (Sunbright[®]ME-050 AL) and 10 kDa (Sunbright[®]ME-100 AL) was obtained from NOF Corporation (Japan). Sodium cyanoborohydride (NaCNBH_3) as reducing agent for PEGylation and L-lysine for terminating the reaction were purchased from Sigma-Aldrich (USA). Caliper LabChip[®]GX II system, HT ProteinExpress LabChip[®] and HT Protein Express Reagent Kit for HT-CGE analysis were obtained from PerkinElmer (USA).

6.2.2 Methods

6.2.2.1 Batch PEGylation and Purification of PEGamers

PEGylation experiments were performed batch-wise in 50 mL Falcon Tubes (BD Biosciences, USA). 25 mM sodium phosphate buffer (pH 7.2) containing 20 mM NaCNBH_3 as reducing agent was used to dissolve lysozyme and mPEG-aldehyde. The lysozyme concentration was kept constant at 5 mg/mL for all PEGylation experiments. mPEG-aldehyde addition was based on the desired molar PEG to protein ratio ($r = N_{PEG}/N_{protein}$ with N being the concentration of moles per volume) of 6.67 [264, 281]. To investigate the influence of the PEG molecular weight on the different stability attributes of PEGylated proteins, 2 kDa, 5 kDa and 10 kDa mPEG-aldehyde was conjugated to lysozyme. For the PEGylation reaction, the tube was continuously shaken in an overhead shaker (Labin-

coLD79, Labinco BV, Netherlands) for 3.5 h at room temperature. The PEGylation reaction was stopped by adding 200 mM of L-lysine according to [253].

6.2.2.2 Isolation of PEGamers by Cation Exchange Chromatography

In order to reduce the influence of unreacted PEG on the binding behavior of the native protein and the PEGamers to the cation exchange resin the PEGylation batch was diluted 1:12 in 10 mM sodium acetate buffer (pH 5) [281]. Preparative separation of PEGamers was performed on an ÄKTA™ purifier system equipped with a Fraction Collector Frac-950 (GE Healthcare, Sweden). As stationary phase a 5 mL prepacked MiniChrom column with Toyopearl GigaCap S-650M resin (Tosoh Bioscience, Deutschland) was used. For column loading, the system was equilibrated in 10 mM sodium acetate buffer (pH 5). Sample application was performed using a 50 mL super loop (GE Healthcare, Sweden). Elution was performed by applying an NaCl step gradient with an elution buffer containing 1 M sodium chloride in 10 mM sodium acetate buffer at pH 5. The NaCl molarities used for the step elution of the different PEGamers are displayed in Table 6.1 in dependence of the molecular weight of the attached PEG molecules. The flow rate for binding and elution was set to 1 mL/min. Fractions of 2 mL were collected into a 96-well deep well plate (VWR, USA). To obtain sufficient sample volume for stability assessment of the different PEGamer species the corresponding fractions of multiple chromatography runs were pooled. Peak allocation to the different PEGamer species and purity determination were performed by high-throughput capillary gel electrophoresis (HT-CGE) using the Caliper LabChip®GX II device (PerkinElmer, USA) as described in [281].

Table 6.1: NaCl steps in mol/L used for the elution of different PEGamer species from Toyopearl GigaCap S-650M at pH 5 in dependency of the PEG molecular weight

	Native lysozyme	mono-PEGylated lysozyme	di-PEGylated lysozyme
$M_w=2$ kDa	1	0.46	0.29
$M_w=5$ kDa	1	0.35	0.16
$M_w=10$ kDa	1	0.25	0.075

6.2.2.3 Sample Conditioning and Concentration Determination

The characterization of the isolated PEGamer species with regard to the different stability attributes required a sample conditioning consisting of buffer exchange (resp. pH-change) and concentration increase. Buffer exchange was carried out using Slide-A-Lyzer™ Dialysis Cassettes (Thermo Fisher Scientific, USA) with a molecular weight cut-off of 2 kDa. The dialysis buffer was thereby determined by the pH value required for the succeeding stability test. Concentrating of protein samples was performed by evaporation using a vacuum concentration unit RVC 2-33CDplus (Martin Christ Gefriertrocknungsanlagen GmbH, Germany) operated at 24 mbar. Lysozyme concentrations were determined using a NanoDrop 2000c UV-Vis spectroscopic device (Thermo Fisher Scientific, USA) using an extinction coefficient of $\epsilon_{280\text{ nm, lysozyme}}^{1\%} = 22.00$ [254]. For PEGylated species the same extinction coefficient was assumed [281]. Since the bound PEG molecules do not absorb at 280 nm [281], the absorption measurement yields the mass concentration of lysozyme molecules in the sample without considering the mass of the bound PEG. To avoid confusion, the mass concentrations of native lysozyme and protein conjugates of different PEG molecular weights were converted into molar concentrations. For this purpose, a molecular weight of lysozyme of 14.3 kDa was used [282]. This approach allows the comparison of stability properties for a constant number of total molecules.

6.2.2.4 Determination of Stability Attributes for PEGylated Lysozyme

Purified lysozyme PEGamers with varying PEGylation degree (non-PEGylated = native, mono-PEGylated and di-PEGylated) and molecular weight of attached PEG (2 kDa, 5 kDa and 10 kDa) were tested for their functional, conformational and colloidal stability.

6.2.2.5 Functional Stability - Activity Assay using *Micrococcus Lysodeikticus*

Quantification of enzyme activity was performed using *Micrococcus lysodeikticus* cells (Sigma Aldrich, USA) as substrate. The kinetic assay is based on the lysis of the bacterial cells by lysozyme resulting in a decrease of turbidity over time. The turbidity was monitored by measuring the absorption at 450 nm (resp. light scattering) with an UV-vis

Infinite M200 plate reader from Tecan (Germany) which was controlled by the software i-control 1.9. Absorption measurements were carried out in 96-well flat-bottom UV-Star[®] full-area micro-plates (Greiner Bio-One, Germany).

The *Micrococcus lysodeikticus* cells were suspended in 25 mM sodium phosphate buffer at pH 7.2. The starting OD value of the *Micrococcus lysodeikticus* suspension was adjusted to 1.7 AU. Samples of native lysozyme and mono-PEGylated as well as di-PEGylated lysozyme with 2 kDa, 5 kDa and 10 kDa PEG molecules attached were adjusted to a concentration of $6,99 \cdot 10^{-2}$ mmol/L (corresponds to 1 mg/mL unmodified protein) in 10 mM sodium acetate buffer (pH 5) as described in section 2.2.3. From this stock solution a serial dilution from $6,99 \cdot 10^{-3}$ mmol/L to $6,99 \cdot 10^{-2}$ mmol/L (corresponds to 0.1 to 1 mg/mL unmodified protein) in $6,99 \cdot 10^{-3}$ mmol/L steps was prepared. Of each diluted sample 7.5 μ L were pipetted to a 96 well micro-plate and 200 μ L *Micrococcus lysodeikticus* suspension were added. Absorption measurements at 450 nm was performed for 10 minutes in 75 s intervals with orbital shaking in between the measurements. A blank consisting of 7.5 μ L 10 mM sodium acetate buffer (pH 5) and 200 μ L *Micrococcus lysodeikticus* suspension was measured likewise. The absorbance values of the protein samples were subtracted from the absorbance values of the *Micrococcus lysodeikticus* blank resulting in a positive slope of the measured values over time. Every sample was measured as triplicate and for calculation of reaction rate the average was used.

6.2.2.6 Conformational Stability - Melting Point Determination

Elevated temperatures and non-physiological concentrations are among the main influencing factors favoring protein unfolding. The exposure of the hydrophobic amino acid residues (e.g. tryptophan) to an aqueous environment upon unfolding results in a shift of the fluorescence emission from blue to red wavelengths [69]. A plot of fluorescence emission wavelength (barycentric mean fluorescence = BCM) against the applied temperature is sigmoidal, with the inflection point being denoted as protein melting point temperature (T_m). An increasing T_m reflects an increase in macroscopic conformational stability [60, 283].

In this study, the combined influence of increased temperature and elevated NaCl concentrations on the conformational stability of native and PEGylated lysozyme species was evaluated by melting point determination. Protein stock solutions were prepared in 100 mM citric buffer (pH 3) and concentrations of native and PEGylated lysozyme solutions were set to 1,89 mmol/L. According to Baumgartner et al. [79] twelve salt solutions

with an uniform increase in NaCl concentration between 0 M and 5 M were prepared by mixing of 100 mM citric buffer (pH 3) and 100 mM citric buffer (pH 3) containing 2.5 M NaCl or 100 mM citric buffer (pH 3) containing 2.5 M NaCl and 100 mM citric buffer (pH 3) containing 5 M NaCl. The samples for melting point determination were generated by mixing equal amounts of protein stock solution and salt solution. Final samples contained 0,94 mmol/L protein and salt concentrations between 0 M and 2.5 M NaCl.

For the prepared samples, T_m was determined non-invasively in multi-cuvette arrays with the Optim[®] II device (Avacta Analytical, England) by measuring the intrinsic fluorescence evoked by the intrinsic tryptophan residues. The system was operated with the Optim 2.1 software. A temperature ramp with 0.25°C/min steps from 20°C to 95°C was performed. The filters UV 266 and Blue 473 were each set to a constant value of 0.25 before each measurement. For export of raw data Igor Pro 6.37 software was used. Obtained raw data was fitted using MATLAB (MathWorks, USA) fits of sigmoidal shape and the inflection point of the fit was assigned as melting point.

6.2.2.7 Colloidal Stability - Generation of Phase Diagrams

Phase diagrams of non-PEGylated lysozyme from chicken egg white were generated earlier [79]. At pH 3 using sodium chloride as precipitant, lysozyme from chicken egg white showed multiple phase transitions including crystallization, precipitation and skin formation. Therefore, pH 3 (100 mM Citric buffer) and sodium chloride as precipitant were selected for investigating the effect of PEGylation on the colloidal stability of proteins. Using the methodology presented by [79] in total four protein phase diagrams for mono-PEGylated lysozyme with 2 kDa, 5 kDa and 10 kDa PEG molecules as well as for di-PEGylated lysozyme with 2 kDa attached PEG molecules were generated on an automated liquid handling station (Freedom EVO[®]200 from Tecan, Germany). Evaluation of phase states was conducted based on photographs taken by the Rock Imager 182/54 automated imaging system (Formulatrix, USA). In order to determine solubility lines the protein concentration in the supernatant of batch systems where a phase transition occurred was determined after 40 days using a NanoDrop 2000c UV-Vis spectroscopic device (Thermo Fisher Scientific, USA) [254].

In order to compare the colloidal stability of native and PEGylated lysozyme samples for additional protein and salt concentration extremes not included in the preliminary screening, two outlying system compositions with NaCl as precipitant were examined.

These systems consisted firstly of 1.52 mmol/L protein and 3.75 M NaCl and secondly of 3.04 mmol/L protein and 2.5 M NaCl. The mixtures were equally prepared in a 24 μ L scale on crystallization plates (MRC Under Oil 96 Well Crystallization Plates purchased from Swissci, Switzerland). In Table 6.2 the required stock solutions and the mixed volumes are displayed. Furthermore, Baumann et al. [284] have shown that native lysozyme precipitates under the influence of 1.25 mol/L sodium sulfate (Na_2SO_4) at pH 3 instantly. No stable solution conditions for lysozyme were detected even for protein concentrations below 2 mg/ml. For this reason, the colloidal stability of native and PEGylated species (2 kDa mono- and di-PEGylated, 5 kDa mono-PEGylated and 10 kDa mono-PEGylated) was additionally investigated using Na_2SO_4 as precipitant. The chosen system composition, required stock solutions and the mixed volumes are displayed in Table 6.2.

Table 6.2: Concentrations of stock solutions for the preparation of the isolated systems for the evaluation of colloidal stability

	1.52 mmol/L protein + 3.75 M NaCl	3.04 mmol/L protein + 2.5 M NaCl	1.52 mmol/L protein + 1.25 M Na_2SO_4
c(Protein) [mg/mL]	87	87	65.25
V(Protein) [μ L]	6	12	8
c(salt) [M]	5	5	1.875
V(Salt) [L]	18	12	16

6.3 Results and Discussion

6.3.1 Preparative Purification of Lysozyme PEGamers

Preparative purification of lysozyme PEGamers was performed by a single cation exchange step. In Fig. 6.1 the resulting CEX chromatograms with an NaCl step gradient for 1:12 diluted PEGylation batches with 2 kDa (A), 5 kDa (B) and 10 kDa (C) are displayed. Native lysozyme had the highest binding affinity to the adsorbent given that a higher salt concentration is required to elute it than for PEGylated species. For PEGylated species, a decrease in binding strength with increasing PEGylation degree was observed for all PEG molecular weights. The comparison of the salt concentration necessary for the elution of PEGylated species in Figure 1A-C indicates that for a constant PEGylation degree the binding strength decreases with increasing PEG molecular weight.

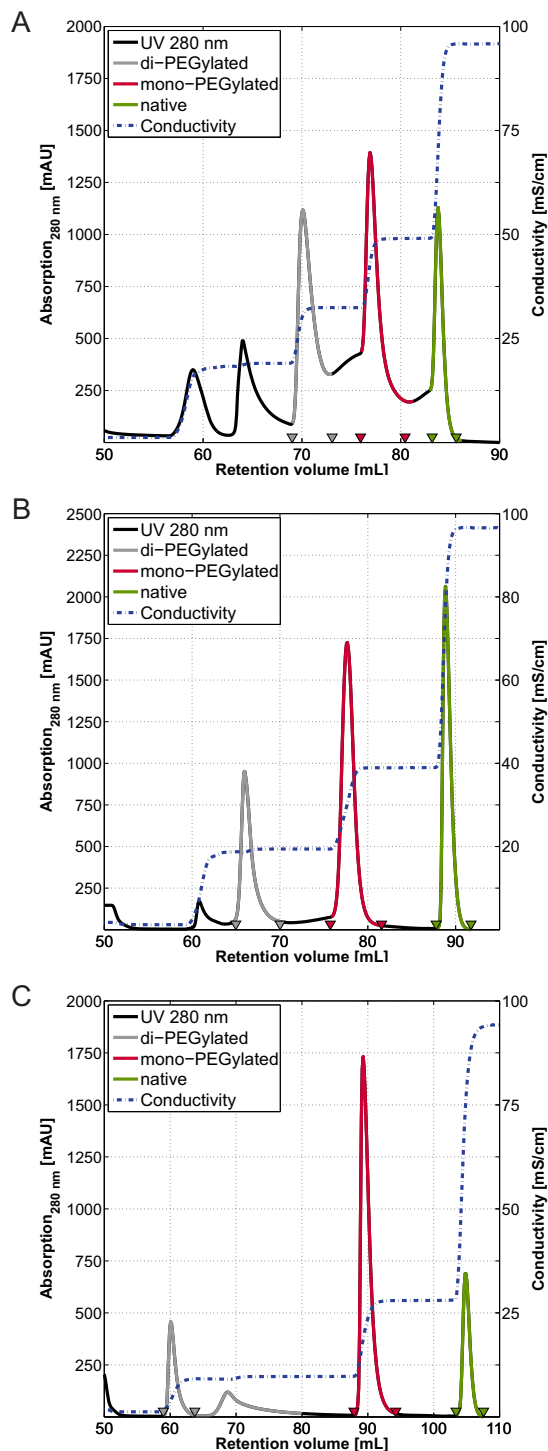


Figure 6.1: CEX chromatograms of 1:12 diluted PEGylation batches ($r=6.67$, pH 7.2, 3.5 h) loaded with a 50 mL loop for 2 kDa PEG (A), 5 kDa PEG (B) and 10 kDa PEG (C). The triangles indicate the respective pooling limits for each PEGamer species.

Modified binding affinities can be explained by weakened electrostatic interactions between protein binding site and adsorber surface due to the attached polymer [149, 258]. Whereas for 5 kDa and 10 kDa the differences in binding strength of the individual PEGamer species were high enough to achieve baseline separation between the individual protein species, the differences in the binding strength for the 2 kDa conjugates were significantly lower. For 2 kDa PEGylation, a very exact adjustment of the salt steps was necessary for a separation which did not allow for a complete baseline separation. Despite the careful selection of salt steps, an isocratic elution of mono-PEGylated lysozyme is apparent in the chromatogram for 2 kDa PEG. By appropriate choice of the pooling limits (indicated in Figure 1 by the triangles) purities above 98.2% were achieved for all PEGamer species (determined by HT-CGE). These findings indicate that the modification of the apparent surface charge of proteins upon PEGylation depends on the PEGylation degree as well as on the PEG molecular weight.

In addition to altering the binding strength, PEGylation also increases the hydrodynamic radius of PEGylated proteins. Previous studies had shown that the increase in size upon PEGylation was solely dependent on the total nominal weight of attached PEG molecules

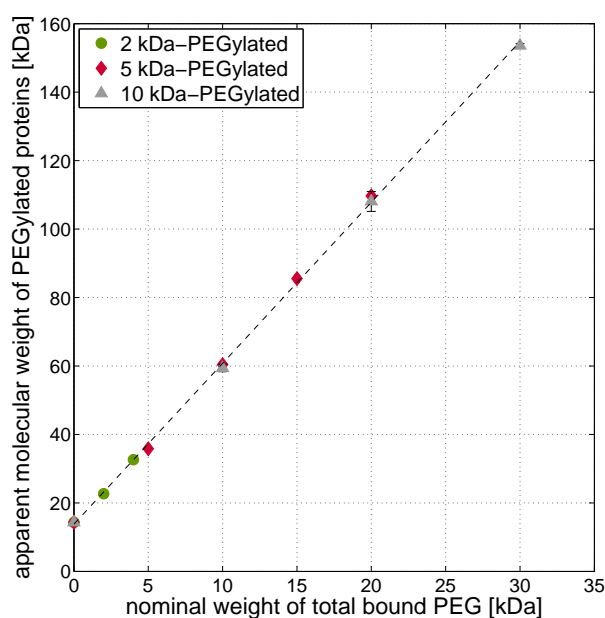


Figure 6.2: Increase in the hydrodynamic radius of PEGylated proteins in dependence of number and molecular weight of attached PEG molecules measured by HT-CGE. The error bars correlate to the 95 % confidence interval (1.96σ).

and regardless of their number [139, 257, 281]. This finding was verified with a linear relationship between the nominal weight of total bound PEG (e.g. 2 kDa di-PEGylated lysozyme has in total 4 kDa PEG attached) and the apparent molecular weight of PEGylated proteins for 2 kDa, 5 kDa and 10 kDa PEG upon HT-CGE analysis (see Fig. 6.2).

6.3.2 Functional Stability - Residual Activity of PEGamers

The effect of PEG molecular weight and PEGylation degree on the catalytic activity of PEGylated lysozyme was investigated. The activity of an enzyme corresponds to the rate of the catalyzed reaction, i.e. the substrate depletion $\Delta c_{substrate}$ per time interval Δt [285]. The reaction rate for lysozyme r_{lys} is therefore described by Eq. 6.1 for a given initial substrate to protein ratio.

$$r_{lys} = \frac{\Delta c_{substrate}}{\Delta t} \propto \frac{\Delta Abs_{450nm}}{\Delta t} \quad (6.1)$$

In this study, the reaction rate was derived from the slope of a linear fit of the measured absorbance values since the absorption at 450 nm is proportional to the concentration of substrate when the substrate is not limiting. For reaction rate calculations, only the linear part of the progression curve (absorption at 450 nm over time) was taken into account (=initial rate period). The Michaelis-Menten equation describes how this reaction rate differs with a changing initial substrate to protein ratio [285]. In order to consider varying substrate to protein ratios into the activity assay, protein concentrations between $6,99 \cdot 10^{-3}$ mmol/L and $6,99 \cdot 10^{-2}$ mmol/L were examined for a constant substrate concentration. The measured reaction rates of these ten protein concentrations were plotted against the nominal protein concentration and again the slope of a linear fit was determined. The respective slope was used as enzyme activity. To allow a comparison for different PEGylated species, calculated activities were normalized to the activity of native lysozyme.

The resulting catalytic activities of native and PEGylated lysozyme species are displayed in Fig. 6.3. With the exception of 2 kDa mono-PEGylated lysozyme, all PEGylated lysozyme species had a lower in vitro activity than the native protein. Increasing the molecular weight of mPEG for a constant PEGylation degree as well as increasing the PEGylation degree for a constant mPEG molecular weight resulted in a decrease in activity. This observation can be explained by steric hindrance resulting in a decreased accessibility of the substrate to the active site. 5 kDa and 10 kDa di-PEGylated lysozyme

showed residual activities below 10% compared to the native protein. Due to these uneconomical residual activities, these two species were not investigated further in the subsequent stability studies. The range of measured residual activities is in line with the residual activities between 8 and 77% for 5 kDa PEGylated lysozyme stated by Da Silva Freitas et al. [278].

Interestingly, 2 kDa mono-PEGylated lysozyme showed an activity increased by 31.1% compared to the native protein, which is rather unusual for water-soluble enzymes. Increased enzyme activities of PEGylated proteins are described in the literature for horseradish peroxidase [286] and laccase [287] in organic surroundings. In organic systems, the attachment of hydrophilic polymers results in the formation of a protein friendly micro-environment which decreases conformational changes of the protein structure in comparison to the native protein. A similar activation phenomenon of trypsin upon polymer modification was reported by Gaertner et al. [288] in aqueous environment. Gaertner et al. attribute the increased activity to an increase in the concentration of the enzyme-substrate-complex due to an altered conformational equilibrium by the attachment of a hydrophilic chain to lysine residues. These results indicate, that the protein conformation

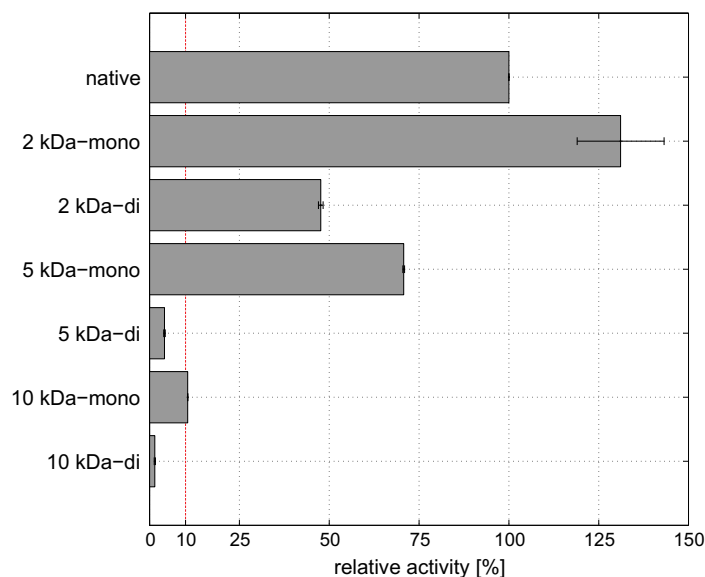


Figure 6.3: Residual enzyme activity (%) of PEGylated lysozyme species towards the substrate *Micrococcus lysodeikticus*. The indicated activity values refer to native lysozyme as reference.

is in addition to steric hindrance another important parameter influencing enzyme activities upon PEGylation. Závodszy et al. state that the enzyme activity and conformational flexibility are closely correlated [265]. In order to investigate the relationship between protein conformation and enzyme activity for PEGylated lysozyme the conformational properties of PEGylated lysozyme were evaluated in this work using intrinsic protein fluorescence.

6.3.3 Conformational Stability - Influence of the Salt Concentration on the Melting Point

To evaluate the influence of PEGylation on the conformational properties of lysozyme, melting temperatures (T_m) were determined using intrinsic protein fluorescence measurements. The influence of PEG molecular weight and PEGylation degree was studied. In Table 6.3 the melting temperatures for all studied protein species without the addition of salt are displayed. The measurement error bars correlate to a 95% confidence interval (1.96σ). All protein species revealed comparable melting temperatures between 60.04 and 62.71 °C. The insignificant differences in the melting temperatures indicate that all conjugates have a similar macroscopic conformational stability as the native protein in the absence of salt.

Table 6.3: Melting temperatures for native and PEGylated lysozyme for 0 M NaCl

Protein species	T_m [°C]	$1.96 * \sigma$
native	62.71	0.52
2 kDa-mono	60.91	0.09
2 kDa-di	60.04	0.08
5 kDa-mono	60.65	0.48
5 kDa-di	62.76	0.28
10 kDa-mono	60.23	0.44
10 kDa-di	62.00	0.45

With an increase in NaCl concentration the melting temperatures decreased for all protein species. These observations are in accordance with the studies of Hofmeister on the destabilizing impact of certain salts on conformational and colloidal stability of proteins [100]. In Fig. 6.4A the melting points of native, mono-PEGylated and di-PEGylated lysozyme are displayed as a function of the NaCl concentration exemplary for the conjugation with 5 kDa PEG. For native lysozyme, no melting points were determined above

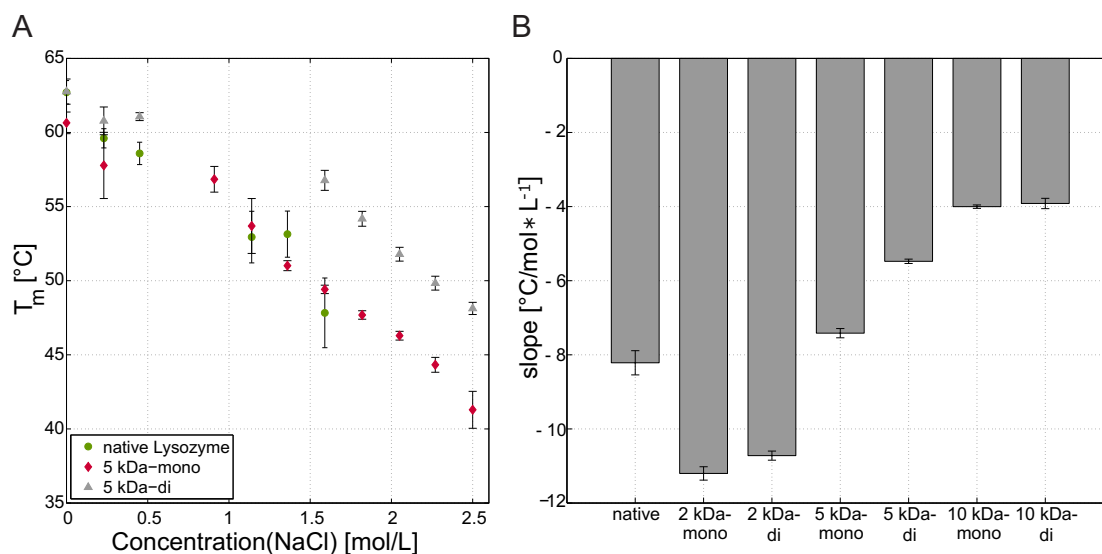


Figure 6.4: A: Melting temperatures of 0,94 mmol/L native, 5 kDa mono-PEGylated and 5 kDa di-PEGylated lysozyme in dependence of NaCl concentration at pH 3. The error bars correlate to the 95 % confidence interval (1.96σ), B: Slope of the linear regression of the melting points vs. NaCl concentration for native as well as 2 kDa, 5 kDa and 10 kDa PEGylated lysozyme.

a NaCl concentration of 1.59 mol/L due to spontaneous precipitation during sample preparation (in accordance with [79]). In a critical salt range between 0.5 und 1.5 mol/L NaCl, the melting curves of several samples deviated markedly from the expected sigmoidal shape. Melting points could therefore not be estimated based on sigmoidal fits and the data points were consequently excluded from the study. In the investigated concentration range, native and 5 kDa mono-PEGylated lysozyme showed comparable trends of the melting points in dependence of the salt concentration and are hence equally destabilized by the addition of salt ions. 5 kDa di-PEGylated lysozyme has the highest melting points at all salt concentrations indicating a lower impact of salt on the conformational stability compared to native and 5 kDa mono-PEGylated lysozyme. Analogous data sets were determined for conjugated lysozyme with 2 kDa and 10 kDa PEG.

In order to assess the influence of different PEG molecular weights and PEGylation degrees on the conformational stability, a linear regression of each dataset was performed. The slopes of these regressions are displayed in Fig. 6.4B. High absolute values of the slope represent a large decrease in melting temperatures with increasing salt concentration. The slopes of 2 kDa mono- and-di-PEGylated lysozyme have a higher absolute value than native lysozyme indicating a higher susceptibility to conformational changes under

the influence of salts. 5 kDa and 10 kDa conjugates are less susceptible to conformational changes under the influence of salts than native lysozyme. Here, no difference between 10 kDa mono- and di-PEGylated lysozyme is detectable within the 95% confidence intervals.

A molecule which is prone to extensive conformational changes under the influence of salts could be less rigid and may exhibit an increased molecular flexibility in the absence of salt. A higher flexibility may explain the observed increase in activity for 2 kDa mono-PEGylated lysozyme due to an improved accessibility of the substrate to the active site. Even though the slope of 2 kDa di-PEGylated lysozyme indicates a higher molecule flexibility compared to native lysozyme no increase in enzyme activity was observed. These results support the thesis that the residual enzyme activity after polymer modification is a combination of steric hindrance and conformational flexibility.

6.3.4 Colloidal Stability - Phase Behavior of PEGylated Lysozyme

In addition to preserving the activity after PEGylation, guaranteeing the solubility of the protein is a fundamental requirement in order to avoid problems during storage or application. In order to obtain information about the colloidal stability of PEGylated lysozyme protein phase diagrams were generated for PEGylated lysozyme with 2 kDa, 5 kDa and 10 kDa PEG in microbatch format at pH 3 under the influence of NaCl. Investigated phase transitions are displayed in Fig. 6.5B-E.

The phase diagram for native lysozyme (Fig. 6.5A) was demonstrated earlier by Baumgartner et al. [79]. For a comparison of the phase behavior on basis of a constant number of molecules, the mass concentrations used by Baumgartner et al. were converted into molar concentrations. The formation of crystals as well as precipitate was observed for native lysozyme. For NaCl concentrations above 1.82 mol/L precipitation was accompanied by skin formation which indicates protein denaturation.

In comparison to native lysozyme, all PEGylated species showed an expansion of the soluble area and a reduced aggregation propensity. For 2 kDa mono-PEGylated lysozyme (Fig. 6.5B) phase transitions to crystallization and precipitation occurred. In comparison to native lysozyme, an approximately 3 fold higher NaCl concentration was required to induce a phase transition at the highest investigated protein concentration. With few exceptions, the complete crystallization range of the native protein was converted into stable protein solution. For 2 kDa mono-PEGylated lysozyme, crystallization and preci-

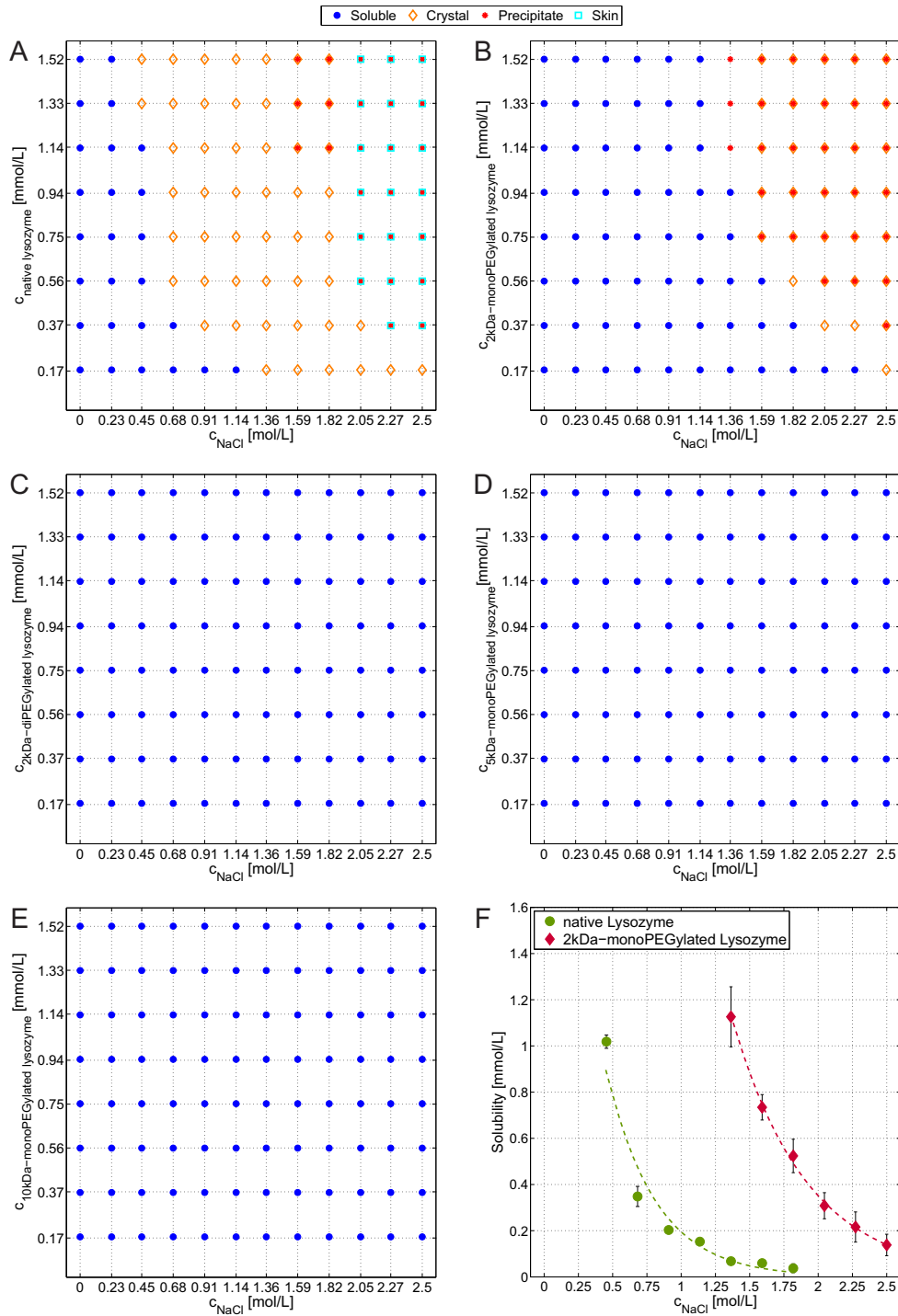


Figure 6.5: Phase diagrams for native (A), 2 kDa mono-PEGylated (B), 2 kDa di-PEGylated (C), 5 kDa mono-PEGylated (D), 10 kDa mono-PEGylated (E) lysozyme with sodium chloride (NaCl) as precipitant at pH 3. Data for the phase diagrams of native lysozyme was taken from Baumgartner et al. [79]. F: Solubility lines of unmodified lysozyme [254] and 2 kDa mono-PEGylated lysozyme at pH 3.

precipitation occurred simultaneously in most cases. Compared to the occurrence of large three-dimensional crystals in the case of native lysozyme, only small needle-shaped crystals and microcrystals were observed in case of 2 kDa mono-PEGylated lysozyme. For 2 kDa di-PEGylated lysozyme (Fig. 6.5C), 5 kDa mono-PEGylated lysozyme (Fig. 6.5D) and 10 kDa mono-PEGylated lysozyme (Fig. 6.5E) the PEGamers were completely soluble in the entire investigated protein and salt concentration range. Skin formation and thus protein denaturation was prevented for all PEG molecular weights and PEGylation degrees.

In Fig. 6.5F the measured solubility values for 2 kDa mono-PEGylated lysozyme are displayed and compared to data for unmodified lysozyme [254]. When the two curves are compared, a considerable increase in solubility is observed. At a constant NaCl concentration of 1.36 mol/L an approximately 11 fold increase in solubility was achieved. The statement that PEGylation results in an increased protein solubility, well-documented in the literature, has been underlined in this systematic study with experimental data.

Although 2 kDa di-PEGylated lysozyme, 5 kDa mono-PEGylated lysozyme and 10 kDa mono-PEGylated lysozyme show the same phase behavior in the investigated concentration range, they reveal a difference in their conformational stability (Fig. 6.4). These results indicate that the measurement of the thermal stability may not be correlated to the phase behavior for PEGylated proteins, although the thermal stability is often used as an indicator of the general protein stability.

In order to induce a phase transition of the PEGamers which were soluble in the entire investigated concentration range, extreme protein and salt conditions were applied. The influence of increased protein concentrations on the one hand and higher NaCl concentrations as well as an additional salt (Na_2SO_4) on the other hand were investigated. In Fig. 6.6 photographs of the protein aggregates formed under the applied conditions are displayed for all PEGamers. Native Lysozyme formed heavy precipitate under all conditions. With increasing PEGylation degree and PEG molecular weight the aggregates changed from precipitate to gelation and even liquid-liquid phase separation occurred. This indicates that the nature of the aggregates is determined for high PEGylation degrees and PEG molecular weights by the properties of the polymer rather than by the properties of the protein itself.

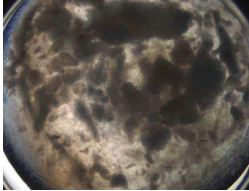
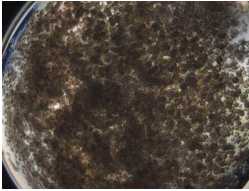
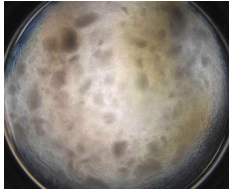
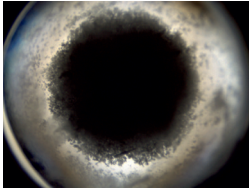
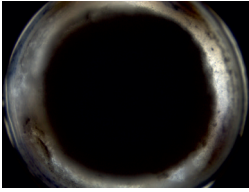
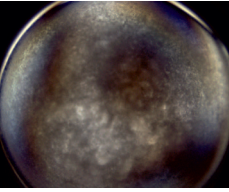
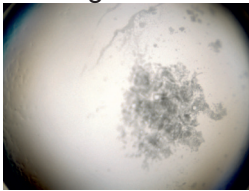
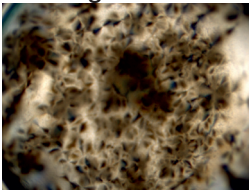
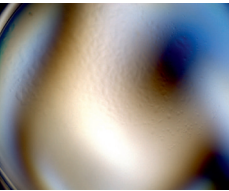
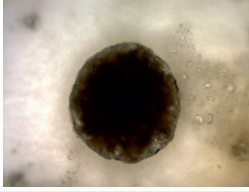
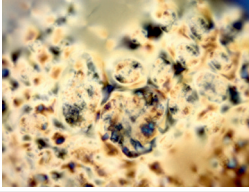
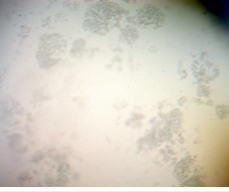
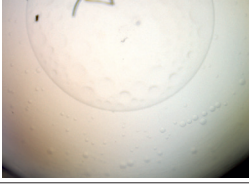
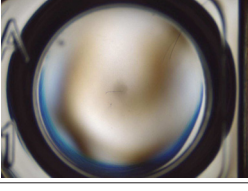
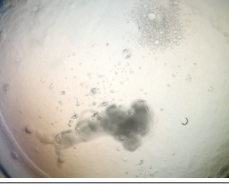
	1.52 mmol/L + 3.75 mol/L NaCl	3.04 mmol/L + 2.5 mol/L NaCl	1.52 mmol/L + 1.25 mol/L Na ₂ SO ₄
native lysozyme	Precipitate 	Precipitate 	Precipitate 
2kDa-mono-PEGylated lysozyme	Precipitate 	Precipitate 	Precipitate 
2kDa-di-PEGylated lysozyme	Precipitate + gelation 	Precipitate + gelation 	Gelation 
5kDa-mono-PEGylated lysozyme	Precipitate + gelation 	Gelation 	Gelation 
10kDa-mono-PEGylated lysozyme	Phase separation + gelation 	Soluble 	Precipitate + gelation 

Figure 6.6: Photographs of phase transitions of native and PEGylated lysozyme species resulting from extreme protein and salt conditions (NaCl and Na₂SO₄).

6.4 Conclusion

Recombinant proteins for pharmaceutical or biotechnological applications are often prone to instabilities during production, formulation and storage. The stability attributes are determined by the complexity of the protein molecule itself and the interplay of environmental conditions determining molecule interactions. The covalent attachment of polyethylene glycol (PEG) to proteins is a promising approach to solve these stability issues. In the presented work, purified samples of lysozyme PEGamers with 2 kDa, 5 kDa and 10 kDa mPEG-aldehyde attached were examined for their functional, conformational and colloidal stability. The automatic generation of protein phase diagrams and the measurement of melting points were found to be helpful tools for understanding mechanisms of protein stabilities. Higher molecular weight PEGs and PEGylation degree resulted in a greater conformational and colloidal stability. However, a reduced in vitro activity was observed. The properties of the conjugates have shown to be a mixture of protein and polymer properties. These findings suggests that in addition to PEG, different synthetic polymers may in future be conjugated to proteins in order to create functional conjugates with tailor-made properties due to the multiplicity of polymers. A careful choice of PEG molecular weight and PEGylation degree enables the fine tuning of protein properties and should be carefully considered for the use of PEGylated proteins upon formulation and storage.

6.5 Acknowledgments

We gratefully acknowledge the financial support by the German Federal Ministry of Education and Research (BMBF). This research work is part of the project ‘Molecular Interaction Engineering: From Nature’s Toolbox to Hybrid Technical Systems’, funding code 031A095B. The authors further acknowledge Tosoh Bioscience GmbH (Griesheim, Germany) for providing chromatographic materials in the context of the Tosoh Chromatography Scholarship 2015.

6.6 References

6. Frokjaer, S. & Otzen, D. E. Protein drug stability: A formulation challenge. *Nat. Rev. Drug Discov* **4**, 298–306 (2005).
25. Chi, E. Y., Krishnan, S., Randolph, T. W. & Carpenter, J. F. Physical stability of proteins in aqueous solution: Mechanism and driving forces in nonnative protein aggregation. *Pharm. Res.* **20**, 1325–1336 (2003).
60. Manning, M. C., Chou, D. K., Murphy, B. M., Payne, R. W. & Katayama, D. S. Stability of protein pharmaceuticals: An update. *Pharm. Res.* **27**, 544–575 (2010).
69. Baumgartner, K., Großhans, S., Schütz, J., Suhm, S. & Hubbuch, J. Prediction of salt effects on protein phase behavior by HIC retention and thermal stability. *Journal of pharmaceutical and biomedical analysis* **128**, 216–225 (2016).
77. Wang, W. Instability, stabilization, and formulation of liquid protein pharmaceuticals. *Int. J. Pharm.* **185**, 129–188 (1999).
79. Baumgartner, K., Galm, L., Nötzold, J., Sigloch, H., Morgenstern, J., Schleining, K., Suhm, S., Oelmeier, S. A. & Hubbuch, J. Determination of protein phase diagrams by microbatch experiments: Exploring the influence of precipitants and pH. *Int. J. Pharm.* **479**, 28–40 (2015).
81. Mahler, H.-C., Friess, W., Grauschopf, U. & Kiese, S. Protein aggregation: Pathways, induction factors and analysis. *J. Pharm. Sci.* **98**, 2909–2934 (2009).
82. Philo, J. S. & Arakawa, T. Mechanisms of protein aggregation. *Current pharmaceutical biotechnology* **10**, 348–351 (2009).
100. Kunz, W., Henle, J. & Ninham, B. W. 'Zur Lehre von der Wirkung der Salze' (about the science of the effect of salts): Franz Hofmeister's historical papers. *Current Opinion in Colloid & Interface Science* **9**, 19–37 (2004).
139. Fee, C. J. & Van Alstine, J. M. Prediction of the viscosity radius and the size exclusion chromatography behavior of PEGylated proteins. *Bioconjugate chemistry* **15**, 1304–1313 (2004).
142. Harris, J. M. & Chess, R. B. Effect of PEGylation on pharmaceuticals. *Nat. Rev. Drug Discov.* **2**, 214–221 (2003).
149. Seely, J. E. & Richey, C. W. Use of ion-exchange chromatography and hydrophobic interaction chromatography in the preparation and recovery of polyethylene glycol-linked proteins. *J. Chromatogr. A* **908**, 235–241 (2001).

238. Baumann, P., Bluthardt, N., Renner, S., Burghardt, H., Osberghaus, A. & Hubbuch, J. Integrated development of up- and processes supported by the Cherry-Tag for real-time tracking of stability and solubility of proteins. *J. Biotech.* **200**, 27–37 (2015).
253. Ottow, K. E., Lund-Olesen, T., Maury, T. L., Hansen, M. F. & Hobley, T. J. A magnetic adsorbent-based process for semi-continuous PEGylation of proteins. *Biotechnol. J.* **6**, 396–409 (2011).
254. Galm, L., Morgenstern, J. & Hubbuch, J. Manipulation of lysozyme phase behavior by additives as function of conformational stability. *Int. J. Pharm.* **494**, 370–380 (2015).
257. Maiser, B., Kröner, F., Dimer, F., Brenner-Weiß, G. & Hubbuch, J. Isoform separation and binding site determination of mono-PEGylated lysozyme with pH gradient chromatography. *J. Chrom. A* **1268**, 102–108 (2012).
258. Yoshimoto, N. & Yamamoto, S. PEGylated protein separations: Challenges and opportunities. *Biotechnol. J.* **7**, 592–593 (2012).
264. Maiser, B., Dimer, F. & Hubbuch, J. Optimization of random PEGylation reactions by means of high throughput screening. *Biotechnol. Bioeng.* **111**, 104–114 (2014).
265. Závodszy, P., Kardos, J., Svingor, Á. & Petsko, G. A. Adjustment of conformational flexibility is a key event in the thermal adaptation of proteins. *PNAS* **95**, 7406–7411 (1998).
266. Schermeyer, M.-T., Sigloch, H., Bauer, K. C., Oelschlaeger, C. & Hubbuch, J. Squeeze flow rheometry as a novel tool for the characterization of highly concentrated protein solutions. *Biotechnol. Bioeng.* **113**, 576–587 (2016).
267. Krishnan, S., Chi, E. Y., Webb, J. N., Chang, B. S., Shan, D., Goldenberg, M., Manning, M. C., Randolph, T. W. & Carpenter, J. F. Aggregation of granulocyte colony stimulating factor under physiological conditions: Characterization and thermodynamic inhibition. *Biochemistry* **41**, 6422–6431 (2002).
268. Chen, B. L., Wu, X., Babuka, S. J. & Hora, M. Solubility of recombinant human tissue factor pathway inhibitor. *J. Pharm. Sci.* **88**, 881–8 (1999).
269. Hansen, C. L., Sommer, M. O. A. & Quake, S. R. Systematic investigation of protein phase behavior with a microfluidic formulator. *PNAS* **101**, 14431–14436 (2004).

-
270. Wang, W. & Roberts, C. J. *Aggregation of therapeutic proteins* 150–151 (Wiley, 2010).
271. Ericsson, U. B., Hallberg, B. M., DeTitta, G. T., Dekker, N. & Nordlund, P. Thermofluor-based high-throughput stability optimization of proteins for structural studies. *Anal. Biochem.* **357**, 289–298 (2006).
272. Baumann, P., Osberghaus, A. & Hubbuch, J. Systematic purification of salt-intolerant proteins by ion-exchange chromatography: The example of human α -galactosidase A. *Eng. Life Sci.* **15**, 195–207 (2015).
273. Kapust, B. R. & Waugh, S. D. Escherichia coli maltose-binding protein is uncommonly effective at promoting the solubility of polypeptides to which it is fused. *Protein Science* **8**, 1668–1674 (1999).
274. Esposito, D. & Chatterjee, D. K. Enhancement of soluble protein expression through the use of fusion tags. *Curr. Opin. Biotechnol.* **17**, 353–358 (2006).
275. Mohan Padmanabha Das, K., Barve, S., Banerjee, S., Bandyopadhyay, S. & Padmanabhan, S. A Novel Thermostability Conferring Property of Cherry Tag and its Application in Purification of Fusion Proteins. *Journal of Microbial & Biochemical Technology* **1**, 59–63 (2009).
276. Azhar, M. & Somashekhar, R. Cloning , expression and purification of human and bovine Enterokinase light chain with Cherry tag and their activity comparison. *Indian J. Applied & Pure Bio.* **29**, 125–132 (2014).
277. Zhang, Y. B., Howitt, J., McCorkle, S., Lawrence, P., Springer, K. & Freimuth, P. Protein aggregation during overexpression limited by peptide extensions with large net negative charge. *Protein Expr. Purif.* **36**, 207–216 (2004).
278. Da Silva Freitas, D. & Abrahao-Neto, J. Biochemical and biophysical characterization of lysozyme modified by PEGylation. *Int. J. Pharm.* **392**, 111–117 (2010).
279. Nie, Y., Zhang, X., Wang, X. & Chen, J. Preparation and stability of N-terminal mono-PEGylated recombinant human endostatin. *Bioconjugate Chemistry* **17**, 995–999 (2006).
280. Basu, A. *et al.* StructureFunction Engineering of Interferon- β -1b for Improving Stability, Solubility, Potency, Immunogenicity, and Pharmacokinetic Properties by Site-Selective Mono-PEGylation. *Bioconjugate Chem.* **17**, 618–630 (2006).

281. Morgenstern, J., Busch, M., Baumann, P. & Hubbuch, J. Quantification of PEGylated proteases with varying degree of conjugation in mixtures: An analytical protocol combining protein precipitation and capillary gel electrophoresis. *J. Chrom. A* **1462**, 153–164 (2016).
282. Smith, R. D., Loo, J. A., Edmonds, C. G., Barinaga, C. J. & Udseth, H. R. New developments in biochemical mass spectrometry: Electrospray ionization. *Anal. Chem.* **62**, 882–899 (1990).
283. Wang, W., Nema, S. & Teagarden, D. Protein aggregation - Pathways and influencing factors. *Int. J. Pharm.* **390**, 89–99 (2010).
284. Baumann, P., Baumgartner, K. & Hubbuch, J. Influence of binding pH and protein solubility on the dynamic binding capacity in hydrophobic interaction chromatography. *J. Chrom. A* **1396**, 77–85 (2015).
285. Nath, A. & Atkins, W. M. A theoretical validation of the substrate depletion approach to determining kinetic parameters. *Drug metabolism and disposition* **34**, 1433–1435 (2006).
286. Jeng, F.-Y. & Lin, S.-C. Characterization and application of PEGylated horseradish peroxidase for the synthesis of poly (2-naphthol). *Process Biochemistry* **41**, 1566–1573 (2006).
287. Vandertol-Vanier, H. A., Vazquez-Duhalt, R., Tinoco, R. & Pickard, M. A. Enhanced activity by poly (ethylene glycol) modification of *Coriolopsis gallica* laccase. *Journal of Industrial Microbiology and Biotechnology* **29**, 214–220 (2002).
288. Gaertner, H. & Puigserver, A. Increased activity and stability of poly (ethylene glycol)-modified trypsin. *Enzyme and microbial technology* **14**, 150–155 (1992).

Stability Assessment of Protein-Polymer Conjugates: Alternative Polymers to Polyethylene Glycol

Josefine Morgenstern^{*,a}, Gabriela Gil Alvaradejo^{*,b,c}, Nicolai Bluthardt^a, Guillaume Delaittre^{**b,c} and Jürgen Hubbuch^{**a}

Josefine Morgenstern^{*,a}, Gabriela Gil Alvaradejo^{*,b,c}, Nicolai Bluthardt^a, Guillaume Delaittre^{**b,c} and Jürgen Hubbuch^{**a}

^a *Institute of Engineering in Life Sciences, Section IV: Biomolecular Separation Science, Karlsruhe Institute of Technology (KIT), 76131 Karlsruhe, Germany*

^b *Institute of Toxicology and Genetics (ITG), Karlsruhe Institute of Technology (KIT), Hermann-von-Helmholtz-Platz 1, 76344 Eggenstein-Leopoldshafen, Germany.*

^c *Preparative Macromolecular Chemistry, Institute for Chemical Technology and Polymer Chemistry (ITCP), Karlsruhe Institute of Technology (KIT), 76128 Karlsruhe, Germany.*

** These authors contributed equally to this work.*

*** Corresponding author.*

Manuscript in preparation.

Abstract

Covalent attachment of synthetic polymers to proteins, known as protein-polymer conjugation, is currently one of the main approaches for improving the physicochemical properties of proteins. The most commonly applied polymer is polyethylene glycol (PEG), having extensive research and clinical track records for its use in biopharmaceuticals. However, the occurrence of allergic reactions or hypersensitivity and the formation of antibodies against PEG conjugates on the one hand and the introduction of controlled radical polymerization techniques and novel monomers on the other hand, is driving the search for alternative polymers for protein conjugation. This study presents the synthesis, purification and protein-conjugation of the alternative polymers, poly-(4-acryloylmorpholine) (PNAM) and poly-(oligoethylene glycol methacrylate) (POEGMA), using lysozyme from chicken egg white as model protein. Conjugate species with different conjugation degrees are investigated for their aggregation behavior and solubility using a high-throughput screening approach. All investigated conjugates show an improved protein solubility when compared to the native protein. To achieve a comparable effect on solubility as PEG, the conjugates required polymers with higher molecular weight or higher conjugation degrees.

Keywords: *PNAM, POEGMA, RAFT polymerization, protein-conjugation, phase behavior, solubility*

7.1 Introduction

The development of recombinant DNA technologies has resulted in a revolution of the biotechnological production of recombinant proteins. Today, industrially produced proteins are widely applied as biocatalysts for the green synthesis of organic materials as well as in the textile, detergent, food processing and pharmaceutical industry. For the latter, drugs based on peptides and proteins have gained a significant share of the pharmaceutical market [13]. The high potential of proteins results from their inherent specificity for molecular targets in the human body, and thus an intervention with minimal side effects. However, the complex molecular structure of proteins and the resulting chemical and physical properties present a challenge for the purification, formulation, storage and delivery of these drugs [289]. Problems that need to be addressed include limited stability, low solubility, short in vivo circulation times, and unwanted immunogenicity [142, 289, 290]. Protein-polymer conjugation has become a central strategy to improve both physicochemical and pharmacokinetic properties of biopharmaceuticals in non-native environments [142].

Protein-polymer conjugates are hybrid molecules generated by the covalent attachment of a synthetic polymer to a native protein. This strategy offers the opportunity to combine the structural and functional features of proteins with the versatility of synthetic polymers to develop novel high performance biomaterials. [291, 292] Requirements for the polymer candidates are biocompatibility, water-solubility and an existing reactive group for the conjugation process [124]. Polyethylene glycol (PEG) is the most commonly applied non-ionic hydrophilic polymer in the pharmaceutical industry. PEG owes its popularity to its FDA approval for use in pharmaceuticals, as well as the long clinical track records and extensive research efforts on PEG conjugates [142]. Despite the positive properties of PEGylated proteins such as increased stability [278], solubility [293] and residence time in the blood stream [294], a series of undesirable effects are reported in literature. These include the occurrence of allergic reactions or hypersensitivity and the formation of antibodies against PEG conjugates (anti-PEG) [295–299]. The formation of anti-PEG leads to an increased clearance rate through the immune system [300] which counteracts the goal of an increased circulation time of the conjugated drug. Furthermore, it is reported that PEG conjugates are not degradable in the human body and that PEG vacuoles are formed in organs such as liver, kidney and spleen [301, 302].

The discussed drawbacks seen in PEG intensified the search for alternative polymers for therapeutic use. A series of synthetic polymers are being investigated and are in

different stages of development [126, 135, 303]. Synthetic polymers owe their versatile range of properties to the availability of different monomers with varying architectures and functional groups [304]. Controlled radical polymerization techniques such as reversible addition-fragmentation chain transfer (RAFT) polymerization allow for an accurate adjustment of the polymer molecular weight with a low dispersity (narrow molecular weight distribution) [292]. The polymer functionality and size as well as the number of the bound polymers is decisive for the physicochemical and biological properties of the protein-polymer conjugate. Fine tuning of these parameters is crucial to optimize activity and stability attributes of the conjugates [292]. However, the underlying physicochemical interactions between polymer and protein as well as the effect of this interaction on the conjugate properties are still not fully understood. The development and processing of conjugates with specific properties and functionalities hence requires the establishment of standardized methods for quantifying the influence of polymer parameters on the resulting molecular properties.

In this study, we investigated the impact of poly-(4-acryloylmorpholine) (PNAM) and poly-(oligoethylene glycol methacrylate) (POEGMA) of different sizes on solubility, aggregation (phase) behavior, and resulting biological activity of the conjugated model protein lysozyme. PNAM is the polymer of the bisubstituted acrylamide derivative N-acryloylmorpholine and has a number of useful properties including its solubility in water and other polar and low-polarity solvents, and low toxicity [305, 306]. Veronese et al. patented in 1997 the activation of PNAM with a single reactive group for the selective monofunctional attachment of PNAM to various surfaces and molecules including biomaterials and bioactive substances such as enzymes and polypeptides [307]. The controlled polymerization of POEGMA was reported by the research group of Armes [308, 309], and it was first used to graft on proteins by Chilkoti et al. [310, 311]. Proteins modified by PNAM and POEGMA showed an increased residence time in blood when compared to the unmodified form [310, 312–316]. Although there are pharmacokinetic investigations on the effect of said polymers, no detailed or systematic studies of their influence on the physical stability of the conjugated proteins have been reported.

In this work, we examined the role of the physicochemical properties of the polymers on the solubility and aggregation behavior of protein-polymer conjugates. We present an automated high-throughput approach to assess the influence of monomer type, molecular weight, and conjugation degree on the stability of protein-polymer conjugates. For the determination of solubility and phase behavior, lysozyme was conjugated to NHS-ester functionalized PNAM or POEGMA in a random reaction. The conjugated species with different conjugation degrees were purified by cation exchange chromatography. Sub-

sequently, protein phase diagrams were generated using an automated liquid handling station. To do so, 96-well systems with varying concentrations of conjugate and precipitant agent (sodium chloride) were prepared on a microtiter plate and examined for phase behavior and solubility. The residual enzyme activity after conjugation was assessed and compared to the native protein using the lysozyme-specific activity assay based on the substrate *M. lysodeikticus*.

7.2 Materials and Methods

7.2.1 Materials

Unless otherwise specified, reagents were used as received without further purification. 4-acryloylmorpholine (Sigma, 97 %), 1,4-dioxane (Sigma, 99 %), dichloromethane (DCM; VWR), diethyl ether (99.5 %, Roth), sinapic acid (Sigma, 98 %), 2,2'-Azobis(2-methylpropanitrile) (AIBN, Aldrich, 98 %), 4-Cyano-4-(phenylcarbonothioylthio)pentanoic acid N-succinimidyl ester (Aldrich), oligo(ethyleneglycol) methyl ether methacrylate 300 (PO-EGMA 300, Sigma), trans-2-[3-(4-tert-Butylphenyl)-2-methyl-2-propenylidene]malononitrile (DCTB, 99 %), and acetonitrile (Sigma, anhydrous, 99.8 %) were used as received. The used buffer substances were sodium citrate tribasic dihydrate (Sigma-Aldrich, USA) for pH 3, sodium acetate trihydrate (Sigma-Aldrich, USA) for pH 5, sodium phosphate monobasic dihydrate (Sigma-Aldrich, USA) and di-sodium hydrogen phosphate dihydrate (Merck, Germany) for pH 7.

7.2.2 Polymer Characterization

¹H nuclear magnetic resonance (NMR) spectroscopy measurements were performed on a Bruker AM 500 spectrometer (500 MHz). All compounds were dissolved in CDCl₃ and the residual solvent peak was used for shift correction (7.26 ppm).

Matrix-assisted laser desorption ionization coupled to time-of-flight (MALDI-ToF) mass spectra were acquired with a 4800 Proteomics Analyzer (Applied Biosystems, Foster City, CA, USA) in positive ion linear mode and a mass range of 1000 to 40000 Da. The laser intensity was set to 4800. The spectra obtained represent the average of laser shots taken by an automatic scheme measuring spectra over the whole spot. The matrices used were

sinapic acid for conjugated proteins and DCTB for the polymer samples. Peak lists were generated using Data Explorer Software 4.0 (Applied Biosystems).

Size exclusion chromatography (SEC) measurements were performed on a TOSOH Eco-SEC HLC-8320 GPC System, comprising an autosampler, a SDV 5 μm bead size guard column (50 \times 8 mm, PSS) followed by three SDV 5 μm columns (300 \times 7.5 mm, subsequently 100 \AA , 1000 \AA and 10⁵ \AA pore size, polystyrene sulfonate (PSS)), and a differential refractive index (DRI) detector using THF as eluent at 30 $^{\circ}\text{C}$ with a flow rate of 1 mL/min. The SEC system was calibrated using linear polystyrene standards ranging from 266 to 252106 g/mol. Before injection the samples were filtered using a 0.2 μm filter.

7.2.3 RAFT Polymerization of 4-Acryloylmorpholine

In a 250 mL round-bottom flask 91.0 mg of 4-cyano-4-(phenylcarbonothioylthio)pentanoic acid N-succinimidyl ester were mixed with 12.0 mg (0.3 eq) of AIBN and 1.129 g (68 eq) of 4-acryloylmorpholine. The mixture was then dissolved in 1,4-dioxane to a monomer final concentration of 1.6 M, and flushed with nitrogen for 30 minutes. The polymerization mixture was heated to 80 $^{\circ}\text{C}$ for 35 minutes. After evaporation of the solvent under reduced pressure and dissolving the residue in DCM, the polymer was precipitated in diethyl ether, centrifuged, separated, and dried under vacuum. The dry product was analyzed by THF SEC, MALDI-ToF, and ¹H NMR spectroscopy.

7.2.4 RAFT Polymerization of Oligo(ethyleneglycol) methyl ether methacrylate 300

In a 250 mL round-bottom flask 361.4 mg of 4-cyano-4-(phenylcarbonothioylthio)pentanoic acid N-succinimidyl ester were mixed with 31.53 mg (0.2 eq) of AIBN, and 12.73 g (44 eq) of oligo(ethyleneglycol) methyl ether methacrylate (OEGMA). The mixture was dissolved in acetonitrile to a RAFT agent final concentration of 16 mM, and flushed with nitrogen for 30 minutes. The polymerization mixture was then heated to 70 $^{\circ}\text{C}$ for 4 hours. After evaporation of the solvent under reduced pressure and dissolving the residue in DCM, the polymer was precipitated in diethyl ether, separated, and dried under vacuum. The dry product was analyzed by THF-SEC, MALDI-ToF, and ¹H NMR spectroscopy.

7.2.5 Protein Conjugation

Conjugation experiments were performed batch-wise in 50 mL Falcon Tubes (BD Biosciences, USA). For conjugation, lysozyme and the respective polymer were dissolved in 25 mM sodium phosphate buffer at pH 7.2. The concentration of lysozyme was set to 0,28 mmol/l. PNAM and POEGMA were added based on a molar polymer to protein ratio ($r = N_{polymer}/N_{protein}$ with N being the concentration of moles per volume) of 2. For the reaction, the tube was continuously shaken in an overhead shaker (LabincoLD79, Labinco BV, Netherlands) for 1 h at room temperature.

7.2.6 Purification of Protein Conjugates

The preparative separation of protein conjugates with varying number of attached polymer molecules was performed on an ÄKTA™ purifier system equipped with a Fraction Collector Frac-950 (GE Healthcare, Sweden). As stationary phase, a 5 ml prepacked Toyopearl GigaCap S-650M cation exchange (CEX) column (TOSOH Bioscience, Germany) was used. For column loading, the system was equilibrated in 10 mM sodium acetate buffer (pH 5). In order to reduce the influence of unbound polymer on the binding behavior of the conjugates to the CEX resin, the conjugation batch was diluted 1:6 in 10 mM sodium acetate buffer (pH 5). Injection of the diluted batch was performed using a 50 mL super loop (GE Healthcare, Sweden). Elution was performed by applying an NaCl step gradient with an elution buffer containing 1 M sodium chloride in 10 mM sodium acetate buffer (pH 5). The NaCl molarities used for the step elution of the different conjugates are displayed in Table 7.1 in dependence of the attached polymer. The flow rate for equilibration, binding and elution was set to 1 ml/min. For process monitoring the absorption at wavelengths of 280 nm (for protein) and 320 nm (for polymer) as well as conductivity were detected continuously. From each chromatographic separation, fractions of 2 mL

Table 7.1: NaCl steps in mol/L used for the elution of different conjugate species from Toyopearl GigaCap S-650M at pH 5 in dependency of the attached polymer.

	Native lysozyme	mono-conjugated lysozyme	di-conjugated lysozyme
PNAM _{3.5kDA}	1	0.36	0.23
PNAM _{7kDA}	1	0.4	0.175
POEGMA _{7.5kDA}	1	0.24	0.12

were collected into a 96-well deep well plate (VWR, USA). To obtain sufficient sample for stability assessment of the different conjugate species the corresponding fractions of multiple chromatographic runs were pooled. Peak allocation to the different conjugate species were performed by MALDI-ToF.

7.2.7 Conditioning and Quantification of Protein Conjugates

The separation of protein-polymer conjugates led to fractions containing different NaCl concentrations. Characterizing the isolated conjugates with regard to activity and phase behavior thus required a sample conditioning consisting of buffer exchange (resp. pH-change) and concentration increase. Buffer exchange was carried out using Slide-A-Lyzer™ Dialysis Cassettes (Thermo Fisher Scientific, USA) with a molecular weight cut-off of 2 kDa. Concentrating of protein samples was performed by evaporation using a vacuum concentration unit RVC 2-33CDplus (Martin Christ Gefriertrocknungsanlagen GmbH, Germany) operated at 24 mbar.

Concentrations of unmodified lysozyme were determined by measuring the absorption at 280 nm using a NanoDrop 2000c UV-Vis spectroscopic device (Thermo Fisher Scientific, USA) and an extinction coefficient of $\epsilon_{280\text{ nm, lysozyme}}^{1\%} = 22.00$ [254]. To convert mass concentrations into molar concentrations, a molecular weight of lysozyme of 14.3 kDa was used [282].

Since the two polymers PNAM and POEGMA also absorb at 280 nm (Supplementary Figure A.2), the total absorption at 280 nm ($A_{280\text{ nm}}$) is described for protein-polymer conjugates by:

$$A_{280\text{ nm}} = A_{280\text{ nm, lysozyme}} + A_{280\text{ nm, polymer}} \quad (7.1)$$

In order to quantify the molar concentration of the protein-polymer conjugates, measurements solely at 280 nm are therefore not sufficient. For the quantification of protein-polymer conjugates, a method based on the differences in the spectra of protein and polymer was applied. At 320 nm, the two polymers absorb light due to the RAFT group [317], while lysozyme does not (Supplementary Figure A.2). Thus, by measuring the absorption at 320 nm and comparing it to a calibration of polymer solutions, it is possible to quantify how much polymer is bound to a protein. For polymer calibration, absorption spectra between 240 nm and 340 nm were recorded for polymer solutions (in conjugation buffer) at 10 concentrations between 0,1 and 1,0 mg/ml using a NanoDrop 2000c UV-Vis spectroscopic device (Thermo Fisher Scientific, USA). Using the respective molecular weight of the polymer, the mass concentrations were converted to molar concentrations.

From the recorded polymer spectra, the absorption values were extracted for 280 nm and 320 nm. By implementing the proportionality

$$K = A_{280nm,polymer} / A_{320nm,polymer} , \quad (7.2)$$

it is possible to rearrange Eq. 7.1 and calculate the absorption $A_{280nm,lysozyme}$ as

$$A_{280nm,lysozyme} = A_{280nm} - K \cdot A_{320nm,polymer} . \quad (7.3)$$

For the K value, the mean value of all K values of the 10 measured polymer concentrations was used. In order to convert the calculated absorption $A_{280nm,lysozyme}$ into a concentration, the extinction coefficient of $\epsilon_{280nm,lysozyme}^{1\%} = 22.00$ was used as for unmodified lysozyme. All concentration measurements were performed as triplicates.

7.2.8 Stability Assessment

7.2.8.1 Functional Atability - Activity Assay Using *M. Lysodeikticus*

In order to evaluate the residual activity of the protein-polymer conjugates after conjugation and separation, a *Micrococcus lysodeikticus*-based activity assay was performed according to [293]. The kinetic assay is based on the lysis of bacterial cells by the enzyme. The decrease in cell density results in a decrease in turbidity over time, which was monitored by measuring the absorbance at 450 nm. To allow a comparison for different conjugated species, the derived activities were normalized to the activity of native lysozyme.

7.2.8.2 Colloidal Stability - Generation of Phase Diagrams

According to [79], in total four protein phase diagrams for mono-PNAM_{3.5 kDa}ylated lysozyme, di-PNAM_{3.5 kDa}ylated lysozyme, mono-PNAM_{7 kDa}ylated lysozyme and mono-POEGMA_{7.5 kDa}lated lysozyme, were generated on an automated liquid handling station (Freedom EVO[®]200 from Tecan, Germany). The pH value was adjusted to 3 using a buffer system of citric acid monohydrate (Merck, Germany) and sodium citrate tribasic dihydrate (Sigma-Aldrich, USA) and a total buffer capacity of 100 mM. The purified conjugated species were concentrated to 3.04 mmol/L \pm 0.07 mmol/L (corresponds to 43.5 mg/mL \pm 1 mg/mL unmodified protein) dialyzed and into 100 mM citric

buffer (pH 3) (=protein stock solution). Eight protein dilution steps between 0.35 and 3.04 mmol/L were prepared by mixing protein stock solution and 100 mM citric buffer (pH 3) on a protein plate. As precipitant, sodium chloride was used. Twelve salt concentrations between 0 and 5 M were created according to [79]. Binary phase diagrams were generated by mixing 12 μL of each diluted protein solution with 12 μL of each prepared salt concentration on a crystallization plate (Swissci, Switzerland) resulting in 96 batch systems with varying composition. As result the protein concentrations varied from 0.17 to 1.52 mmol/L and the salt concentrations from 0 M to 2.5 M. Evaluation of phase states was conducted based on photographs taken by the Rock Imager 182/54 automated imaging system (Formulatrix, USA). In order to determine solubility lines the protein concentration in the supernatant of batch systems where a phase transition occurred was determined after 40 days using a NanoDrop 2000c UV-vis spectroscopic device.

7.3 Results and Discussion

7.3.1 Polymer Synthesis

The disadvantages of PEG, already discussed in previous sections, increased the interest in alternative polymers for use in therapeutics. Synthetic polymers, such as PNAM and POEGMA, are some of the potential alternatives being investigated. The selected polymers for this study can be prepared via RAFT polymerization, which allows not only the synthesis of polymers with defined sizes and narrow dispersities, but also the introduction of a functional group to the end chain for further modification by selecting the appropriate RAFT agent. Its relatively simple experimental setup when compared to PEG (e.g., no handling of gaseous monomer), and the possibility to scale up its synthesis make these polymers attractive for potential uses in biomedical fields.

A commercially available RAFT agent with an activated NHS ester was used for the polymer synthesis. The use of NHS esters to bind lysine residues is a well-known technique for protein conjugation [318]. Table 7.2 summarizes the features of the polymers used for this study. As expected, the polymers synthesized show a narrow dispersity ($D < 1.10$), and the survival of the activated ester group for protein conjugation is shown via UV spectra (Supplementary Figure A.2) and ^1H NMR (Supplementary Figures A.4, A.5 and A.6).

Table 7.2: Summary of the characterization of the three polymers synthesized for this study.

	Monomeric units	$M_{n,SEC}$	$M_{n,NMR}$	D
PNAM _{3.5kDa}	22	1900	3500	1.08
PNAM _{7kDa}	47	3800	7100	1.09
POEGMA _{7.5kDa}	24	6700	7600	1.10

7.3.2 Protein Conjugation and Purification

Preparative purification of lysozyme species with different number of attached polymer molecules was performed by a single cation exchange step. In Fig 7.1 the resulting CEX chromatograms with an NaCl step gradient for 1:6 diluted conjugation batches are displayed for PNAM_{3.5 kDa} (A), PNAM_{7 kDa} (B) and POEGMA_{7.5 kDa} (C). The first 50 ml of the chromatographic purification run correspond to the loading phase and are hence not displayed here. The green line indicates the absorption at 280 nm (UV_{280nm}) at which both protein and polymer absorb. The red line indicates the absorption at 320 nm (UV_{320nm}) at which only the polymer absorbs. Conjugation species with varying degree of conjugation were assigned to the individual peaks of the CEX chromatogram by MALDI-ToF. The results of this fractional analysis are shown in Fig 7.2 and will be discussed in the following. For a first estimation of the conjugation degree, however, the ratio of UV_{320nm} to UV_{280nm} can be used. Fractions containing only protein but no polymer do not absorb at 320 nm. In Fig 7.1 A und C, it can be seen that the native fractions for PNAM_{3.5 kDa} and POEGMA_{7.5 kDa} contain slight impurities of the respective polymer. However, these fractions were not used for further experiments within the study. The higher the degree of conjugation, the higher the ratio of UV_{320nm} to UV_{280nm} . For all three investigated polymers, native lysozyme had the highest binding affinity to the adsorbent given that a higher salt concentration is required to elute it than for conjugated species. For conjugated species, a decrease in binding strength with increasing conjugation degree was observed. These results are in accordance with the purification of PEGylated lysozyme published earlier [293]. Modified binding strength can be explained by weakened electrostatic interactions between protein binding site and adsorber surface due to the attached polymer [149, 258, 319].

The successful separation of each conjugated species was proven via MALDI-ToF (Fig 7.2). A sample of the raw mixture obtained after the conjugation experiment was taken for

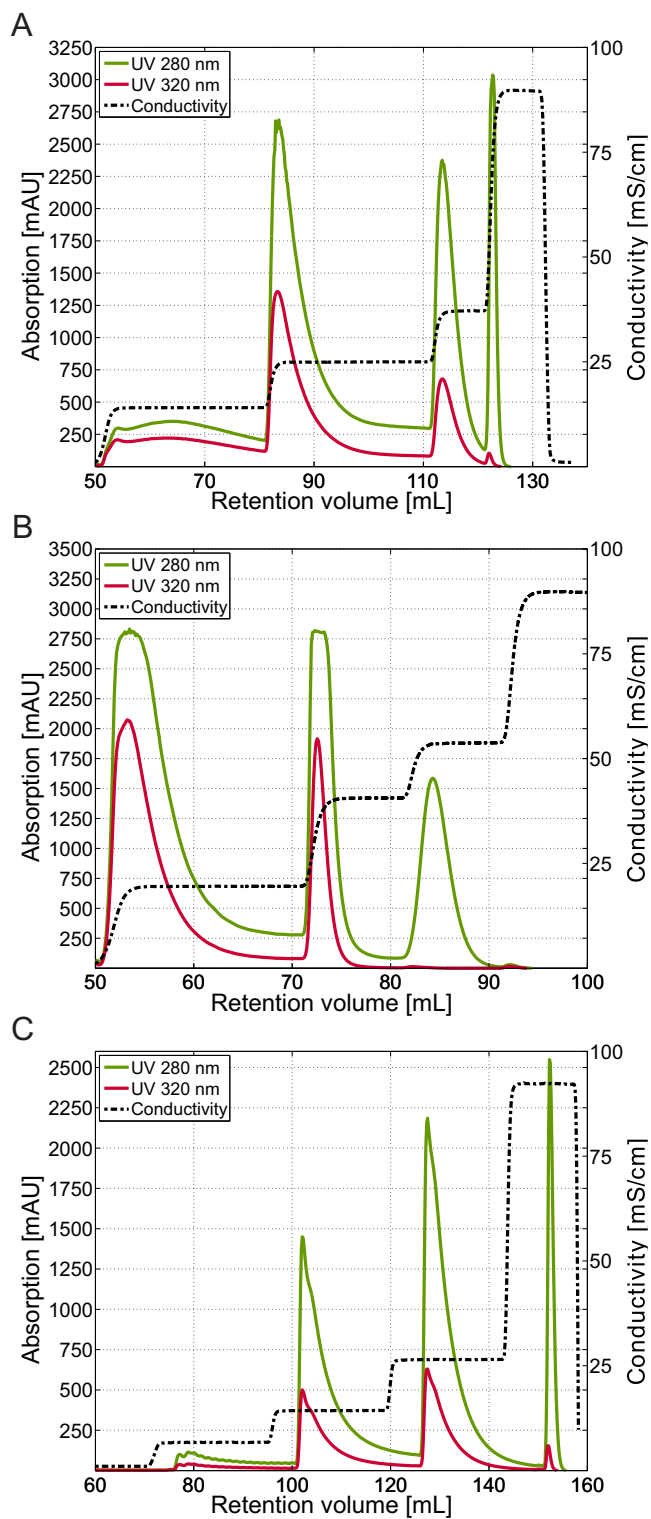


Figure 7.1: CEX chromatograms of 1:6 diluted conjugation batches ($r = 2$, pH 7.2, 1 h) loaded with a 50 mL loop for PNAM_{3.5} kDa (A), PNAM₇ kDa (B) and POEGMA_{7.5} kDa (C).

each polymer. At this point and without any purification step, the MALDI spectra show, in all cases, three main different distributions (Fig 7.2B, D, and F), which correspond to a mixture of native and conjugated protein. The signal at approximately 14.3 kDa is a narrow distribution that can be assigned to native unreacted lysozyme, while the higher mass value species correspond to the polymer-protein conjugates obtained. Samples collected after separation using CEX chromatography were then analyzed via MALDI and assigned to a protein or polymer-protein species (Fig 7.22 B, D, and F). In the case of conjugation experiments using either PNAM_{3.5 kDa} or PNAM_{7 kDa}, the spectra of the first and second eluted species on CEX show a monomodal distribution. The maximum of these signals add up to two and one polymer chains attached on one protein, respectively. As previously mentioned, the last species to elute is lysozyme, as seen from the signal at 14.3 kDa on the MALDI spectra for all cases. Analysis of the separation of the PEOGMA-lysozyme conjugates using MALDI show a similar pattern in the case of the native and mono conjugated protein. Although a signal of native protein is still visible on the spectrum of the mono conjugated species, further characterization of the sample

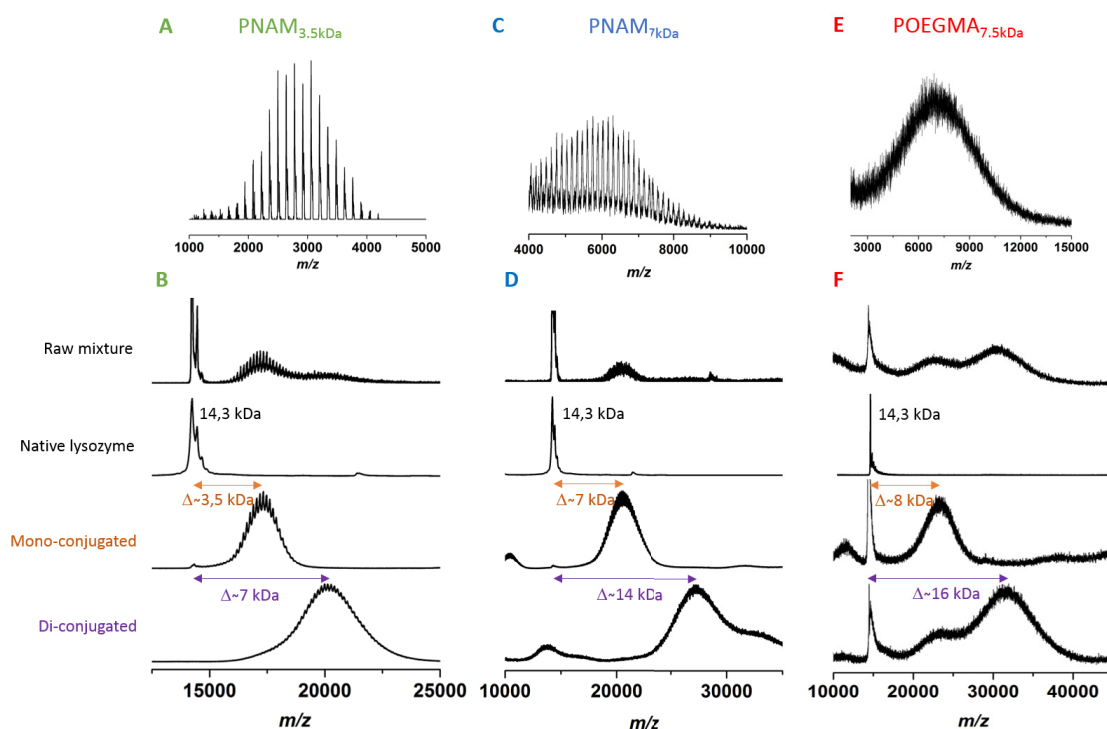


Figure 7.2: MALDI spectra of the synthesized polymers (top) and the conjugated fractions separated using CEX chromatography (bottom).

using high-throughput capillary gel electrophoresis (Supplementary Figure A.7) and SEC (Supplementary Figure A.8) have proven the high purity of the mono conjugate. The higher conjugates corresponding to the first eluted species on CEX, however, show more than one distribution and were, therefore, not used for further experiments.

7.3.3 Stability Assessment

7.3.3.1 Functional Stability

The functional stability of the purified protein-polymer conjugates was studied using a lysozyme specific activity assay based on the substrate *M. lysodeikticus*. The assay procedure and calculation of the residual enzyme activities were performed according to [293]. The resulting catalytic activities of native, PNAMylated and POEGMALated lysozyme species are displayed in Fig. 7.3. With the exception of mono-PNAM_{3.5 kDa}ylated lysozyme, all conjugated species had a lower in vitro activity than the native protein. For PNAM, increasing the molecular weight of the polymer for a constant conjugation degree as well as increasing the conjugation degree for a constant polymer molecular weight resulted in a decreased residual activity. These results are in accordance with the activities of

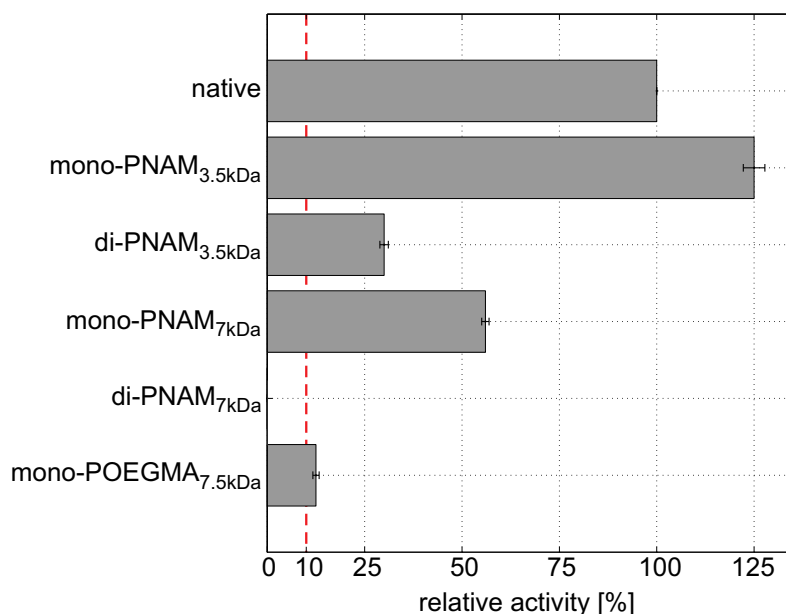


Figure 7.3: Residual lysozyme activity (%) of protein-polymer conjugates towards the substrate *M. lysodeikticus*. The indicated activity values refer to native lysozyme as reference.

PEGylated lysozyme species published earlier [293]. For PEG, changes in enzyme activities upon PEGylation have shown to result from a combination of steric hindrance and molecular flexibility. It can be assumed, that similar mechanism apply for the here studied polymers. di-PNAM_{7 kDa}ylated lysozyme showed no residual activity. When comparing mono-PNAM_{7 kDa}ylated and mono-POEGMA_{7.5 kDa}lated lysozyme, the PNAM-conjugates exhibit a significantly higher residual activity of 56 % compared to 13.5 % for the POEGMA-conjugates. The low residual activity obtained for di-POEGMA_{7.5 kDa}lated lysozyme gives grounds to expect a residual activity of below 10 % for di-POEGMA_{7.5 kDa}lated lysozyme. Due to these uneconomical residual activities, di-PNAM_{7 kDa}ylated and di-POEGMA_{7.5 kDa}lated lysozyme were not investigated further in the subsequent stability study.

7.3.3.2 Colloidal Stability

In addition to conserving the biological functionality after the conjugation, the resulting physicochemical properties of the hybrid molecules are of major interest. In this study, the solubility and the phase behavior of the conjugates are investigated as an important physicochemical property. To obtain information about the colloidal stability of the conjugated lysozyme species, protein phase diagrams were generated for lysozyme conjugated with PNAM_{3.5 kDa}, PNAM_{7 kDa} and POEGMA_{7.5 kDa} in microbatch format at pH 3 under the influence of NaCl. The investigated phase transitions are displayed in Fig 7.4B-E. The phase diagram for native lysozyme Fig 7.4A was generated earlier by Baumgartner et al. [79]. For a comparison of the phase behavior on basis of a constant number of molecules, the mass concentrations used by Baumgartner et al. were converted into molar concentrations. The formation of crystals as well as precipitate was observed for native lysozyme. For NaCl concentrations above 1.82 mol/L precipitation was accompanied by skin formation which indicates protein denaturation.

Compared to native lysozyme, all conjugated species featured a reduced aggregation propensity which manifests in an extension of the soluble area. For mono-PNAM_{3.5 kDa}ylated lysozyme (Fig 7.4B), the NaCl concentration initiating a phase transition for the highest investigated protein concentration was twice as high when compared to native lysozyme. The visual evaluation of the phase diagrams revealed phase transitions to crystallization, precipitation and gelation. For all occurring phase transitions, the formation of precipitate was observed. For moderate salt and protein concentrations, precipitate was accomplished by gelation and the formation of microcrystals. Except for the deficiency

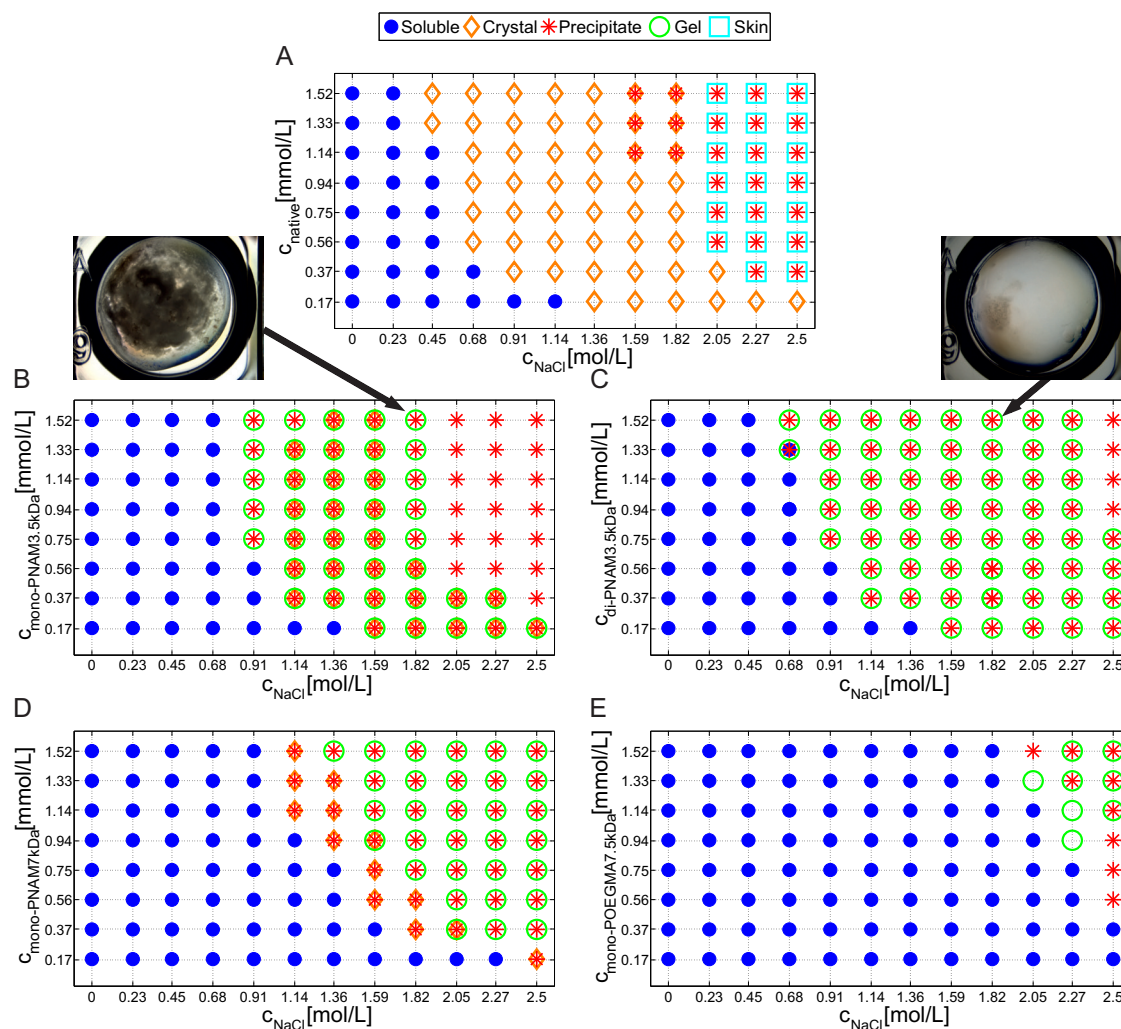


Figure 7.4: Phase diagrams for native (A), 3.5 kDa mono-PNAMylated (B), 3.5 kDa di-PNAMylated (C), 7 kDa mono-PNAMylated (D), 7.5 kDa mono-POEGMAlyated (in preparation and therefore at day 7) (E) lysozyme with sodium chloride (NaCl) as precipitant at pH 3. Data for the phase diagrams of native lysozyme was taken from [79].

of microcrystals and a slight increase in the gelation area, the resulting phase diagram of mono- and di-PNAM_{3.5} kDa_{ylated} lysozyme (Fig 7.4B and C, respectively) show similar features. However, the resulting aggregates differ greatly in their appearance as shown by the photographs in Fig 7.4 (conjugate concentration of 1,52 mmol/l and a NaCl concentration of 1,82 mol/l). In the case of mono-PNAM_{3.5} kDa_{ylated} lysozyme, heavy precipitation

occurs resulting in a visible dark area. For di-PNAM_{3.5 kDa}ylated lysozyme, the phase transition is predominated by gelation and only light precipitate is formed. For a higher conjugation degree, the properties of the conjugates seem to be rather dominated by the polymer properties than by those of the native protein. PNAM is a hydrophilic polymer that increases the hydrodynamic radius of the protein by binding water molecules. Thereby the interactions of salts ions and protein charges are weakened. Moreover, the bound polymer masks hydrophobic patches on the protein surface. Since the present salt ions have less interactions and the hydrophobic patches are less accessible, the hydrophobic forces are weaker and a higher precipitant agent concentration is necessary to induce protein-based aggregation. However, these same high salt concentrations seem to lead to physically crosslinked polymer gels. Crosslinking by ionic interactions is a known strategy for hydrogel formation, that does not necessarily require the presence of ionic groups in the polymer for gel formation [320, 321]. Mono-POEGMA_{7.5 kDa}ylated lysozyme shows the largest soluble area of all investigated conjugate species. For the highest protein concentration used, 2.05 M NaCl was necessary to induce phase transition for the POEGMAylated lysozyme compared to 0.45 M NaCl for unmodified lysozyme. Precipitation and gelation preexisted for the conjugated species. For POEGMA the outstanding reduction of the aggregation propensity is contrasted by the already discussed extreme decrease of the residual biological activity. This example clearly demonstrates that a careful choice of the polymer type, molecular weight and number of bound molecules must be made depending on the requirements of the particular application.

To quantify the impact of the polymer attachment on the solubility increase, the conjugate concentration in the supernatant of the batch systems with observed phase transition was measured after 40 days of incubation. In Fig. 7.5, the measured solubility curves for mono- and di-PNAM_{3.5 kDa}ylated lysozyme as well as for mono-PNAM_{7 kDa}ylated lysozyme are displayed. The solubility curves for native lysozyme [254] and mono-PEG_{2 kDa}ylated lysozyme [293] have been published earlier. As already expected from the phase diagrams, all conjugated species show a higher solubility under the influence of NaCl at pH 3. Surprisingly, 3.5 kDa di-PNAMylated lysozyme exhibits a lower solubility than 3.5 kDa mono-PNAMylated lysozyme at moderate salt concentrations. For high salt concentrations, the two solubility curves approach each other. Based on the assumption that two attached polymer chains lead to a higher shielding effect, di-PNAM_{3.5 kDa}ylated lysozyme was expected to be more stable than mono-PNAM_{3.5 kDa}ylated lysozyme. A possible explanation is the higher proportion of bound water molecules by two polymer chains compared to one polymer chain. Compared to the mono-conjugated species, the

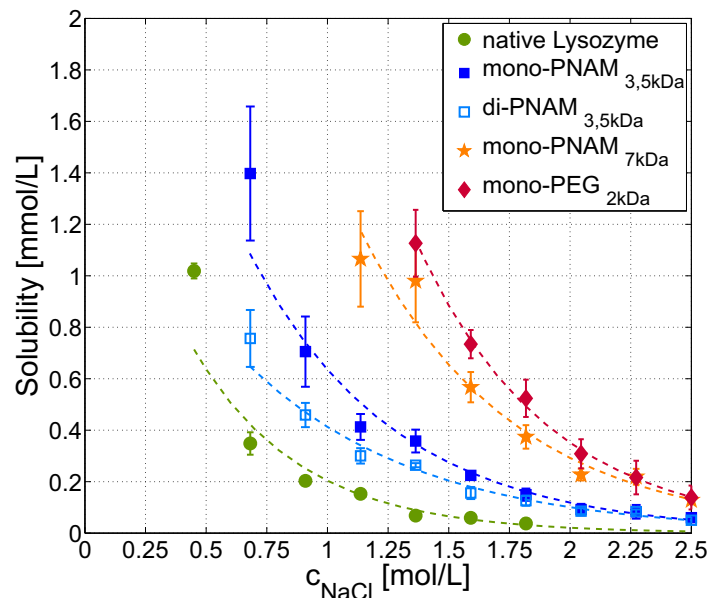


Figure 7.5: Solubility lines of unmodified lysozyme [254], mono-PNAM_{3.5 kDa}ylated lysozyme, di-PNAM_{3.5 kDa}ylated lysozyme, mono-PNAM_{7 kDa}ylated lysozyme and mono-PEG_{2 kDa}ylated lysozyme [293] at pH 3. Solubility line for mono-POEGMA_{7.5 kDa}ylated lysozyme is in preparation.

residual water necessary for a solvation of the protein conjugates is reduced which may cause the observed decrease in solubility. The solubility line of mono-PNAM_{7 kDa}ylated lysozyme behaves similarly to that of mono-PEG_{2 kDa}ylated lysozyme. It can be stated that due to the difference in polymer architecture, a higher molecular weight of PNAM is required to achieve the same stabilizing effect as by PEG.

At the point of handing in this thesis, the phase experiment for mono-POEGMA_{7.5 kDa}ylated lysozyme is in its 40 days incubation period and the solubility line is not yet measured. Based on the optical evaluation of the phase diagrams, however, a higher solubility is expected when compare to mono-PEG_{2 kDa}ylated lysozyme.

7.4 Conclusion

In this study, the polymers PNAM and POEGMA were synthesized by RAFT polymerization and conjugated to lysozyme from chicken egg white. The resulting conjugate properties result from a combination of protein and polymer properties. By shielding the

protein surface, the attached polymer simultaneously led to a decrease in the in vitro activity and an increase in the equilibrium solubility under a combined influence of extreme salt concentrations and pH value. The here presented method constitutes a helpful tool for optimizing polymer parameters for a tradeoff between enhanced physicochemical properties and reduced in vitro activity.

7.5 Acknowledgments

We gratefully acknowledge the financial support by the German Federal Ministry of Education and Research (BMBF). This research work is part of the project ‘Molecular Interaction Engineering: From Nature’s Toolbox to Hybrid Technical Systems’, funding code 031A095B. G.G.A. thanks the Mexican National Council for Science and Technology (Conacyt) for a doctoral research scholarship. Frank Kirschhöfer, Boris Köhl, and Dr. Gerald Brenner-Weiss (IFG, KIT) are acknowledged for providing access to and support on MALDI-ToF.

7.6 References

13. EvaluatePharma. *World Preview 2015, Outlook to 2020* <http://info.evaluategroup.com/rs/607-YGS-364/images/wp15.pdf>. [Online; accessed 12/2016].
79. Baumgartner, K., Galm, L., Nötzold, J., Sigloch, H., Morgenstern, J., Schleining, K., Suhm, S., Oelmeier, S. A. & Hubbuch, J. Determination of protein phase diagrams by microbatch experiments: Exploring the influence of precipitants and pH. *Int. J. Pharm.* **479**, 28–40 (2015).
124. Katre, N. V. The conjugation of proteins with polyethylene glycol and other polymers: Altering properties of proteins to enhance their therapeutic potential. *Advanced Drug Delivery Reviews* **10**, 91–114 (1993).
126. Pelegri-O’Day, E. M., Lin, E.-W. & Maynard, H. D. Therapeutic protein-polymer conjugates: Advancing beyond PEGylation. *Journal of the American Chemical Society* **136**, 14323–14332 (2014).
135. Knop, K., Hoogenboom, R., Fischer, D. & Schubert, U. S. Poly (ethylene glycol) in drug delivery: Pros and cons as well as potential alternatives. *Angewandte Chemie International Edition* **49**, 6288–6308 (2010).

142. Harris, J. M. & Chess, R. B. Effect of PEGylation on pharmaceuticals. *Nat. Rev. Drug Discov.* **2**, 214–221 (2003).
149. Seely, J. E. & Richey, C. W. Use of ion-exchange chromatography and hydrophobic interaction chromatography in the preparation and recovery of polyethylene glycol-linked proteins. *J. Chromatogr. A* **908**, 235–241 (2001).
242. Rose, J. R., Salto, R. & Craik, C. S. Regulation of autoproteolysis of the HIV-1 and HIV-2 proteases with engineered amino acid substitutions. *Journal of Biological Chemistry* **268**, 11939–11945 (1993).
243. Tiukinhoy-Laing, S. D., Huang, S., Klegerman, M., Holland, C. K. & McPherson, D. D. Ultrasound-facilitated thrombolysis using tissue-plasminogen activator-loaded echogenic liposomes. *Thrombosis Research* **119**, 777–784 (2007).
244. Sinha, V. R. & Trehan, A. Biodegradable microspheres for protein delivery. *Journal of Controlled Release* **90**, 261–280 (2003).
254. Galm, L., Morgenstern, J. & Hubbuch, J. Manipulation of lysozyme phase behavior by additives as function of conformational stability. *Int. J. Pharm.* **494**, 370–380 (2015).
258. Yoshimoto, N. & Yamamoto, S. PEGylated protein separations: Challenges and opportunities. *Biotechnol. J.* **7**, 592–593 (2012).
278. Da Silva Freitas, D. & Abrahao-Neto, J. Biochemical and biophysical characterization of lysozyme modified by PEGylation. *Int. J. Pharm.* **392**, 111–117 (2010).
282. Smith, R. D., Loo, J. A., Edmonds, C. G., Barinaga, C. J. & Udseth, H. R. New developments in biochemical mass spectrometry: Electrospray ionization. *Anal. Chem.* **62**, 882–899 (1990).
289. Manning, M. C., Patel, K. & Borchardt, R. T. Stability of protein pharmaceuticals. *Pharm. Res.* **6**, 903–918 (1989).
290. Harris, J. M., Martin, N. E. & Modi, M. Pegylation. *Clinical pharmacokinetics* **40**, 539–551 (2001).
291. Biedermann, F., Rauwald, U., Zayed, J. M. & Scherman, O. A. A supramolecular route for reversible protein-polymer conjugation. *Chemical Science* **2**, 279–286 (2011).

-
292. Lucius, M., Falatach, R., McGlone, C., Makaroff, K., Danielson, A., Williams, C., Nix, J. C., Konkolewicz, D., Page, R. C. & Berberich, J. A. Investigating the Impact of Polymer Functional Groups on the Stability and Activity of Lysozyme–Polymer Conjugates. *Biomacromolecules* **17**, 1123–1134 (2016).
293. Morgenstern, J., Baumann, P., Brunner, C. & Hubbuch, J. Effect of PEG molecular weight and PEGylation degree on the physical stability of PEGylated lysozyme. *Int. J. Pharm.* **519**, 408–417 (2017).
294. Abuchowski, A., Van Es, T., Palczuk, N. & Davis, F. Alteration of immunological properties of bovine serum albumin by covalent attachment of polyethylene glycol. *J. Biol. Chem.* **252**, 3578–3581 (1977).
295. Richter, A. W. & Åkerblom, E. Antibodies against polyethylene glycol produced in animals by immunization with monomethoxy polyethylene glycol modified proteins. *International Archives of Allergy and Immunology* **70**, 124–131 (1983).
296. Richter, A. W. & Åkerblom, E. Polyethylene glycol reactive antibodies in man: Titer distribution in allergic patients treated with monomethoxy polyethylene glycol modified allergens or placebo, and in healthy blood donors. *International Archives of Allergy and Immunology* **74**, 36–39 (1984).
297. Sundry, J. S., Ganson, N. J., Kelly, S. J., Scarlett, E. L., Rehrig, C. D., Huang, W. & Hershfield, M. S. Pharmacokinetics and pharmacodynamics of intravenous PEGylated recombinant mammalian urate oxidase in patients with refractory gout. *Arthritis & Rheumatology* **56**, 1021–1028 (2007).
298. Garay, R. P., El-Gewely, R., Armstrong, J. K., Garratty, G. & Richette, P. Antibodies against polyethylene glycol in healthy subjects and in patients treated with PEG-conjugated agents. *Expert Opinion on Drug Delivery* **9**, 1319–1323 (2012).
299. Schellekens, H., Hennink, W. E. & Brinks, V. The immunogenicity of polyethylene glycol: Facts and fiction. *Pharm. Res.* **30**, 1729–1734 (2013).
300. Armstrong, J., Hempel, G., Koling, S., Chan, L., Fisher, T., Meiselman, H. & Garratty, G. Antibody against poly (ethylene glycol) adversely affects PEG-asparaginase therapy in acute lymphoblastic leukemia patients. *Cancer* **110**, 103–111 (2007).
301. Ulbricht, J., Jordan, R. & Luxenhofer, R. On the biodegradability of polyethylene glycol, polypeptoids and poly (2-oxazoline) s. *Biomaterials* **35**, 4848–4861 (2014).
302. Qi, Y. & Chilkoti, A. Protein-polymer conjugation - moving beyond PEGylation. *Current opinion in chemical biology* **28**, 181–193 (2015).

303. Ozer, I. & Chilkoti, A. Site-Specific and Stoichiometric Stealth Polymer Conjugates of Therapeutic Peptides and Proteins. *Bioconjugate chemistry* **28**, 713–723 (2017).
304. Krishna, O. D. & Kiick, K. L. Protein-and peptide-modified synthetic polymeric biomaterials. *Peptide Science* **94**, 32–48 (2010).
305. Ranucci, E., Spagnoli, G., Sartore, L., Ferruti, P., Caliceti, P., Schiavon, O. & Veronese, F. M. Synthesis and molecular weight characterization of low molecular weight end-functionalized poly (4-acryloylmorpholine). *Macromolecular Chemistry and Physics* **195**, 3469–3479 (1994).
306. D'Agosto, F., Hughes, R., Charreyre, M.-T., Pichot, C. & Gilbert, R. G. Molecular weight and functional end group control by RAFT polymerization of a bisubstituted acrylamide derivative. *Macromolecules* **36**, 621–629 (2003).
307. Veronese, F. M., Schiavon, O., Caliceti, P., Sartore, L., Ranucci, E. & Ferruti, P. *Polymers of N-acryloylmorpholine activated at one end and conjugates with bioactive materials and surfaces* US Patent 5,629,384. 1997.
308. Wang, X.-S., Lascelles, S., Jackson, R. & Armes, S. Facile synthesis of well-defined water-soluble polymers via atom transfer radical polymerization in aqueous media at ambient temperature. *Chemical Communications*, 1817–1818 (1999).
309. Wang, X.-S. & Armes, S. Facile atom transfer radical polymerization of methoxy-capped oligo (ethylene glycol) methacrylate in aqueous media at ambient temperature. *Macromolecules* **33**, 6640–6647 (2000).
310. Gao, W., Liu, W., Mackay, J. A., Zalutsky, M. R., Toone, E. J. & Chilkoti, A. In situ growth of a stoichiometric PEG-like conjugate at a protein's N-terminus with significantly improved pharmacokinetics. *PNAS* **106**, 15231–15236 (2009).
311. Gao, W., Liu, W., Christensen, T., Zalutsky, M. R. & Chilkoti, A. In situ growth of a PEG-like polymer from the C terminus of an intein fusion protein improves pharmacokinetics and tumor accumulation. *PNAS* **107**, 16432–16437 (2010).
312. Bovera, R., Ottolina, G., Carrea, G., Ferruti, P. & Veronese, F. M. Modification of lipase from *Pseudomonas* sp. with poly (acryloylmorpholine) and study of its catalytic properties in organic solvents. *Biotechnology letters* **16**, 1069–1074 (1994).
313. Schiavon, O., Caliceti, P., Ferruti, P. & Veronese, F. Therapeutic proteins: A comparison of chemical and biological properties of uricase conjugated to linear or branched poly (ethylene glycol) and poly (N-acryloylmorpholine). *Il Farmaco* **55**, 264–269 (2000).

-
314. Giardino, R., Giavaresi, G., Fini, M., Torricelli, P. & Guzzardella, G. A. The role of different chemical modifications of superoxide dismutase in preventing a prolonged muscular ischemia/reperfusion injury. *Artificial Cells, Blood Substitutes, and Biotechnology* **30**, 189–198 (2002).
315. Bencini, M., Ranucci, E., Ferruti, P., Manfredi, A., Trotta, F. & Cavalli, R. Poly (4-acryloylmorpholine) oligomers carrying a β -cyclodextrin residue at one terminus. *Journal of Polymer Science Part A: Polymer Chemistry* **46**, 1607–1617 (2008).
316. Cummings, C. S., Campbell, A. S., Baker, S. L., Carmali, S., Murata, H. & Russell, A. J. Design of Stomach Acid-Stable and Mucin-Binding Enzyme Polymer Conjugates. *Biomacromolecules* **18**, 576–586 (2017).
317. Skrabania, K., Miasnikova, A., Bivigou-Koumba, A. M., Zehm, D. & Laschewsky, A. Examining the UV-vis absorption of RAFT chain transfer agents and their use for polymer analysis. *Polymer Chemistry* **2**, 2074–2083 (2011).
318. Roberts, M., Bentley, M. & Harris, J. Chemistry for peptide and protein PEGylation. *Adv. Drug Deliv. Rev.* **64**, 116–127 (2012).
319. Morgenstern, J., Wang, G., Baumann, P. & Hubbuch, J. Model-Based Investigation on the Mass Transfer and Adsorption Mechanisms of Mono-Pegylated Lysozyme in Ion-Exchange Chromatography. *Biotechnol. J.* doi:10.1002/biot.201700255 (2017).
320. Hennink, W. & Van Nostrum, C. Novel crosslinking methods to design hydrogels. *Advanced drug delivery reviews* **64**, 223–236 (2012).
321. Hoffman, A. S. Hydrogels for biomedical applications. *Advanced drug delivery reviews* **64**, 18–23 (2012).
361. Kittelmann, J., Ottens, M. & Hubbuch, J. Robust high-throughput batch screening method in 384-well format with optical in-line resin quantification. *J. Chrom. B* **988**, 98–105 (2015).

Model-based Investigation on the Mass Transfer and Adsorption Mechanisms of Mono-PEGylated Lysozyme in Ion-Exchange Chromatography

Josefine Morgenstern*, Gang Wang*, Pascal Baumann and Jürgen Hubbuch**

Institute of Engineering in Life Sciences, Section IV: Biomolecular Separation Science, Karlsruhe Institute of Technology (KIT), 76131 Karlsruhe, Germany

** These authors contributed equally to this work.*

*** Corresponding author. Biotechnology journal 12/9 (2017), accepted manuscript.*

Abstract

Recent studies highlighted the potential of PEGylated proteins to improve stabilities and pharmacokinetics of protein drugs. Ion-exchange chromatography (IEX) is among the most frequently used purification methods for PEGylated proteins. However, the underlying physical mechanisms allowing for a separation of different PEGamers (proteins with a varying number of attached PEG molecules) are not yet fully understood.

In this work, mechanistic chromatography modeling was applied to gain a deeper understanding of the mass transfer and adsorption/desorption mechanisms of mono-PEGylated proteins in IEX. Using a combination of the general rate model (GRM) and the steric mass action (SMA) isotherm, simulation results in good agreement with the experimental data were achieved. During linear gradient elution of proteins attached with PEG of different molecular weight, similar peak heights and peak shapes at constant gradient length were observed. A superimposed effect of increased desorption rate and reduced diffusion rate as a function of the hydrodynamic radius of PEGylated proteins was identified to be the reason of this anomaly. That is why the concept of the diffusion-desorption-compensation effect is proposed. In addition to the altered elution orders, PEGylation resulted in a considerable decrease of maximum binding capacity. By using the SMA model in a kinetic formulation, the adsorption behavior of PEGylated proteins in the highly concentrated state was described mechanistically. An exponential increase in the steric hindrance effect with increasing PEG molecular weight was observed. This suggests the formation of multiple PEG layers in the interstitial space between bound proteins and an associated shielding of ligands on the adsorber surface to be the cause of the reduced maximum binding capacity. The presented *in silico* approach thus complements the hitherto proposed theories on the binding mechanisms of PEGylated proteins in IEX.

Keywords: *Mechanistic modeling, ion-exchange chromatography, PEGylated proteins, diffusion-desorption-compensation effect, shielding*

8.1 Introduction

It is estimated that in 2020 about 46% of the sales volume of the 100 highest-selling pharmaceutical products will be achieved by biopharmaceutical products [13]. Biopharmaceuticals contain active substances based on biological molecules, such as recombinant proteins. Compared to conventional small molecular pharmaceuticals, proteins have a complex three-dimensional structure allowing for a more efficient and specific intervention in cellular metabolic pathways. The efficacy of systemically administered protein drugs however, may be hampered by a low bioavailability due to a poor solubility under physiological conditions, a short in vivo half-life due to a rapid elimination by the body and proteolysis. A promising approach to overcoming these drawbacks is the covalent attachment of polyethylene glycol (PEG) to protein drugs [142]. As early as in 1977, the group of Abuchowski and Davis found an increased blood circulation half-life and a reduced immunogenicity of PEGylated proteins compared to the native form [133, 294]. Additional positive effects of PEGylation are an increased thermal stability as well as a higher solubility allowing for higher concentrated protein formulations [293]. Two successfully approved PEGylated protein drugs are interferon α -2a (Pegasys[®], Hoffman-LaRoche) for the treatment of hepatitis C and granulocyte-colony stimulating factor (Neulasta[®], Amgen) for the treatment of leukemia.

The emergence of conjugates with varying number (PEGamers) and site of attachment (positional isoforms) upon PEGylation reactions creates a need for a thorough purification in order to gain regulatory approval [130, 322]. Ion-exchange chromatography (IEX) is among the most frequently used purification methods for PEGylated proteins [129, 130]. Understanding the underlying physical mechanisms is an important prerequisite to optimize, control, predict, and scale-up the separation of PEGamers to pilot and production level. In this context, mechanistic modeling provides an excellent opportunity to generate various information about mass transport and adsorption isotherm parameters *in silico*.

The physico-chemical properties and thus the behavior of a protein in chromatographic separation processes are significantly influenced by its PEGylation [130, 322]. Due to the high hydration of the hydrophilic PEG, PEGylated proteins have a distinctly higher hydrodynamic radius than unmodified proteins with the same molecular weight. A non-linear correlation introduced by Fee and Van Alstine allows a reliably mathematical prediction of the hydrodynamic radius $h_{R,PEGprot}$ based on the molecular weight of the protein and the attached PEG [130, 139]. In case of chromatographic separation, the

PEG ‘cloud’ around the protein results in an increased distance between protein binding site and adsorber surface [322]. Seely and Richey [149] observed that the elution order of different PEGamers was the same in both cation-exchange and anion-exchange chromatography. They proposed the ‘charge-shielding effect’ which links the weakened electrostatic interactions to the increased distance between protein binding site and adsorber surface. A deeper process understanding was achieved by Yamamoto et al. [323] using mechanistic chromatography modeling. They applied the stoichiometric displacement model (SDM) to verify the ‘charge-shielding effect’ quantitatively and associated it with the decreased elution volume of PEGamers. Moreover, it was shown that mono-PEGylated proteins are bound to the ion-exchange adsorber with binding sites similar to the unmodified protein. In following studies, this model was applied to PEGylated lysozyme and BSA [150, 324]. The aforementioned contributions demonstrated the successful application of mechanistic modeling to understand the adsorption behavior of PEGylated proteins in the linear region of the adsorption isotherm.

This work presents a full investigation of the behavior of mono-PEGylated proteins in IEX based on mechanistic chromatography modeling. In contrast to previous studies, information on the adsorption and desorption behavior in the non-linear region of the isotherm, i.e. the overloaded state, is included by using the steric mass action (SMA) model [155] in kinetic formulation. Compared to the equilibrium isotherm used hitherto, the kinetic formulation is suitable for the description of protein behavior in higher concentrated state on adsorber surface. To further account for mass transfer effects within the chromatography column the general rate model (GRM) [325] is employed. To best of our knowledge, mechanistic modeling of polymer grafted proteins in IEX using a combination of GRM and SMA isotherm has not been studied. By connecting these two approaches, this study delivers supplements by the quantitative investigation on the film diffusion, pore diffusion, charge and shielding parameters, as well as the adsorption and desorption rate coefficients.

The model protein lysozyme from chicken egg was chosen as PEGylation target and conjugated to activated PEG of three different molecular weights (2 kDa, 5 kDa and 10 kDa). The preparative isolation of the mono-PEGylated species was carried out using a single cation-exchange (CEX) chromatography step. For each purified protein species, three linear gradient elution (LGE) experiments with different gradient slopes were conducted to confirm the constancy of the characteristic charge. Breakthrough experiments were carried out to gain insight into the binding behavior of PEGylated proteins in the highly non-linear region and to investigate whether the perceivable behavior of PEGylated pro-

teins originates from adsorption/desorption or mass transfer. Confidence intervals at 95 % level were calculated for parameter estimates.

8.2 Materials and Methods

8.2.1 Adsorber, Proteins, and Chemicals

All stock solutions and buffers were prepared with ultra-pure water (PURELAB Ultra water purification system, ELGA Labwater, Germany), filtrated using a cellulose-acetate filter with a membrane cut-off of 0.22 μm (Satorius, Germany) and degassed by sonication. The used buffer substances were sodium acetate trihydrate (Sigma-Aldrich, USA) for pH 5 and sodium phosphate monobasic dihydrate (Sigma-Aldrich, USA) as well as di-sodium hydrogen phosphate dihydrate (Merck, Germany) for pH 7.0 and pH 7.2, respectively. Hydrochloric acid and sodium hydroxide (NaOH) for pH adjustment were obtained from Merck (Germany). Lysozyme from chicken egg-white (no. HR7-110) was purchased from Hampton Research (USA). Methoxy-PEG-propionaldehyde (mPEG-aldehyde) with an average molecular weight (MW) of 2 kDa (Sunbright[®]ME-020 AL), 5 kDa (Sunbright[®]ME-050 AL) and 10 kDa (Sunbright[®]ME-100 AL) was obtained from NOF Corporation (Japan). Sodium cyanoborohydride (NaCNBH₃) and L-lysine were purchased from Sigma-Aldrich (USA). For preparative isolation of PEGamers as well as for modeling purposes, the strong cation-exchange (CEX) chromatography adsorber medium TOYOPEARL[®] GigaCap S-650M (Tosoh Bioscience, Germany) was used. It is a high capacity polymer grated cation exchange resin based on hydroxylated methacrylic polymer with a 100 nm pore size and a 75 μm particle size. For preparative isolation of PEGamer species, 5 mL pre-packed MiniChrom columns (dimension: 100 mm \times 8 mm) and for modeling purposes, a pre-packed 0.965 mL Toyoscreen[®] column (dimension: 30 mm \times 6.4 mm) were used. Between the runs, the resin media were stored in 20 % ethanol. The storage solution was removed by prolonged equilibration with ultra-pure water and flushed with binding and elution buffer before experimentation. Sodium chloride (NaCl) used for protein elution was purchased from Merck (Germany). 0.5 M NaOH (Merck, Germany) was used for cleaning-in-place.

8.2.2 Instrumentation and Software

pH adjustment of all buffers was performed using a five-point calibrated pH-meter HI-3220 (Hanna Instruments, USA) equipped with a SenTix[®]62 pH electrode (Xylem Inc., USA). Protein concentration measurements were conducted using a NanoDrop2000c UV-vis spectrophotometer (Thermo Fisher Scientific, USA). Purity of isolated mono-PEGylated lysozyme was determined by high-throughput capillary gel electrophoresis (HT-CGE) using the Caliper LabChip[®]GX II device (PerkinElmer, USA). For data processing and purity determination, the LabChip[®]GX 3.1 software (PerkinElmer, USA) was used.

Preparative isolation of mono-PEGylated lysozyme species was performed on an ÄKTA[™] purifier system equipped with a Fraction Collector Frac-950 (GE Healthcare, Sweden). All experiments for chromatography model calibration were carried out using an Ettan liquid chromatography (LC) system with the UV monitor UV-900 (3 mm optical path length), pump unit P-905, dynamic single chamber mixer M-925 (90 μ l mixer volume), and conductivity cell pH/C-900 (all GE Healthcare, Little Chalfont, Buckinghamshire, UK). The UNICORN 5.31 software (GE Healthcare, UK) was used to control both chromatographic systems and to record the signals. The protein chromatography simulation software ChromX (GoSilico, Germany) was used for the numerical simulations of the system of partial differential equations, estimation of model parameters, as well as for statistical analysis [158]. Other data evaluations were conducted in Matlab[®] R2016a (MathWorks, USA).

8.2.3 PEGylation Reaction

As reaction buffer 25 mM sodium phosphate (pH 7.2) containing 20 mM sodium cyanoborohydride (NaCNBH₃) as reducing agent was used. PEGylation experiments were performed batch-wise in 50 mL Falcon Tubes (BD Biosciences, USA). Lysozyme (5 mg/mL) and mPEG-aldehyde were dissolved in the reaction buffer with a molar polymer to protein ratio of 6.67:1 [264, 281]. The tube was continuously shaken in an overhead shaker LabincoLD79 (Labinco BV, Netherlands) for 3.5 h at 25°C. The PEGylation reaction was stopped by adding 200 mM of L-lysine according to [253].

8.2.4 Preparative Purification of Mono-PEGylated Lysozyme

For preparative isolation of mono-PEGylated lysozyme, the stopped PEGylation batch was diluted to a ratio of 1:12 in 10 mM sodium acetate buffer (pH 5) [281]. For column loading, the system was equilibrated in 10 mM sodium acetate buffer (pH 5). Sample application was performed using a 50 mL super loop (GE Healthcare, Sweden). Elution was initiated by applying an NaCl step gradient with 10 mM sodium acetate buffer (pH 5) containing 1.0 M sodium chloride. The NaCl molarities used for the step elution of the different PEGamers are displayed in Tab. 8.1 as a function of the molecular weight of the attached PEG molecules. The flow rate for binding and elution was set to 1 mL/min. Fractions of 2 mL were collected into a 96-well deep well plate (VWR, USA). To obtain sufficient sample volume for the linear gradient and the breakthrough experiments, fractions containing mono-PEGylated lysozyme of multiple chromatography runs were pooled.

Table 8.1: NaCl steps in mM used for the elution of different PEGamer species from Toyopearl GigaCap S-650M at pH 5 as a function of the PEG molecular weight

	Native lysozyme	mono-PEGylated lysozyme	di-PEGylated lysozyme
$M_w=2$ kDa	1000	460	290
$M_w=5$ kDa	1000	350	160
$M_w=10$ kDa	1000	250	75

To ensure similar binding conditions for all PEG molecular weights during the calibration runs, the mono-PEGylated samples were concentrated to approximately $3.76 \cdot 10^{-4}$ M. This was accomplished by evaporation using a vacuum concentration unit RVC 2-33CDplus (Martin Christ Gefriertrocknungsanlagen GmbH, Germany) operated at 24 mbar. After concentrating, the protein samples were transferred to 25 mM sodium phosphate buffer (pH 7) using Slide-A-Lyzer™ Dialysis Cassettes (Thermo Fisher Scientific, USA) with a molecular weight cut-off of 2 kDa. All chromatography experiments were carried out at 25°C.

8.2.5 Offline Identification and Quantification of PEGamer Species

Purity of isolated mono-PEGylated lysozyme was determined by high-throughput capillary gel electrophoresis (HT-CGE) as described in [281]. The experiments were performed

with an HT Protein Express LabChip[®] and an HT Protein Express Reagent Kit (Perkin Elmer, Hopkinton, MA, USA). The LabChip[®] installation, sample preparation and analysis were performed according to the manufacturer's standard protocol [326]. Sample preparation was performed in skirted 96-well polypropylene twin.tec[®] PCR plates from Eppendorf (Hamburg, Germany). Molecular weight determination was performed according to protein standards from the HT Protein Express Reagent Kit.

For protein quantification, absorption measurements at 280 nm were performed. Since the bound PEG molecules do not absorb at 280 nm, the extinction coefficient of $\epsilon_{280\text{ nm, lysozyme}}^{1\%} = 22.00$ was used for native as well as for mono-PEGylated lysozyme [79, 281]. Appropriate blanks were subtracted. Molar concentrations were calculated using a lysozyme molecular mass of 14.6 kDa [327]. The final concentrations of native lysozyme and mono-PEGylated species attached with 2 kDa, 5 kDa, and 10 kDa PEG used for the linear gradient and breakthrough experiments were $3.87 \cdot 10^{-4} \pm 7.19 \cdot 10^{-7}$ M, $3.63 \cdot 10^{-4} \pm 1.41 \cdot 10^{-7}$ M, $3.60 \cdot 10^{-4} \pm 1.61 \cdot 10^{-7}$ M, and $3.81 \cdot 10^{-4} \pm 1.57 \cdot 10^{-5}$ M, respectively. The slight deviations in PEGamer concentrations are due to concentrating and buffer exchange. For subsequent modeling the exact concentrations were employed.

8.2.6 Chromatography System Characterization

Tracer pulse injections at constant flow rate of 0.33 mL/min were carried out to characterize the ÄKTA[™] system and chromatography column. For determination of the interstitial volume of the column, 25 μ L of 10 g/L non-interacting, non-pore-penetrating tracer blue dextran 2000 kDa (Sigma-Aldrich, St. Louis, MO, USA) in ultra-pure water was used. 25 μ L of 1%(v/v) pore-penetrating, non-interacting tracer acetone (Merck, Darmstadt, Germany) in ultra-pure water was used to determine system and total voidage of the column. The UV signals at 260 nm were recorded for that purpose. All measurements were corrected with respect to system dead volumes. The ionic capacity Λ of GigaCap S-650M was determined via acid-base titration following Huuk and coworkers [157].

8.2.7 Linear Gradient Experiments for Model Calibration

Protein solutions with lysozyme and its PEGylated species were prepared in binding buffer (25 mM sodium phosphate buffer, pH 7.0). Before injection, the protein solutions were filtrated with a membrane cut-off of 0.22 μ m.

Linear gradient elution (LGE) experiments were used for determining model parameters for native lysozyme, lysozyme attached with PEG 2 kDa, PEG 5 kDa, and PEG 10 kDa. Protein solutions were injected via a 100 μL loop. After a post-loading wash step of 1 CV binding buffer, elution was carried out by increasing the salt gradient from 0 M to 1.0 M NaCl. From low-salt and high-salt buffer, linear gradients with a gradient length of 15 CV, 20 CV, and 25 CV were mixed within the LC system. After that, the column was stripped over 3 CV at an NaCl concentration of 1.0 M and re-equilibrated for 5 CV binding buffer. To ensure a constant residence time, all experiments were carried out at a flow rate of 0.33 mL/min.

8.2.8 Breakthrough Experiments for Model Calibration

Breakthrough experiments were used for modeling of the SMA isotherm model in the non-linear region. Protein solutions with native lysozyme, lysozyme attached with PEG 2 kDa, PEG 5 kDa, and PEG 10 kDa were prepared in binding buffer and injected via a 50 mL superloop (GE Healthcare, UK). The loading was carried out under strong binding condition at 0 M NaCl until 100 % breakthrough was observed. To ensure a constant residence time, all experiments were carried out at a flow rate of 0.33 mL/min.

8.2.9 General Rate Model

In the presented study, the general rate model (GRM) was employed to cover convection and diffusion within a one-dimensional chromatography column of length L . Here, the concentrations of all components i in the bulk phase c , in the pore phase c_p , and adsorbed to the stationary phase q depend on time t and axial position x . Eq. 8.1 describes the mass transfer between the bulk phase and the pore phase depending on the flow velocity u , axial dispersion D_{ax} , bed porosity ε_b , film diffusion coefficient k_{film} , particle radius r_p , and the concentrations c and c_p . The chosen Danckwerts boundary conditions are shown in Eqs. 8.2 and 8.3. In Eq. 8.4 the mass transfer between the pore phase and the stationary phase is described to be dependent on the radial position in the pore r ,

pore diffusion coefficient D_{pore} , particle porosity ε_p , film diffusion coefficient k_{film} , and concentrations in the bulk phase c , pore phase c_p , and stationary phase q .

$$\frac{\partial c_i(x, t)}{\partial t} = -u(t) \frac{\partial c_i(x, t)}{\partial x} + D_{ax} \frac{\partial^2 c(x, t)}{\partial x^2} \quad (8.1)$$

$$- \frac{1 - \varepsilon_b}{\varepsilon_b} k_{film, i} \frac{3}{r_p} (c_i(x, t) - c_{p, i}(x, t))$$

$$\frac{\partial c_i(0, t)}{\partial x} = \frac{u(t)}{D_{ax}} (c_i(0, t) - c_{in, i}(t)) \quad (8.2)$$

$$\frac{\partial c_i(L, t)}{\partial x} = 0 \quad (8.3)$$

$$\frac{\partial c_{p, i}(x, t)}{\partial t} = \begin{cases} \frac{1}{r^2} \frac{\partial}{\partial r} (r^2 D_{p, i} \frac{\partial c_{p, i}(x, t)}{\partial r}) - \frac{1 - \varepsilon_p}{\varepsilon_p} \frac{\partial q_i(x, t)}{\partial t} & \text{for } r \in (0, r_p), \\ \frac{k_{film, i}}{\varepsilon_p D_{p, i}} (c_i(x, t) - c_{p, i}(x, t)) & \text{for } r = r_p, \\ 0 & \text{for } r = 0. \end{cases} \quad (8.4)$$

8.2.10 Adsorption Isotherm Model

Based on the stoichiometric displacement model (SDM) [328], Brooks and Cramer derived the steric mass action (SMA) isotherm model by introducing the shielding factor σ , which accounts for the sterically hindered binding sites on the adsorber surface due to protein binding [155]. In Eq. 8.5, the kinetic formulation according to Nilsson and coworkers is shown [156]. It describes the protein concentration in the stationary phase q as a function of q itself, in the pore phase c_p , and salt concentration $c_{p, salt}$ in the pore phase.

$$k_{kin, i} \frac{\partial q_i(x, t)}{\partial t} = k_{eq, i} (\Lambda - \sum_{j=1}^k (\nu_j + \sigma_j) q_j(x, t))^{\nu_i} c_{p, i}(x, t) - c_{p, salt}(x, t)^{\nu_i} q_i(x, t), \quad \forall i \neq salt \quad (8.5)$$

Eq. 8.6 describes the salt concentration in the stationary phase as a function of proteins bound to the adsorber surface.

$$q_{salt}(x, t) = \Lambda - \sum_{j=1}^k \nu_j q_j(x, t) \quad (8.6)$$

Instead of the adsorption rate coefficient k_{ads} and the desorption rate coefficient k_{des} , the equilibrium coefficient $k_{eq} = k_{ads}/k_{des}$ and the kinetic coefficient $k_{kin} = 1/k_{des}$ were used. In this way, parameter estimation was simplified, since k_{eq} and k_{kin} correlate mainly

with the retention time and peak height, respectively [158]. ν is the characteristic charge, also known as the number of binding sites directly involved in binding. Λ is the column-specific ionic binding capacity equal to the number of potential binding sites. Here, the SMA isotherm has been chosen to cover the overloading state in investigated breakthrough experiments. For the description of low protein loading as usually applied in the step gradient experiments for preparative separation, the SDM isotherm would be sufficient. The kinetic formulation has been chosen out of several reasons. According to Carta and Jungbauer, protein adsorption is often slower than small molecules because of limitations in the binding kinetics. In addition, a true adsorption equilibrium may not be established since the protein may undergo molecular changes due to unfolding, aggregation, or degradation before reaching equilibrium with the surface [188]. Furthermore, Toyopearl GigaCap S-650M is a hydroxylated methacrylic polymer grafted adsorber providing high ligand density. As result, fast adsorption rates may be favored initially, but with increasing protein binding, steric crowding and electrostatic repulsion may limit the access to binding sites [329, 330].

8.2.11 Numerical Methods

The chromatograms resulting from LGE and breakthrough experiments were used to estimate the parameters with the inverse method [331]. The adaptive simulated annealing (ASA) [332] yielding the first guess was followed by the Levenberg-Marquardt (LM) algorithm [333] for the fine adjustment of the parameter estimates. Subsequently, the confidence intervals at 95 % level were calculated to verify estimation reliability. Discretization in space on a grid with equidistant nodes and θ -scheme discretization in time were carried out by employing the finite element method and the fractional step [334], respectively. Picard iteration was employed to approximate the solution of the non-linear equation system [335].

8.3 Results

8.3.1 PEGylation and Purification

In case of lysozyme, six lysine residues and the N-terminal amino group are available as binding sites for the PEG aldehyde reaction [257]. The large number of binding sites allows for the formation of different PEGamers. Preparative isolation of the mono-PEGylated species was performed by a single cation-exchange step. In Fig. 8.1 the resulting chromatograms are shown for 1:12 diluted PEGylation batches with 2 kDa (a), 5 kDa (b) and 10 kDa (c) PEG. After peak fractionation, HT-CGE analysis was performed according to [281] to verify purity and PEGylation degree. As observed and discussed by [129, 149, 258], a decrease in elution volume with increasing PEGylation degree was observed for all PEG molecular weights. The red areas in Figs. 8.1a-c indicate the respective pooling limits for the mono-PEGylated species based on purity requirements greater than 97%. Purity was determined by HT-CGE analysis according to the analytical protocol established by [281]. The resulting fluorescence signals of HT-CGE for the native lysozyme and the purified mono-PEGylated species with a concentration of $6.99 \cdot 10^{-5}$ M showed a distinct peak broadening of PEGylated proteins compared to the native species (Supplementary Fig. A.9). By using the calibration established by [281], this peak broadening was taken into account in the calculation of purities.

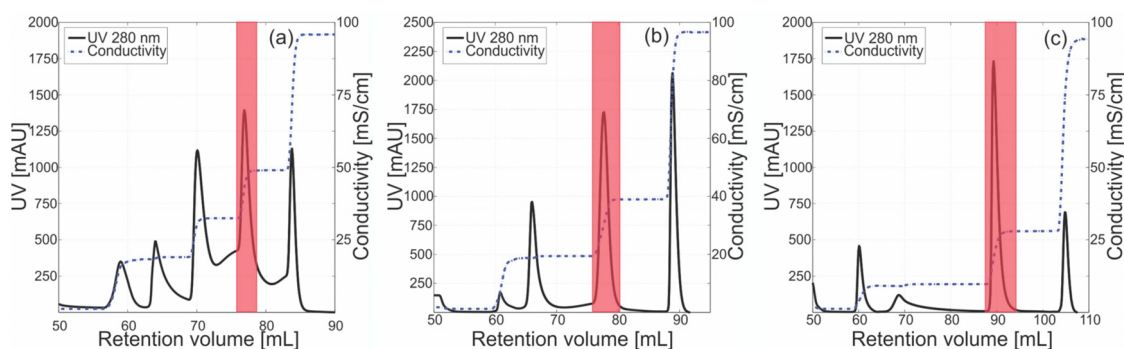


Figure 8.1: Chromatograms of preparative CEX for 1:12 diluted PEGylation batches ($r=6.67$, pH 7.2, 3.5 h) loaded with a 50 mL loop for 2 kDa PEG (a), 5 kDa PEG (b) and 10 kDa PEG (c). The red area indicates the respective pooling limits for the mono-PEGylated species.

8.3.2 System Characteristics

Tracer experiments were carried out to determine the system parameters bed voidage, particle voidage, and axial dispersion. The ionic capacity was determined by applying acid-base titration. The results are shown in Tab. 8.2. The axial dispersion was found to be similar to literature data [336].

Table 8.2: For the Toyoscreen column, the voidages and axial dispersion are calculated from the retention volume and peak broadening of tracer injections. The ionic capacity is determined by acid-base titration.

		GigaCap S-650M
Particle diameter	d_p	75 μm
Bed voidage	ε_b	0.414
Particle voidage	ε_p	0.779
Total voidage	ε_t	0.871
Axial dispersion [mm^2/s]	D_{ax}	$6.691 \cdot 10^{-2}$
Ionic capacity [M]	Λ	1.389

8.3.3 Linear Gradient Elution and Breakthrough Experiments

Linear gradient experiments were carried out to generate information about proteins in the linear region of the adsorption isotherm. The retention time of every protein species over three different salt gradient lengths yielded information about the isotherm parameters characteristic charge ν and equilibrium coefficient k_{eq} . The height, width, and shape of the elution peaks provided partial information about the mass transfer parameters film diffusion coefficient k_{film} and pore diffusion coefficient D_{pore} . Thus, by employing ASA and LM, ν and k_{eq} were estimated with high reliability, for k_{film} and D_{pore} an initial guess was delivered. As can be seen by comparing the dashed lines in Figs. 8.2a, d, g, and j, lysozyme in its native form was the strongest binding species for all investigated gradient lengths. Comparison of the elution peaks of native and PEGylated species at a constant gradient length in Fig. 8.2 reveals that the elution times decreased with increasing PEG chain length. Except for the different elution times of all protein species, their peak heights and widths are highly similar at each salt gradient conditions. A small shoulder peak behind the main peak can be seen in Fig. 8.2d-f, indicating a small amount of a stronger binding protein species. Presumably this species is by unmodified

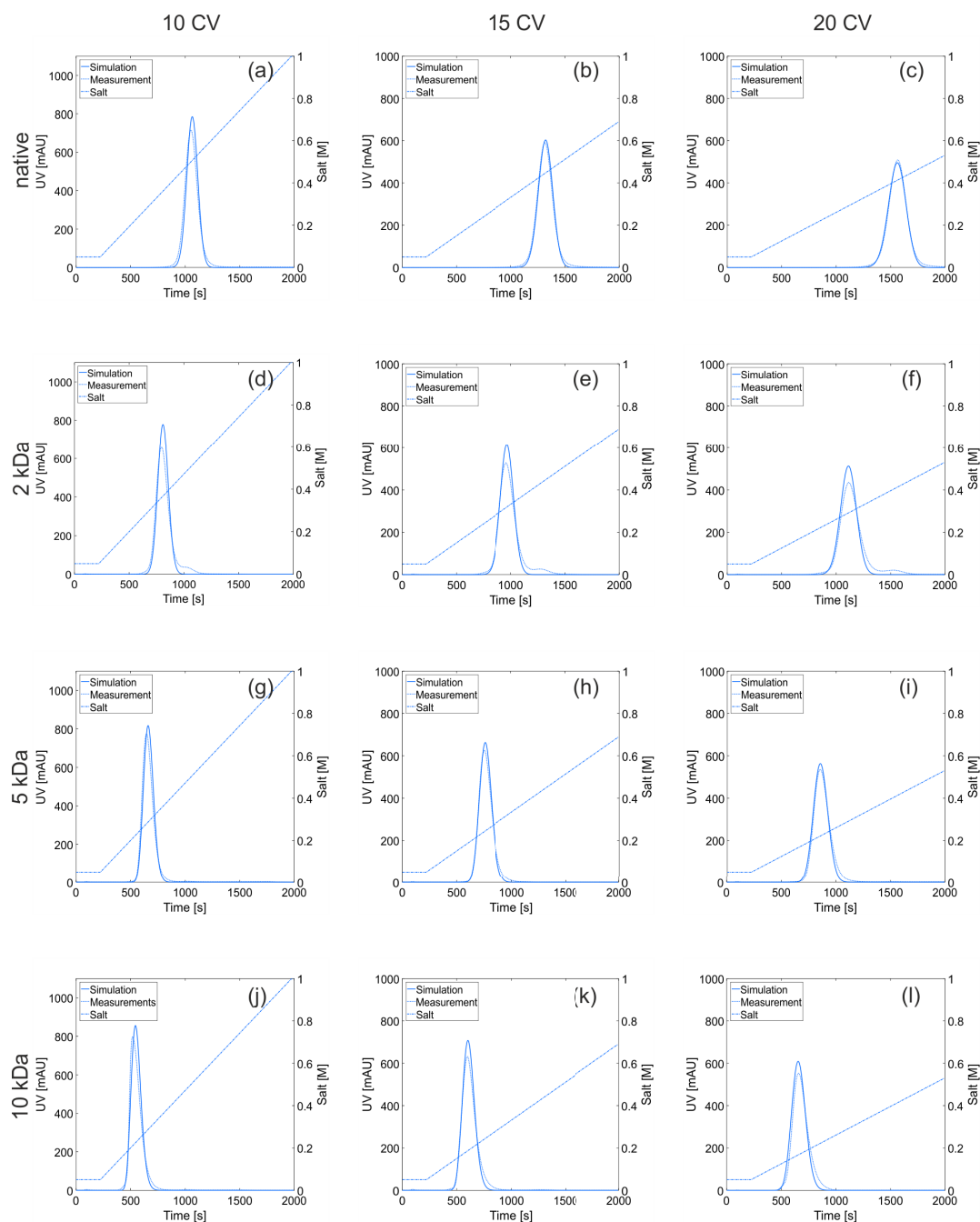


Figure 8.2: Plots of UV signals over process run-time for bind-and-elute experiments. Dashed lines display the UV signals measured at the column outlet and the adjusted linear salt gradients. Solid lines represent the simulated chromatograms. The elution peaks of native lysozyme, lysozyme attached with 2 kDa PEG, 5 kDa PEG, and 10 kDa PEG by applying linear salt gradients from 0.05 M to 1.0 M over 10 CV, 15 CV, and 20 CV are shown in (a) - (c), (d) - (f), (g) - (i), and (j) - (l). Similar peak heights and widths, but different retention times can be seen for different protein species. Here, the Toyoscreen column was employed.

lysozyme, since for the 2 kDa PEGylation no peak baseline separation between the different PEGamer species could be achieved in preparative chromatography (compare Fig. 8.1a).

Additionally, breakthrough experiments were carried out under strong binding condition. The 280 nm signals were highly non-linear above 2000 mAU and reached the detector saturation at approximately 2500 mAU. As shown by the dashed lines in Fig. 8.3, lysozymes with 10 kDa, 5 kDa and 2 kDa PEG attached, and the native lysozyme exhibited their breakthrough in successive order. Based on this information, the shielding parameter σ was estimated and the correlation between k_{kin} and k_{film} that both affect the peak height in the linear part of the adsorption isotherm was dissolved.

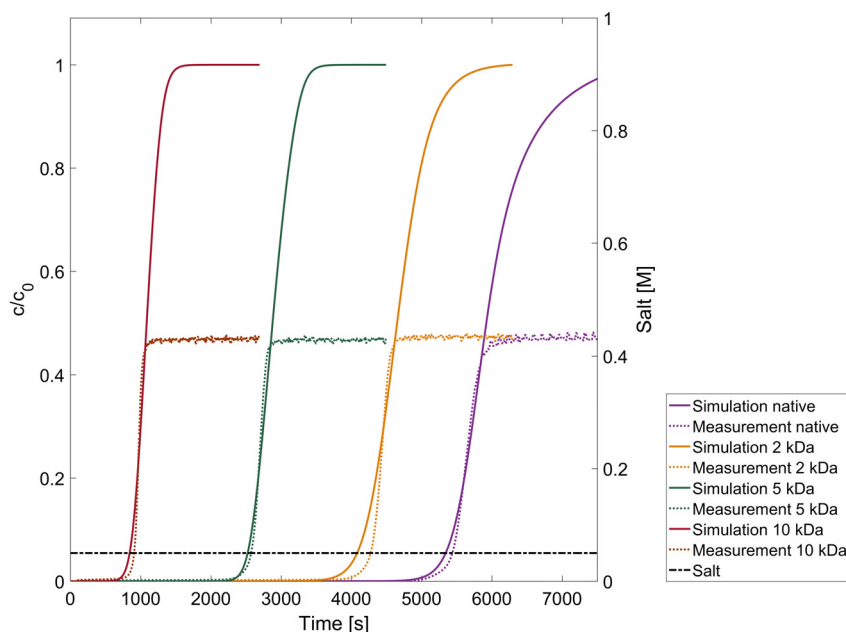


Figure 8.3: Plots of normalized protein concentration over process run-time for breakthrough experiments. Dashed lines display the normalized protein concentrations calculated from UV Fig. 8.2 as solid lines. In all cases, a good agreement between simulations and signals measured at the column outlet and the constant salt concentration at 0.05 M. Solid lines represent the normalized protein concentrations calculated from the simulated chromatograms. The native lysozyme and lysozyme attached with 2 kDa PEG, 5 kDa PEG, and 10 kDa PEG are shown in purple, yellow, green, and red, respectively. Here, the Toyoscreen column was employed.

The final parameter estimates and the related confidence intervals at 95 % level are summarized in Tab. 8.3. The simulated LGE for the four protein species are displayed in measurements was found for the retention time, peak width, and peak shape. Overall, the conformity was highest for the native lysozyme. The peak heights of PEGylated species were slightly overestimated. The simulated breakthrough curves for all protein species are displayed in Fig. 8.3. Here, the model accurately accounted for the overall slopes and reflected the process relevant times at 10 % and 50 % breakthrough. The relative offsets for the process times at 10 % breakthrough were 1.83 % for lysozyme in the native condition, 3.53 % for lysozyme attached with 2 kDa PEG, 1.93 % for lysozyme attached with 5 kDa, and 4.17 % for lysozyme attached with 10 kDa.

Table 8.3: Parameters of the mass transfer model and kinetic isotherm formulation estimated from bind-and-elute experiments with linear salt gradient and breakthrough curves using the inverse method are shown for native and mono-PEGylated lysozyme species. Confidence intervals at 95 % level reflect the reliability of the parameter estimates.

Parameter	Native	2 kDa PEGylated	5 kDa PEGylated	10 kDa PEGylated
k_{film} [mm/s]	$9.95 \cdot 10^{-2}$ $\pm 5.20 \cdot 10^{-2}$	$8.92 \cdot 10^{-2}$ $\pm 5.49 \cdot 10^{-2}$	$6.62 \cdot 10^{-2}$ $\pm 3.12 \cdot 10^{-2}$	$4.07 \cdot 10^{-2}$ $\pm 2.53 \cdot 10^{-2}$
D_{pore} [mm ² /s]	$2.85 \cdot 10^{-4}$ $\pm 2.38 \cdot 10^{-5}$	$1.33 \cdot 10^{-4}$ $\pm 7.56 \cdot 10^{-6}$	$8.42 \cdot 10^{-5}$ $\pm 2.08 \cdot 10^{-6}$	$5.75 \cdot 10^{-5}$ $\pm 2.28 \cdot 10^{-6}$
k_{eq} [-]	$4.62 \cdot 10^{-2}$ $\pm 9.16 \cdot 10^{-5}$	$5.94 \cdot 10^{-3}$ $\pm 2.79 \cdot 10^{-5}$	$1.16 \cdot 10^{-3}$ $\pm 5.13 \cdot 10^{-6}$	$1.92 \cdot 10^{-5}$ $\pm 1.48 \cdot 10^{-6}$
k_{kin} [sM ^{-ν}]	$3.94 \cdot 10^{-2}$ $\pm 7.56 \cdot 10^{-4}$	$4.58 \cdot 10^{-3}$ $\pm 2.10 \cdot 10^{-4}$	$2.31 \cdot 10^{-4}$ $\pm 6.74 \cdot 10^{-5}$	$6.34 \cdot 10^{-6}$ $\pm 2.82 \cdot 10^{-5}$
ν [-]	4.21 $\pm 1.82 \cdot 10^{-3}$	4.21 $\pm 2.65 \cdot 10^{-3}$	4.20 $\pm 1.10 \cdot 10^{-3}$	4.22 $\pm 1.56 \cdot 10^{-3}$
σ [-]	5.61 $\pm 1.27 \cdot 10^{-2}$	6.81 $\pm 1.35 \cdot 10^{-2}$	9.79 $\pm 1.67 \cdot 10^{-2}$	25.90 $\pm 1.08 \cdot 10^{-1}$

8.3.4 Mass Transfer and Kinetic Phenomena

The GRM assumes that the adsorbent particles have a spherical shape and a uniform diameter. The shape of PEGylated proteins is influenced by the surrounding PEG layer which is highly dynamic. Due to the high hydration of PEG, PEGylated proteins have a significantly greater hydrodynamic radius than unmodified proteins with a comparable

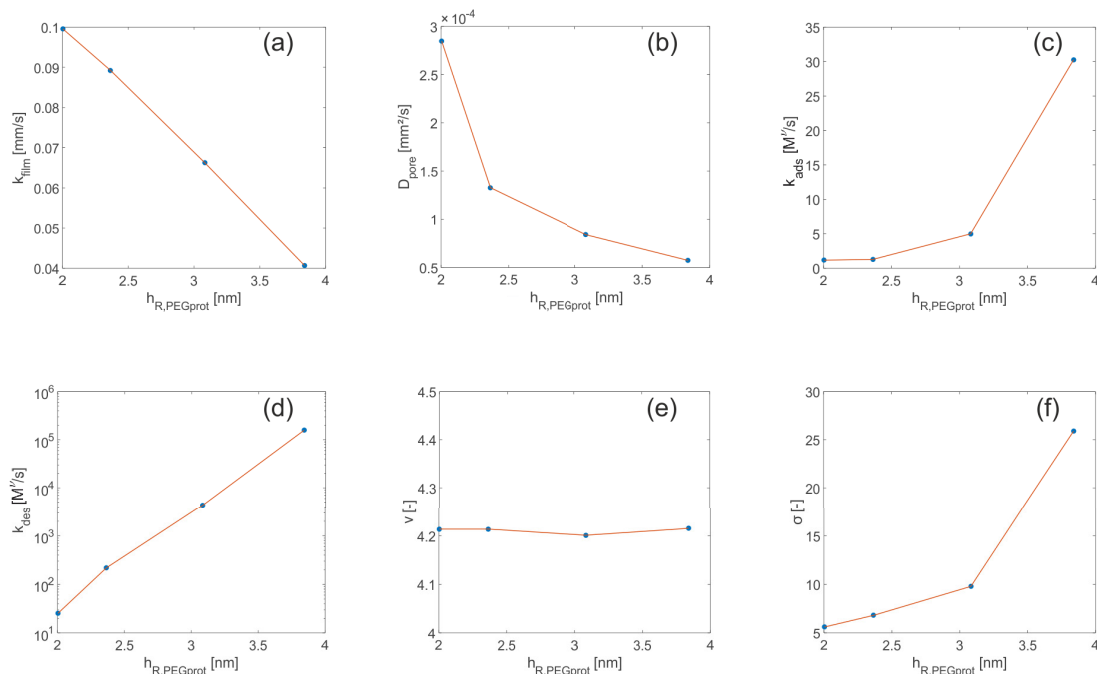


Figure 8.4: (a) - (f) the show film diffusion coefficient, pore diffusion coefficient, adsorption coefficient, desorption coefficient, characteristic charge, and shielding factor versus the hydrodynamic radius $h_{R,PEGprot}$ of PEGamers. $h_{R,PEGprot}$ takes into account the non-linear relationship between conjugate size and total molecular weight of attached PEG [130, 139]. Blue dots from left to right represent the native lysozyme and lysozyme attached with 2 kDa PEG, 5 kDa PEG, and 10 kDa PEG.

molecular weight. Fee and Van Alstine introduced a nonlinear relationship between the degree of PEGylation in terms of total molecular weight of PEG attached and the hydrodynamic radius of the PEGylated protein [130, 139]. This non-linearity is the reason why the behavior of conjugated proteins in IEX must necessarily be described as a function of the hydrodynamic radius and not in terms of the total molecular weight of attached polymer. According to the correlation introduced by Fee and Van Alstine [130], the hydrodynamic radii $h_{R,PEGprot}$ were calculated to be 2.00 nm, 2.37 nm, 3.08 nm, and 3.84 nm for the four lysozyme species with increasing PEG MW.

For lysozyme, the mass transfer coefficient k_{eff} calculated according to $1/k_{eff} = 1/k_{pore} + 1/k_{film}$ with the internal mass transfer resistance $k_{pore} = 10D_{pore}\epsilon_p/d_p$ [151] was found to be consistent with literature data [336]. An approximately linear decrease of the film diffusion coefficient k_{film} with increasing $h_{R,PEGprot}$ was determined as displayed in Fig. 8.4 a. A comparable dependency was reported by Mejía-Manzano et al. [337] for affinity chro-

matography. As shown in Fig. 8.4 b, the pore diffusion coefficient D_{pore} decreased reciprocally with increasing $h_{R,PEGprot}$ according to the Stokes-Einstein equation qualitatively. The adsorption and desorption rate coefficients $k_{ads} = k_{eq}/k_{kin}$ and $k_{des} = 1/k_{kin}$ were calculated and are displayed in Figs. 8.4 c and d. With increasing PEG MW, both k_{ads} and k_{des} showed an exponential increase. A similar trend has been observed by Mejía-Manzano et al. [337] for affinity chromatography. The increase of k_{des} exceeded the increase of k_{ads} by more than two orders of magnitude. For native and 5 kDa mono-PEGylated lysozyme, k_{eq} was found to be of the same magnitude as reported in the literature [150].

8.3.5 Characteristic Charge and Shielding

The characteristic charges ν of PEGylated lysozyme (4.20-4.22) were found to be equal to the value determined for native lysozyme (4.21) as shown in Fig. 8.4 e. ν was unaffected by PEGylation degree and PEG chain length. This finding was consistent with data delivered by Abe and coworker [150]. A small shielding factor σ of 5.61 was found for the native lysozyme. With increasing PEG chain length, σ increased from 6.81 for 2 kDa to 9.79 for 5 kDa, and up to 25.90 for 10 kDa PEG as displayed in Fig. 8.4 f. The dependency of σ on the hydrodynamic radius was highly non-linear. Based on the definition of q_{max} being $\Lambda/(\sigma + \nu)$, the maximal binding capacity q_{max} for the four protein species was calculated to be $1.41 \cdot 10^{-1}$ M for native species, $1.26 \cdot 10^{-1}$ M for 2 kDa PEGylated species, $9.93 \cdot 10^{-2}$ M for 5 kDa PEGylated species and $4.61 \cdot 10^{-2}$ M for 10 kDa PEGylated species. q_{max} was found to be reduced by 10.6 % when attached with 2 kDa PEG by 29.6 % when attached with 5 kDa PEG, and by 67.3 % when attached with 10 kDa PEG compared to the native lysozyme species.

8.4 Discussion

PEGylation is commonly used in biopharmaceutical industry to improve protein stabilities and pharmacokinetics of protein drugs. However, the currently used reaction mechanisms and conditions usually result in a heterogeneous product mixture of unreacted protein and conjugates with varying number and modification site of attached polymers [130, 322]. For this reason, purification processes of PEGylated proteins are imperative. Chromatographic processes based on electrostatic interactions e.g. ion-exchange chromatography, are among the most effective purification processes for this application

[324]. So far, the development of ion-exchange steps for the purification of the individual PEGamers has been driven mainly by expert-based or experimental approaches (high-throughput process development and statistical design of experiments). These approaches are time-consuming and cost-intensive due to the wide variety of proteins and polymers (linear vs. branched, molecular weight etc.). Mechanistic modeling and simulations can help to reduce the number of experiments during process optimization by *in silico* predictions [143]. From the perspective of process development, the parameters estimated by mechanistic modeling can be used for process up scaling, process optimization, and process control, meeting the demands of the Quality by Design approach (QbD) proposed by the US food and drug administration (FDA) [338].

In our work, the SMA isotherm in kinetic formulation coupled with the GRM produced a comprehensive description of the adsorption and desorption behavior on the adsorber surface, steric hindrance, and the mass transfer for native lysozyme and its PEGylated species. The model parameters k_{film} , D_{pore} , k_{eq} , k_{kin} , ν , and σ were determined and k_{ads} , k_{des} , $h_{R,PEGprot}$, and q_{max} were calculated to improve the mechanistic understanding of PEGylated proteins in CEX. It should be mentioned, that the PEGylation reaction usually delivers various PEGamer isoforms. In the presented case, the isoforms behaved highly similar and could not be separated with the used CEX setup. Hence all isoforms of each lysozyme species had to be modeled as lumped components, resulting in slight overestimation of the peak heights.

As reported by many researchers, PEGylated proteins elute earlier than their native analogs [149, 150, 324]. Based on the observation of the elution order of different PEGylated species being the same in both cation-exchange and anion-exchange chromatography, Seely and Richey suggested the ‘charge-shielding effect’ to explain this phenomenon [149]. Later, Abe and coworkers applied the equilibrium stoichiometric displacement isotherm model (SDM) to describe the retention time of PEGylated proteins in linear gradient experiments and determined similar numbers of binding sites for lysozyme and BSA attached with PEG of different lengths. Furthermore, they reported the decrease of a lumped parameter consisting of the equilibrium coefficient, the binding site, and the ionic binding capacity with increasing PEG chain length [150]. In this way, the ‘charge-shielding effect’ hypothesis was verified and the equilibrium coefficient was identified to be responsible for the weaker binding of PEGylated proteins [150].

k_{film} showed a linear dependency on $h_{R,PEGprot}$ as expected according to the correlation suggested by Jungbauer and Carta [188]. Its decrease with increasing PEG chain length was to be reflected by broader and lower elution peaks. However, the LGE under same operating conditions showed similar peak heights and widths for all PEGylated and na-

tive species. Considering the fact that there is a strongly exponential correlation of k_{des} with $h_{R,PEGprot}$, a diffusion-desorption-compensation effect is suggested to be responsible for the uniformity in peak heights and width. The faster desorption of proteins attached with longer PEG chain may be neutralized by the slower film diffusion. This hypothesis is highly consistent with the widely accepted view of the ‘charge-shielding effect’, since weaker charged proteins increasingly tend to undergo desorption. D_{pore} showed a reciprocal correlation with $h_{R,PEGprot}$, as had been expected according to the Stokes-Einstein equation [339], which is reflected by slight tailing of elution peaks in LGE. D_{pore} was found to exceed the molecular diffusion coefficient for native lysozyme. As intensively studies in literature, there are two opinions to explain this effect. Carta et al. and Rodrigues et al. [340–342] introduced the convection-enhanced effective intra-particle diffusivity. Many more experimental examples of intra-particle convection in protein chromatography could be found in the literature [343–347]. However, convective mass transfer into the bead interior was observed for large pores ($> 5000 \text{ \AA}$)[347, 348]. For small pores up to 700 \AA , Nash et al. assumed diffusional mass transport only. For the TOYOPEARL[®] GigaCap S-650M resin having an average pore size of 1000 \AA , the observed molecular diffusion coefficient cannot be explained completely by convective mass transport in the pores. An additional effect observed by Dziennik et al. [349] for porous resins with high charge density applies to TOYOPEARL[®] GigaCap S-650M. They found indications that non-diffusive mechanisms of electrostatic origin could enhance protein uptake rates in ion exchange particles, resulting in enhanced effective pore diffusivities.

The shielding factor σ showed an exponential increase with increasing PEG chain length. In comparison to native lysozyme, approximately 12 %, 43 %, and 207 % more free binding sites are sterically hindered by the species with 2 kDa, 5 kDa, and 10 kDa PEG attached, respectively. In contrast to this, ν was found to be independent of PEGylation and PEG chain length, indicating the same binding orientation for all species. Thus, the steric hindrance of free binding sites was identified to be the main contributor to the observed exponential decrease of molar binding capacity q_{max} upon PEGylation. It is indicated that the longer PEG chains of an adsorbed protein make many more free binding sites inaccessible than the shorter ones or equally sized unmodified proteins. Fee and Van Alstine proposed a correlation for the average shape of the PEG-layers around a protein over timescale [130, 322]. These layers are expected to have increasing degree of dynamics with increasing PEG molecular weight [350]. This concept could also explain the non-linearity in k_{ads} , k_{des} , and σ shown in Fig. 8.4c, d, f.

Especially in the overloading state under strong binding condition, a high density of proteins bound could result in formation of multiple PEG chain layers covering adjacent

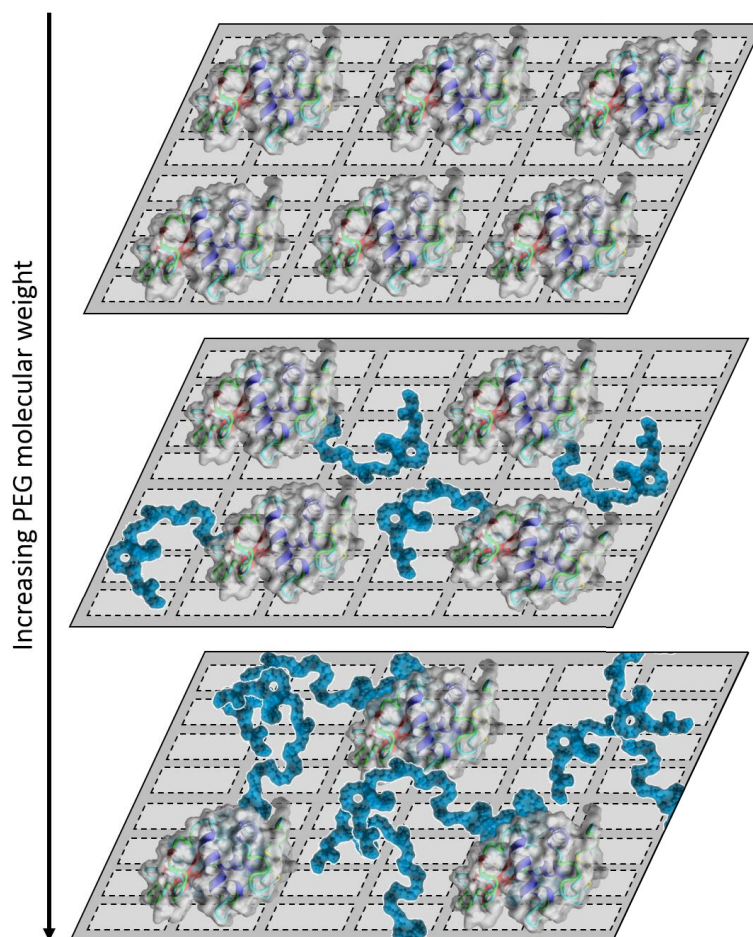


Figure 8.5: Molecular picture of the adsorption of lysozymes on an adsorber surface. Increasing PEG chain length results in the formation of multiple PEG chain layers hindering the binding of further lysozymes. The reduction of accessible binding sites explains the observed decrease in binding capacity upon protein PEGylation. (Molecular graphic of lysozyme (PDB: 1LYZ) was created with YASARA (www.yasara.org)).

free binding sites. The multiple PEG chain layers would not shield the electrostatic interactions, but keep the proteins in the mobile phase distant from the adsorber surface, so that the electrostatic attraction would become weak and binding impossible. This hypothesis is schematically represented by Fig. 8.5. Along the increasing binding density, several transitional states are supposed to exist. First, in the linear part of the adsorption isotherm, the proteins could distribute uniformly on the adsorber surface; secondly,

unfavorable binding sites between the proteins covered by thin PEG chain layers could be occupied, though the electrostatic attraction could already be reduced; finally, the multiple PEG chain layers could become dominant, so that the electrostatic attraction could disappear and binding could be suppressed. This concept is consistent with the observation made by Blaschke and coworkers [351]. They found that adsorption was less enthalpy-driven at higher loading states for proteins attached with longer PEG chains. Of course, the PEG-layers around PEGylated proteins are not static, rather of dynamic nature. Thus, the mechanistic chromatography model describes the average behavior of lysozyme species in CEX. As suggested by Fee et al., the dynamicism of PEG-layers tend to increase with increasing PEG chain length. This concept could be an alternative explanation for the nontrivial behavior of PEGylated lysozymes observed in the presented work.

Using mechanistic chromatography modeling and considering insights provided by former pioneer work, the hydrodynamics and thermodynamics of PEGylated lysozymes in CEX were investigated. The diffusion-desorption-compensation effect was introduced to explain the anomaly of peak heights and widths remaining constant in spite of an increasing hydrodynamic radius. Additionally, it reflects the exponential dependency of the shielding factor on the MW of PEGylated proteins and suggests that multiple PEG chain layers formed in the overloading state are responsible for this non-trivial phenomenon. Thus, the model view of PEGylated proteins' behavior in CEX was supplemented by the overloading state.

This study clearly demonstrates that mechanistic chromatography modeling can be applied to describe PEGylated proteins with high accuracy and reliability. Thus it has great potential for the optimization, prediction, and scale-up of purification processes for PEGylated proteins. A future challenge is to show whether the separation of positional isoforms can be predicted by this kind of simulation. In this respect, a combination of mechanistic chromatography modelling combined with molecular modeling could be profitable.

8.5 Acknowledgments

This project partly received funding from the European Union's Horizon 2020 Research and Innovation Programme under grant agreement No 635557. Furthermore, we would like to acknowledge the further financial support by the German Federal Ministry of Education and Research (BMBF) within the project 'Molecular Interaction Engineering:

From Nature's Toolbox to Hybrid Technical Systems', funding code 031A095B. We want to thank Carina Brunner for her reliable and persistent support in the laboratory. Last but not least, we kindly thank Johannes Winderl for useful discussions related to this work. The authors declare no conflict of interest.

8.6 References

13. EvaluatePharma. *World Preview 2015, Outlook to 2020* <http://info.evaluategroup.com/rs/607-YGS-364/images/wp15.pdf>. [Online; accessed 12/2016].
79. Baumgartner, K., Galm, L., Nötzold, J., Sigloch, H., Morgenstern, J., Schleining, K., Suhm, S., Oelmeier, S. A. & Hubbuch, J. Determination of protein phase diagrams by microbatch experiments: Exploring the influence of precipitants and pH. *Int. J. Pharm.* **479**, 28–40 (2015).
129. Pasut, G. & Veronese, F. State of the art in PEGylation: the great versatility achieved after forty years of research. *Journal of Controlled Release* **161**, 461–472 (2012).
130. Fee, C. J. & Van Alstine, J. M. PEG-proteins: Reaction engineering and separation issues. *Chemical engineering science* **61**, 924–939 (2006).
133. Abuchowski, A., McCoy, J., Palczuk, N., van Es, T. & Davis, F. Effect of covalent attachment of polyethylene glycol on immunogenicity and circulating life of bovine liver catalase. *J. Biol. Chem.* **252**, 3582–3586 (1977).
139. Fee, C. J. & Van Alstine, J. M. Prediction of the viscosity radius and the size exclusion chromatography behavior of PEGylated proteins. *Bioconjugate chemistry* **15**, 1304–1313 (2004).
142. Harris, J. M. & Chess, R. B. Effect of PEGylation on pharmaceuticals. *Nat. Rev. Drug Discov.* **2**, 214–221 (2003).
143. Nfor, B. K., Verhaert, P. D., van der Wielen, L. A. M., Hubbuch, J. & Ottens, M. Rational and systematic protein purification process development: The next generation. *Trends Biotechnol.* **27**, 673–679 (2009).
149. Seely, J. E. & Richey, C. W. Use of ion-exchange chromatography and hydrophobic interaction chromatography in the preparation and recovery of polyethylene glycol-linked proteins. *J. Chromatogr. A* **908**, 235–241 (2001).

150. Abe, M., Akbarzaderaleh, P., Hamachi, M., Yoshimoto, N. & Yamamoto, S. Interaction mechanism of mono-PEGylated proteins in electrostatic interaction chromatography. *Biotechnol. J.* **5**, 477–483 (2010).
151. Schmidt-Traub, H., Schulte, M. & Seidel-Morgenstern, A. *Preparative Chromatography* 291 (WILEY-VCH, 2012).
155. Brooks, C. A. & Cramer, S. M. Steric mass-action ion exchange: Displacement profiles and induced salt gradients. *AIChE Journal* **38**, 1969–1978 (1992).
156. Jakobsson, N., Karlsson, D., Axelsson, J. P., Zacchi, G. & Nilsson, B. Using computer simulation to assist in the robustness analysis of an ion-exchange chromatography step. *J. Chromatogr. A* **1063**, 99–109 (2005).
157. Huuk, T., Briskot, T., Hahn, T. & Hubbuch, J. A versatile noninvasive method for adsorber quantification in batch and column chromatography based on the ionic capacity. *Biotechnol. Progr.* **32**, 666–677 (2016).
158. Hahn, T., Huuk, T., Heuveline, V. & Hubbuch, J. Simulating and Optimizing Preparative Protein Chromatography with ChromX. *J. Chem. Educ.* **92**, 1497–1502 (2015).
188. Carta, G. & Jungbauer, A. *Protein Chromatography Process Development and Scale-up* (WILEY-VCH, 2010).
253. Ottow, K. E., Lund-Olesen, T., Maury, T. L., Hansen, M. F. & Hobley, T. J. A magnetic adsorbent-based process for semi-continuous PEGylation of proteins. *Biotechnol. J.* **6**, 396–409 (2011).
257. Maiser, B., Kröner, F., Dimer, F., Brenner-Weiß, G. & Hubbuch, J. Isoform separation and binding site determination of mono-PEGylated lysozyme with pH gradient chromatography. *J. Chrom. A* **1268**, 102–108 (2012).
258. Yoshimoto, N. & Yamamoto, S. PEGylated protein separations: Challenges and opportunities. *Biotechnol. J.* **7**, 592–593 (2012).
264. Maiser, B., Dimer, F. & Hubbuch, J. Optimization of random PEGylation reactions by means of high throughput screening. *Biotechnol. Bioeng.* **111**, 104–114 (2014).
281. Morgenstern, J., Busch, M., Baumann, P. & Hubbuch, J. Quantification of PEGylated proteases with varying degree of conjugation in mixtures: An analytical protocol combining protein precipitation and capillary gel electrophoresis. *J. Chrom. A* **1462**, 153–164 (2016).

-
293. Morgenstern, J., Baumann, P., Brunner, C. & Hubbuch, J. Effect of PEG molecular weight and PEGylation degree on the physical stability of PEGylated lysozyme. *Int. J. Pharm.* **519**, 408–417 (2017).
294. Abuchowski, A., Van Es, T., Palczuk, N. & Davis, F. Alteration of immunological properties of bovine serum albumin by covalent attachment of polyethylene glycol. *J. Biol. Chem.* **252**, 3578–3581 (1977).
322. Janson, J.-C. in: Chap. 14 (John Wiley & Sons, 2012).
323. Yamamoto, S., Fujii, S., Yoshimoto, N. & Akbarzadehlaleh, P. Effects of protein conformational changes on separation performance in electrostatic interaction chromatography: Unfolded proteins and PEGylated proteins. *J. Biotechnol.* **132**, 196–201 (2007).
324. Yoshimoto, N., Isakari, Y., Itoh, D. & Yamamoto, S. PEG chain length impacts yield of solid-phase protein PEGylation and efficiency of PEGylated protein separation by ion-exchange chromatography: Insights of mechanistic models. *Biotechnol. J.* **8**, 801–810 (2013).
325. Guiochon, G. & Beaver, L. A. Separation science is the key to successful biopharmaceuticals. *J. Chromatogr. A* **1218**, 8836–8858 (2011).
326. PerkinElmer. *LabChip GX/GX II - User Manual* http://www.perkinelmer.com/Content/LST_Software_Downloads/LabChip_GX_User_Manual.pdf. [Online; accessed 01/2017].
327. Research, H. *Lysozyme - User Guide HR7-110* http://hamptonresearch.com/documents/product/hr006812_711020.pdf. [Online; accessed 01/2017].
328. Velayudhan, A. & Horvath, C. Preparative chromatography of proteins - analysis of the multivalent ion-exchange formalism. *J. Chromatogr. A* **443**, 13–29 (1988).
329. Lenhoff, A. M. Protein adsorption and transport in polymer-functionalized ion-exchangers. *J. Chromatogr. A* **1218**, 8748–8759 (2011).
330. Wittmann, A., Haupt, B. & Ballauff, M. Adsorption of proteins on spherical polyelectrolyte brushes in aqueous solution. *Phys. Chem. Chem. Phys.* **5**, 1671–1677 (2003).
331. Hahn, T., Baumann, P., Huuk, T., Heuveline, V. & Hubbuch, J. UV absorption-based inverse modeling of protein chromatography. *Eng. Life Sci.* **16**, 99–106 (2016).

332. Kaczmariski, K. & Antos, D. Use of simulated annealing for optimization of chromatographic separations. *Acta Chromatogr.* **17**, 20–45 (2006).
333. Devernay, F. *C/C++ Minpack* <http://devernay.free.fr/hacks/cminpack/>. [Online; accessed 01/2017].
334. Glowinski, R. *Finite element methods for incompressible viscous flow*. In *Numerical Methods for Fluids (Part 3)* 3–1176 (Elsevier, 2003).
335. Quarteroni, A. & Valli, A. *Numerical approximation of partial differential equations* 160 (Springer, 1994).
336. Wang, G., Briskot, T., Hahn, T., Baumann, P. & Hubbuch, J. Estimation of adsorption isotherm and mass transfer parameters in protein chromatography using artificial neural networks. *J. Chromatogr. A* **1487**, 211–217 (2017).
337. Mejia-Manzano, L. A., Sandoval, G., Lienqueo, M. E., Moisset, P., Rito-Palomares, M. & Asenjo, J. A. Simulation of mono-PEGylated lysozyme separation in heparin affinity chromatography using a general rate model. *J. Chem. Technol. Biotechnol.* doi:10.1002/jctb.5309 (2017).
338. ICH. *International Conference on Harmonisation of Technical Requirements for Registration of Pharmaceuticals for Human Use, ICH-Endorsed Guide for ICH Q8/Q9/Q10 Implementation* http://www.ich.org/fileadmin/Public_Web_Site/ICH_Products/Guidelines/Quality/Q8_9_10_QAs/PtC/Quality_IWG_PtCR2_6dec2011.pdf. [Online; accessed 07/2017].
339. Einstein, A. On the movement of small particles suspended in stationary liquids required by the molecular-kinetic theory of heat. *Ann. Phys.* **17**, 549–560 (1905).
340. Carta, G., Gregory, M. E. & Kirwan, D. J. Chromatography with permeable supports: Theory and comparison with experiments. *Sep. Technol.* **2**, 62–72 (1992).
341. Carta, G. & Rodrigues, A. E. Diffusion and convection in chromatographic processes using permeable particles with a bidisperse pore structure. *Chem. Eng. Sci.* **48**, 3927–3935 (1993).
342. Rodrigues, A. E., Lu, Z. P., Loureiro, J. M. & Carta, G. Peak resolution in linear chromatography: Effects of intraparticle convection. *J. Chromatogr. A* **653**, 189–xx198 (1993).
343. Frey, D. D., Schweinheim, E. & Horvath, C. Effect of intraparticle convection on the chromatography of biomacromolecules. *Biotechnol. Progr.* **9**, 273–284 (1993).

-
344. Freitag, R., Frey, D. & Horvath, C. Effect of bed compression on high-performance liquid-chromatography columns with gigaporous polymeric packings. *J. Chromatogr. A* **686**, 165–177 (1994).
345. Pfeiffer, J. F., Chen, J. C. & Hsu, J. T. Permeability of gigaporous particles. *AIChE J.* **42**, 932–939 (1996).
346. Gustavsson, P. E., Mosbach, K., Nilsson, K. & Larsson, P. O. Superporous agarose as an affinity-chromatography support. *J. Chromatogr. A* **776**, 197–203 (1997).
347. Nash, D. C. & Chase, H. A. Comparison of diffusion and diffusion-convection matrices for use in ion-exchange separations of proteins. *J. Chromatogr. A* **807**, 185–207 (1998).
348. Lloyd, L. L. Rigid macroporous copolymers as stationary phases in high-performance liquid chromatography. *J. Chromatogr. A* **544**, 201–217 (1991).
349. Dziennik, S. R., Belcher, E. B., Barker, G. A., DeBergalis, M. J., Fernandez, S. E. & Lenhoff, A. M. Nondiffusive mechanisms enhance protein uptake rates in ion exchange particles. *PNAS* **100**, 420–425 (2003).
350. Van Alstine, J. M. & Malmsten, M. Poly (ethylene glycol) Amphiphiles: Surface Behavior of Biotechnical Significance. *Langmuir* **13**, 4044–4053 (1997).
351. Blaschke, T., Varon, J., Werner, A. & Hasse, H. Microcalorimetric study of the adsorption of PEGylated lysozyme on a strong cation exchange resin. *J. Chromatogr. A* **1218**, 4720–4726 (2011).

Assessment of Hydrogels for Biopharmaceutical Purposes
Using a Combination of 3D Printing and High-Throughput
Screening

Josefine Morgenstern*, Carsten Philipp Radtke*, Cathrin Dürr and Jürgen Hubbuch**

*Institute of Engineering in Life Sciences, Section IV: Biomolecular Separation Science,
Karlsruhe Institute of Technology (KIT), 76131 Karlsruhe, Germany*

** These authors contributed equally to this work.*

*** Corresponding author. Manuscript in preparation.*

Abstract

Synthetic hydrogels provide an effective and convenient way to administer high molecular weight protein drugs. However, the release kinetics of these proteins from hydrogels depend on the highly complex physical and chemical properties of the hydrogel, the surrounding solution conditions and the protein itself. The objective of this work was the development of an rapid and cost-effective tool for the investigation of the influences of these variables on occurring interactions. The fulfillment and realization of this aim was successfully achieved by a combination of hydrogel 3D printing and high-throughput screening techniques. In a case study, the lysozyme uptake and release profiles of hydrogel structures with different compositions (polyethylene glycol-diacrylate and acrylic acid) under the influence of varying surrounding buffer conditions was investigated. In comparison with literature data, it was shown that the approach presented here leads to very similar data for the used materials and thus constitutes a helpful tool for the development of hydrogel-based drug delivery systems.

Keywords: *3D printing, photopolymerization, controlled drug delivery, protein uptake and release, high-throughput screening*

9.1 Introduction

Advances in medical technology and the pharmaceutical sector have created a better understanding of the root cause of a variety of diseases in recent years. Biopharmaceuticals based on recombinant proteins, such as monoclonal antibodies or therapeutic enzymes, promise highly effective therapies with minimal side effects due to their high selectivity for certain cells or metabolic pathways in the human body. Moreover, recombinant proteins can treat diseases resulting from insufficient or deficient production of endogenous proteins [170]. The increasing use of pharmaceutical proteins has created a need for new methods of controlled administration of these compounds [167]. In this context, polymeric carrier systems arouse the interest of academia and industry for the controlled spatial and temporal release of biotherapeutics [162, 163]. For use in the clinical field, these polymers must meet the requirements of biocompatibility and immunological acceptance while integrating elements of responsive behavior to give a well-defined reaction to external conditions [163].

Proteins are found in human tissues mainly in aqueous environments. In order to mimic this natural environment and thus to preserve the native protein conformation, hydrophilic polymers are suitable to administer pharmaceutical proteins. These polymers are capable of absorbing large amounts of water or biological fluids and can be interlinked to three-dimensional networks. Therefore those hydrophilic networks are often referred to as hydrogels. The presence of chemical and/or physical crosslinks renders hydrogels insoluble in water after network formation. [161]

Hydrogels are already used as a matrix for the oral administration of small molecule drugs [352]. Also, hydrogel-based formulations present a promising approach for the oral administration of protein drugs since the molecule is protected from harsh conditions and degradation by endogenous enzymes in the gastrointestinal tract [167]. Thus, for example, considerable efforts for the development and clinical testing of oral delivery forms for insulin have been made [353–355]. Further, hydrogels may be applied directly to a wound or implanted near the site of action. This approach results in a depot formulation from which the drug slowly elutes and thus maintains a high local concentration in the surrounding tissues over an extended period of time [165].

The network structure and the thermodynamic nature of all compounds involved determine the protein release profile of these networks [321]. The molecular weight and content of the polymer as well as the addition of crosslinking agents determine the density of crosslinks in the gel matrix and thus the mesh size [167]. The mesh size of the

swollen network affects the physical properties of the gel, such as mechanical strength, degradation and diffusion of captured molecules [170]. By the addition of ionizable or hydrophobic hydrogel monomers, additional interactions of the proteins with the polymer network can be promoted [167]. On the protein side, mainly the molecular weight, the composition of the amino acids and thus the distribution of charged and hydrophobic residues on the surface of the protein as well as the three-dimensional structure of the protein affect the release properties from the hydrogel [167]. The interaction-based uptake and release of biomolecules is determined by the ratio of the interaction between the hydrogel and the protein as well as the protein and the surrounding solution [163]. There are many theoretical approaches to describe network structure, mesh size, swelling behavior and mass transport of biomolecules in hydrogels [161]. The high number of variables, however, makes a comprehensive mechanistic understanding of protein-hydrogel interaction difficult. Furthermore, the theoretical predictability of the uptake and release profiles is aggravated by the multiplicity of combinable proteins and hydrogel materials [356]. A sound experimental data base is essential for theoretical knowledge building of the various interactions occurring between the hydrogels, proteins and the liquid environment. In this context, high-throughput screenings (HTS) may help to understand the complexity affecting the drug delivery result [357]. HTS offer an accurate, rapid, and cost-saving method to study hydrogel-protein interactions and the influence of surrounding solution conditions while covering a high number of potential process parameters at the same time. The standard HTS-format in biotechnology are multi-well plates, which are handled by highly automated pipetting stations [358–361]. For hydrogels, however, a fast and reproducible method to crosslink precursor solutions into a HTS-compatible shape is still missing. 3D printing offers the herefore needed outstanding possibility to polymerize precursor solutions to any shape [362]. In case of 3D bioprinting, the printing materials, or bioinks, are composed of biocompatible matrix materials such as hydrogels or their precursors, additives and biological components.

This study aims to implement three dimensional hydrogel structures into multi-well plates for the investigation of hydrogel-protein interactions on liquid-handling stations. Therefore, hollow hydrogel cylinders fitting into standard 48-well plates were produced using 3D bioprinting. This shape provides a large surface to volume ratio for the observation of transport phenomena while ensuring a non-destructive operation of the automated pipetting tips. Lysozyme from chicken egg white was used as a model protein to study the drug uptake and release behavior from polyethylene glycol-diacrylate (PEG-DA)-based hydrogels. PEG-DA was photochemically crosslinked using a DLP (digital light processing)-based stereolithography system. Two approaches for the incorporation of pro-

teins in hydrogels are compared. In the first approach, the hydrogel was printed without protein and subsequently loaded with protein (PostFabLoading). This approach increases the probability of preserving the biological activity of the protein, reduces, however, the maximum utilization of the protein due to partitioning limitations [169]. In order to maximize the protein uptake different polymer contents and pH values as well as the addition of the comonomer acrylic acid (AA) were investigated. For the second approach, the protein was part of the bioink and consequently present during the polymerization process (PrintLoading). This approach may result in activity loss due to potential reactions with the hydrogel polymer, resulting radicals or the energy input necessary for crosslinking. After hydrogel formation and protein loading, the release was examined under different solution conditions (pH and ionic strength). In order to ensure protein integrity after the release, an activity assay was performed.

9.2 Materials and Methods

All solutions were prepared with ultra-pure water ($0.55 \mu\text{S}/\text{cm}$) obtained from a PURE-LAB Ultra water purification system (ELGA Labwater, Germany). The 25 mM multicomponent buffer with a linear buffering range from pH 3 to pH 9 consisted of the buffer substances AMPSO (2-hydroxy-3-[(1-hydroxy-2-methylpropan-2-yl)amino]propane-1-sulfonic acid) (Sigma-Aldrich), TAPSO (3-[[1,3-dihydroxy-2-(hydroxymethyl)propan-2-yl]amino]-2-hydroxypropane-1-sulfonic acid)(Sigma-Aldrich), MES 1-hydrate (2-morpholinoethanesulfonic acid) (AppliChem), sodium acetate trihydrate (Sigma-Aldrich, USA) and formic acid (Merck Millipore). The buffer recipe is summarized in Table 9.1. Potassium chlo-

Table 9.1: Composition of 25 mM multicomponent buffer with a linear buffering range from pH 3 to pH 9 calculated according to [363]. The used buffer substances are displayed with the corresponding pK_a value and molarity.

Buffer component	pK_a value [-]	molarity [mM]
AMPSO	9.14	42.44
TAPSO	7.64	33.90
MES 1-hydrate	6.10	38.03
Sodium acetate trihydrate	4.76	27.56
Formic acid	3.75	37.43

ride (KCl) and di-potassium hydrogen phosphate (K_2HPO_4) for the size exclusion chromatography running buffer were purchased from VWR. Dulbecco's Phosphate buffered saline (PBS) (ThermoFisher Scientific) and sodium chloride (Merck Millipore) were used for protein release studies. pH adjustment of all buffers within a range of ± 0.05 units was performed using a five-point calibrated pH-meter HI-3220 (Hanna Instruments, USA) with a SenTix[®] 62 pH electrode (Xylem Inc., USA). For pH correction hydrochloric acid and sodium hydroxide were obtained from Merck (Germany). All buffers were filtered using a 0.2 μ m cellulose-acetate filter (Sartorius, Germany) and degassed for chromatographic purposes.

Polyethylene glycol-diacrylate (PEG-DA, average MW 575), 2,2-Dimethoxy-2-phenylacetophenone (DMPA) and acrylic acid for bioink preparation were obtained from Sigma-Aldrich. Protein solutions were prepared using chicken egg-white lysozyme (subsequently referred to as lysozyme) from Hampton Research.

9.2.1 3D Printing of PEG-DA-based Hydrogels

9.2.1.1 Preparation of Bioinks

The used mass concentrations of all components are summarized in Table 9.2 for all studied bioinks. To prevent premature polymerization, all ink components were weighed in and stored in lightproof centrifuge tubes (50 ml Tube Cellstar[®], Greiner Bio-One).

Table 9.2: Composition of bioinks. The percentage of a component %(w/w) refers to the total weight of all components. The lysozyme stock solution was prepared by dissolving 6,45 %(w/w) in ultrapure water.

	PEG-DA (MW 575)	ultra-pure water	acrylic acid	DMPA	lysozyme stock solution
PEG-DA ₅₀	50	49	-	1	-
PEG-DA ₇₅	75	24	-	1	-
PEG-DA ₉₀	90	9	-	1	-
PEG-DA ₇₅ AA _{7.5}	75	16.5	7.5	1	-
PEG-DA ₇₅ AA ₁₅	75	9	15	1	-
PEG- DA ₇₅ Lys _{1.55}	75	-	-	1	9.6

The ink was mixed on an overhead shaker for at least 24 hours to ensure complete dissolution of the photoinitiator.

9.2.1.2 3D Fabrication of Hydrogels

A commercially available B9Creator DLP 3D printer (version 1.2, B9Creations) equipped with an modified projector (D912HD, vivitek) as light source was used to polymerize the bioinks. The CAD model of the hollow cylinder was created in Solid Edge ST7 (Siemens PLM Software) and exported as a stereolithography file (.stl) into the 3D printer software (B9Creator). The hollow cylinders have an outer diameter of 9.45 mm, a wall thickness of 0.82 mm and a height of 7 mm. This results in a total volume of the hollow cylinder of 155.6 mm³ before being swollen in water. The model was sliced to layers of 200 μm thickness and the configuration of the printer was set to an x, y resolution of 30 μm . Before printing, calibration of the build table and automatic focusing of the projector was performed. Depending on the ink composition printer settings were adjusted in order to achieve complete polymerization and 3D objects free from defects. The applied settings for the different bioinks are summarized in Table 9.3. Except the changes stated here, the bioinks were printed with the default settings for the commercial ink B9R-1-Red from B9Creations. Since a complete filling of the tank with bioink was too material-consuming, the ink was gradually applied manually. The necessary time for ink application was achieved by setting the post-release delay to 10 seconds. Four cylinders were produced simultaneously in one printing run. The irradiation by the projector led to a clouding

Table 9.3: Adapted printing parameters for the various ink compositions (see Table 2).

	Exposure settings base	Exposure settings over	Attach lay- ers	Attach base	Attach Over
PEG-DA ₅₀	25	1	1	20	1
PEG-DA ₇₅	20	1	1	15	1
PEG-DA ₉₀	20	1	1	15	1
PEG-DA ₇₅ AA _{7.5}	20	1	1	30	1
PEG-DA ₇₅ AA ₁₅	28	1	1	50	1
PEG-DA ₇₅ Lys _{1.55}	11	1	2	12	1

of the silicone layer which is built-in to prevent adhesion of the printed structure to the resin vat. This effect was amplified by increasing the content of AA in the bioinks. Therefore, the silicone layer was exchanged at regular intervals according to the specification of B9Creations using Elastosil[®] RT 601 (Wacker Chemie).

9.2.1.3 Determination of Protein Uptake and Release by 3D Printed Hydrogel Cylinders

Loading of Hydrogels with Protein

For PrintLoading, the protein is present during the printing process. The fabrication of the protein containing hydrogel cylinders is already described in section 9.2.1.2. The amount of lysozyme that was entrapped within the hydrogel was determined by assuming the same weight percent of lysozyme in the precursor solution to be also present in the polymerized hydrogel.

To perform the PostFabLoading of the printed hydrogel cylinders, a lysozyme solution of 40 mg/ml was prepared using the 25 mM multicomponent buffer of respective pH. Protein concentration measurements were conducted using a NanoDrop2000c UV-Vis spectrophotometer (Thermo Fisher Scientific) and an extinction coefficient of $\epsilon_{280\text{ nm, lysozyme}}^{1\%} = 22.00$ [254]. The 3D-printed cylinders were stored in ultra-pure water for at least 24 h in order to deplete unpolymerized bioink components. For the uptake experiments, the cylinders were drained, patted dry and placed in the wells of a 48-well plate (48 Well Cell Culter Cluster, Costar[®]). Using a fully automated pipetting station Freedom EVO[®] 200 (Tecan) the cylinders were equilibrated for 30 min in 400 μl multicomponent buffer of the respective pH. After equilibration, 300 μl of the buffer were withdrawn and replaced by the 40 mg/ml protein solution yielding a concentration of 30 mg/ml for the uptake experiments. During incubation, the 48-well plates were covered to avoid evaporation and shaken at 200 rpm on a Te-Shake orbital mixer (Tecan). After 0, 2, 4, 6, 8, 10 and 12 hours, the supernatant was removed from a triplet of cylinders of equal composition and examined by analytical size exclusion chromatography (SEC) for the remaining protein concentration. For all experiments carried out, only one measurement value is generated from the supernatant of each hydrogel cylinder of a 48-well plate. Thus, the multiple determination of a data point as well as the different time steps within a protein uptake series result from different cylinders.

The chromatography runs were performed using a Dionex UltiMate[®] 3000 liquid chromatography system (ThermoFisher Scientific) equipped with a HPG-3400RS pump, a

WPS-3000TFC analytical autosampler, a TCC3000RS column thermostat and a DAD-3000RS detector. As stationary phase, an Acquity UPLC[®] BEH200 SEC 1.7 μm (4.6 x 30mm) column (Waters) was used. Analysis was performed at a flow rate of 0.2 ml/min using a 200 mM K_2HPO_4 buffer at pH 7 containing 250 mM KCl. The injection volume was set to 20 μl using double loop overflow.

Protein Release from Hydrogels

Protein release was studied using the 25 mM multicomponent buffer at three different pH values (3, 7 and 9) and under the influence of three different sodium chloride concentrations (0 M, 0.15 M and 0.5 M). Furthermore, the protein release under physiological conditions was tested using phosphate buffered saline (PBS). To study the protein release from the loaded hydrogels, cylinders were incubated for 12 h with protein solution for PostFabLoading as described in section 9.2.1.3. After incubation, the protein solution was withdrawn and the hydrogels were washed with 1 ml ultra-pure water by single-time uptake and dispensing with a pipette. The Printed cylinders were rinsed with ultra-pure water for 10 s after the printing process.

For the protein release studies, 500 μl of the release buffer to be screened was added to each cylinder. During incubation, the 48-well plates was shaken at 200 rpm. Kinetics were recorded using a NanoDrop2000c UV-Vis spectrophotometer and an extinction coefficient of $\epsilon_{280\text{ nm, lysozyme}}^{1\%} = 22.00$. For each time point, 3 μl of sample were withdrawn and analyzed. The multiple determination of a data point within one protein release series results from three independent cylinders.

In order to evaluate biological integrity after the fabrication process, the released protein was analyzed for residual activity using *Micrococcus lysodeikticus*-based activity assay according to [293]. This method was slight modified by measuring the activities only at a protein concentration of 0.3 mg/ml. The slope of the absorption at 450 nm over time was used as activity and related to the activity of reference sample containing native lysozyme at pH 7. Moreover, samples were analyzed by analytical SEC in order to monitor the formation of aggregates (c.f. section 9.2.1.3).

9.3 Results and Discussion

PEG-DA-based hydrogels were fabricated by photopolymerization with a DLP-based stereolithography system using DMPA as a photoinitiator. DMPA photofragments to highly reactive methyl radicals, which initiate photopolymerization by attacking the carbon-carbon double (C=C) bonds present in the acrylate groups of PEG-DA and acrylic acid [167, 364]. This radical photopolymerization leads to linear chain growth as well as to branched and crosslinked structures forming a three-dimensional network [364]. The two components PEG-DA and acrylic acid absorb water in an aqueous environment and thus create an ideal environment to incorporate biomolecules in this three-dimensional network. In this study, two methods to introduce the biomolecule into the hydrogels are investigated. Firstly, the hydrogel is polymerized and subsequently incubated in concentrated drug solutions (post-fabrication equilibrium partitioning = PostFabLoading) [169] and secondly, the protein is present in the bioink during the polymerization (PrintLoading) [167]. The hydrogels loaded in both ways are tested for their release behavior and the residual activity of the incorporated protein.

9.3.1 3D Printing of PEG-DA-based Hydrogels

The presented setup with the B9Creator and the modified projector was well suited to produce hydrogel structures from all prepared ink compositions. With the UV filter removed from the projector the emission spectra and the irradiance was adequate to polymerize hydrogel layers of 200 μm and hollow cylinders could be build up. To ensure a proper print result, the applied printing parameters (c.f. Table 9.3) had to be adapted for the varying bioink formulations (c.f. Table 9.2). The aim of the adaptations was the production of hydrogel structures with a minimum of reject and waste. Furthermore, the duration of light exposure was optimized in regard to print result, total print time, and in the specific case preventing inadequate irradiation of the protein. Adjusting the suitable print settings as well as the application of the ink were the most crucial steps for a successful printing procedure. Insufficient exposure settings for the attaching layer concluded in poor attachment and the occurring of polymerized parts in the applied ink (see Fig. 9.1A). Also incomplete structures were developing when the freshly printed layer had no contact to the already consisting layer. In the later printing process, air bubbles or the lack of applied ink could disrupt the resulting hydrogel structure as shown in Fig. 9.1B. It is in the nature of this printing technique, that unintended absence of

polymerizable material during the printing process inevitably causes malformations in the resulting structure. Nonetheless, commensurate ink application in combination with the adapted printing parameters (c.f. Table 9.3) resulted in a high repeatability in the production of flawless hydrogel cylinders for the further use in this study (see Fig. 9.1C). An increasing amount of PEG-DA in the bioink resulted in shorter exposure times needed for good printing outcomes. This need for lower energy input at the given layer height can be explained by the concentration dependent amount of possible crosslinking sites [365]. To generate flawless hydrogel structures from bioinks containing 75 % PEG-DA and additional acrylic acid an increase in the exposure time was required compared to bioinks without acrylic acid. The reaction rate of this copolymerization seems to be slowed down with increasing percentage of acrylic acid. Different reactivities of PEG-DA and acrylic acid can be used as an explanation for this shift. The applied exposure times could be reduced for the bioink PEG-DA₇₅Lys_{1.55}. This was influenced by the noticeable turbidity (see Fig. 9.1), which was already visible before the polymerization and probably occurred due to precipitated lysozyme in this ink. The turbidity increased the absorbance of luminous energy which resulted in a faster polymerization process.

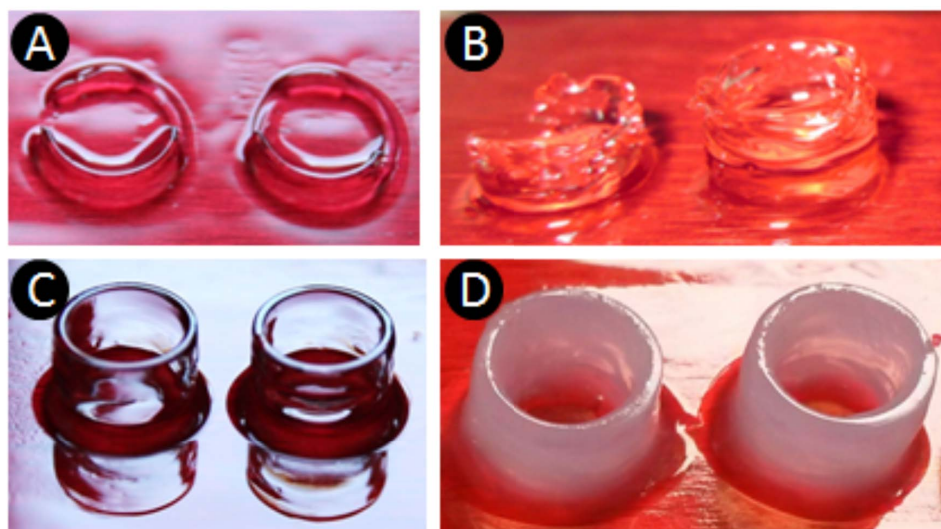


Figure 9.1: Photographs of printed hydrogel structures from PEG-DA₇₅ (A-C) and PEG-DA₇₅Lys_{1.55} (D). Underexposure led to insufficient adherence of the hydrogel at the build platform (A). Unbalanced ink application and air bubbles resulted in partially defective structures (B). Flawless hollow hydrogel cylinders as they have been used in the presented study (C). PrintLoading cylinders with noticeable turbidity due to incorporated protein (D).

9.3.2 Protein Uptake During Post-Fabrication Equilibrium Partitioning

Post-fabrication equilibrium partitioning (PostFabLoading) of lysozyme to PEG-DA-based hydrogels was studied using the bioinks PEG-DA₅₀, PEG-DA₇₅, PEG-DA₉₀, PEG-DA₇₅AA_{7.5} and PEG-DA₇₅AA₁₅. The protein uptake was determined by measuring the lysozyme concentration in the supernatant of incubated hydrogel cylinders at regular time intervals by analytical SEC. The amount of loaded protein was calculated by the difference between the amount of protein in the protein stock solution and in the supernatant. The relative protein uptake was defined by Eq. 9.1, where m_{loaded} and m_{stock} are the mass of the loaded protein and the mass of the total protein in the stock solution, respectively.

$$Relative\ protein\ uptake = \frac{m_{loaded}}{m_{stock}} \cdot 100\% \quad (9.1)$$

In Fig. 9.2, the relative protein uptake is displayed for different bioink compositions and loading conditions. The error bars indicate the standard deviation of a triple determination from the supernatant of three independent hydrogel cylinders. In Fig. 9.2A, the influence of PEG-DA mass fraction in the bioink on the relative protein uptake at pH 7 is shown. Over a time of 12 hours, the hydrogels with an initial PEG-DA mass fraction of 50 % exhibit the highest uptake of up to 40 % of the initial applied protein mass. The course of the protein uptake curve for the hydrogels with 75 % and 90 % PEG-DA are very similar and achieve a maximum of approximately 20 % in the studied 12 h. These observations are consistent with the work of Zhang and coworkers [366] who describe that a higher PEG-DA concentration leads to a more compact hydrogel structure with higher crosslinking density. A higher crosslinking density restricts the swelling of the hydrogel and results in a reduced meshsize which in turn hinders protein diffusion into and out of the hydrogel. For all three curves, the increase in protein uptake is highest during the first 6 h and almost reaches a plateau value after 10 h. The plateau value reflects the maximal protein absorption capacity of the hydrogel, which is denoted as protein uptake at saturation [367]. Zaho et al. [367] have observed similar results for the uptake of lysozyme by glycerol diglycidylether crosslinked oxidized starch microgels. They found a absorption time of 4 h to be sufficient for the microgel to reach saturation during protein absorption.

In Fig. 9.2B it is demonstrated, how the relative protein uptake of PEG-DA-based hydrogels can be increased by addition of the comonomer acrylic acid. Firstly, it can be

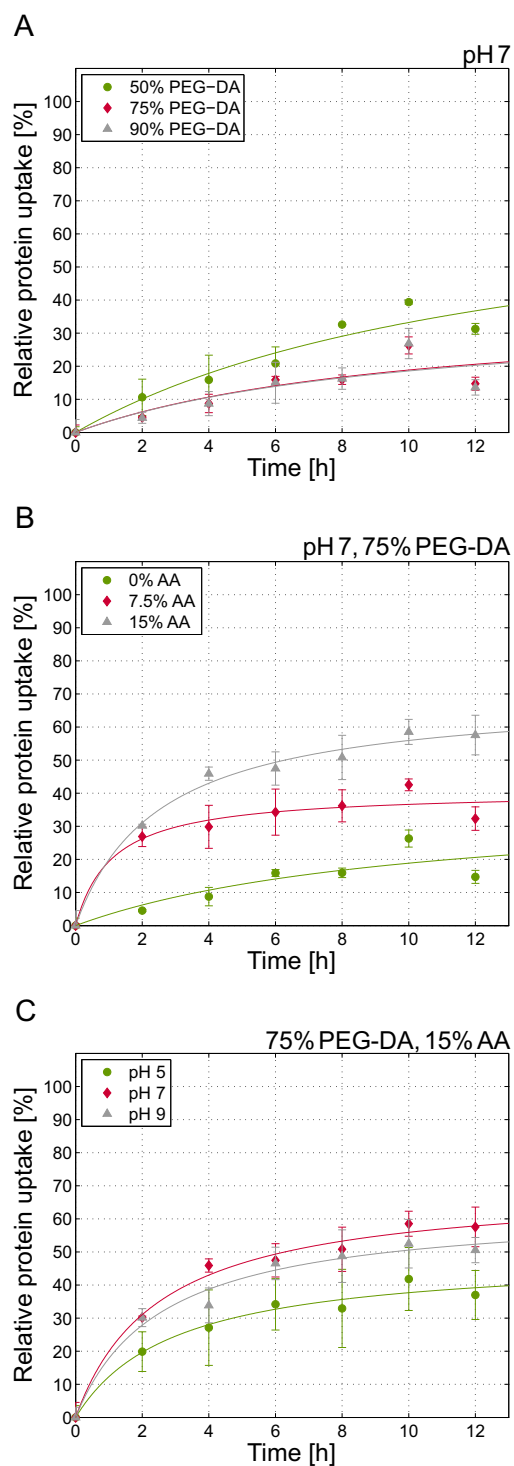


Figure 9.2: PostFabLoading of PEG-DA-based hydrogels with lysozyme: Relative protein uptake of hydrogels with varying mass fraction of PEG-DA at pH 7 (A), with 75 % PEG-DA and varying mass fraction of the comonomer acrylic acid at pH 7 (B) and different loading pH values for 75 % PEG-DA and 15 % acrylic acid (C).

seen that the protein uptake rises more steeply in the first 4 h than without acrylic acid. This indicates that lysozyme absorbs with higher affinity to hydrogels containing acrylic acid. This observation can be explained by the introduction of an ionic character to the hydrogel by the addition of acrylic acid [167]. At pH 7, acrylic acid is negatively charged due to its pK_a of 4.25 [368] while the net charge of lysozyme is positive ($pI=11.3$ [257]). Therefore, electrostatic interactions occur between protein and ionized acrylic acid. Secondly, the protein uptake at saturation increases approximately linearly with increasing mass fraction of acrylic acid. This linear increase can be explained by the introduction of exactly one negative charge per molecule acrylic acid into the hydrogel. Doubling the acrylic acid content therefore leads to a doubling of the binding sites for the protein. An unlimited increase in the acrylic acid content is, however, not possible, because the molecule has only one free double bond and thus weakens the network structure of the hydrogel.

In Fig. 9.2C, the effect of the solution pH on the protein uptake is shown for the bioink PEG-DA₇₅AA₁₅ containing 75 % PEG-DA and 15 % acrylic acid. When comparing the three pH values, the lowest protein uptake is achieved at pH 5. The curves of pH 7 and pH 9 are identical within the error bars. Since pH 7 and pH 9 are more than two pH-steps higher than the pK_a value of acrylic acid, a complete deprotonation of all acid groups can be assumed for both pH values. According to the calculation of the protein charge with H^{++} [369], the net charge of lysozyme is +8 at pH 7 and pH 9. These assumptions apply to the identical protein uptake curves at pH 7 and pH 9. In contrast, pH 5 is very close to the pK_a value of the acrylic acid. Since the pK_a value indicates the pH value at which 50 % of the acid groups are deprotonated, it is possible that not all acid groups are deprotonated at pH 5. This would result in a reduced number of negative charges available to the protein for the interactions, and thus can explain the lower protein uptake.

9.3.3 Protein Release from Loaded Hydrogels

To study the release profiles for the protein-loaded hydrogels, the hollow cylinders were incubated in different release buffers for 150 min. During this period, samples were regularly taken and the contained protein was quantified by means of absorption measurements. The resulting release profiles are displayed in Fig. 9.3 for 0 M and 0.15 M NaCl in the release buffer. The results for 0.5 M NaCl in the release buffer are displayed Supplementary Fig. A.10), since they differed only slightly from the results with 0.15 M NaCl.

In all experiments, PBS behaves as the multicomponent buffer at pH 7 containing 0.15 M sodium chloride. In Fig. 9.3A-D, the lysozyme release profiles for hydrogel cylinders consisting of 75 % PEG-DA and 0 % AA (in the bioink) are displayed. These hydrogels are uncharged since they are formed exclusively by crosslinking uncharged PEG-DA chains. For the two loading methods PostFabLoading (Fig. 9.3A and B) and PrintLoading (Fig. 9.3C and D), neither the pH of the surrounding solution nor the salt concentration has any influence on the release profile. The transport of the protein therefore appears to be driven exclusively by diffusive processes. When comparing PostFabLoading and PrintLoading for a given solution condition, it is noticeable that the maximum protein released is higher for PrintLoaded hydrogels. This difference can not be attributed to different concentration gradients since hydrogel cylinders of both loading methods contain the same amount of protein after the loading process. The most probable cause for the difference in the maximum protein release between PostFabLoaded and PrintLoaded hydrogels is an unequal swelling state at the beginning of the release experiments. Hydrogel water content will affect the release profile because water in the matrix is the medium through which proteins will diffuse [167]. The PostFabLoaded hydrogels are already completely swollen due to their storage, equilibrium and protein loading and have thus reached their equilibrium water content (EWC) [167]. In contrast, the PrintLoaded hydrogels were only washed for 10 s in ultra-pure water immediately after printing to reduce uncontrolled protein release during the washing process. The addition of buffer during the release experiments induced the swelling process and thus led to an increasing mesh size during the release process. An increased gel mesh size allows more protein to diffuse out of the hydrogel [366]. The generally low release rates indicate the existence of intermolecular interactions such as hydrogen bonds or Van-der-Waals forces which appear to be stronger between lysozyme and PEG-DA than between lysozyme and the surrounding solution. In case of PrintLoaded hydrogels, covalent binding of the protein to the gel is also possible by free radical addition or Michael addition between lysine residues and acrylate groups of the polymer [167, 370]. Since being present during the printing process, the protein may additionally be enclosed inaccessibly in closed or too narrow pores.

In Fig. 9.3E and F, lysozyme release profiles from hydrogels containing 75 % PEG-DA and 15 % AA are shown. Comparing Fig. 9.3E and F with Fig. 9.3A and B, it can be seen that the release of lysozyme from acrylic acid containing hydrogels is slower than from acrylic acid-free hydrogels. These observations suggest an affinity-based mechanism of release, as is was already discussed for the protein uptake experiments. For 0 M sodium

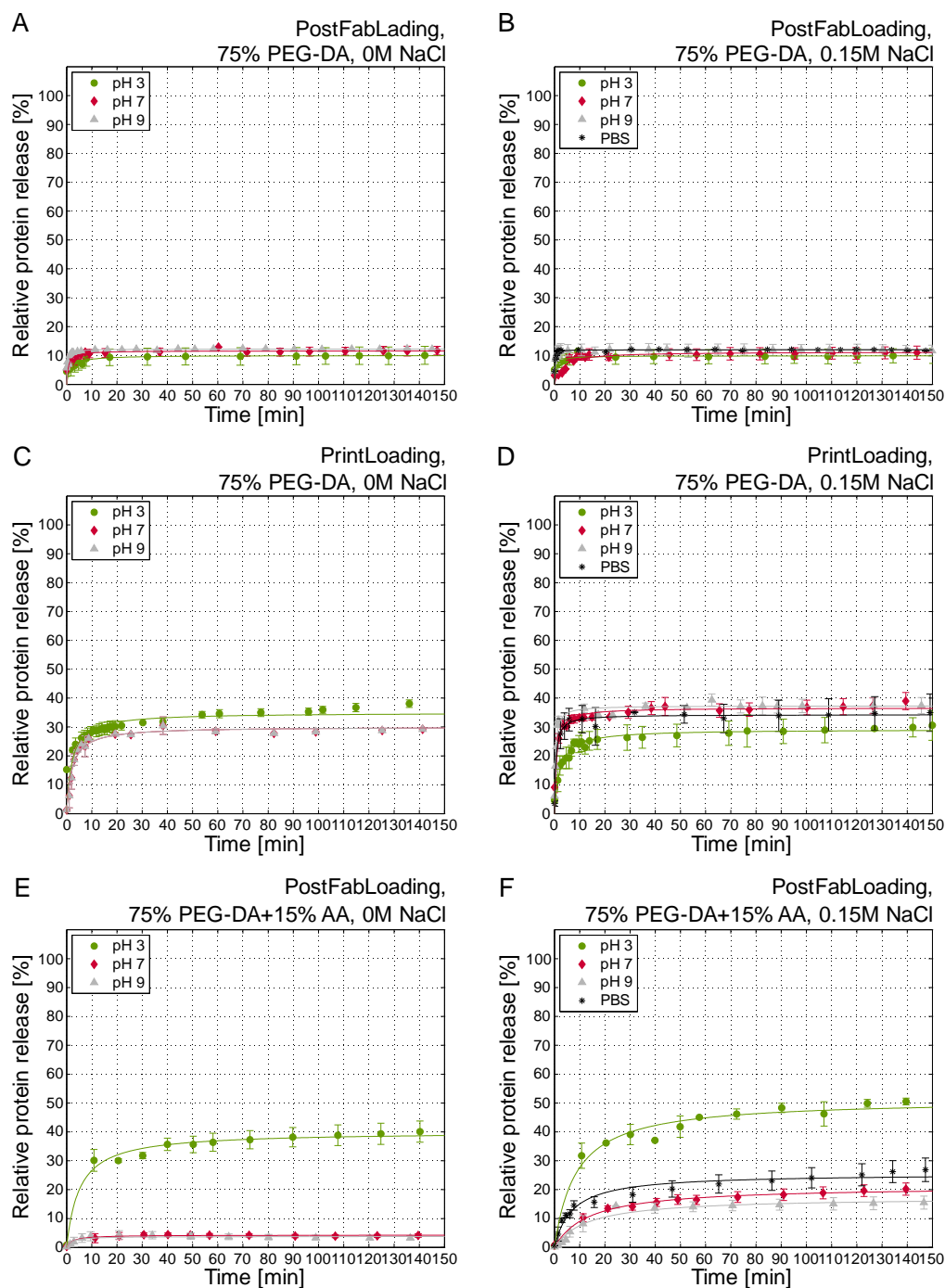


Figure 9.3: Relative protein release under the influence of 0 M NaCl in the release buffer (PostFabLoaded hydrogels from 75 % PEG-DA (A), PrintLoaded hydrogels from 75 % PEG-DA (C) and PostFabLoaded hydrogels from 75 % PEG-DA and 15 % AA (E)) and under the influence of 0.15 M NaCl in the release buffer (PostFabLoaded hydrogels from 75 % PEG-DA (B), PrintLoaded hydrogels from 75 % PEG-DA (D) and PostFabLoaded hydrogels from 75 % PEG-DA and 15 % AA (F)).

chloride in the release buffer (Fig. 9.3E), a clear dependency of the protein release on the pH value of the surrounding solution can be seen. At pH 3, the maximum protein release is 10 fold greater than at pH 7 and pH 9. Since pH 3 is below the pK_a of acrylic acid, the acid groups in the hydrogel are protonated and thus uncharged. Due to the pH change of pH 7 during the loading to pH 3 during release, the protein which was absorbed via electrostatic attraction is released. These results are in accordance with the work of Zhang and coworkers [366], who have described a fast initial burst release of proteins at pH 2.0 due to a squeezing mechanism. Since there are no electrostatic attractions between hydrogel and lysozyme at pH 3, the addition of salt ions (compare Fig. 9.3F) also has no significant effect on the release. At pH 7 and pH 9, the acid groups of acrylic acid, however, are deprotonated and thus negatively charged. Since lysozyme has a net charge of +8 (calculated with H^{++} [369]) at both pH 7 and pH 9, the protein is equally retained in the hydrogel by means of electrostatic interactions. When salt is added (compare Fig. 9.3F), the salt ions compete with the proteins for the charges of the hydrogel and displace the proteins. This effect has been discussed by various authors including Brooks and Cramer [155] in the context of ion exchange chromatography.

9.3.4 Activity Examination of the Released Lysozyme

Following the release studies, the gained samples were examined regarding their residual enzyme activity compared to native lysozyme. In Fig. 9.4, the determined relative activity of all samples is shown. The way of carrying out the assay could have led to partially pronounced standard deviations. Therefore, we defined a relative activity of $100\% \pm 10\%$ as unimpaired preservation of activity. It can be seen, that the buffer conditions of the release procedure also had an influence on the activity of the released lysozyme in the diluted assay conditions. For the lysozyme released from PostFabLoading PEG-DA₇₅ a slightly positive effect can be seen for the presence of NaCl in the release buffer but no reliable statement can be made due to the standard deviations. The positive influence of the salt could definitely be observed for the release at pH 3 PrintLoading and even more clearly at pH 7 and pH 9 PostFabLoading PEG-DA₇₅AA₁₅. The salt significantly alleviated the negative impact on the activity initiated by the loading into acrylic acid containing hydrogels and the subsequent release with buffers at pH 7 and pH 9. The lysozyme released in PBS showed a slightly smaller activity than the comparable multi-component buffer at pH 7 with 0.15 M NaCl. Comparing the two executed approaches

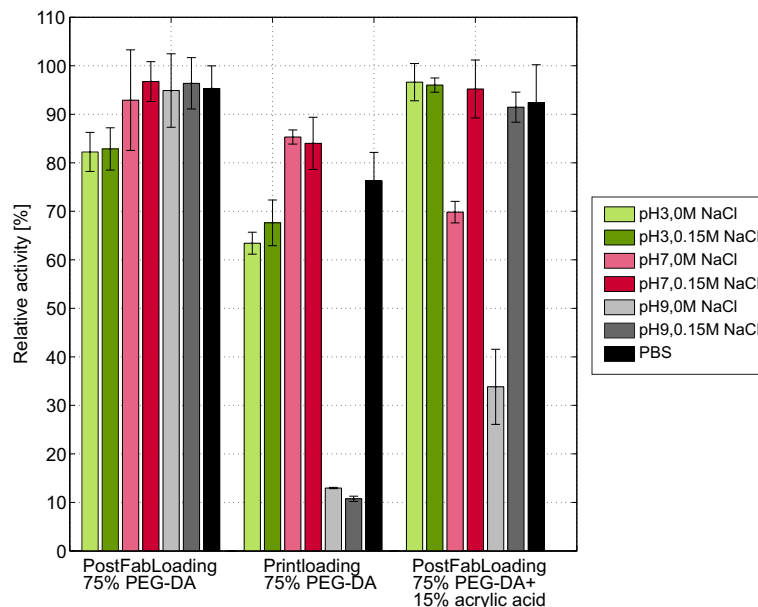


Figure 9.4: Comparison of the relative activities of released lysozyme relating to the loading method and ink composition.

PostFabLoading and PrintLoading at given pH, a negative impact of the PrintLoading procedure could be determined. This impact was strongly evident for the released lysozyme at pH 9.

In order to further investigate the reduced activity, released protein samples from PostFabLoaded and PrintLoaded hydrogels without acrylic acid at pH 9 and 0 M NaCl were analyzed using analytical SEC. The results are displayed in Fig. 9.5. The protein sample from PostFabLoading resulted in a single peak which could be attributed to a reference sample of native lysozyme. The protein sample from PrintLoading, however, contained larger and smaller protein species, which eluted earlier and later than native lysozyme, respectively. The loss in activity during the PrintLoading process may therefore be attributed to the formation of precipitate and fragments of lysozyme due to the bioink composition and effects triggered by irradiation. The turbidity of the applied bioink and resulting hydrogels could serve as a first indication of protein aggregation during the printing process.

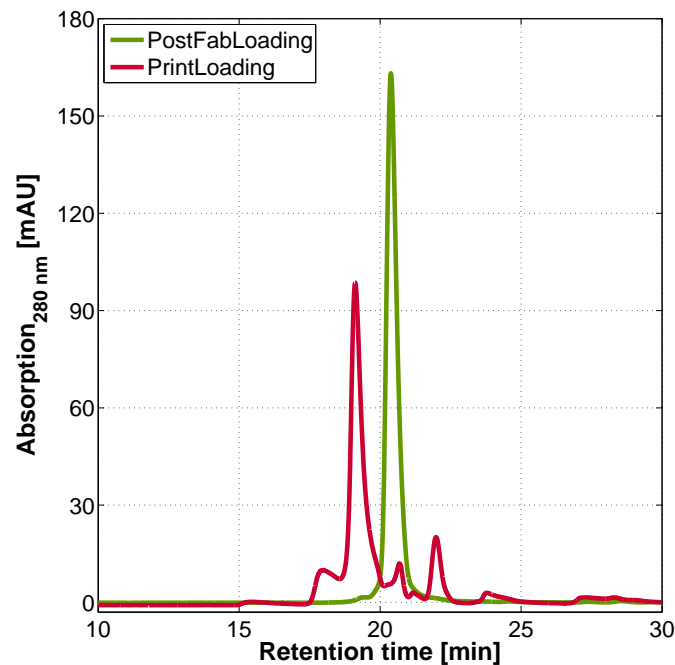


Figure 9.5: Analytical SEC comparing released lysozyme form PostFabLoading and PrintLoading for PEG-DA-based hydrogels without acrylic acid at pH 9 and 0 M NaCl.

9.4 Conclusion

Protein uptake and release of hydrogels depends on the right combination of hydrogel materials, protein and surrounding solution conditions. This study has demonstrated that mechanisms and effects of protein adsorption and release by hydrogels already described in the literature could be reproduced reliably by the presented combination of 3D printing and high-throughput screening. Thus, a helpful tool was developed for the rapid and cost-effective optimization of new hydrogel materials with regard to the physical, biological and material transport requirements at the site of action. The development of oral delivery products and implanted reservoir systems for biopharmaceutical proteins may profit from the here presented approach. In order to further qualify this approach for high-throughput studies, we are in the process of automating the printing procedure.

Furthermore, the results demonstrated that the direct incorporation of proteins into the bioinks may lead to the formation of inactive species during the printing process.

The development of suitable stabilization strategies for hydrogel-based biopharmaceutical products are therefore of the utmost interest to meet this challenge.

9.5 Acknowledgments

We gratefully acknowledge the financial support by the German Federal Ministry of Education and Research (BMBF). This research work is part of the project ‘Molecular Interaction Engineering: From Nature’s Toolbox to Hybrid Technical Systems’, funding code 031A095B. The authors further acknowledge Rebecca L. Hoffman, Dominik S. G. Hiltmann and Nicolai Bluthardt for their support in the laboratory.

9.6 References

105. Wiendahl, M., Völker, C., Husemann, I., Krarup, J., Staby, A., Scholl, S. & Hubbuch, J. A novel method to evaluate protein solubility using a high throughput screening approach. *Chemical Engineering Science* **64**, 3778–3788 (2009).
155. Brooks, C. A. & Cramer, S. M. Steric mass-action ion exchange: Displacement profiles and induced salt gradients. *AIChE Journal* **38**, 1969–1978 (1992).
160. Kim, S. W., Bae, Y. H. & Okano, T. Hydrogels: Swelling, drug loading, and release. *Pharm. Res.* **9**, 283–290 (1992).
161. Peppas, N. A., Bures, P., Leobandung, W. S. & Ichikawa, H. Hydrogels in pharmaceutical formulations. *European journal of pharmaceuticals and biopharmaceutics* **50**, 27–46 (2000).
162. Langer, R. & Tirrell, D. A. Designing materials for biology and medicine. *Nature* **428**, 487–492 (2004).
163. Liechty, W. B., Kryscio, D. R., Slaughter, B. V. & Peppas, N. A. Polymers for drug delivery systems. *Annual review of chemical and biomolecular engineering* **1**, 149–173 (2010).
165. Hoare, T. R. & Kohane, D. S. Hydrogels in drug delivery: Progress and challenges. *Polymer* **49**, 1993–2007 (2008).

-
167. Mellott, M. B., Searcy, K. & Pishko, M. V. Release of protein from highly cross-linked hydrogels of poly (ethylene glycol) diacrylate fabricated by UV polymerization. *Biomaterials* **22**, 929–941 (2001).
169. Lin, C.-C. & Anseth, K. S. PEG hydrogels for the controlled release of biomolecules in regenerative medicine. *Pharm. Res.* **26**, 631–643 (2009).
170. Sharpe, L. A., Daily, A. M., Horava, S. D. & Peppas, N. A. Therapeutic applications of hydrogels in oral drug delivery. *Expert opinion on drug delivery* **11**, 901–915 (2014).
173. Malda, J., Visser, J., Melchels, F. P., Jüngst, T., Hennink, W. E., Dhert, W., Groll, J. & Hutmacher, D. W. 25th anniversary article: Engineering hydrogels for biofabrication. *Advanced materials* **25**, 5011–5028 (2013).
254. Galm, L., Morgenstern, J. & Hubbuch, J. Manipulation of lysozyme phase behavior by additives as function of conformational stability. *Int. J. Pharm.* **494**, 370–380 (2015).
257. Maiser, B., Kröner, F., Dimer, F., Brenner-Weiß, G. & Hubbuch, J. Isoform separation and binding site determination of mono-PEGylated lysozyme with pH gradient chromatography. *J. Chrom. A* **1268**, 102–108 (2012).
293. Morgenstern, J., Baumann, P., Brunner, C. & Hubbuch, J. Effect of PEG molecular weight and PEGylation degree on the physical stability of PEGylated lysozyme. *Int. J. Pharm.* **519**, 408–417 (2017).
321. Hoffman, A. S. Hydrogels for biomedical applications. *Advanced drug delivery reviews* **64**, 18–23 (2012).
352. Ferreira, L., Vidal, M. M. & Gil, M. H. Evaluation of poly (2-hydroxyethyl methacrylate) gels as drug delivery systems at different pH values. *Int. J. Pharm.* **194**, 169–180 (2000).
353. Hari, P. R., Chandy, T. & Sharma, C. P. Chitosan/calcium–alginate beads for oral delivery of insulin. *Journal of Applied Polymer Science* **59**, 1795–1801 (1996).
354. Chaturvedi, K., Ganguly, K., Nadagouda, M. N. & Aminabhavi, T. M. Polymeric hydrogels for oral insulin delivery. *Journal of controlled release* **165**, 129–138 (2013).
355. Zou, X., Zhao, X. & Ye, L. Synthesis of cationic chitosan hydrogel with long chain alkyl and its controlled glucose-responsive drug delivery behavior. *RSC Advances* **5**, 96230–96241 (2015).

356. Brandl, F., Hammer, N., Blunk, T., Tessmar, J. & Goepferich, A. Biodegradable hydrogels for time-controlled release of tethered peptides or proteins. *Biomacromolecules* **11**, 496–504 (2010).
357. Oliveira, M. B. & Mano, J. F. High-throughput screening for integrative biomaterials design: Exploring advances and new trends. *Trends in biotechnology* **32**, 627–636 (2014).
358. Hertzberg, R. P. & Pope, A. J. High-throughput screening: New technology for the 21st century. *Current opinion in chemical biology* **4**, 445–451 (2000).
359. Bensch, M., Schulze Wierling, P., von Lieres, E. & Hubbuch, J. High throughput screening of chromatographic phases for rapid process development. *Chemical engineering & technology* **28**, 1274–1284 (2005).
360. Capelle, M. A. H., Gurny, R. & Arvinte, T. High throughput screening of protein formulation stability: Practical considerations. *European journal of pharmaceuticals and biopharmaceutics* **65**, 131–148 (2007).
361. Kittelmann, J., Ottens, M. & Hubbuch, J. Robust high-throughput batch screening method in 384-well format with optical in-line resin quantification. *J. Chrom. B* **988**, 98–105 (2015).
362. Wang, J., Goyanes, A., Gaisford, S. & Basit, A. W. Stereolithographic (SLA) 3D printing of oral modified-release dosage forms. *Int. J. Pharm.* **503**, 207–212 (2016).
363. Kröner, F. & Hubbuch, J. Systematic generation of buffer systems for pH gradient ion exchange chromatography and their application. *J. Chrom. A* **1285**, 78–87 (2013).
364. Sirkar, K. & Pishko, M. V. Amperometric biosensors based on oxidoreductases immobilized in photopolymerized poly (ethylene glycol) redox polymer hydrogels. *Anal. Chem.* **70**, 2888–2894 (1998).
366. Zhang, L., Ma, Y., Zhao, C., Zhu, X., Chen, R. & Yang, W. Synthesis of pH-responsive hydrogel thin films grafted on PCL substrates for protein delivery. *Journal of Materials Chemistry B* **3**, 7673–7681 (2015).
367. Zhao, L., Chen, Y., Li, W., Lu, M., Wang, S., Chen, X., Shi, M., Wu, J., Yuan, Q. & Li, Y. Controlled uptake and release of lysozyme from glycerol diglycidyl ether cross-linked oxidized starch microgel. *Carbohydrate polymers* **121**, 276–283 (2015).

368. Morris, G. E., Vincent, B. & Snowden, M. J. Adsorption of Lead Ions onto N-Isopropylacrylamide and Acrylic Acid Copolymer Microgels. *Journal of colloid and interface science* **190**, 198–205 (1997).
369. VirginiaTech. *H++* <http://biophysics.cs.vt.edu/index.php>. [Online; accessed 05/2017].
370. Hammer, N., Brandl, F. P., Kirchof, S., Messmann, V. & Goepferich, A. M. Protein Compatibility of Selected Cross-linking Reactions for Hydrogels. *Macromolecular bioscience* **15**, 405–413 (2015).

Conclusion and Outlook

The development and production of recombinant protein drugs is hampered by the occurrence of protein instabilities. Protein aggregation due to low solubility or unfolding of the molecule is among the most frequent instabilities. The main focus of this work was the development of processing and formulation strategies for the production of stable protein therapeutics. The challenge of laborious empirical process optimizations and the lack of mechanistic understanding of the underlying protein interactions was addressed by using high-throughput screening (HTS) methods in miniaturized scale and computer-based approaches.

In this context, the following stabilization strategies were addressed:

- Addition of stabilizing solution additives
- Covalent attachment of biocompatible polymers (protein conjugation)
- Incorporation into hydrogels

As binary reference system in which aggregation occurs intensively, the model protein lysozyme (from chicken egg white) under the influence of the salt sodium chloride was used in all studies. For the unstabilized lysozyme, the phase transitions crystallization, precipitation and skin formation occur. Skin formation is an indication for protein denaturation. [79]

In the first part of the thesis, it was shown that solution additives can alter both the aggregation behavior and the solubility of proteins. The effect of the investigated additives was found to depend on the stability of the protein conformation. For system conditions in which the protein conformation in the binary system was unstable, a stabilization of the protein conformation could be achieved by the addition of polyethylene glycol (PEG) and glycerol. However, no change in the protein solubility was observed. For

system conditions where the protein conformation was stable in the binary system, these additives exhibited a significant increase in lysozyme solubility.

The ability of PEG to stabilize protein conformation and to increase solubility initiated the investigation on how the covalent attachment of PEG to the protein (PEGylation) influences aggregation behavior and solubility. In order to monitor PEGylation reactions and to identify conjugate species with different number of attached PEG molecules (PEGamers), an HTS-compatible analytical method based on a calibrated capillary gel electrophoresis was developed. This method was found to be highly effective for large data sets as it provides a low sample consumption and analysis time, a high resolution allowing for peak baseline separation and a high sensitivity. For structural unstable proteins, this method was successfully supplemented by a precipitation step for the preservation of the sample composition. With regard to the stabilization of lysozyme, PEGylation resulted in a complete suppression of protein denaturation and an enormous increase in protein solubility. The presented experimental method is a valuable tool to optimize PEG molecular weight and PEGylation degree with regard to a compromise between increased conformational and colloid stability and residual protein activity.

While PEG remains useful for the stabilization of therapeutic proteins, some limitations in its clinical use have begun to emerge driving the development of alternatives. For this reason, two alternative, biocompatible polymers PNAM and POEGMA were synthesized and investigated for their suitability for protein stabilization. Both polymers induced an increased solubility compared to unmodified lysozyme. Compared to PEG, however, higher molecular weight polymers were required to achieve a comparable effect on solubility, which entailed a significant reduction of residual activity. Nonetheless, it was demonstrated that the methods for analysis, purification and stability assessment developed with PEGylated proteins are readily transferable to novel molecular systems. The presented high-throughput approach hence facilitates and accelerates the search for more effective and economically viable alternatives.

For the large-scale production of protein conjugates, ion exchange chromatography (IEX) is one of the most important methods for the separation of differently conjugated species. In order to transfer chromatographic processes from laboratory to production scale, knowledge of the underlying mass transfer and adsorption/desorption parameters is conducive. In this thesis, mechanistic chromatography modeling was applied to determine these parameters based on a small number of experiments. This study demonstrates, that an increase in PEG molecular weight results in slower film diffusion, faster desorption and an exponential increase in shielded ligands. These observations help to explain decreased retention time and binding capacities for PEGylated proteins.

In the last part of the thesis, functionalized PEG was investigated as a hydrogel material for the incorporation and release of lysozyme. Hydrogel-based protein delivery systems have gained momentum in the recent past as they protect the drug from harmful environments, such as enzymes or the low pH value in the stomach of a human body. However, chemical structure and molecular weight of the polymer, crosslinking density as well as surrounding solution conditions influence the diffusion and adsorption of captured molecules. The diversity of tunable features aggravates a mechanistic prediction of the protein release from hydrogels. To address this issue, a rapid and cost-effective HTS tool for the determination of protein release profiles from PEG-based hydrogels was developed. In order to crosslink the hydrogel precursors to high-throughput compatible structures, 3D printing was successfully applied for all studied materials. A modification of protein-hydrogel interactions was achieved both by copolymerization of PEG-diacrylate and acrylic acid as well as by changing the surrounding solution conditions. In comparison with literature data, it was shown that the approach presented here leads to verisimilar data for the used materials and thus constitutes a helpful tool for the development of hydrogel-based drug delivery systems. During the study, however, protein precipitation occurred when lysozyme was present during network formation.

In summary, the approaches presented in this work significantly accelerate and simplify the experimental evaluation of protein stabilities and thus make a valuable contribution to the development and processing of stable protein therapeutics. Prospective studies will focus on the integration of protein conjugation and hydrogel formation via 3D printing. An advantage could be a reduction in the observed instabilities when the protein is present during network formation. Moreover, protein conjugation using bi-functionalized polymers is conceivable. This approach would enable the attachment to the protein on the one end and the incorporation into the polymeric hydrogel network with the other end. The result would be a one-step immobilization of proteins into hydrogels and thus the creation of novel hybrid materials having both biological and polymer properties. In order to crosslink hydrogels to arbitrary three-dimensional geometries, 3D printing has shown to be a promising tool. The implementation of the proposed concept using 3D printing allows to shape these functional hybrid materials into technically relevant objects such as patient-specific implants, bioreactors or biosensors.

Comprehensive Reference List

1. Vermonden, T., Censi, R. & Hennink, W. E. Hydrogels for protein delivery. *Chemical Reviews* **112**, 2853–2888 (2012).
2. Tuomi, T., Santoro, N., Caprio, S., Cai, M., Weng, J. & Groop, L. The many faces of diabetes: A disease with increasing heterogeneity. *The Lancet* **383**, 1084–1094 (2014).
3. Serratrice, C., Carballo, S., Serratrice, J. & Stirnemann, J. Imiglucerase in the management of Gaucher disease type 1: An evidence-based review of its place in therapy. *Core Evidence* **11**, 37 (2016).
4. Ananyeva, N., Khrenov, A., Darr, F., Summers, R., Sarafanov, A. & Saenko, E. Treating haemophilia A with recombinant blood factors: A comparison. *Expert Opin. Pharmacother.* **5**, 1061–1070 (2004).
5. Forloni, G., Terreni, L., Bertani, I., Fogliarino, S., Invernizzi, R., Assini, A., Ribizzi, G., Negro, A., Calabrese, E. & Volonté, M. A. Protein misfolding in Alzheimer's and Parkinson's disease: Genetics and molecular mechanisms. *Neurobiology of aging* **23**, 957–976 (2002).
6. Frokjaer, S. & Otzen, D. E. Protein drug stability: A formulation challenge. *Nat. Rev. Drug Discov* **4**, 298–306 (2005).
7. Jameel, F. & Hershenson, S. *Formulation and process development strategies for manufacturing biopharmaceuticals* (John Wiley & Sons, 2010).
8. Watson, J. D. & Crick, F. H. C. Molecular structure of nucleic acids. *Resonance* **9**, 96–98 (2004).
9. Cohen, S. N., Chang, A. C., Boyer, H. W. & Helling, R. B. Construction of biologically functional bacterial plasmids in vitro. *PNAS* **70**, 3240–3244 (1973).

10. Hermeling, S., Crommelin, D. J., Schellekens, H. & Jiskoot, W. Structure-immunogenicity relationships of therapeutic proteins. *Pharm. Res.* **21**, 897–903 (2004).
11. Walsh, G. & Murphy, B. *Biopharmaceuticals, an industrial perspective* (Springer Science & Business Media, 2013).
12. Dingermann, T. Recombinant therapeutic proteins: Production platforms and challenges. *Biotechnol. J.* **3**, 90–97 (2008).
13. EvaluatePharma. *World Preview 2015, Outlook to 2020* <http://info.evaluategroup.com/rs/607-YGS-364/images/wp15.pdf>. [Online; accessed 12/2016].
14. Strohl, W. R. & Knight, D. M. Discovery and development of biopharmaceuticals: Current issues. *Curr. Opin. Biotechnol.* **20**, 668–672 (2009).
15. Otto, R., Santagostino, A. & Schrader, U. *From Science to Operations: Questions, Choices, and Strategies for Success in Biopharma* (McKinsey & Company, New York, 2014).
16. Wurm, F. M. Production of recombinant protein therapeutics in cultivated mammalian cells. *Nat. Biotechnol.* **22**, 1393–1398 (2004).
17. Peraman, R., Bhadraya, K. & Padmanabha Reddy, Y. Analytical quality by design: A tool for regulatory flexibility and robust analytics. *Int. J. Anal. Chem.* **2015** (2015).
18. Schiestl, M., Stangler, T., Torella, C., Cepeljnik, T., Toll, H. & Grau, R. Acceptable changes in quality attributes of glycosylated biopharmaceuticals. *Nat. Biotechnol.* **29**, 310–313 (2011).
19. Lawrence, X. Pharmaceutical quality by design: product and process development, understanding, and control. *Pharm. Res.* **25**, 781–791 (2008).
20. Branden, C. *et al.* *Introduction to protein structure* (Garland Science, 1999).
21. Berg, J., Tymoczko, J. & Stryer, L. in (WH Freeman New York, 2002).
22. Pace, C. N., Shirley, B. A., McNutt, M. & Gajiwala, K. Forces contributing to the conformational stability of proteins. *The FASEB journal* **10**, 75–83 (1996).
23. Von Hippel, P. H. & Wong, K. Y. On the conformational stability of globular proteins. *The Journal of Biological Chemistry* **240**, 3909–3923 (1965).
24. Munson, M., Balasubramanian, S., Fleming, K. G., Nagi, A. D., O'Brien, R., Sturtevant, J. M. & Regan, L. What makes a protein a protein? Hydrophobic core designs that specify stability and structural properties. *Protein Science* **5**, 1584–1593 (1996).

-
25. Chi, E. Y., Krishnan, S., Randolph, T. W. & Carpenter, J. F. Physical stability of proteins in aqueous solution: Mechanism and driving forces in nonnative protein aggregation. *Pharm. Res.* **20**, 1325–1336 (2003).
 26. Dong, A., Prestrelski, S. J., Allison, S. D. & Carpenter, J. F. Infrared spectroscopic studies of lyophilization-and temperature-induced protein aggregation. *J. Pharm. Sci.* **84**, 415–424 (1995).
 27. Wang, W. & Roberts, C. J. *Aggregation of therapeutic proteins* (John Wiley & Sons, 2010).
 28. Kumar, S. & Nussinov, R. Close-range electrostatic interactions in proteins. *Chem-BioChem* **3**, 604–617 (2002).
 29. Rose, G. D., Geselowitz, A. R., Lesser, G. J., Lee, R. H. & Zehfus, M. H. Hydrophobicity of amino acid residues in globular proteins. *Science* **229**, 834–839 (1985).
 30. Skoog, B. & Wichman, A. Calculation of the isoelectric points of polypeptides from the amino acid composition. *Trac-Trends in Analytical Chemistry* **5**, 82–83 (1986).
 31. Hendsch, Z. S. & Tidor, B. Do salt bridges stabilize proteins? A continuum electrostatic analysis. *Protein Science* **3**, 211–226 (1994).
 32. Petsko, G. A. & Ringe, D. *Protein structure and function* (New Science Press, 2004).
 33. Schmitt, L. Biochemie. Eine Einführung für Mediziner und Naturwissenschaftler. Von Werner Müller-Esterl. *Angewandte Chemie* **117**, 4025–4025 (2005).
 34. Teague, S. J. Implications of protein flexibility for drug discovery. *Nat. Rev. Drug Discov.* **2**, 527–541 (2003).
 35. Teilum, K., Olsen, J. G. & Kragelund, B. B. Functional aspects of protein flexibility. *Cellular and Molecular Life Sciences* **66**, 2231 (2009).
 36. Derjaguin, B. v. & Landau, L. Theory of the stability of strongly charged lyophobic sols and the adhesion of strongly charged particles in solutions of electrolytes. *Acta Physicochim. USSR* **14**, 633–662 (1941).
 37. Overbeek, J. T. G. & Verwey, E. *Theory of the Stability of Lyophobic Colloids: The interaction of Sol Particles Having an Electric Double Layer* (Elsevier, New York, 1948).

38. Derjaguin, B. v. & Landau, L. Theory of the stability of strongly charged lyophobic sols and of the adhesion of strongly charged particles in solutions of electrolytes. *Progress in Surface Science* **43**, 30–59 (1993).
39. Harvey, S. C. Treatment of electrostatic effects in macromolecular modeling. *Proteins: Structure, Function, and Bioinformatics* **5**, 78–92 (1989).
40. Schubert, H. Grundlagen des Agglomerierens. *Chemie Ingenieur Technik* **51**, 266–277 (1979).
41. Parsegian, V. A. *Van der Waals forces: A handbook for biologists, chemists, engineers, and physicists* (Cambridge University Press, 2005).
42. Pfeifer-Lehmann, O. *Untersuchung der Adhäsionskräfte in interaktiven Pulvermischungen zur Inhalation und deren Veränderung in Abhängigkeit von der Dichtigkeit der Verpackung* PhD thesis (Johannes Gutenberg-Universität Mainz, 2010).
43. Israelachvili, J. N. *Intermolecular and surface forces* (Academic press, 2015).
44. Chiew, Y., Kuehner, D., Blanch, H. & Prausnitz, J. Molecular thermodynamics for salt-induced protein precipitation. *AIChE Journal* **41**, 2150–2159 (1995).
45. Lund, M. & Jönsson, B. A mesoscopic model for protein-protein interactions in solution. *Biophys. J.* **85**, 2940–2947 (2003).
46. Flickinger, M. C. *Downstream industrial biotechnology: Recovery and purification* (John Wiley & Sons, 2013).
47. Saluja, A. & Kalonia, D. S. Nature and consequences of protein-protein interactions in high protein concentration solutions. *Int. J. Pharm.* **358**, 1–15 (2008).
48. Hu, X., Cebe, P., Weiss, A. S., Omenetto, F. & Kaplan, D. L. Protein-based composite materials. *Materials Today* **15**, 208–215 (2012).
49. Leckband, D. & Sivasankar, S. Forces controlling protein interactions: Theory and experiment. *Colloids and surfaces B: Biointerfaces* **14**, 83–97 (1999).
50. Israelachvili, J. & Pashley, R. The hydrophobic interaction is long range, decaying exponentially with distance. *Nature* **300**, 341–342 (1982).
51. Scopes, R. K. *Protein purification: Principles and practice* (Springer Science & Business Media, 2013).
52. Roth, C. M., Neal, B. L. & Lenhoff, A. M. Van der Waals interactions involving proteins. *Biophys. J.* **70**, 977–987 (1996).

-
53. Galm, L., Amrhein, S. & Hubbuch, J. Predictive approach for protein aggregation: Correlation of protein surface characteristics and conformational flexibility to protein aggregation propensity. *Biotechnol. Bioeng.* **114**, 1170–1183 (2017).
 54. Jiang, L., Gao, Y., Mao, F., Liu, Z. & Lai, L. Potential of mean force for protein–protein interaction studies. *Proteins: Structure, Function, and Bioinformatics* **46**, 190–196 (2002).
 55. Liu, S., Zhang, C., Zhou, H. & Zhou, Y. A physical reference state unifies the structure-derived potential of mean force for protein folding and binding. *Proteins: Structure, Function, and Bioinformatics* **56**, 93–101 (2004).
 56. Remington, J. P. *Remington: The science and practice of pharmacy* (Lippincott Williams & Wilkins, 2006).
 57. George, M. & Abraham, T. E. Polyionic hydrocolloids for the intestinal delivery of protein drugs: Alginate and chitosan—a review. *Journal of controlled release* **114**, 1–14 (2006).
 58. Bailon, P. & Berthold, W. Polyethylene glycol-conjugated pharmaceutical proteins. *Pharm. Sci. Technol. Today* **1**, 352–356 (1998).
 59. Rosenberg, A. S. Effects of protein aggregates: An immunologic perspective. *The AAPS journal* **8**, E501–E507 (2006).
 60. Manning, M. C., Chou, D. K., Murphy, B. M., Payne, R. W. & Katayama, D. S. Stability of protein pharmaceuticals: An update. *Pharm. Res.* **27**, 544–575 (2010).
 61. Berkowitz, S. A., Engen, J. R., Mazzeo, J. R. & Jones, G. B. Analytical tools for characterizing biopharmaceuticals and the implications for biosimilars. *Nat. Rev. Drug Discov.* **11**, 527 (2012).
 62. Anfinsen, C. B. Principles that govern the folding of protein chains. *Science* **181**, 223–230 (1973).
 63. Lumry, R., Biltonen, R. & Brandts, J. F. Validity of the “two-state” hypothesis for conformational transitions of proteins. *Biopolymers* **4**, 917–944 (1966).
 64. Shaw, K. L., Scholtz, J. M., Pace, C. N. & Grimsley, R. G. Determining the conformational stability of a protein using urea denaturation curves. *Protein Structure, Stability, and Interactions* **490**, 41–55 (2009).
 65. Brady, G. P. & Sharp, K. A. Entropy in protein folding and in protein–protein interactions. *Current opinion in structural biology* **7**, 215–221 (1997).

66. Hilser, V. J., Gómez, J. & Freire, E. The enthalpy change in protein folding and binding: Refinement of parameters for structure-based calculations. *Proteins: Structure, Function, and Bioinformatics* **26**, 123–133 (1996).
67. Rees, D. C. & Robertson, A. D. Some thermodynamic implications for the thermostability of proteins. *Protein Science* **10**, 1187–1194 (2001).
68. Vivian, J. T. & Callis, P. R. Mechanisms of tryptophan fluorescence shifts in proteins. *Biophys. J.* **80**, 2093–2109 (2001).
69. Baumgartner, K., Großhans, S., Schütz, J., Suhm, S. & Hubbuch, J. Prediction of salt effects on protein phase behavior by HIC retention and thermal stability. *Journal of pharmaceutical and biomedical analysis* **128**, 216–225 (2016).
70. Ambrose, E. & Elliott, A. The structure of synthetic polypeptides. II. Investigation with polarized infra-red spectroscopy. *Proceedings of the Royal Society of London A: Mathematical, Physical and Engineering Sciences* **205**, 47–60 (1951).
71. Ambrose, E. & Elliott, A. Infra-red spectroscopic studies of globular protein structure. *Proceedings of the Royal Society of London A: Mathematical, Physical and Engineering Sciences* **208**, 75–90 (1951).
72. Güldenhaupt, J. *ATR-FTIR-spectroscopic analysis of membrane-bound Ras* PhD thesis (Ruhr-University Bochum, 2010).
73. Barth, A. Infrared spectroscopy of proteins. *Biochimica et Biophysica Acta (BBA)-Bioenergetics* **1767**, 1073–1101 (2007).
74. Jackson, M. & Mantsch, H. H. The use and misuse of FTIR spectroscopy in the determination of protein structure. *Critical reviews in biochemistry and molecular biology* **30**, 95–120 (1995).
75. Pelton, J. T. & McLean, L. R. Spectroscopic methods for analysis of protein secondary structure. *Anal. Biochem.* **277**, 167–176 (2000).
76. Atkins, P. W. & De Paula, J. *Physikalische chemie* (John Wiley & Sons, 2013).
77. Wang, W. Instability, stabilization, and formulation of liquid protein pharmaceuticals. *Int. J. Pharm.* **185**, 129–188 (1999).
78. Asherie, N. Protein crystallization and phase diagrams. *Methods* **34**, 266–272 (2004).

-
79. Baumgartner, K., Galm, L., Nötzold, J., Sigloch, H., Morgenstern, J., Schleining, K., Suhm, S., Oelmeier, S. A. & Hubbuch, J. Determination of protein phase diagrams by microbatch experiments: Exploring the influence of precipitants and pH. *Int. J. Pharm.* **479**, 28–40 (2015).
 80. Ducruix, A. F. & Ries-Kautt, M. M. Solubility diagram analysis and the relative effectiveness of different ions on protein crystal growth. *Methods* **1**, 25–30 (1990).
 81. Mahler, H.-C., Friess, W., Grauschopf, U. & Kiese, S. Protein aggregation: Pathways, induction factors and analysis. *J. Pharm. Sci.* **98**, 2909–2934 (2009).
 82. Philo, J. S. & Arakawa, T. Mechanisms of protein aggregation. *Current pharmaceutical biotechnology* **10**, 348–351 (2009).
 83. Faber, C. *Measurement and Prediction of Protein Phase Behaviour and Protein-Protein Interactions* PhD thesis (Technical University of Denmark, 2006).
 84. Middaugh, C. R., Tisel, W. A., Haire, R. N. & Rosenberg, A. Determination of the apparent thermodynamic activities of saturated protein solutions. *Journal of Biological Chemistry* **254**, 367–370 (1979).
 85. Boistelle, R. & Astier, J. Crystallization mechanisms in solution. *Journal of Crystal Growth* **90**, 14–30 (1988).
 86. Garcia-Ruiz, J. M. Nucleation of protein crystals. *Journal of structural biology* **142**, 22–31 (2003).
 87. Panchenko, A. & Przytycka, T. *Protein-protein Interactions and Networks: Identification, Computer Analysis, and Prediction* (Springer Science, 2008).
 88. Cromwell, M., Hilario, E. & Jacobson, F. Protein aggregation and bioprocessing. *The AAPS journal* **8**, E572–E579 (2006).
 89. Fink, A. L. Protein aggregation: Folding aggregates, inclusion bodies and amyloid. *Folding and design* **3**, R9–R23 (1998).
 90. Roberts, C. J. Non-native protein aggregation kinetics. *Biotechnol. Bioeng.* **98**, 927–938 (2007).
 91. Treuheit, M. J., Kosky, A. A. & Brems, D. N. Inverse relationship of protein concentration and aggregation. *Pharm. Res.* **19**, 511–516 (2002).
 92. Jezek, J., Rides, M., Derham, B., Moore, J., Cerasoli, E., Simler, R. & Perez-Ramirez, B. Viscosity of concentrated therapeutic protein compositions. *Advanced drug delivery reviews* **63**, 1107–1117 (2011).

93. Van Oss, C. Hydrophobicity of biosurfaces—origin, quantitative determination and interaction energies. *Colloids and Surfaces B: Biointerfaces* **5**, 91–110 (1995).
94. Kumar, V., Dixit, N., Zhou, L. L. & Fraunhofer, W. Impact of short range hydrophobic interactions and long range electrostatic forces on the aggregation kinetics of a monoclonal antibody and a dual-variable domain immunoglobulin at low and high concentrations. *Int. J. Pharm.* **421**, 82–93 (2011).
95. Minton, A. P. The effect of volume occupancy upon the thermodynamic activity of proteins: Some biochemical consequences. *Molecular and cellular biochemistry* **55**, 119–140 (1983).
96. Kuznetsova, I. M., Zaslavsky, B. Y., Breydo, L., Turoverov, K. K. & Uversky, V. N. Beyond the excluded volume effects: Mechanistic complexity of the crowded milieu. *Molecules* **20**, 1377–1409 (2015).
97. Pegram, L. M., Wendorff, T., Erdmann, R., Shkel, I., Bellissimo, D., Felitsky, D. J. & Record, M. T. Why Hofmeister effects of many salts favor protein folding but not DNA helix formation. *PNAS* **107**, 7716–7721 (2010).
98. Zhao, H. Protein stabilization and enzyme activation in ionic liquids: Specific ion effects. *J. Chem. Technol. Biotechnol.* **91**, 25–50 (2016).
99. Tsumoto, K., Ejima, D., Senczuk, A. M., Kita, Y. & Arakawa, T. Effects of salts on protein–surface interactions: Applications for column chromatography. *J. Pharm. Sci.* **96**, 1677–1690 (2007).
100. Kunz, W., Henle, J. & Ninham, B. W. 'Zur Lehre von der Wirkung der Salze' (about the science of the effect of salts): Franz Hofmeister's historical papers. *Current Opinion in Colloid & Interface Science* **9**, 19–37 (2004).
101. Arakawa, T. & Timasheff, S. N. Mechanism of protein salting in and salting out by divalent cation salts: Balance between hydration and salt binding. *Biochemistry* **23**, 5912–5923 (1984).
102. Arakawa, T. Hydration as a Major Factor in Preferential Solvent- Protein Interactions. *Cryst. Growth Des.* **2**, 549–551 (2002).
103. Sawyer, W. H. & Puckridge, J. The dissociation of proteins by chaotropic salts. *Journal of Biological Chemistry* **248**, 8429–8433 (1973).
104. Myerson, A. *Handbook of industrial crystallization* (Butterworth-Heinemann, 2002).

-
105. Wiendahl, M., Völker, C., Husemann, I., Krarup, J., Staby, A., Scholl, S. & Hubbuch, J. A novel method to evaluate protein solubility using a high throughput screening approach. *Chemical Engineering Science* **64**, 3778–3788 (2009).
 106. Trevino, S. R., Scholtz, J. M. & Pace, C. N. Measuring and increasing protein solubility. *J. Pharm. Sci.* **97**, 4155–4166 (2008).
 107. Berg, A., Schuetz, M., Dismar, F. & Hubbuch, J. Automated measurement of apparent protein solubility to rapidly assess complex parameter interactions. *Food and Bioproducts Processing* **92**, 133–142 (2014).
 108. Liang, K., Ricco, R., Doherty, C. M., Styles, M. J., Bell, S., Kirby, N., Mudie, S., Haylock, D., Hill, A. J. & Doonan, C. J. Biomimetic mineralization of metal-organic frameworks as protective coatings for biomacromolecules. *Nature communications* **6**, 1–8 (2015).
 109. Trevino, S. R., Scholtz, J. M. & Pace, C. N. Amino acid contribution to protein solubility: Asp, Glu, and Ser contribute more favorably than the other hydrophilic amino acids in RNase Sa. *Journal of molecular biology* **366**, 449–460 (2007).
 110. Hamada, H., Arakawa, T. & Shiraki, K. Effect of additives on protein aggregation. *Current pharmaceutical biotechnology* **10**, 400–407 (2009).
 111. Ohtake, S., Kita, Y. & Arakawa, T. Interactions of formulation excipients with proteins in solution and in the dried state. *Advanced drug delivery reviews* **63**, 1053–1073 (2011).
 112. Yancey, P. H., Clark, M. E., Hand, S. C., Bowlus, R. D. & Somero, G. N. Living with water stress: Evolution of osmolyte systems. *Science* **217**, 1214–1222 (1982).
 113. Yancey, P. H. Water Stress, Osmolytes and Proteins. *American Zoologist* **41**, 699–709 (2001).
 114. Bolen, D. W. Protein stabilization by naturally occurring osmolytes. *Protein structure, stability, and folding* **168**, 17–36 (2001).
 115. Arakawa, T. & Timasheff, S. Stabilization of protein structure by sugars. *Biochemistry* **21**, 6536–6544 (1982).
 116. Arakawa, T. & Timasheff, S. The stabilization of proteins by osmolytes. *Biophys. J.* **47**, 411–414 (1985).
 117. Auton, M., Bolen, D. W. & Rösgen, J. Structural thermodynamics of protein preferential solvation: Osmolyte solvation of proteins, aminoacids, and peptides. *Proteins: Structure, Function, and Bioinformatics* **73**, 802–813 (2008).

118. Collins, K. D. Ions from the Hofmeister series and osmolytes: Effects on proteins in solution and in the crystallization process. *Methods* **34**, 300–311 (2004).
119. Golovanov, A. P., Hautbergue, G. M., Wilson, S. A. & Lian, L.-Y. A simple method for improving protein solubility and long-term stability. *Journal of the American Chemical Society* **126**, 8933–8939 (2004).
120. Mitragotri, S., Burke, P. A. & Langer, R. Overcoming the challenges in administering biopharmaceuticals: Formulation and delivery strategies. *Nat. Rev. Drug Discov.* **13**, 655–672 (2014).
121. Polson, A., Potgieter, G., Largier, J., Mears, G. & Joubert, F. The fractionation of protein mixtures by linear polymers of high molecular weight. *Biochimica et Biophysica Acta (BBA)-General Subjects* **82**, 463–475 (1964).
122. Atha, D. H. & Ingham, K. C. Mechanism of precipitation of proteins by polyethylene glycols. Analysis in terms of excluded volume. *J. Biol. Chem.* **256**, 12108–12117 (1981).
123. Kumar, V., Sharma, V. K. & Kalonia, D. S. Effect of polyols on polyethylene glycol (PEG)-induced precipitation of proteins: Impact on solubility, stability and conformation. *Int. J. Pharm.* **366**, 38–43 (2009).
124. Katre, N. V. The conjugation of proteins with polyethylene glycol and other polymers: Altering properties of proteins to enhance their therapeutic potential. *Advanced Drug Delivery Reviews* **10**, 91–114 (1993).
125. Seyfried, B. K., Marchetti-Deschmann, M., Siekmann, J., Bard, M. J., Scheiflinger, F., Turecek, P. L. & Allmaier, G. Microchip capillary gel electrophoresis of multiply PEGylated high-molecular-mass glycoproteins. *Biotechnol. J.* **7**, 635–641 (2012).
126. Pelegri-O'Day, E. M., Lin, E.-W. & Maynard, H. D. Therapeutic protein-polymer conjugates: Advancing beyond PEGylation. *Journal of the American Chemical Society* **136**, 14323–14332 (2014).
127. Thordarson, P., Le Droumaguet, B. & Velonia, K. Well-defined protein–polymer conjugates—synthesis and potential applications. *Applied microbiology and biotechnology* **73**, 243 (2006).
128. Jung, B. & Theato, P. Chemical strategies for the synthesis of protein–polymer conjugates. *Bio-synthetic polymer conjugates*, 37–70 (2012).

-
129. Pasut, G. & Veronese, F. State of the art in PEGylation: the great versatility achieved after forty years of research. *Journal of Controlled Release* **161**, 461–472 (2012).
 130. Fee, C. J. & Van Alstine, J. M. PEG-proteins: Reaction engineering and separation issues. *Chemical engineering science* **61**, 924–939 (2006).
 131. Tsutsumi, Y., Onda, M., Nagata, S., Lee, B., Kreitman, R. J. & Pastan, I. Site-specific chemical modification with polyethylene glycol of recombinant immunotoxin anti-Tac (Fv)-PE38 (LMB-2) improves antitumor activity and reduces animal toxicity and immunogenicity. *PNAS* **97**, 8548–8553 (2000).
 132. Dozier, J. K. & Distefano, M. D. Site-specific PEGylation of therapeutic proteins. *International journal of molecular sciences* **16**, 25831–25864 (2015).
 133. Abuchowski, A., McCoy, J., Palczuk, N., van Es, T. & Davis, F. Effect of covalent attachment of polyethylene glycol on immunogenicity and circulating life of bovine liver catalase. *J. Biol. Chem.* **252**, 3582–3586 (1977).
 134. Abuchowski, A., van Es, T., Palczuk, N. C. & Davis, F. F. Alteration of Immunological Properties of Bovine Serum Albumin by Covalent Attachment of Polyethylene Glycol. *Journal of Biological Chemistry* **252**, 3578–3581 (1977).
 135. Knop, K., Hoogenboom, R., Fischer, D. & Schubert, U. S. Poly (ethylene glycol) in drug delivery: Pros and cons as well as potential alternatives. *Angewandte Chemie International Edition* **49**, 6288–6308 (2010).
 136. Jevševar, S., Kunstelj, M. & Porekar, V. G. PEGylation of therapeutic proteins. *Biotechnol. J.* **5**, 113–128 (2010).
 137. Turecek, P. L., Bossard, M. J., Schoetens, F. & Ivens, I. A. PEGylation of biopharmaceuticals: A review of chemistry and nonclinical safety information of approved drugs. *J. Pharm. Sci.* **105**, 460–475 (2016).
 138. Ryan, S. M., Mantovani, G., Wang, X., Haddleton, D. M. & Brayden, D. J. Advances in PEGylation of important biotech molecules: Delivery aspects. *Expert opinion on drug delivery* **5**, 371–383 (2008).
 139. Fee, C. J. & Van Alstine, J. M. Prediction of the viscosity radius and the size exclusion chromatography behavior of PEGylated proteins. *Bioconjugate chemistry* **15**, 1304–1313 (2004).
 140. Fee, C. J. Size comparison between proteins PEGylated with branched and linear poly (ethylene glycol) molecules. *Biotechnol. Bioeng.* **98**, 725–731 (2007).

141. Cunningham-Rundles, C., Zhuo, Z., Griffith, B. & Keenan, J. Biological activities of polyethylene-glycol immunoglobulin conjugates resistance to enzymatic degradation. *Journal of immunological methods* **152**, 177–190 (1992).
142. Harris, J. M. & Chess, R. B. Effect of PEGylation on pharmaceuticals. *Nat. Rev. Drug Discov.* **2**, 214–221 (2003).
143. Nfor, B. K., Verhaert, P. D., van der Wielen, L. A. M., Hubbuch, J. & Ottens, M. Rational and systematic protein purification process development: The next generation. *Trends Biotechnol.* **27**, 673–679 (2009).
144. Zhang, F., Liu, M.-R. & Wan, H.-T. Discussion about several potential drawbacks of PEGylated therapeutic proteins. *Biological and Pharmaceutical Bulletin* **37**, 335–339 (2014).
145. Lutz, J.-F. Polymerization of oligo (ethylene glycol)(meth) acrylates: Toward new generations of smart biocompatible materials. *Journal of Polymer Science Part A: Polymer Chemistry* **46**, 3459–3470 (2008).
146. Chiefari, J., Chong, Y., Ercole, F., Krstina, J., Jeffery, J., Le, T., Mayadunne, R., Meijs, G., Moad, C. & Moad, G. Living free-radical polymerization by reversible addition- fragmentation chain transfer: The RAFT process. *Macromolecules* **31**, 5559–5562 (1998).
147. Brocchini, S. in *Polymeric Drug Delivery Techniques - Translating Polymer Science for Drug Delivery* (Sigma Aldrich Materials Science).
148. Shu, J. Y., Panganiban, B. & Xu, T. Peptide-polymer conjugates: From fundamental science to application. *Annual review of physical chemistry* **64**, 631–657 (2013).
149. Seely, J. E. & Richey, C. W. Use of ion-exchange chromatography and hydrophobic interaction chromatography in the preparation and recovery of polyethylene glycol-linked proteins. *J. Chromatogr. A* **908**, 235–241 (2001).
150. Abe, M., Akbarzaderaleh, P., Hamachi, M., Yoshimoto, N. & Yamamoto, S. Interaction mechanism of mono-PEGylated proteins in electrostatic interaction chromatography. *Biotechnol. J.* **5**, 477–483 (2010).
151. Schmidt-Traub, H., Schulte, M. & Seidel-Morgenstern, A. *Preparative Chromatography* 291 (WILEY-VCH, 2012).

-
152. Piatkowski, W., Antos, D. & Kaczmarski, K. Modeling of preparative chromatography processes with slow intraparticle mass transport kinetics. *J. Chrom. A* **988**, 219–231 (2003).
 153. Guiochon, G., Felinger, A. & Shirazi, D. *Fundamentals of preparative and nonlinear chromatography* (Academic Press, 2006).
 154. Wang, G., Hahn, T. & Hubbuch, J. Water on hydrophobic surfaces: Mechanistic modeling of hydrophobic interaction. *J. Chrom. A* **1465**, 71–78 (2016).
 155. Brooks, C. A. & Cramer, S. M. Steric mass-action ion exchange: Displacement profiles and induced salt gradients. *AIChE Journal* **38**, 1969–1978 (1992).
 156. Jakobsson, N., Karlsson, D., Axelsson, J. P., Zacchi, G. & Nilsson, B. Using computer simulation to assist in the robustness analysis of an ion-exchange chromatography step. *J. Chromatogr. A* **1063**, 99–109 (2005).
 157. Huuk, T., Briskot, T., Hahn, T. & Hubbuch, J. A versatile noninvasive method for adsorber quantification in batch and column chromatography based on the ionic capacity. *Biotechnol. Progr.* **32**, 666–677 (2016).
 158. Hahn, T., Huuk, T., Heuveline, V. & Hubbuch, J. Simulating and Optimizing Preparative Protein Chromatography with ChromX. *J. Chem. Educ.* **92**, 1497–1502 (2015).
 159. Webster, J. G. & Hendee, W. R. *Encyclopedia of Medical Devices and Instrumentation, Volumes 1–4* (AIP, 1989).
 160. Kim, S. W., Bae, Y. H. & Okano, T. Hydrogels: Swelling, drug loading, and release. *Pharm. Res.* **9**, 283–290 (1992).
 161. Peppas, N. A., Bures, P., Leobandung, W. S. & Ichikawa, H. Hydrogels in pharmaceutical formulations. *European journal of pharmaceuticals and biopharmaceutics* **50**, 27–46 (2000).
 162. Langer, R. & Tirrell, D. A. Designing materials for biology and medicine. *Nature* **428**, 487–492 (2004).
 163. Liechty, W. B., Kryscio, D. R., Slaughter, B. V. & Peppas, N. A. Polymers for drug delivery systems. *Annual review of chemical and biomolecular engineering* **1**, 149–173 (2010).
 164. Peppas, N. & Korsmeyer, R. Dynamically swelling hydrogels in controlled release applications. *Hydrogels in medicine and pharmacy* **3**, 109–136 (1987).

165. Hoare, T. R. & Kohane, D. S. Hydrogels in drug delivery: Progress and challenges. *Polymer* **49**, 1993–2007 (2008).
166. Ahmed, E. Hydrogel: Preparation, characterization, and applications: A review. *JAR* **6**, 105–121 (2015).
167. Mellott, M. B., Searcy, K. & Pishko, M. V. Release of protein from highly cross-linked hydrogels of poly (ethylene glycol) diacrylate fabricated by UV polymerization. *Biomaterials* **22**, 929–941 (2001).
168. Gombotz, W. R. & Pettit, D. K. Biodegradable polymers for protein and peptide drug delivery. *Bioconjugate chemistry* **6**, 332–351 (1995).
169. Lin, C.-C. & Anseth, K. S. PEG hydrogels for the controlled release of biomolecules in regenerative medicine. *Pharm. Res.* **26**, 631–643 (2009).
170. Sharpe, L. A., Daily, A. M., Horava, S. D. & Peppas, N. A. Therapeutic applications of hydrogels in oral drug delivery. *Expert opinion on drug delivery* **11**, 901–915 (2014).
171. Yang, J. *Stent having cover with drug delivery capability* US Patent 6,379,382. 04/2002.
172. Murphy, S. V., Skardal, A. & Atala, A. Evaluation of hydrogels for bio-printing applications. *Journal of Biomedical Materials Research Part A* **101**, 272–284 (2013).
173. Malda, J., Visser, J., Melchels, F. P., Jüngst, T., Hennink, W. E., Dhert, W., Groll, J. & Hutmacher, D. W. 25th anniversary article: Engineering hydrogels for biofabrication. *Advanced materials* **25**, 5011–5028 (2013).
174. Gross, B., Erkal, J., Lockwood, S., Chen, C. & Spence, D. Evaluation of 3D printing and its potential impact on biotechnology and the chemical sciences. *Anal. Chem.* **86**, 3240–3253 (2014).
175. Murphy, S. V. & Atala, A. 3D bioprinting of tissues and organs. *Nat. Biotechnol.* **32**, 773–785 (2014).
176. Yu, D. G., Zhu, L.-M., Branford-White, C. J. & Yang, X. L. Three-dimensional printing in pharmaceuticals: Promises and problems. *J. Pharm. Sci.* **97**, 3666–3690 (2008).
177. Goole, J. & Amighi, K. 3D printing in pharmaceuticals: A new tool for designing customized drug delivery systems. *Int. J. Pharm.* **499**, 376–394 (2016).

-
178. Rengier, F., Mehndiratta, A., von Tengg-Kobligk, H., Zechmann, C. M., Unterhinninghofen, R., Kauczor, H.-U. & Giesel, F. L. 3D printing based on imaging data: Review of medical applications. *International journal of computer assisted radiology and surgery* **5**, 335–341 (2010).
179. Dababneh, A. B. & Ozbolat, I. T. Bioprinting technology: A current state-of-the-art review. *Journal of Manufacturing Science and Engineering* **136**, 061016 (2014).
180. Jean-Pierre, F. in (Gardner Publications, Inc., Cincinnati, 1995).
181. Melchels, F., Feijen, J. & Grijpma, D. W. A review on stereolithography and its applications in biomedical engineering. *Biomaterials* **31**, 6121–6130 (2010).
182. B9Creations. *B9Creator Technology* <https://www.b9c.com/media/files/Brochures/b9creator-brochure.pdf>. [Online; accessed 07/2017].
183. Yañez-Soto, B., Liliensiek, S., Murphy, C. & Nealey, P. Biochemically and topographically engineered poly (ethylene glycol) diacrylate hydrogels with biomimetic characteristics as substrates for human corneal epithelial cells. *Journal of biomedical materials research Part A* **101**, 1184–1194 (2013).
184. Roberts, C. J. Therapeutic protein aggregation: Mechanisms, design, and control. *Trends in biotechnology* **32**, 372–380 (2014).
185. Shire, S. J., Shahrokh, Z. & Liu, J. Challenges in the development of high protein concentration formulations. *J. Pharm. Sci.* **93**, 1390–1402 (2004).
186. Agrawal, N., Kumar, S., Wang, X., Helk, B., Singh, S. & Trout, B. Aggregation in protein-based biotherapeutics: Computational studies and tools to identify aggregation-prone regions. *J. Pharm. Sci.* **100**, 5081–5095 (2011).
187. Veronese, F. M. & Pasut, G. PEGylation, successful approach to drug delivery. *Drug Discovery Today* **10**, 1451–1458 (2005).
188. Carta, G. & Jungbauer, A. *Protein Chromatography Process Development and Scale-up* (WILEY-VCH, 2010).
189. Scopes, R. K. in *Protein Purification* 41–71 (Springer, 1987).
190. Basu, S. K., Govardhan, C. P., Jung, C. W. & Margolin, A. L. Protein crystals for the delivery of biopharmaceuticals. *Expert. Opin. Biol. Ther.* **4**, 301–317 (2004).
191. Jen, A. & Merkle, H. P. Diamonds in the rough: Protein crystals from a formulation perspective. *Pharm. Res.* **18**, 1483–1488 (2001).
192. Brange, J. & Vølund, A. Insulin analogs with improved pharmacokinetic profiles. *Advanced drug delivery reviews* **35**, 307–335 (1999).

193. Vajo, Z., Fawcett, J. & Duckworth, W. C. Recombinant DNA technology in the treatment of diabetes: Insulin analogs. *Endocrine reviews* **22**, 706–717 (2001).
194. Yang, M. X., Shenoy, B., Disttler, M., Patel, R., McGrath, M., Pechenov, S. & Margolin, A. L. Crystalline monoclonal antibodies for subcutaneous delivery. *PNAS* **100**, 6934–6939 (2003).
195. Dzwolak, W., Ravindra, R., Lendermann, J. & Winter, R. Aggregation of bovine insulin probed by DSC/PPC calorimetry and FTIR spectroscopy. *Biochemistry* **42**, 11347–11355 (2003).
196. Feng, Y. W., Ooishi, A. & Honda, S. Aggregation factor analysis for protein formulation by a systematic approach using FTIR, SEC and design of experiments techniques. *Journal of pharmaceutical and biomedical analysis* **57**, 143–152 (2012).
197. Kendrick, B. S., Cleland, J. L., Lam, X., Nguyen, T., Randolph, T. W., Manning, M. C. & Carpenter, J. F. Aggregation of recombinant human interferon gamma: Kinetics and structural transitions. *J. Pharm. Sci.* **87**, 1069–1076 (1998).
198. Matheus, S., Friess, W., Schwartz, D. & Mahler, H.-C. Liquid high concentration IgG1 antibody formulations by precipitation. *J. Pharm. Sci.* **98**, 3043–3057 (2009).
199. Harries, D. & Rösgen, J. A practical guide on how osmolytes modulate macromolecular properties. *Methods in cell biology* **84**, 679–735 (2008).
200. Arakawa, T. & Timasheff, S. N. Preferential interactions of proteins with solvent components in aqueous amino acid solutions. *Arch. Biochem. Biophys.* **224**, 169–177 (1983).
201. Arakawa, T. & Timasheff, S. N. Mechanism of polyethylene glycol interaction with proteins. *Biochemistry* **24**, 6756–6762 (1985).
202. Lee, J. & Lee, L. Preferential solvent interactions between proteins and polyethylene glycols. *Journal of Biological Chemistry* **256**, 625–631 (1981).
203. Timasheff, S. N. & Arakawa, T. Mechanism of protein precipitation and stabilization by co-solvents. *Journal of Crystal Growth* **90**, 39–46 (1988).
204. Webb, J. N., Webb, S. D., Cleland, J. L., Carpenter, J. F. & Randolph, T. W. Partial molar volume, surface area, and hydration changes for equilibrium unfolding and formation of aggregation transition state: High-pressure and cosolute studies on recombinant human IFN-gamma. *PNAS* **98**, 7259–7264 (2001).

-
205. Santoro, M. M., Liu, Y., Khan, S. M., Hou, L. X. & Bolen, D. Increased thermal stability of proteins in the presence of naturally occurring osmolytes. *Biochemistry* **31**, 5278–5283 (1992).
206. Poddar, N., Ansari, Z., Singh, R., Moosavi-Movahedi, A. & Ahmad, F. Effect of monomeric and oligomeric sugar osmolytes on ΔG_D , the Gibbs energy of stabilization of the protein at different pH values: Is the sum effect of monosaccharide individually additive in a mixture? *Biophys. Chem.* **138**, 120–129 (2008).
207. Singh, L. R., Poddar, N. K., Dar, T., Kumar, R. & Ahmad, F. Protein and DNA destabilization by osmolytes: The other side of the coin. *Life sciences* **88**, 117–125 (2011).
208. Macchi, F., Eisenkolb, M., Kiefer, H. & Otzen, D. E. The effect of osmolytes on protein fibrillation. *International journal of molecular sciences* **13**, 3801–3819 (2012).
209. Granata, V., Palladino, P., Tizzano, B., Negro, A., Berisio, R. & Zagari, A. The effect of the osmolyte trimethylamine N-oxide on the stability of the prion protein at low pH. *Biopolymers* **82**, 234–240 (2006).
210. Natalello, A., Liu, J., Ami, D., Doglia, S. M. & de Marco, A. The osmolyte betaine promotes protein misfolding and disruption of protein aggregates. *Proteins: Structure, Function, and Bioinformatics* **75**, 509–517 (2009).
211. Singh, L. R., Dar, T. A., Rahman, S., Jamal, S. & Ahmad, F. Glycine betaine may have opposite effects on protein stability at high and low pH values. *Biochimica et Biophysica Acta (BBA)-Proteins and Proteomics* **1794**, 929–935 (2009).
212. Kaushik, J. K. & Bhat, R. Why is trehalose an exceptional protein stabilizer? An analysis of the thermal stability of proteins in the presence of the compatible osmolyte trehalose. *Journal of Biological Chemistry* **278**, 26458–26465 (2003).
213. Howard, S. B., Twigg, P. J., Baird, J. K. & Meehan, E. J. The solubility of hen egg-white lysozyme. *Journal of Crystal Growth* **90**, 94–104 (1988).
214. Retailleau, P., Ries-Kautt, M. & Ducruix, A. No salting-in of lysozyme chloride observed at low ionic strength over a large range of pH. *Biophys. J.* **73**, 2156–2163 (1997).
215. Cohn, E. The physical chemistry of proteins. *Physiological Reviews* **5**, 349–437 (1925).

216. Zeelen, J. P. Interpretation of the crystallization drop results. *Protein Crystallization Techniques, Strategies, and Tips*, TM Bergfors, Ed. (International University Line, CA, 1999), 131 (2009).
217. McPherson, A. Introduction to protein crystallization. *Methods* **34**, 254–265 (2004).
218. Curtis, R., Prausnitz, J. & Blanch, H. Protein-protein and protein-salt interactions in aqueous protein solutions containing concentrated electrolytes. *Biotechnol. Bioeng.* **57**, 11–21 (1998).
219. Guo, B., Kao, S., McDonald, H., Asanov, A., Combs, L. L. & Wilson, W. W. Correlation of second virial coefficients and solubilities useful in protein crystal growth. *Journal of crystal growth* **196**, 424–433 (1999).
220. Haas, C., Drenth, J. & Wilson, W. W. Relation between the solubility of proteins in aqueous solutions and the second virial coefficient of the solution. *The Journal of Physical Chemistry B* **103**, 2808–2811 (1999).
221. Ruppert, S., Sandler, S. & Lenhoff, A. Correlation between the osmotic second virial coefficient and the solubility of proteins. *Biotechnology progress* **17**, 182–187 (2001).
222. Durbin, S. & Feher, G. Crystal growth studies of lysozyme as a model for protein crystallization. *Journal of Crystal Growth* **76**, 583–592 (1986).
223. Heidner, E. Protein crystallizations: The functional dependence of the nucleation rate on the protein concentration and the solubility. *Journal of Crystal Growth* **44**, 139–144 (1978).
224. Kam, Z., Shore, H. & Feher, G. On the crystallization of proteins. *Journal of molecular biology* **123**, 539–555 (1978).
225. Bruzdzziak, P., Panuszko, A. & Stangret, J. Influence of osmolytes on protein and water structure: A step to understanding the mechanism of protein stabilization. *The Journal of Physical Chemistry B* **117**, 11502–11508 (2013).
226. Auton, M., Rösger, J., Sinev, M., Holthausen, L. M. F. & Bolen, D. W. Osmolyte effects on protein stability and solubility: A balancing act between backbone and side-chains. *Biophys. Chem.* **159**, 90–99 (2011).
227. Bolen, D. & Baskakov, I. V. The osmophobic effect: Natural selection of a thermodynamic force in protein folding. *Journal of molecular biology* **310**, 955–963 (2001).

-
228. Li, Q., Yi, L., Marek, P. & Iverson, B. L. Commercial proteases: Present and future. *FEBS Letters* **587**, 1155–1163 (2013).
229. Craik, C. S., Page, M. J. & Madison, E. L. Proteases as therapeutics. *Biochemical Journal* **435**, 1–16 (2011).
230. Sheehan, J. J. & Tsirka, S. E. Fibrin-modifying serine proteases thrombin, tPA, and plasmin in ischemic stroke: A review. *Glia* **50**, 340–350 (2005).
231. WorldHealthOrganization. *Media centre* <http://www.who.int/mediacentre/factsheets/fs310/en/>. [Online; accessed 07/2017].
232. Chen, W. T. Membrane proteases: Roles in tissue remodeling and tumour invasion. *Current Opinion in Cell Biology* **4**, 802–809 (1992).
233. Weidle, U. H., Buckel, P. & Wienberg, J. Amplified expression constructs for human tissue-type plasminogen activator in Chinese hamster ovary cells: Instability in the absence of selective pressure. *Gene* **66**, 193–203 (1988).
234. Rouf, S. A., Moo-Young, M. & Chisti, Y. Tissue-type plasminogen activator: Characteristics, applications and production technology. *Biotechnology advances* **14**, 239–266 (1996).
235. Kim, J. Y., Kim, J. K., Park, J. S., Byun, Y. & Kim, C. K. The use of PEGylated liposomes to prolong circulation lifetimes of tissue plasminogen activator. *Biomaterials* **30**, 5751–5756 (2009).
236. Terpe, K. Overview of bacterial expression systems for heterologous protein production: From molecular and biochemical fundamentals to commercial systems. *Applied Microbiology and Biotechnology* **72**, 211–222 (2006).
237. Li, Y. Self-cleaving fusion tags for recombinant protein production. *Biotechnology Letters* **33**, 869–881 (2011).
238. Baumann, P., Bluthardt, N., Renner, S., Burghardt, H., Osberghaus, A. & Hubbuch, J. Integrated development of up- and processes supported by the Cherry-Tag for real-time tracking of stability and solubility of proteins. *J. Biotech.* **200**, 27–37 (2015).
239. Kapust, R. B., Tózsér, J., Fox, J. D., Anderson, D. E., Cherry, S., Copeland, T. D. & Waugh, D. S. Tobacco etch virus protease: Mechanism of autolysis and rational design of stable mutants with wild-type catalytic proficiency. *Protein engineering* **14**, 993–1000 (2001).

240. Ohana, R. F., Encell, L. P., Zhao, K., Simpson, D., Slater, M. R., Urh, M. & Wood, K. V. HaloTag7: A genetically engineered tag that enhances bacterial expression of soluble proteins and improves protein purification. *Protein Expr. Purif.* **68**, 110–120 (2009).
241. Arnau, J., Lauritzen, C., Petersen, G. E. & Pedersen, J. Current strategies for the use of affinity tags and tag removal for the purification of recombinant proteins. *Protein Expr. Purif.* **48**, 1–13 (2006).
242. Rose, J. R., Salto, R. & Craik, C. S. Regulation of autoproteolysis of the HIV-1 and HIV-2 proteases with engineered amino acid substitutions. *Journal of Biological Chemistry* **268**, 11939–11945 (1993).
243. Tiukinhoy-Laing, S. D., Huang, S., Klegerman, M., Holland, C. K. & McPherson, D. D. Ultrasound-facilitated thrombolysis using tissue-plasminogen activator-loaded echogenic liposomes. *Thrombosis Research* **119**, 777–784 (2007).
244. Sinha, V. R. & Trehan, A. Biodegradable microspheres for protein delivery. *Journal of Controlled Release* **90**, 261–280 (2003).
245. Lutz, J. F. & Börner, H. G. Modern trends in polymer bioconjugates design. *Progress in Polymer Science* **33**, 1–39 (2008).
246. Mehvar, R. Modulation of the pharmacokinetics and pharmacodynamics of proteins by polyethylene glycol conjugation. *Journal of pharmacy and pharmaceutical sciences* **3**, 125–136 (2000).
247. Pfister, D. & Morbidelli, M. Process for protein PEGylation. *Journal of Controlled Release* **180**, 134–149 (2014).
248. Gaberc-Porekar, V., Zore, I., Podobnik, B. & Menart, V. Obstacles and pitfalls in the PEGylation of therapeutic proteins. *Current Opinion in Drug Discovery and Development* **11**, 242 (2008).
249. Zillies, J. C., Zwioerek, K., Winter, G. & Coester, C. Method for quantifying the PEGylation of gelatin nanoparticle drug carrier systems using asymmetrical flow field-flow fractionation and refractive index detection. *Anal. Chem.* **79**, 4574–4580 (2007).
250. Hansen, S. K., Maiser, B. & Hubbuch, J. Rapid quantification of protein–polyethylene glycol conjugates by multivariate evaluation of chromatographic data. *J. Chrom. A* **1257**, 41–47 (2012).

-
251. Roberts, M. J. & Harris, J. M. Attachment of degradable poly(ethylene glycol) to proteins has the potential to increase therapeutic efficacy. *J. Pharm. Sci.* **87**, 1440–1445 (1998).
252. Jiang, L., He, L. & Fountoulakis, M. Comparison of protein precipitation methods for sample preparation prior to proteomic analysis. *J. Chrom. A* **1023**, 317–320 (2004).
253. Ottow, K. E., Lund-Olesen, T., Maury, T. L., Hansen, M. F. & Hobley, T. J. A magnetic adsorbent-based process for semi-continuous PEGylation of proteins. *Biotechnol. J.* **6**, 396–409 (2011).
254. Galm, L., Morgenstern, J. & Hubbuch, J. Manipulation of lysozyme phase behavior by additives as function of conformational stability. *Int. J. Pharm.* **494**, 370–380 (2015).
255. Gasteiger, E., Hoogland, C., Gattiker, A., Duvaud, S., Wilkins, M. R., Appel, R. D. & Bairoch, A. *Protein identification and analysis tools on the ExPASy server* (Springer, 2005).
256. Oelmeier, S. A., Dimer, F. & Hubbuch, J. Application of an aqueous two-phase systems high-throughput screening method to mAb HCP separation. *Biotechnol. Bioeng.* **108**, 69–81 (2011).
257. Maiser, B., Kröner, F., Dimer, F., Brenner-Weiß, G. & Hubbuch, J. Isoform separation and binding site determination of mono-PEGylated lysozyme with pH gradient chromatography. *J. Chrom. A* **1268**, 102–108 (2012).
258. Yoshimoto, N. & Yamamoto, S. PEGylated protein separations: Challenges and opportunities. *Biotechnol. J.* **7**, 592–593 (2012).
259. Zheng, C. Y., Ma, G. & Su, Z. Native PAGE eliminates the problem of PEG-SDS interaction in SDS-PAGE and provides an alternative to HPLC in characterization of protein PEGylation. *Electrophoresis* **28**, 2801–2807 (2007).
260. Odom, O. W., Kudlicki, W., Kramer, G. & Hardesty, B. An effect of polyethylene glycol 8000 on protein mobility in sodium dodecyl sulfate-polyacrylamide gel electrophoresis and a method for eliminating this effect. *Anal. Biochem.* **245**, 249–252 (1997).
261. Dai, S. & Tam, K. C. Isothermal titration calorimetry studies of binding interactions between polyethylene glycol and ionic surfactants. *The Journal of Physical Chemistry B* **105**, 10759–10763 (2001).

262. Maltesh, C. & Somasundamn, P. Effect of Binding of Cations to Polyethylene Glycol on Its Interactions with Sodium Dodecyl Sulfate. *Langmuir* **8**, 1926–1930 (1992).
263. Moosmann, A., Blath, J., Lindner, R., Müller, E. & Böttinger, H. Aldehyde PEGylation kinetics: A standard protein versus a pharmaceutically relevant single chain variable fragment. *Bioconjugate chemistry* **22**, 1545–1558 (2011).
264. Maiser, B., Dismer, F. & Hubbuch, J. Optimization of random PEGylation reactions by means of high throughput screening. *Biotechnol. Bioeng.* **111**, 104–114 (2014).
265. Závodszy, P., Kardos, J., Svingor, Á. & Petsko, G. A. Adjustment of conformational flexibility is a key event in the thermal adaptation of proteins. *PNAS* **95**, 7406–7411 (1998).
266. Schermeyer, M.-T., Sigloch, H., Bauer, K. C., Oelschlaeger, C. & Hubbuch, J. Squeeze flow rheometry as a novel tool for the characterization of highly concentrated protein solutions. *Biotechnol. Bioeng.* **113**, 576–587 (2016).
267. Krishnan, S., Chi, E. Y., Webb, J. N., Chang, B. S., Shan, D., Goldenberg, M., Manning, M. C., Randolph, T. W. & Carpenter, J. F. Aggregation of granulocyte colony stimulating factor under physiological conditions: Characterization and thermodynamic inhibition. *Biochemistry* **41**, 6422–6431 (2002).
268. Chen, B. L., Wu, X., Babuka, S. J. & Hora, M. Solubility of recombinant human tissue factor pathway inhibitor. *J. Pharm. Sci.* **88**, 881–8 (1999).
269. Hansen, C. L., Sommer, M. O. A. & Quake, S. R. Systematic investigation of protein phase behavior with a microfluidic formulator. *PNAS* **101**, 14431–14436 (2004).
270. Wang, W. & Roberts, C. J. *Aggregation of therapeutic proteins* 150–151 (Wiley, 2010).
271. Ericsson, U. B., Hallberg, B. M., DeTitta, G. T., Dekker, N. & Nordlund, P. Thermofluor-based high-throughput stability optimization of proteins for structural studies. *Anal. Biochem.* **357**, 289–298 (2006).
272. Baumann, P., Osberghaus, A. & Hubbuch, J. Systematic purification of salt-intolerant proteins by ion-exchange chromatography: The example of human α -galactosidase A. *Eng. Life Sci.* **15**, 195–207 (2015).

-
273. Kapust, B. R. & Waugh, S. D. Escherichia coli maltose-binding protein is uncommonly effective at promoting the solubility of polypeptides to which it is fused. *Protein Science* **8**, 1668–1674 (1999).
274. Esposito, D. & Chatterjee, D. K. Enhancement of soluble protein expression through the use of fusion tags. *Curr. Opin. Biotechnol.* **17**, 353–358 (2006).
275. Mohan Padmanabha Das, K., Barve, S., Banerjee, S., Bandyopadhyay, S. & Padmanabhan, S. A Novel Thermostability Conferring Property of Cherry Tag and its Application in Purification of Fusion Proteins. *Journal of Microbial & Biochemical Technology* **1**, 59–63 (2009).
276. Azhar, M. & Somashekhar, R. Cloning , expression and purification of human and bovine Enterokinase light chain with Cherry tag and their activity comparison. *Indian J. Applied & Pure Bio.* **29**, 125–132 (2014).
277. Zhang, Y. B., Howitt, J., McCorkle, S., Lawrence, P., Springer, K. & Freimuth, P. Protein aggregation during overexpression limited by peptide extensions with large net negative charge. *Protein Expr. Purif.* **36**, 207–216 (2004).
278. Da Silva Freitas, D. & Abrahao-Neto, J. Biochemical and biophysical characterization of lysozyme modified by PEGylation. *Int. J. Pharm.* **392**, 111–117 (2010).
279. Nie, Y., Zhang, X., Wang, X. & Chen, J. Preparation and stability of N-terminal mono-PEGylated recombinant human endostatin. *Bioconjugate Chemistry* **17**, 995–999 (2006).
280. Basu, A. *et al.* StructureFunction Engineering of Interferon- β -1b for Improving Stability, Solubility, Potency, Immunogenicity, and Pharmacokinetic Properties by Site-Selective Mono-PEGylation. *Bioconjugate Chem.* **17**, 618–630 (2006).
281. Morgenstern, J., Busch, M., Baumann, P. & Hubbuch, J. Quantification of PEGylated proteases with varying degree of conjugation in mixtures: An analytical protocol combining protein precipitation and capillary gel electrophoresis. *J. Chrom. A* **1462**, 153–164 (2016).
282. Smith, R. D., Loo, J. A., Edmonds, C. G., Barinaga, C. J. & Udseth, H. R. New developments in biochemical mass spectrometry: Electrospray ionization. *Anal. Chem.* **62**, 882–899 (1990).
283. Wang, W., Nema, S. & Teagarden, D. Protein aggregation - Pathways and influencing factors. *Int. J. Pharm.* **390**, 89–99 (2010).

284. Baumann, P., Baumgartner, K. & Hubbuch, J. Influence of binding pH and protein solubility on the dynamic binding capacity in hydrophobic interaction chromatography. *J. Chrom. A* **1396**, 77–85 (2015).
285. Nath, A. & Atkins, W. M. A theoretical validation of the substrate depletion approach to determining kinetic parameters. *Drug metabolism and disposition* **34**, 1433–1435 (2006).
286. Jeng, F.-Y. & Lin, S.-C. Characterization and application of PEGylated horseradish peroxidase for the synthesis of poly (2-naphthol). *Process Biochemistry* **41**, 1566–1573 (2006).
287. Vandertol-Vanier, H. A., Vazquez-Duhalt, R., Tinoco, R. & Pickard, M. A. Enhanced activity by poly (ethylene glycol) modification of *Coriopsis gallica* laccase. *Journal of Industrial Microbiology and Biotechnology* **29**, 214–220 (2002).
288. Gaertner, H. & Puigserver, A. Increased activity and stability of poly (ethylene glycol)-modified trypsin. *Enzyme and microbial technology* **14**, 150–155 (1992).
289. Manning, M. C., Patel, K. & Borcharadt, R. T. Stability of protein pharmaceuticals. *Pharm. Res.* **6**, 903–918 (1989).
290. Harris, J. M., Martin, N. E. & Modi, M. Pegylation. *Clinical pharmacokinetics* **40**, 539–551 (2001).
291. Biedermann, F., Rauwald, U., Zayed, J. M. & Scherman, O. A. A supramolecular route for reversible protein-polymer conjugation. *Chemical Science* **2**, 279–286 (2011).
292. Lucius, M., Falatach, R., McGlone, C., Makaroff, K., Danielson, A., Williams, C., Nix, J. C., Konkolewicz, D., Page, R. C. & Berberich, J. A. Investigating the Impact of Polymer Functional Groups on the Stability and Activity of Lysozyme–Polymer Conjugates. *Biomacromolecules* **17**, 1123–1134 (2016).
293. Morgenstern, J., Baumann, P., Brunner, C. & Hubbuch, J. Effect of PEG molecular weight and PEGylation degree on the physical stability of PEGylated lysozyme. *Int. J. Pharm.* **519**, 408–417 (2017).
294. Abuchowski, A., Van Es, T., Palczuk, N. & Davis, F. Alteration of immunological properties of bovine serum albumin by covalent attachment of polyethylene glycol. *J. Biol. Chem.* **252**, 3578–3581 (1977).

-
295. Richter, A. W. & Åkerblom, E. Antibodies against polyethylene glycol produced in animals by immunization with monomethoxy polyethylene glycol modified proteins. *International Archives of Allergy and Immunology* **70**, 124–131 (1983).
296. Richter, A. W. & Åkerblom, E. Polyethylene glycol reactive antibodies in man: Titer distribution in allergic patients treated with monomethoxy polyethylene glycol modified allergens or placebo, and in healthy blood donors. *International Archives of Allergy and Immunology* **74**, 36–39 (1984).
297. Sundry, J. S., Ganson, N. J., Kelly, S. J., Scarlett, E. L., Rehrig, C. D., Huang, W. & Hershfield, M. S. Pharmacokinetics and pharmacodynamics of intravenous PEGylated recombinant mammalian urate oxidase in patients with refractory gout. *Arthritis & Rheumatology* **56**, 1021–1028 (2007).
298. Garay, R. P., El-Gewely, R., Armstrong, J. K., Garratty, G. & Richette, P. Antibodies against polyethylene glycol in healthy subjects and in patients treated with PEG-conjugated agents. *Expert Opinion on Drug Delivery* **9**, 1319–1323 (2012).
299. Schellekens, H., Hennink, W. E. & Brinks, V. The immunogenicity of polyethylene glycol: Facts and fiction. *Pharm. Res.* **30**, 1729–1734 (2013).
300. Armstrong, J., Hempel, G., Koling, S., Chan, L., Fisher, T., Meiselman, H. & Garratty, G. Antibody against poly (ethylene glycol) adversely affects PEG-asparaginase therapy in acute lymphoblastic leukemia patients. *Cancer* **110**, 103–111 (2007).
301. Ulbricht, J., Jordan, R. & Luxenhofer, R. On the biodegradability of polyethylene glycol, polypeptoids and poly (2-oxazoline) s. *Biomaterials* **35**, 4848–4861 (2014).
302. Qi, Y. & Chilkoti, A. Protein-polymer conjugation - moving beyond PEGylation. *Current opinion in chemical biology* **28**, 181–193 (2015).
303. Ozer, I. & Chilkoti, A. Site-Specific and Stoichiometric Stealth Polymer Conjugates of Therapeutic Peptides and Proteins. *Bioconjugate chemistry* **28**, 713–723 (2017).
304. Krishna, O. D. & Kiick, K. L. Protein-and peptide-modified synthetic polymeric biomaterials. *Peptide Science* **94**, 32–48 (2010).
305. Ranucci, E., Spagnoli, G., Sartore, L., Ferruti, P., Caliceti, P., Schiavon, O. & Veronese, F. M. Synthesis and molecular weight characterization of low molecular weight end-functionalized poly (4-acryloylmorpholine). *Macromolecular Chemistry and Physics* **195**, 3469–3479 (1994).

306. D'Agosto, F., Hughes, R., Charreyre, M.-T., Pichot, C. & Gilbert, R. G. Molecular weight and functional end group control by RAFT polymerization of a bisubstituted acrylamide derivative. *Macromolecules* **36**, 621–629 (2003).
307. Veronese, F. M., Schiavon, O., Caliceti, P., Sartore, L., Ranucci, E. & Ferruti, P. *Polymers of N-acryloylmorpholine activated at one end and conjugates with bioactive materials and surfaces* US Patent 5,629,384. 1997.
308. Wang, X.-S., Lascelles, S., Jackson, R. & Armes, S. Facile synthesis of well-defined water-soluble polymers via atom transfer radical polymerization in aqueous media at ambient temperature. *Chemical Communications*, 1817–1818 (1999).
309. Wang, X.-S. & Armes, S. Facile atom transfer radical polymerization of methoxy-capped oligo (ethylene glycol) methacrylate in aqueous media at ambient temperature. *Macromolecules* **33**, 6640–6647 (2000).
310. Gao, W., Liu, W., Mackay, J. A., Zalutsky, M. R., Toone, E. J. & Chilkoti, A. In situ growth of a stoichiometric PEG-like conjugate at a protein's N-terminus with significantly improved pharmacokinetics. *PNAS* **106**, 15231–15236 (2009).
311. Gao, W., Liu, W., Christensen, T., Zalutsky, M. R. & Chilkoti, A. In situ growth of a PEG-like polymer from the C terminus of an intein fusion protein improves pharmacokinetics and tumor accumulation. *PNAS* **107**, 16432–16437 (2010).
312. Bovara, R., Ottolina, G., Carrea, G., Ferruti, P. & Veronese, F. M. Modification of lipase from *Pseudomonas* sp. with poly (acryloylmorpholine) and study of its catalytic properties in organic solvents. *Biotechnology letters* **16**, 1069–1074 (1994).
313. Schiavon, O., Caliceti, P., Ferruti, P. & Veronese, F. Therapeutic proteins: A comparison of chemical and biological properties of uricase conjugated to linear or branched poly (ethylene glycol) and poly (N-acryloylmorpholine). *Il Farmaco* **55**, 264–269 (2000).
314. Giardino, R., Giavaresi, G., Fini, M., Torricelli, P. & Guzzardella, G. A. The role of different chemical modifications of superoxide dismutase in preventing a prolonged muscular ischemia/reperfusion injury. *Artificial Cells, Blood Substitutes, and Biotechnology* **30**, 189–198 (2002).
315. Bencini, M., Ranucci, E., Ferruti, P., Manfredi, A., Trotta, F. & Cavalli, R. Poly (4-acryloylmorpholine) oligomers carrying a β -cyclodextrin residue at one terminus. *Journal of Polymer Science Part A: Polymer Chemistry* **46**, 1607–1617 (2008).

-
316. Cummings, C. S., Campbell, A. S., Baker, S. L., Carmali, S., Murata, H. & Russell, A. J. Design of Stomach Acid-Stable and Mucin-Binding Enzyme Polymer Conjugates. *Biomacromolecules* **18**, 576–586 (2017).
317. Skrabania, K., Miasnikova, A., Bivigou-Koumba, A. M., Zehm, D. & Laschewsky, A. Examining the UV-vis absorption of RAFT chain transfer agents and their use for polymer analysis. *Polymer Chemistry* **2**, 2074–2083 (2011).
318. Roberts, M., Bentley, M. & Harris, J. Chemistry for peptide and protein PEGylation. *Adv. Drug Deliv. Rev.* **64**, 116–127 (2012).
319. Morgenstern, J., Wang, G., Baumann, P. & Hubbuch, J. Model-Based Investigation on the Mass Transfer and Adsorption Mechanisms of Mono-Pegylated Lysozyme in Ion-Exchange Chromatography. *Biotechnol. J.* doi:10.1002/biot.201700255 (2017).
320. Hennink, W. & Van Nostrum, C. Novel crosslinking methods to design hydrogels. *Advanced drug delivery reviews* **64**, 223–236 (2012).
321. Hoffman, A. S. Hydrogels for biomedical applications. *Advanced drug delivery reviews* **64**, 18–23 (2012).
322. Janson, J.-C. in. Chap. 14 (John Wiley & Sons, 2012).
323. Yamamoto, S., Fujii, S., Yoshimoto, N. & Akbarzadehlaleh, P. Effects of protein conformational changes on separation performance in electrostatic interaction chromatography: Unfolded proteins and PEGylated proteins. *J. Biotechnol.* **132**, 196–201 (2007).
324. Yoshimoto, N., Isakari, Y., Itoh, D. & Yamamoto, S. PEG chain length impacts yield of solid-phase protein PEGylation and efficiency of PEGylated protein separation by ion-exchange chromatography: Insights of mechanistic models. *Biotechnol. J.* **8**, 801–810 (2013).
325. Guiochon, G. & Beaver, L. A. Separation science is the key to successful biopharmaceuticals. *J. Chromatogr. A* **1218**, 8836–8858 (2011).
326. PerkinElmer. *LabChip GX/GX II - User Manual* http://www.perkinelmer.com/Content/LST_Software_Downloads/LabChip_GX_User_Manual.pdf. [Online; accessed 01/2017].
327. Research, H. *Lysozyme - User Guide HR7-110* http://hamptonresearch.com/documents/product/hr006812_711020.pdf. [Online; accessed 01/2017].

328. Velayudhan, A. & Horvath, C. Preparative chromatography of proteins - analysis of the multivalent ion-exchange formalism. *J. Chromatogr. A* **443**, 13–29 (1988).
329. Lenhoff, A. M. Protein adsorption and transport in polymer-functionalized ion-exchangers. *J. Chromatogr. A* **1218**, 8748–8759 (2011).
330. Wittmann, A., Haupt, B. & Ballauff, M. Adsorption of proteins on spherical polyelectrolyte brushes in aqueous solution. *Phys. Chem. Chem. Phys.* **5**, 1671–1677 (2003).
331. Hahn, T., Baumann, P., Huuk, T., Heuveline, V. & Hubbuch, J. UV absorption-based inverse modeling of protein chromatography. *Eng. Life Sci.* **16**, 99–106 (2016).
332. Kaczmarek, K. & Antos, D. Use of simulated annealing for optimization of chromatographic separations. *Acta Chromatogr.* **17**, 20–45 (2006).
333. Devernay, F. *C/C++ Minpack* <http://devernay.free.fr/hacks/cminpack/>. [Online; accessed 01/2017].
334. Glowinski, R. *Finite element methods for incompressible viscous flow*. In *Numerical Methods for Fluids (Part 3)* 3–1176 (Elsevier, 2003).
335. Quarteroni, A. & Valli, A. *Numerical approximation of partial differential equations* 160 (Springer, 1994).
336. Wang, G., Briskot, T., Hahn, T., Baumann, P. & Hubbuch, J. Estimation of adsorption isotherm and mass transfer parameters in protein chromatography using artificial neural networks. *J. Chromatogr. A* **1487**, 211–217 (2017).
337. Mejia-Manzano, L. A., Sandoval, G., Lienqueo, M. E., Moisset, P., Rito-Palomares, M. & Asenjo, J. A. Simulation of mono-PEGylated lysozyme separation in heparin affinity chromatography using a general rate model. *J. Chem. Technol. Biotechnol.* doi:10.1002/jctb.5309 (2017).
338. ICH. *International Conference on Harmonisation of Technical Requirements for Registration of Pharmaceuticals for Human Use, ICH-Endorsed Guide for ICH Q8/Q9/Q10 Implementation* http://www.ich.org/fileadmin/Public_Web_Site/ICH_Products/Guidelines/Quality/Q8_9_10_QAs/PtC/Quality_IWG_PtCR2_6dec2011.pdf. [Online; accessed 07/2017].
339. Einstein, A. On the movement of small particles suspended in stationary liquids required by the molecular-kinetic theory of heat. *Ann. Phys.* **17**, 549–560 (1905).

-
340. Carta, G., Gregory, M. E. & Kirwan, D. J. Chromatography with permeable supports: Theory and comparison with experiments. *Sep. Technol.* **2**, 62–72 (1992).
341. Carta, G. & Rodrigues, A. E. Diffusion and convection in chromatographic processes using permeable particles with a bidisperse pore structure. *Chem. Eng. Sci.* **48**, 3927–3935 (1993).
342. Rodrigues, A. E., Lu, Z. P., Loureiro, J. M. & Carta, G. Peak resolution in linear chromatography: Effects of intraparticle convection. *J. Chromatogr. A* **653**, 189–xx198 (1993).
343. Frey, D. D., Schweinheim, E. & Horvath, C. Effect of intraparticle convection on the chromatography of biomacromolecules. *Biotechnol. Progr.* **9**, 273–284 (1993).
344. Freitag, R., Frey, D. & Horvath, C. Effect of bed compression on high-performance liquid-chromatography columns with gigaporous polymeric packings. *J. Chromatogr. A* **686**, 165–177 (1994).
345. Pfeiffer, J. F., Chen, J. C. & Hsu, J. T. Permeability of gigaporous particles. *AIChE J.* **42**, 932–939 (1996).
346. Gustavsson, P. E., Mosbach, K., Nilsson, K. & Larsson, P. O. Superporous agarose as an affinity-chromatography support. *J. Chromatogr. A* **776**, 197–203 (1997).
347. Nash, D. C. & Chase, H. A. Comparison of diffusion and diffusion-convection matrices for use in ion-exchange separations of proteins. *J. Chromatogr. A* **807**, 185–207 (1998).
348. Lloyd, L. L. Rigid macroporous copolymers as stationary phases in high-performance liquid chromatography. *J. Chromatogr. A* **544**, 201–217 (1991).
349. Dziennik, S. R., Belcher, E. B., Barker, G. A., DeBergalis, M. J., Fernandez, S. E. & Lenhoff, A. M. Nondiffusive mechanisms enhance protein uptake rates in ion exchange particles. *PNAS* **100**, 420–425 (2003).
350. Van Alstine, J. M. & Malmsten, M. Poly (ethylene glycol) Amphiphiles: Surface Behavior of Biotechnical Significance. *Langmuir* **13**, 4044–4053 (1997).
351. Blaschke, T., Varon, J., Werner, A. & Hasse, H. Microcalorimetric study of the adsorption of PEGylated lysozyme on a strong cation exchange resin. *J. Chromatogr. A* **1218**, 4720–4726 (2011).
352. Ferreira, L., Vidal, M. M. & Gil, M. H. Evaluation of poly (2-hydroxyethyl methacrylate) gels as drug delivery systems at different pH values. *Int. J. Pharm.* **194**, 169–180 (2000).

353. Hari, P. R., Chandy, T. & Sharma, C. P. Chitosan/calcium–alginate beads for oral delivery of insulin. *Journal of Applied Polymer Science* **59**, 1795–1801 (1996).
354. Chaturvedi, K., Ganguly, K., Nadagouda, M. N. & Aminabhavi, T. M. Polymeric hydrogels for oral insulin delivery. *Journal of controlled release* **165**, 129–138 (2013).
355. Zou, X., Zhao, X. & Ye, L. Synthesis of cationic chitosan hydrogel with long chain alkyl and its controlled glucose-responsive drug delivery behavior. *RSC Advances* **5**, 96230–96241 (2015).
356. Brandl, F., Hammer, N., Blunk, T., Tessmar, J. & Goepferich, A. Biodegradable hydrogels for time-controlled release of tethered peptides or proteins. *Biomacromolecules* **11**, 496–504 (2010).
357. Oliveira, M. B. & Mano, J. F. High-throughput screening for integrative biomaterials design: Exploring advances and new trends. *Trends in biotechnology* **32**, 627–636 (2014).
358. Hertzberg, R. P. & Pope, A. J. High-throughput screening: New technology for the 21st century. *Current opinion in chemical biology* **4**, 445–451 (2000).
359. Bensch, M., Schulze Wierling, P., von Lieres, E. & Hubbuch, J. High throughput screening of chromatographic phases for rapid process development. *Chemical engineering & technology* **28**, 1274–1284 (2005).
360. Capelle, M. A. H., Gurny, R. & Arvinte, T. High throughput screening of protein formulation stability: Practical considerations. *European journal of pharmaceuticals and biopharmaceutics* **65**, 131–148 (2007).
361. Kittelmann, J., Ottens, M. & Hubbuch, J. Robust high-throughput batch screening method in 384-well format with optical in-line resin quantification. *J. Chrom. B* **988**, 98–105 (2015).
362. Wang, J., Goyanes, A., Gaisford, S. & Basit, A. W. Stereolithographic (SLA) 3D printing of oral modified-release dosage forms. *Int. J. Pharm.* **503**, 207–212 (2016).
363. Kröner, F. & Hubbuch, J. Systematic generation of buffer systems for pH gradient ion exchange chromatography and their application. *J. Chrom. A* **1285**, 78–87 (2013).
364. Sirkar, K. & Pishko, M. V. Amperometric biosensors based on oxidoreductases immobilized in photopolymerized poly (ethylene glycol) redox polymer hydrogels. *Anal. Chem.* **70**, 2888–2894 (1998).

-
365. Arcaute, K., Mann, B. K. & Wicker, R. B. in *Stereolithography* 299–331 (Springer, 2011).
366. Zhang, L., Ma, Y., Zhao, C., Zhu, X., Chen, R. & Yang, W. Synthesis of pH-responsive hydrogel thin films grafted on PCL substrates for protein delivery. *Journal of Materials Chemistry B* **3**, 7673–7681 (2015).
367. Zhao, L., Chen, Y., Li, W., Lu, M., Wang, S., Chen, X., Shi, M., Wu, J., Yuan, Q. & Li, Y. Controlled uptake and release of lysozyme from glycerol diglycidyl ether cross-linked oxidized starch microgel. *Carbohydrate polymers* **121**, 276–283 (2015).
368. Morris, G. E., Vincent, B. & Snowden, M. J. Adsorption of Lead Ions onto N-Isopropylacrylamide and Acrylic Acid Copolymer Microgels. *Journal of colloid and interface science* **190**, 198–205 (1997).
369. VirginiaTech. *H++* <http://biophysics.cs.vt.edu/index.php>. [Online; accessed 05/2017].
370. Hammer, N., Brandl, F. P., Kirchhof, S., Messmann, V. & Goepferich, A. M. Protein Compatibility of Selected Cross-linking Reactions for Hydrogels. *Macromolecular bioscience* **15**, 405–413 (2015).

Abbreviations and parameters

Abbreviations

3D	three-dimensional
AA	acrylic acid
Abs	absorption
API	active pharmaceutical ingredient
ASA	adaptive simulated annealing
BCM	barycentric mean fluorescence
BMBF	Bundesministerium für Bildung und Forschung = German Federal Ministry of Education and Research
CAD	computer-aided design
CGE	capillary gel electrophoresis
CEX	cation-exchange chromatography
CMC	critical micelle concentration
CQA	critical quality attributes
CV	column volumes
Cys	cysteine
DDS	drug delivery system
DLP	digital light processing
DMPA	2,2-Dimethoxy-2-phenylacetophenone
DoE	Design of Experiments
DSP	downstream processing
EO	ethylene oxide
EWG	equilibrium water content
FDA	Food and Drug Administration

FT-IR	Fourier-Transformed-Infrared
G-CSF	granulocyte colonystimulating factor
Gln	glutamine
GMO	genetically modified organism
GRM	general rate model
HIC	hydrophobic interaction chromatography
HT-CGE	high-throughput capillary gel electrophoresis
HTS	high-throughput screening
IEX	ion-exchange chromatography
LC	liquid chromatography
LGE	linear gradient elution
LM	Levenberg-Marquardt
Lys	lysine
mAb	monoclonal antibodies
MALDI-TOF	Matrix-Assisted Laser Desorption Ionization–Time of Flight
MD	molecular dynamic
MIE	Molecular Interaction Engineering
MS	mass spectrometry
NaCl	sodium chloride
NHS	N-Hydroxysuccinimide
NMR	Nuclear Magnetic Resonance
PBS	phosphate buffered saline
PEG	polyethylene glycol
PEG-DA	polyethylene glycol-diacrylate
pI	isoelectric point
PLA	polylactic acid
PNAM	poly-(N-acryloylmorpholine)
POEGMA	poly-(oligo(ethylene glycol)methacrylate)
PVA	poly(vinyl alcohol)
PVP	polyvinylpyrrolidone
QbD	Quality by Design
RAFT	reversible addition-fragmentation chain transfer
SDM	stoichiometric displacement model
SDS	sodium dodecyl sulfate
SEC	size-exclusion chromatography
SLA	sterolithography

SMA	steric mass action
TCA	trichloroacetic acid
tPA	tissue plasminogen activator
Tyr	tyrosine
USP	upstream processing
UV	ultraviolet
vdW	van-der-Waals
vis	visible

Parameters

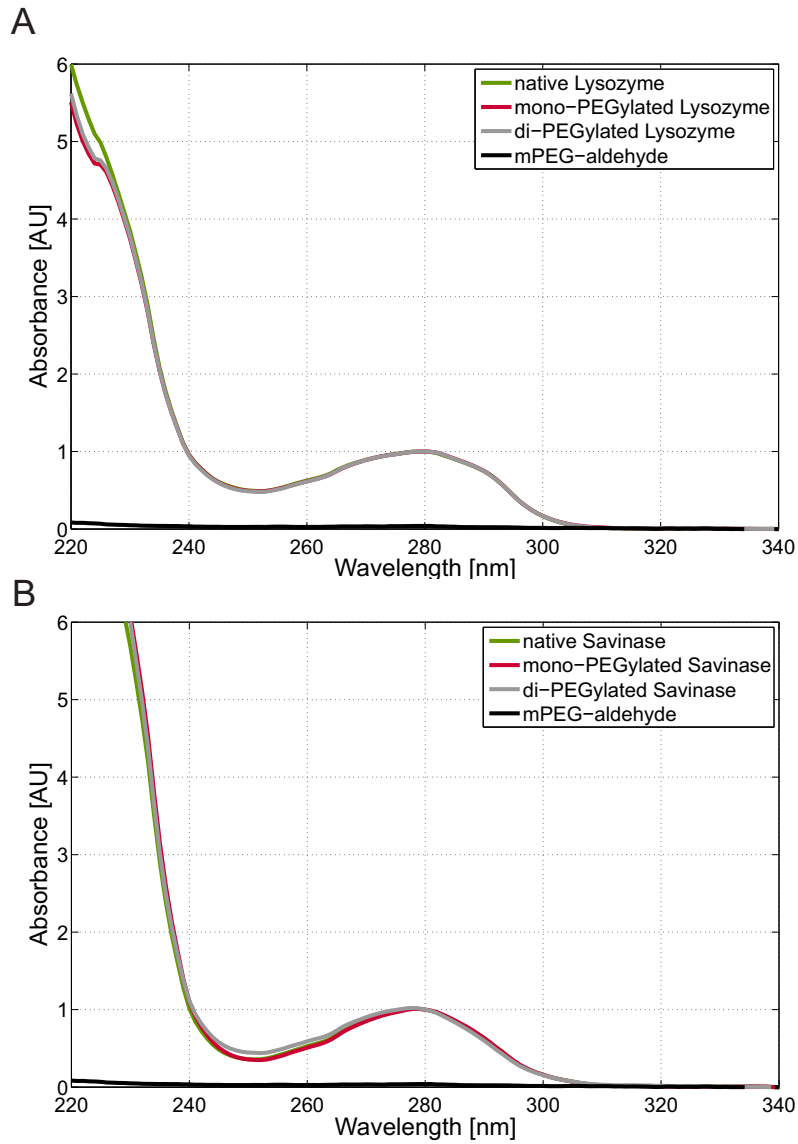
a	activity (effective concentration)
c	concentration
D_{ax}	axial dispersion coefficient
D_p	pore diffusion coefficient
d	diameter
F	force
G	Gibbs free energy
H	enthalpy
H_a	Hamaker constant
k_{ads}	adsorption coefficient
k_{des}	desorption coefficient
k_e	Coulomb's constant
k_{eq}	equilibrium coefficient
k_{film}	film diffusion coefficient
k_{kin}	reaction velocity coefficient
Q	charge
q	concentration on the stationary phase
R	universal gas constant
r	radial pore position or ratio
r_p	particle radius
S	entropy
S_a	activity-related supersaturation
S_c	concentration-related supersaturation

T	temperature
T_m	melting temperature
t	time
u	flow velocity
x	distance or position

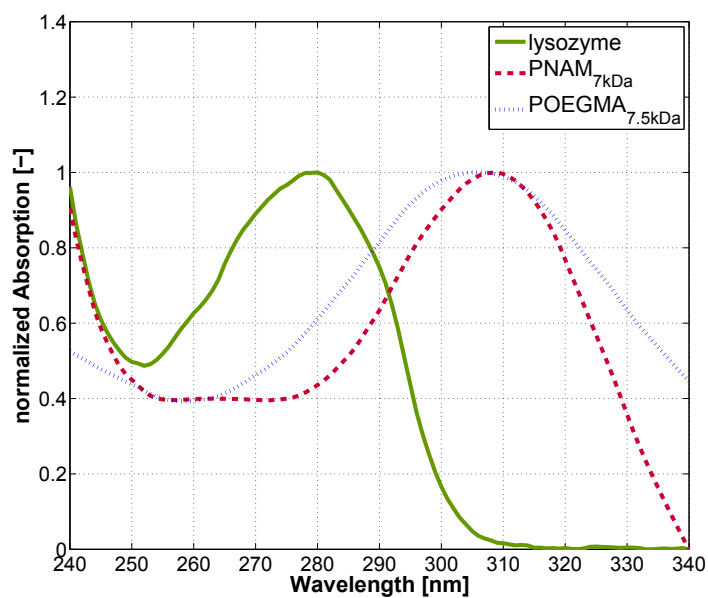
Greek symbols

γ	activity coefficient
ε	extinction coefficient
ε_b	bed porosity
$\tilde{\mu}$	molar chemical potential
ν	characteristic binding charge
σ	steric shielding factor or standard deviation

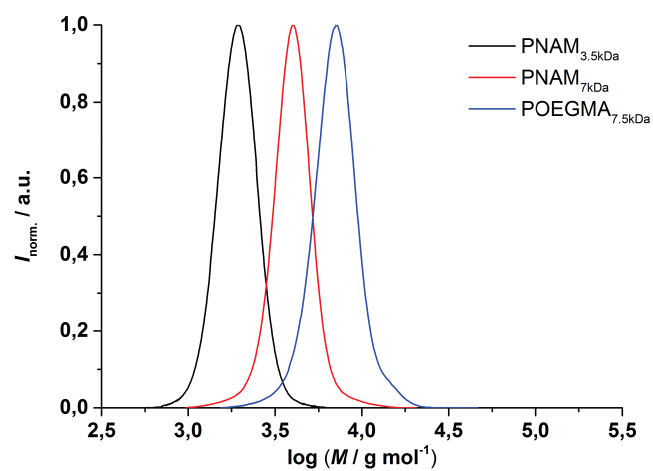
Supplementary Figures



Supplementary Figure A.1: Absorption spectra of native, mono-PEGylated and di-PEGylated Lysozyme (A) and of native, mono-PEGylated and di-PEGylated Savinase (B) normalized to 280nm.

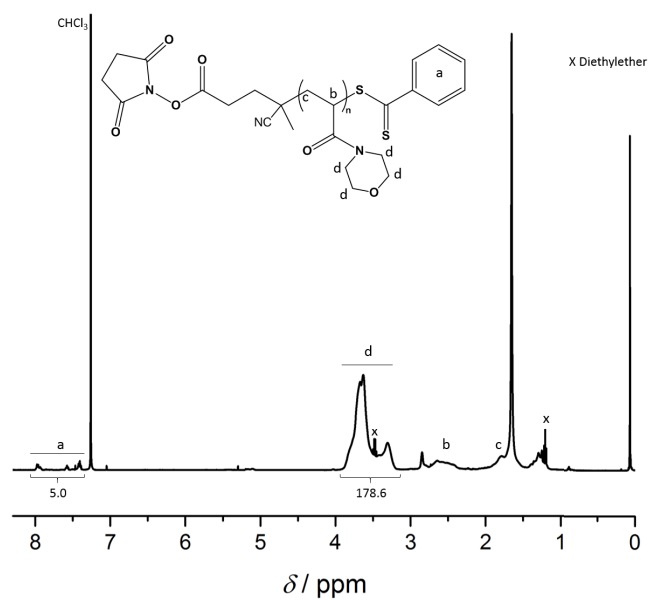


Supplementary Figure A.2: Absorption spectra of lysozyme, PNAM_{7kDa} and POEGMA_{7.5kDa} normalized to their absorption maximum.

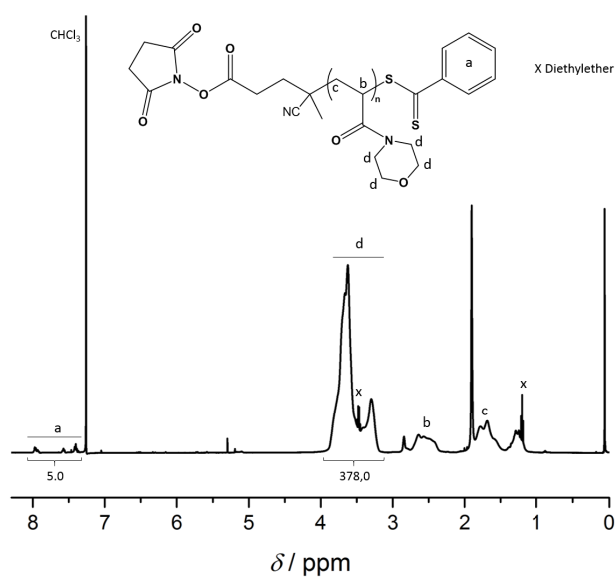


Supplementary Figure A.3: THF-SEC traces of the synthesized polymers PNAM_{3.5kDa}, PNAM_{7kDa}, POEGMA_{7.5kDa}.

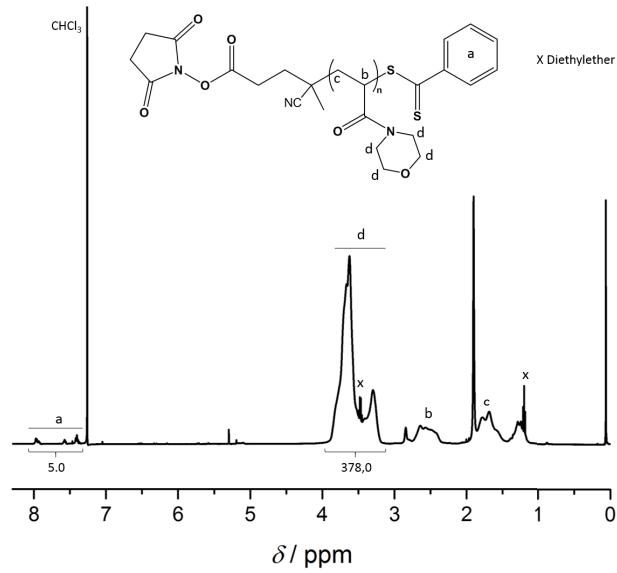
Appendix A Supplementary Figures



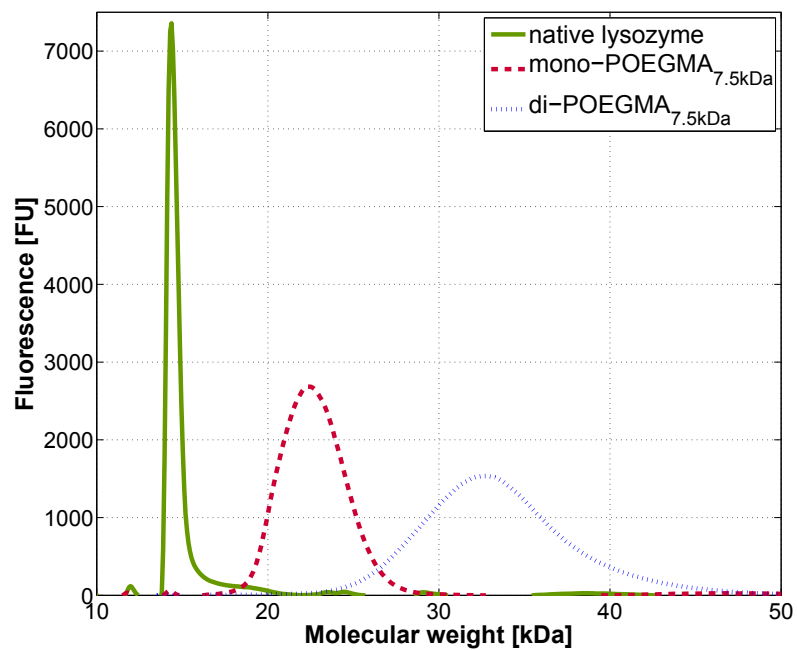
Supplementary Figure A.4: ^1H NMR spectrum of the purified PNAM_{3.5kDa}.



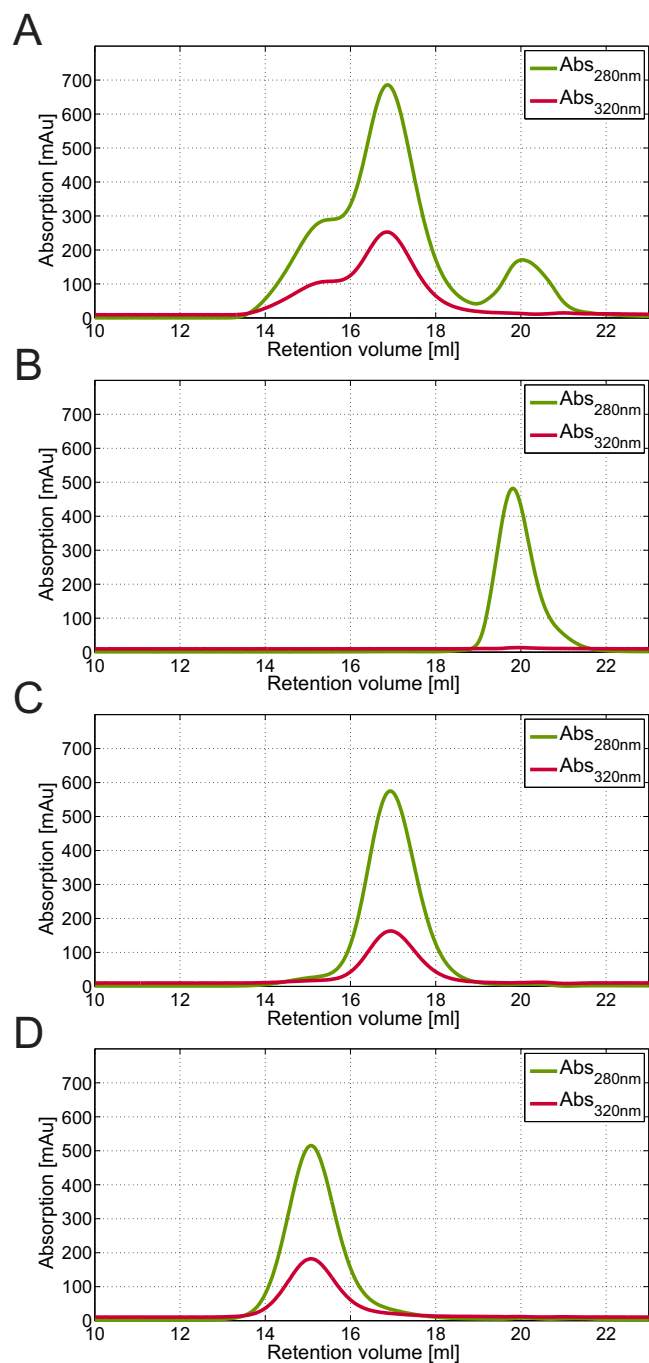
Supplementary Figure A.5: ^1H NMR spectrum of the purified PNAM_{7kDa}.



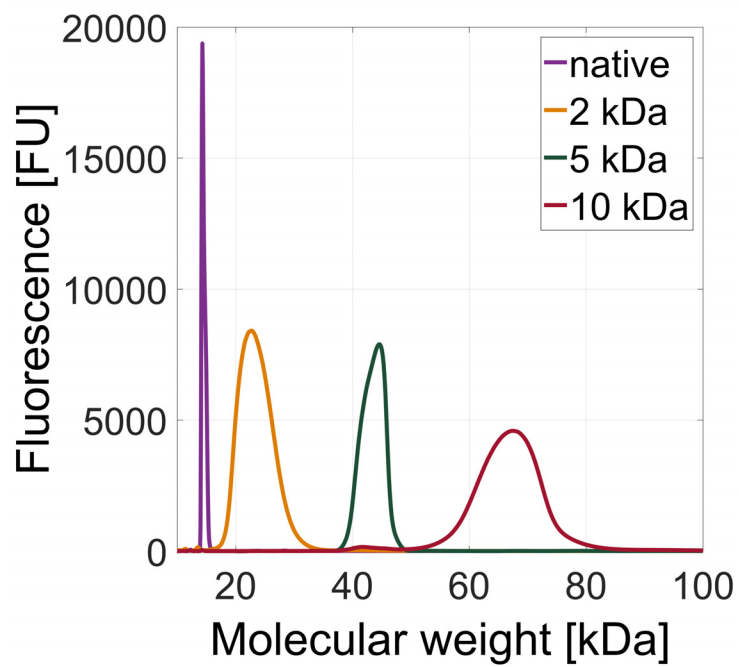
Supplementary Figure A.6: ^1H NMR spectrum of the purified POEGMA $_{7.5\text{kDa}}$.



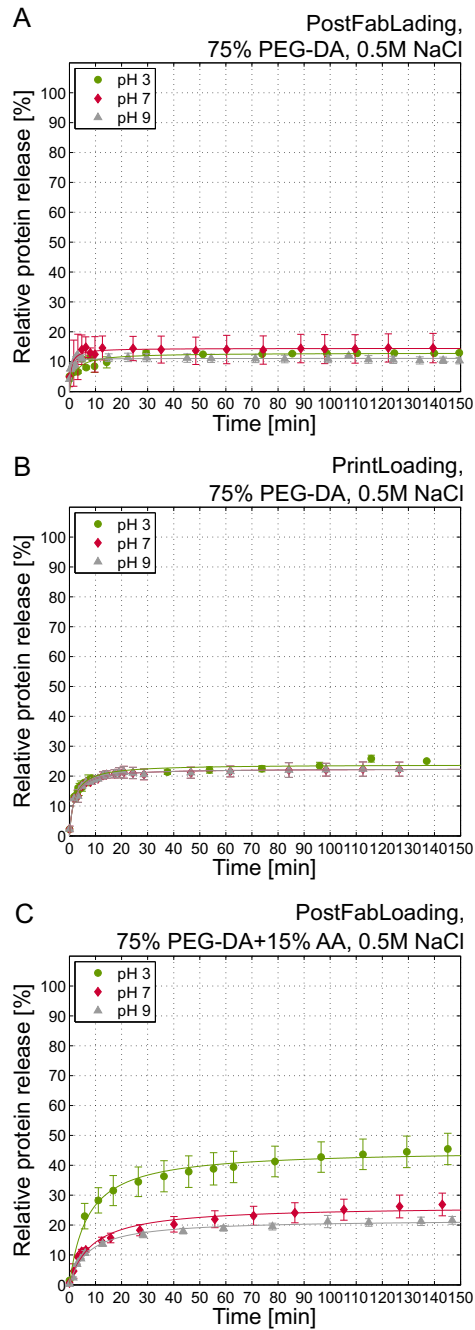
Supplementary Figure A.7: Analysis of the purified POEGMA-lysozyme conjugates using high-throughput capillary gel electrophoresis (HT-CGE) according to Morgenstern et al. [281].



Supplementary Figure A.8: SEC chromatograms of the POEGMA conjugation batch (A) and the purified species of native lysozyme (B), mono-conjugated lysozyme (C) and di-conjugated lysozyme (D). The separation was performed on a Superdex200Increase 10/300 (GE Healthcare, Uppsala, Sweden) using a 25 mM sodium phosphate buffer with 150 mM sodium chloride at pH 7.2.



Supplementary Figure A.9: HT-CGE fluorescence signals of native lysozyme as well as lysozyme attached with 2 kDa PEG, 5 kDa PEG, and 10 kDa PEG. All protein concentrations were set to $6.99 \cdot 10^{-5}$ M.



Supplementary Figure A.10: Relative protein release under the influence of 0.5 M NaCl in the release buffer: PostFabLoaded hydrogels from 75 % PEG-DA (A), PrintLoaded hydrogels from 75 % PEG-DA (B) and PostFabLoaded hydrogels from 75 % PEG-DA and 15 % AA (C).